Journal of Biosci

CONTENTS

Instructions to authors

Authors should send papers to: The Editor, 'Journal of Bioscie
No. 8005, C. V. Raman Avenue, Bangalore 560 080.

Three copies of the paper must be submitted.

The papers must present results of original work. Submission
that it has not been previously published and is not under con
further, that if accepted, it will not be published elsewhere.

*Authors are invited to suggest names and addresses of three ex
paper. The choice of referees will however remain with the editor*

Typescript

Papers must be typed (on one side only) double-spaced and wi
bond paper (280 × 215 mm). This also applies to the abstract
references each of which should be typed on separate sheets.

Title page

- The title of the paper must be brief and contain words useful
- The names with initials of authors and the address of the in
  must be given.
- An abbreviated running title of not more than 50 letters (in
- The address for communication (with telephone, telex and fa

Abstract

Papers must have an abstract (typed on a separate page) of no
significant results reported.

Keywords

Three to six keywords must be provided.

Text

- The paper must be divided into sections preferably starti
  'Discussion'

Figures and Photographs

- All figures should be numbered consecutively in arabic numerals text. Original figures should be drawn with India ink on tracing p
- *Please do not submit photographs of line drawings.*
- Good photocopies of all figures should accompany each copy of t
- Photographs should be numbered consecutively along with the order of appearance in the text. They should be assembled toget plates.
- Do not include line drawings and photographs in the same plate.
- Photographs should be sharp, of high contrast and on glossy pape
- Xerox copies of photographs are unsatisfactory for refereeing; three be submitted, both black and white and colour photographs are v

References

References should be cited in the text by author and year, not by nu authors, reference should be made to the first author followed by *et a* of the paper should be listed alphabetically by authors' names, follow full title of the paper, name of the journal (abbreviated according Periodicals, Butterworths, London), volume number, initial and final p should include: name(s) of author(s), initials, year of publication, title initials and name(s) of editor(s) if any, preceded by ed(s), place of referred to. References to these must include the year, the title of submitted and the university.

Examples

Mani A and Prabhu V K K 1986 Significance of critical develop: endocrine mediated precocious metamorphosis in *Oryctes rhinoceros Indian Acad. Sci. (Anim. Sci.)* **95** 379–385

Zar J H 1974 *Biostatistical analysis* (New Jersey: Prentice Hall)

Samiwala E B 1987 *DNA cloning in Haemophilus influenzae*, Ph. Bombay.

Ramanna M S and Hermsen J H Th 1979 Genome relationships in t *and taxonomy of Solanaceae* (eds) J G Hawkes, R N Lester and A G S pp 647–654

Abbreviations, symbols, units etc

The authors should follow *internationally agreed rules* especially th Commission on Biochemical Nomenclature (CBN). The journal will

Announcement

The *Journal of Biosciences* now incorporates *P...
Sciences) and *Proceedings* (*Plant Sciences*). Pap...
all areas of biology. These include

Molecular Biology
Genetics
Developmental Biology
Biophysics
Biochemistry
Immunology
Endocrinology
Medical Biology

Neurobi...
Ecology
Physiolo...
Etholog...
Evolutio...
Environ...
Sensory

Editorial

This is the first number of *Journal of Biosciences* incorporat
Sciences) and *Proceedings* (*Plant Sciences*). This merger m
have happened to the biology journals of the Academy i
course too early to say whether merging in itself will prov
the extent to which the merged journal will succeed
contemporary Indian biological research effort, and time,
against which the Academy decided to revamp its biology
specialized journals in biology—with 19 issues per year
have too many landmark papers to present. It made sens
journals of biology—*Journal of Genetics* being the other
year but bearing the better papers in the modern are
frequently published outside India.

It is often said that the main reason why Indian scien
journals is to ensure greater exposure and recognition. T
Some of the foreign journals they publish in are 'exotic'
or universities outside the country of publication. The trut
recognition do not follow merely because a finding is report
a discovery has intrinsic merit and significance, it will surf
regardless of which journal reported it. Great theories like S
even need a formal journal to spread their message
mimeographed the manuscript he sent to the *Annalen der P*
to a dozen or so European and British physicists, a
immortality.

On behalf of the Council and Fellowship of the Acad
Editors and Members of the Editorial Boards of the mer
decades of service in the cause of the growth of Indian
Editorial Board Members of the *Journal of Bioscie*
consented to continue to serve on the new Editorial Bo:

Reduction of ultraviolet-induced mitotic delay by c
irradiated plasmodia of *Physarum polycephalum*

P R JAYASREE and R VIMALA NAIR* (née

Department of Zoology, University of Calicut, Calicut 673 6

Abstract. Synchronously mitotic surface plasmodia of *Phys* violet-irradiated at different times during G2-phase (−4 h metaphase), and treated immediately thereafter with varying was observed that ultraviolet-induced mitotic delay is methylxanthine. In plasmodia irradiated between −4 and − the effect was concentration-dependent and the need for obtaining the reduction in delay was apparent. However, hig toxic when applied at this part of the cycle and led to r obtained with UV alone. The most striking observation ma phase-specific precipitous effect seen in those plasmodia irra mitosis which almost eliminated the long delay due to ultrav are discussed in the context of some of the known effects of mitosis-promoting factor. It is proposed that the significε induced mitotic delay reported here is due to the reactivation mitosis-promoting factor by caffeine. Alternatively, it is poss the inactivation of this factor by ultraviolet.

1. Introduction

shown to induce mitotic delay in this organism (B
addition to causing delay, UV-irradiation is also kno
in *Physarum* (Devi *et al* 1968). We report here the
induced, G2-phase mitotic delay by different conc
organism. The concentration-dependency of this effect
much of the G2-phase. However, any concentration
found sufficient to achieve this in plasmodia irradi
mitosis. This is a time when early indications of ci
visible under a microscope and extra sensitivity to UV
Kumari and Nair 1984).

2. Materials and methods

Macroplasmodia (surface plasmodia) containing synch
prepared (Guttes and Guttes 1964) from shaken cult
polycephalum (M_3C strain) maintained on the sem
Daniel and Baldwin (1964). Both macro- and micro-p
24°C. For irradiations a Philips 15-W germicidal la
approximately 90% of the UV-energy at 2537Å (Jag
dose delivered was 1400 Jm^{-2}, at a dose rate of 7·18 J

Aliquots from a stock solution (6 mg ml^{-1}) of ca
were added to the culture medium of the respectiv
different concentrations (50–750 μg ml^{-1}) of the drug
The sister macroplasmodia used in a set of expe
pooled microplasmodial suspension. The perturbation
times during the G2-phase preceding the second pos
plasmodium was cut into seven sectors. Six of them w
as control. Immediately after irradiation, five of the

Table 1. Effect of different concentrations of caffeine on U

Category of experiment Plasmodia	Early G2			Late G	
	A	B	C	D	E
Time of UV-irradiation (h^{min}) before metaphase	3^{45}	2^{20}	1^{25}	0^{55}	0^{50}
Delay (h^{min})					
UV	9^{00}	8^{55}	7^{50}	9^{55}	7^{10}
UV + caffeine (μg ml^{-1})					
50	8^{25}	7^{55}	6^{15}	9^{30}	7^{15}
	(6)	(11)	(20)	(4)	(101)*
100	9^{30}	6^{45}	4^{50}	9^{30}	1^{30}
	(106)*	(24)	(38)	(4)	(79)
250	7^{10}	6^{10}	4^{05}	1^{40}	1^{05}
	(20)	(31)	(48)	(83)	(85)
500	8^{30}	9^{00}	9^{15}	1^{25}	1^{05}
	(6)	(101)*	(118)*	(86)	(85)
750	12^{00}	11^{55}	12^{35}	0^{45}	1^{25}
	(133)*	(134)*	(161)*	(92)	(80)

The data from 8 plasmodia (A–H) are horizontally arranged, from the ea to the perturbation timings in them, which is given with respect to the me the respective control sector. Plasmodia A–C, E and G are sisters from on sisters from another experiment. Plasmodium D is from a third experiment basis of the time of metaphase in the respective control sector) obtained in a plasmodium are given sequentially below it (vertical column) and the pe in delay is given in parentheses. The percentage reduction/increase in de case of the different irradiated and caffeine-treated (UV + caffeine) sec corresponding irradiated (UV) sector as 100%.
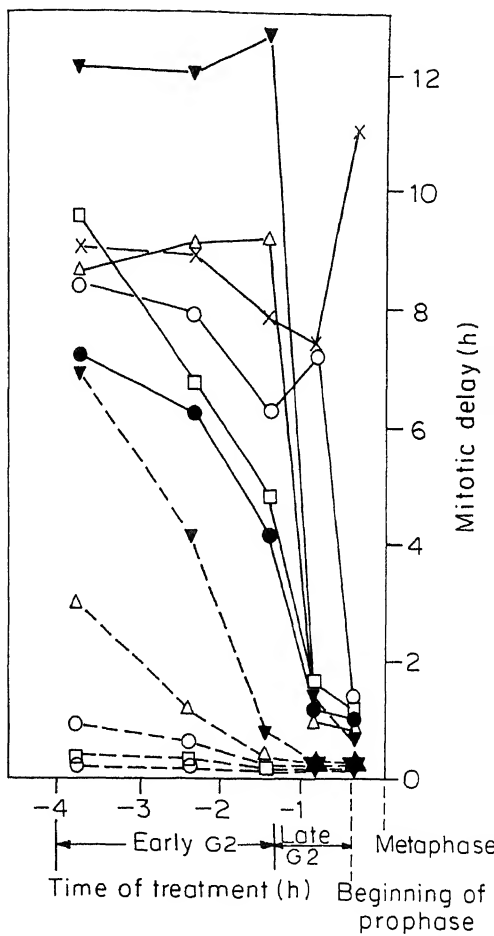
scussion

ck *et al* (1978) reported a concentration-dependent reduction of γ-ray ir
delay by caffeine in *P. polycephalum*. Their data show that, just as
studies, in those plasmodia irradiated earlier during G2 (74 min
red to 27 min before control metaphase), the protective effect of the l
tration of the drug employed by them (10 mM) was not evident beca
ic effect on longer exposure.

phase-specific effect reported by us is highly precipitous in nature
rally most interesting from the point of view of mitosis-cont
nisms. For example, this is the phase when maximal phosphorylation
in *P. polycephalum* (Bradbury *et al* 1974). The importance of phosp
of proteins involved in mitosis, particularly that of histones, in the in
osis and cell proliferation has been highlighted in a series of recent r
hy and Newport 1988; Murray and Krischner 1989; Pardee 1989). It ha
ted by Daniel and Oleinick (1984) that the reduction in γ-ray induced
by caffeine and some other phosphodiesterase inhibitors (Oleinick *et a*
to adjustments in cyclic nucleotide levels. The change they observed
vas a transient elevation of cyclic AMP followed by an increase in
Earlier to this, some others have proposed the involvement of cyclic A
duction of X-ray induced mitotic delay in the case of mammalian cells
Boynton *et al* 1974; Walters *et al* 1974).

osis-promoting factor (MPF) or the maturation-promoting factor, first
be present in the unfertilized egg cytoplasm of certain amphibians
larkert 1971; Reynhout and Smith 1974), has been ascribed with the fun
horylating some of the proteins involved in the structural changes ass
mitosis, such as chromatin condensation, nuclear envelope breakdov
ay and Krischner 1989). This protein has been assayed biochemic
e H1 kinase or as a MPF in biological assays (O'Farrell *et al* 1989) ar
respects similar to a certain maturation-promoting activity (MPA) re

to MPF (called as MPA by them in this paper) t
Moreover, they observed that agents which promote ch
as Mg^{2+} or polyamines partially restore the MPF of th
extracts.

Unlike UV, caffeine is known to induce premature
and advance mitosis in Syrian hamster fibroblast cell
replicative state of the cell (Schlegel and Pardee 1986
chromosome-condensing effect of caffeine has also bee
Physarum (P R Jayasree and R Vimala Nair, unpublish
the results of their study Schlegel and coworkers have
advancing effect of caffeine is because of its ability to se
related protein, which is generally fairly labile. Althoug
characterized to any great extent by them, because of its
and because of its G2-specificity, it would appear to be
(MPA) extracted from various cell types (Masui and M
Smith 1974; Adlakha *et al* 1984; O'Farrell *et al* 1989) in
et al 1988). It would then appear that the reduction of U
Physarum, reported here, could either be due to the rea
MPF-like activity by caffeine or because of the preventic
the drug. Further studies are in progress to elucidate thi

Acknowledgements

Reduction of UV-induced mitotic delay by caffeine

Jagger J 1967 *Introduction to research in ultraviolet photobiology* (New Jersey: Pr

Kumari P A V and Nair V R 1984 Mitotic delays and macromolecular synthesis
plasmodia of *Physarum polycephalum*; *Exp. Cell Res.* **151** 104–111

Masui Y and Markert C 1971 Cytoplasmic control of nuclear behaviour during
frog oocytes; *J. Exp. Zool.* **177** 129–146

Murray A W and Krischner M W 1989 Dominoes and Clocks: The union of two
Science **246** 614–621

O'Farrell P H, Edgar B A, Lakich D and Lehner C F 1989 Directing cell divisi
Science **246** 635–640

Oleinick N L 1972 The radiation-sensitivity of mitosis and the synthesis of thymi
polycephalum: a comparison to the sensitivity to actinomycin D and cycloh
638–653

Oleinick N L, Brewer E N and Rustad R C 1978 The reduction of radiation-in
caffeine: a test of the cyclic AMP hypothesis; *Int. J. Radiat. Biol.* **33** 69–73

Pardee A 1989 G1 events and regulation of cell proliferation; *Science* **246** 603–6

Reynhout J K and Smith L D 1974 Studies on the appearance and nature of
factor in the cytoplasm of amphibian oocytes exposed to progesterone; *Dev.*

Scaife J F 1971 Cyclic 3′,5′-adenosine monophosphate: its possible role in mam
radiation induced mitotic G2 delay; *Int. J. Radiat. Biol.* **19** 191–195

Schlegel R and Pardee A B 1986 Caffeine-induced uncoupling of mitosis from
replication in mammalian cells; *Science* **232** 1264–1266

Schlegel R, Croy R G and Pardee A B 1987 Exposure to caffeine and suppress
combine to stabilize the proteins and RNA required for premature mitotic ev
85–91

Walters R A, Gurley L R and Tobey R A 1974 Effects of caffeine on radiati
associated with cell-cycle traverse of mammalian cells; *Biophys. J.* **14** 99–118

Synthesis of actinomycin-insensitive RNA d
irradiation mitotic cycle, in the synchronously
Physarum polycephalum

W P S INDIRABAI and R VIMALA NAIR

Department of Zoology, University of Calicut, Calicut 6

Abstract. A sucrose density gradient analysis of ³H-uri
first postirradiation mitotic cycle of *Physarum polycep*
classes of RNA synthesized during this period are re
actinomycin D. In fact, the synthesis is found to be great
heterogenously sedimenting synthetic activity here may
and its precursors or more than one kind of RNA. Furth
meaningful in view of the actinomycin insensitivity of
itself to this antibiotic.

Keywords. Ultraviolet-irradiation; transcription; actin
mitotic cycle; *Physarum polycephalum*.

1. Introduction

Nuclear divisions in the multinucleated, syncytial plas
Physarum polycephalum, are synchronous and rh
multinucleated state makes the plasmodia highly resista

al 1968b; Guttes *et al* 1969), such that no further mitosis
the drug (Kumari and Nair 1983). The complete actinom
irradiation mitotic cycle in this system is also accompa
activity of this drug on the rate of overall RNA
Sachsenmaier 1973; Sachsenmaier and Dworzak 1976). Ce
studies also confirmed this (Kumari and Nair 1983).
subjected ^{3}H-uridine pulse-labelled RNA from the irrad
density gradient centrifugation. This showed that
synthesize preferentially low molecular weight RNA typ
that there is an overall reduction in the rate of synthe
Nair 1981). As a follow-up of this, we have now analysed
of the RNA synthesized by the irradiated plasmodia befo
employing essentially similar methods for isolation and a
Kumari and Nair (1981). It is found that while all th
synthesized during the delay period prior to the firs
actinomycin as much as the control system, complete resi
of RNA synthesized during the cycle after the first PIM
are discussed here.

2. Materials and methods

2.1 *Culturing of the organism and determination of mitot*

The Wisconsin strain (M3C) of *Physarum polyc*
microplasmodia in shaken cultures on a semi-defined m
Baldwin 1964), at a temperature of 24°C. Mitotically sy
plasmodia were made by the coalescence of pooled m
(0.4 ml aliquots) on Whatman No. 40 filter paper (Gutte
of macroplasmodia made from pooled microplasm
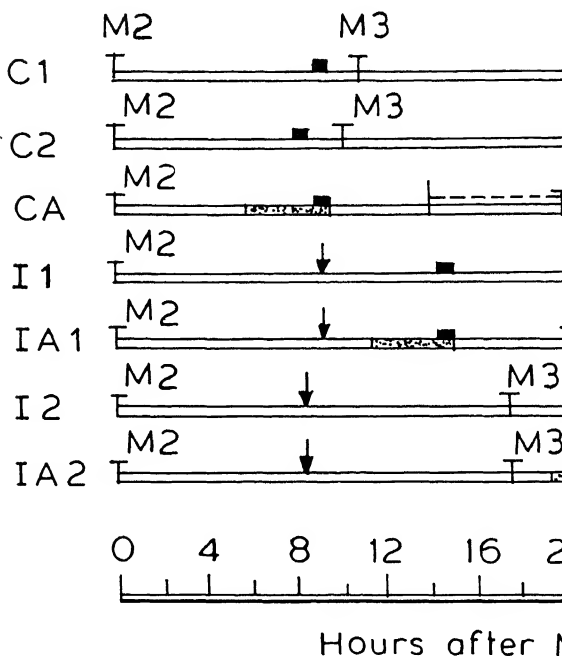
Figure 1. Schedule of irradiation, actinomycin treatment a

C1 and C2, Control plasmodia; RNA analysis data for C
plasmodium, treated with actinomycin, RNA analysis data
irradiated plasmodia, RNA analysis data given in figures
IA2, irradiated plasmodia, treated with actinomycin, RNA
and 7 respectively. The schedule for irradiation, actinomy
labelling for plasmodia, whose RNA analysis data are given
those for figures 6 and 7, except that the ³H-uridine pul
schedule refers to the data given in figures 2–9 and table 1.

M2, Second PEM; M3, third PEM in the case of contro

actions in sucrose gradients, the sedimentation pattern of which are given in figures 2–7.

dpm/region[b]	dpm/absorbance[c]	Inhibition due to actinomycin/irradiation or both based on unirradiated controls[a] (%)		Inhibition or increase (f) due to actinomycin calculated with respect to irradiated system (IA 1 compared to I1 and IA2 compared to I2) (%)
		C1	C2	
8,230	1600	—	—	—
11,440	3030	—	—	—
6,190	3990	—	—	—
	(1·9; 2·5; 1·7)			
9,520	1490	—	—	—
5,600	2030	—	—	—
4,140	2520	—	—	—
	(1·4; 1·7; 14)			
1,650	340	78·75	77·18	—
1,620	620	79·54	69·46	—
1,120	1330	66·67	47·22	—
	(1·8; 3·9; 2·8)			

340	70	95·62	95·30	75·00
260	110	96·37	94·58	74·42
570	410	89·72	83·73	70·07
	(1·6; 5·9; 4·6)			— — —
3,590	680	57·50	54·36	—
2,940	1110	63·37	45·32	—
1,840	1280	67·92	49·21	—
	(1·6; 1·9; 1·4)			
4,910	880	45·00	40·94	(↑) 29·41
2,810	1220	59·75	39·90	(↑) 9·91
1,690	1990	50·13	21·03	(↑) 55·47
	(1·4; 2·3; 1·9)			

...ree regions represented by the respective peaks.

...ponding region.

...bers of region H, with respect to the density changes of series I, II, III...

extracted twice with 3 ml phenol at 60°C and twice
time adding 0·2 ml diethylpyrocarbonate to the
precipitated from the aqueous layer of the final extr
ethanol (− 20°C), containing 2% sodium acetate. Th
centrifugation for 45 min at 10,000 rpm (12,000 *g*) in
L8–55M ultracentrifuge. This was then dissolved i:
0·1 M sodium chloride, 0·1 mM magnesium chloride,
(buffer II) and was precipitated, as above, once mor
− 20°C.

RNA thus extracted was fractionated on a linear
The sucrose solutions were made using buffer II. T
buffer II was layered on top of a 4·6 ml gradient.
45,000 rpm (243,000 *g*) in a Beckman SW 50·1 rotor f
of 10 drops each were collected in tubes. To each tu
added and the absorbancy was measured at 260
spectrophotometer. The sedimentation coefficients
Physarum, which include the two types of ribosom
taken to be 26S, 19S and 4S, respectively and are bas
al 1970; Zellweger and Braun 1971; Grant 1973).

2.4 *Assay of radioactivity*

For radioactivity assay, aliquots from each of the a
Whatman GF/C glass fibre filters and counted in a
using a toluene, PPO, POPOP cocktail.

2.5 *Quantitative evaluation of the gradients*

A quantitative evaluation of the RNA fraction in th
given in table 1. For this, the fractions in a gradient

on a comparative basis, in an irradiated system, there
molecular weight RNAs when compared to rRNA (figur

Total inhibition due to irradiation and actinomycin
RNA isolated during the UV-induced, extended G2-ph
irradiation mitosis is more than that due to actinomyci
system (compare type IA1 with CA in table 1). In other
of irradiation and actinomycin on RNA synthesis is seen
this time, the extent of sensitivity of the irradiated sys
different from that shown by the control (figures 2 and
and 5). On an average, more than 70% inhibition o
sedimentation classes of RNA is seen in the irrad
plasmodia in comparison with the corresponding irrad
type IA1 with I1 in table 1). About the same percentage i
by actinomycin in the case of control, unirradiated plas
to types C1 or C2 in table 1). In fact, in the low mo
percentage inhibition induced by actinomycin in the ir
more than that in the control (types Ia1 and I1 in table
or C2).

The characteristics of the RNA synthesized in the ir
the first postirradiation mitosis is very different, whe
described synthesis during the delay period prior to that
still substantial inhibition of transcription when comp
increased after the first PIM. What is perhaps more strik
insensitivity of all the sedimentation classes of RNA syn
In fact, the synthetic activity is greater in the drug-treat
(figures 6 and 7 and table 1). The higher synthetic a
category can also be shown after shorter ^{3}H-uridine pu
comparison here is made with respect to the correspond
Percentage-wise, the increased synthesis is greater in
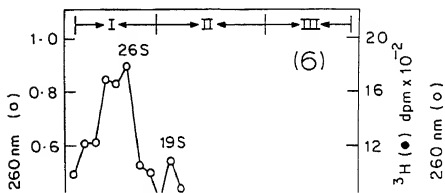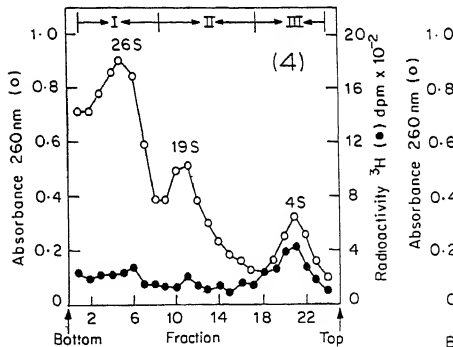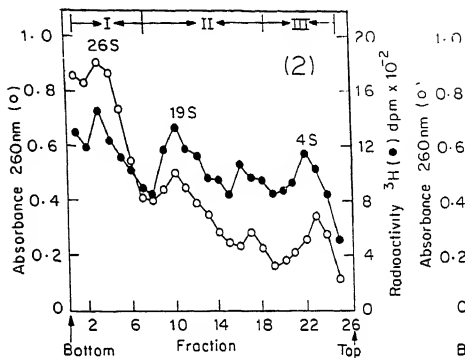
RNA/DNA and protein/DNA ratios, at the time of th[...]
radiation are much larger than that seen in the c[...]
corresponding undelayed mitosis (Devi *et al* 1968a). Si[...]
just as in any cellular systems, is accounted for by rR1[...]
synthesis to a great extent, helps in bringing down, the [...]
to the control level.

It is known that the sensitivity of the *P. polycephalu*[...]
mitotic delay induced by actinomycin, decreased rapidl[...]
that, following the first PIM, the plasmodia remaine[...]
actinomycin exposure for a few mitotic cycles (Devi an[...]
Nair 1983). In view of this, the present demonstration[...]
insensitive, heterogenously sedimenting RNA synthe[...]
irradiation mitotic cycle assumes importance. Moreo[...]
particularly in the low molecular weight region of the g[...]
drug-treated plasmodia (compare figure 6 with figure 7[...]

There have been many reports of lower sensitivity o[...]
some RNA types in the presence of actinomycin in di[...]
cells treated with low concentrations of actinomycin, sy[...]
can be inhibited without a corresponding decrease in t[...]
in the nucleoplasm (Perry and Kelley 1968). An increase[...]
synthesis, following the addition of actinomycin [...]
hepatoma cell cultures, led Tomkins *et al* (1969) to pr[...]
an unstable-mRNA specific, suppressor protein, thus [...]
the mRNA for the above aminotransferase. In Tomki[...]
actinomycin, no further synthesis of the unstable mR[...]
protein will occur and hence the superinduction of [...]

Figures 2–9. Sucrose density gradient analysis of RN[...]

presence. With respect to superinduction, the
Physarum appears to be analogous to the above
has been reported that nucleolar 4–7S RNA
experimental animals with actinomycin (Busch
has also been used to amplify the labelling of mito
Grivell 1971). Benecke and Penman (1977) also re
of small nuclear RNAs of discrete sizes between
are not affected by a certain concentration of acti
is susceptible. They observed that this class of RI
with the chromatin and nuclear matrix, is
concentrations of α-amanitin.

It is known that rRNA synthesis in *P. polyce*
to the action of actinomycin (Mittermayer *et al*
case of other eukaryotes (Penman *et al* 1968). Ther
our system in all probability must represent so
resistant synthesis is seen at a time when the rat
increased (figure 6 and table 1), over its severe r
prior to the first PIM (figure 4 and table 1). In
point out that both in the irradiated system p
control, approximately 20% of the heterogenou
was found not to be susceptible to the fairly
($200 \ \mu g \ ml^{-1}$) used by us in the present studies. It
the first PIM, the predominant synthetic activity
irradiation mitotic cycle would be an ideal system
this RNA(s) showing a fairly high resistance to
the observed increased synthesis in the presence
sedimenting synthetic activity here, with increa
weight region, may represent a single species of
than one kind of RNA. It would also be interest
if some of this RNA(s) to the reported actino

P and Grivell L A 1971 Mitochondrial ribosomes; *FEBS Lett.* **13** 73–88

H and Smetana K 1970 *The nucleolus* (New York: Academic Press)

J W and Baldwin H H 1964 Methods of culture for plasmodial myxomycetes; *Me siol.* **1** 9–41

R and Guttes E 1972 Macromolecular syntheses and mitosis in UV-irradiated pla *ysarum polycephalum*; *Radiat. Res.* **51** 410–430

R, Guttes E and Guttes S 1968a Effects of ultraviolet light on mitosis in *Physarum poly . Cell Res.* **50** 589–598

R, Guttes E and Guttes S 1968b Effect of actinomycin C on mitosis and DNA sy *ysarum polycephalum*; *19th Annual AIBS meeting*, Columbus, Ohio, Sept. 3–7

ak E and Sachsenmaier W 1973 Advanced initiation of synchronous nuclear division in *ycephalum* following UV-irradiation: effects of actinomycin C; *Publ. Univ. Innsbruck (A* 19

W D 1972 The effect of α-amanitin and $(NH_4)_2SO_4$ on RNA synthesis in nuclei an ated from *Physarum polycephalum* at different times during the cell cycle; *Eur. J. Bioche*

W D 1973 RNA synthesis during the cell cycle in *Physarum polycephalum*; in *The ce elopment and differentiation* (eds) M Balls and F S Billet (London: Cambridge University 109

E and Guttes S 1964 Mitotic synchrony in the plasmodia of *Physarum polycephalum* an chronization by coalescence of microplasmodia; *Methods Cell Physiol.* **1** 43–53

E, Guttes S and Devi V R 1969 Electron microscope study of mitosis in normal and act ated nuclei of *Physarum polycephalum*; *III Int. Congr. on Protozoology* Leningrad, July 2

E, Guttes S and Rusch H P 1961 Morphological observations on growth and differ *ysarum polycephalum* grown in pure culture; *Dev. Biol.* **3** 588–614

i P A V and Nair V R 1981 Preferential synthesis of low-molecular-weight RNA in UV smodia of *Physarum polycephalum*; *Radiat. Res.* **88** 37–46

i P A V and Nair V R 1983 Transcription in ultraviolet-irradiated plasmodia of *ycephalum*; *J. Biosci.* **5** 365–375

i P A V and Nair V R 1984 Mitotic delays and macro-molecular synthesis in G2 phase smodia of *Physarum polycephalum*; *Exp. Cell Res.* **151** 104–111

P W, Chet I and Rusch H P 1970 Electrophoretic characterization of ribosomal F *ysarum polycephalum*; *Biochim. Biophys. Acta* **209** 569–572

mayer C, Braun R and Rusch H P 1964 RNA synthesis in the mitotic cycle of *ycephalum*; *Biochim. Biophys. Acta* **91** 399–405

Histidine-15 and lytic activity of lysozyme

MADHURI M UGRANKAR, G KRISH
BALA S PRABHANANDA

Chemical Physics Group, Tata Institute of Fundamental
Bombay 400 005, India

Abstract. The literature data on the activity of histic
lysozyme are conflicting: the modified enzyme is reporte
activity or less activity by different authors. Amino acid
of the single His-15. Detailed activity studies on His-15
diethyl pyrocarbonate) lysozyme have shown that the con
specific choices of ionic strengths and cell wall substr
attributed to the substrate being negatively charged. (
though histidine-15 is far removed from the active
modification or binding of the negatively-charged s
conformation around the active site. However, the cha
chemically modifying His-15 is small.

Keywords. Lysozyme; histidine modification; *Microco*
potential in catalysis; pK-shifts.

1. Introduction

In the recent past, there has been considerable interest in
far removed from the active site of enzyme in the substr
reactions (Krishnamoorthy *et al* 1979; Grütter and Math

which His-15 is modified with iodoacetic acid. H
reported increased activity (110–112%) when only
contrast with this report, Piszkiewicz and Bruice (196
observation of a decrease in lytic activity (40–45%)
15. On the other hand, Parsons *et al* (1969) did r
activity.

Since the lysozyme activity towards cell wall su
strength-dependent (Davis *et al* 1969; Maurel and
the explanation of the conflicting results reported in
specific choice of ionic strength in the experimen
undertaken to examine such a possibility and to find
above mentioned contradicting results. Two types of
15 have been used for this purpose. (i) Carboxyr
procedure of Parsons *et al* (1969) using iodoacetic aci
15 by the reaction of lysozyme with diethyl pyrocarb
two types of chemical modifications enable us to l
activity behaviours when the charges on the ch
different. Apart from clarifying the conflicting repo
shown the importance of His-15 in the regulation of
walls.

2. Materials and methods

HEW lysozyme, DPC and *M. luteus* were obtained
acid from Aldrich (USA). Carbethoxyhistidine-15
prepared by adding 8 μl of 250 mM DPC in ethyl a
lysozyme in 50 mM Bistris buffer at pH 5·5. The
against 10 mM Bistris at pH 7, after allowing the rea

variation in the activity measured in the four measureme
observed were confirmed by duplicating the experiments
solutions. Experiments were also carried out using K
strength and at other pH conditions to confirm that the
not due to the specific choices of electrolyte or pH.

3. Results

The chemical modifications of lysozyme described in th
under conditions such that His-15 was specifically alte
under our conditions generated only one carbethoxyhistid
the enzyme as shown by its optical absorption at 240
restoration of activity to the 100% level by hydroxylami
Reaction with iodoacetic acid was carried out under cor
described by Parsons *et al* (1969) who had shown by
specific reaction at the single histidine residue.

The hypothesis that the differences in the experime
different authors [which are not explicitly mentioned in t
et al 1963; Parsons *et al* 1969)] could be responsible for t
confirmed by studying the lytic activities at different ion
concentrations as shown below.

At low ionic strengths, the activity of CE lysozyme is
lysozyme at all the substrate concentrations used in our
2). However, the activity of CM lysozyme at low ionic st
HEW lysozyme at low substrate concentrations (figures 1
that of HEW lysozyme at higher substrate concentrations
observations are well beyond the experimental errors and
reported by Kravchenko *et al* (1963) or Parsons *et al* (19
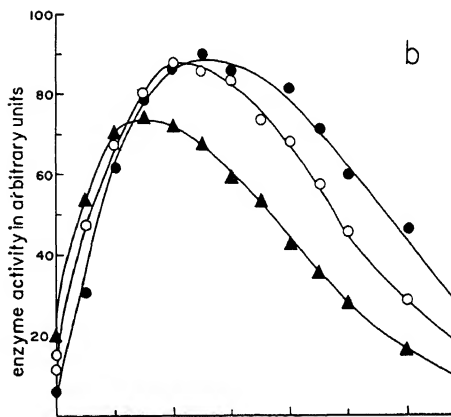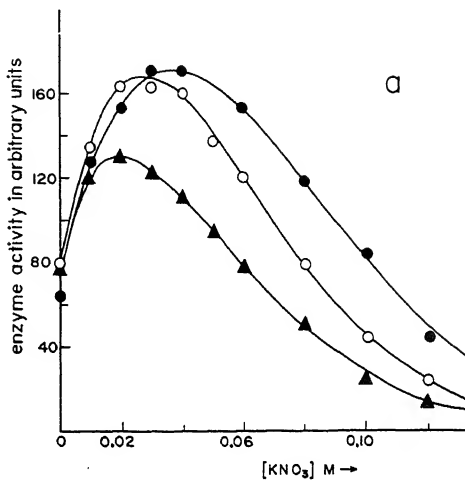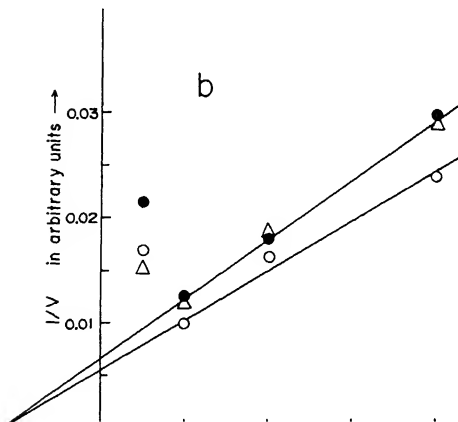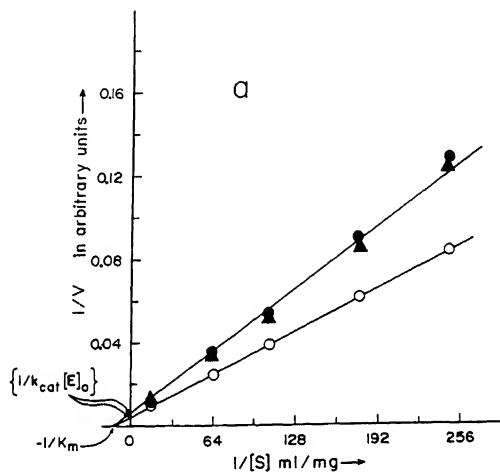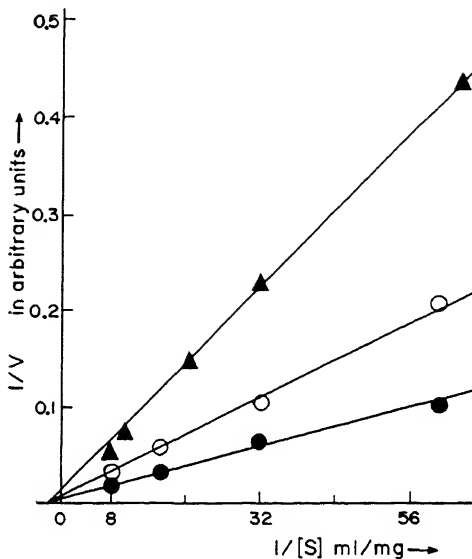
Figure 3. Lineweaver-Burk plots for HEW Lyso[...] lysozyme (▲), at high ionic strength. $[KNO_3] =$ [...] and temperature 24°C. Buffer concentration was 2[...]
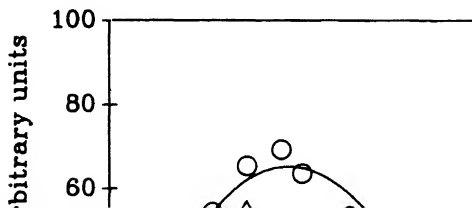
optimum activity shifts to smaller values, (ii) the diff
enzyme preparations observed at low and high ionic st
due to differences in k_{cat} and (iii) the pH of optimum ac
smaller value. These three predictions are observed in t
data in figures 1 and 2 show clearly that the conflicting
1963; Piskiewicz and Bruice 1968; Hartdgen 1967; Pars
of modification of His-15 could be due to different ex
ionic strength and substrate concentration) employed
activity. The data also suggest a conformational cha
lysozyme on chemically modifying His-15. Furthermo
conformation near the active site, inferred from the sl
maximum activity in the case of CM lysozyme (figure
decrease in the maximum k_{cat}. A parallel situation i
between the inactivation due to oxidation of Trp-108 a
35 observed in X-ray studies (Blake *et al* 1967).

At low ionic strengths and at high substrate con
product formation decreases with increase in substrate
suggesting the possibility of substrate inhibition of ly
ionic strengths have also been observed by Verhamme
HEW lysozyme. The results were best understood in
1988) in which a second substrate binds to the enzy
leading to an inactive complex (ES_2). The rate of
(Verhamme *et al* 1988).

$$\frac{1}{V} = \frac{1}{k_{cat}[E]_0}\left[1 + \frac{K_m}{[S]} + \frac{[S]}{K_2} \right],$$

where K_m is the Michaelis constant and $K_2 = [ES]\cdot$
explains the "deviations" from the straight line behav
smaller deviation observed for CM lysozyme (figure 2b)

the possibility of such changes in the activity even
when charged substrates are involved.

References

Blake C C F, Johnson L N, Mair G A, North A C T, Phillips D C
    egg-white lysozyme; *Nature (London)* **206** 757–761

Blake C C F, Johnson L N, Mair G A, North A C T, Phillips D C
    egg-white lysozyme at 2 Å resolution; *Proc. R. Soc. (London)*

Blake C C F 1968 The preparation of isomorphous derivatives;

Davis R C, Neuberger A and Wilson B M 1969 The dependence
    strength; *Biochim. Biophys. Acta* **178** 294–305

Goux W J and Allerhand A 1979 Studies of chemically modified
    13 NMR spectroscopy; *J. Biol. Chem.* **254** 2210–2213

Grütter M G and Mathews B W 1982 Amino acid substitution f
    T4 lysozyme reduce catalytic activity and suggest that the C
    in substrate binding; *J. Mol. Biol.* **154** 525–535

Hartdgen F J 1967 *Chemical modification of lysozyme*, Ph. D. the

Imoto T, Johnson L N, North A C T, Phillips D C and Rupley
    enzymes (ed.) P D Boyer (New York: Academic Press) vol 7,

Jolles J, Spotorno G and Jolles P 1965 Lysozymes character.
    histidine less lysozyme; *Nature (London)* **208** 1204–1205

Kravchenko N A, Kleopina G V and Kaverzneva E D 196
    lysozyme: Carboxymethylation of the imidazole group of histi
    Biochim. Biophys. Acta **92** 412–414

Krishnamoorthy G, Prabhananda B S and Gurnani S 1979 Bro
    active site environment: A temperature-jump study; *Biopolym*

Krishnamoorthy G and Prabhananda B S 1982 Phenolsulfoph
    lysozyme activity towards cell wall substrates; *Biochim. Bioph*

Maurel P and Douzou P 1976 Catalytic implications of electr
    lysozyme as a model; *J. Mol. Biol.* **102** 253–264

Miles E W 1977 Modification of histidyl residues in proteins
    Enzymol. **47** 431–442

Parsons S M, Jao L, Dahlquist F W, Borders C L, Jr, Groff T, Ra

Conformation of azidothymidine: an anti-AIDS

ANIL SARAN* and R P OJHA[†]

Chemical Physics Group, Tata Institute of Fundamenta
Colaba, Bombay 400 005, India
[†]Permanent address: Physics Department, Gorakhpur
India

Abstract. The nucleoside antibiotic, 3′-azido-3′-deoxythy
has shown great promise in inhibiting the human immun
mortality among AIDS patients. Conformational prope
investigated by quantum-mechanical PCILO method
parent nucleoside, thymidine. The results indicate great
similarity is remarkably striking in the situations that
result has important biological significance in e
azidothymidine.

1. Introduction

The rapid spread of the previously unknown infectious
deficiency syndrome (AIDS) has caused a worldwide
disease effectively. AIDS has been conclusively shown t
immuno deficiency virus (HIV) by Gallo *et al* (1984) and
been engaged in carrying out various studies to understa
structure and functions (Vogel *et al* 1988; Lapatto *et*
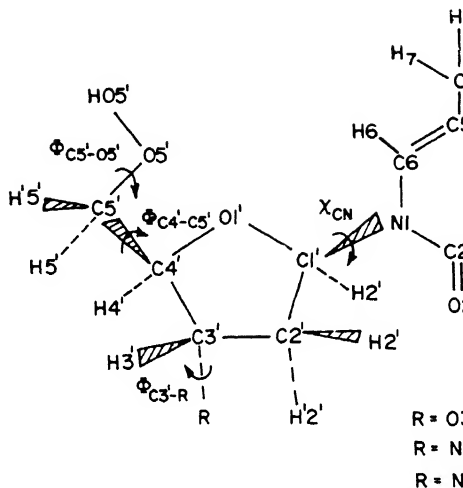
Figure 1. Schematic diagram of AZT and thymid

(see figure 1) is *anti* for both molecules of AZT: χ
and 3·5° for AZT-molecule B. The conformation aro
is *gg* ($\phi_{C4'-C5'} = 50\cdot7°$) in AZT-molecule A while f
= 173·6°). An independent X-ray crystallographic
reported by Parthasarathy and Kim (1988) which i
to those reported by Camerman *et al* (1987). Camer
crystal conformation of AZT molecules A and B
phosphate moieties A and B of a highly hydr
dinucleotide, 5′-phosphothymidylyl (3′-5′) thymidine
et al (1976). Although the two structures are grossly
they differ considerably in details. Evidence of this i

around C4'-C5' bond is predominantly *gg*. These solut
variance with those obtained in the solid state from X
authors also reported very briefly the predominance o
C4'-C5' for both molecules of AZT by the PCILO me
studies on the conformation of AZT molecule carried
indicate that AZT has C3'-endo sugar pucker and the
glycosyl and C4'-C5' bonds are, respectively, *anti* and *gg*.
cluded that AZT has no unusual features but has confo
very similar to those of standard deoxypyrimidines. These
at variance with those obtained in the solid state from

The conformation of nucleoside antibiotics has
laboratory for several years (Saran 1981, 1987, 198
established an important correlation between the co
activity of nucleoside antibiotics. AZT is a nucleoside a
consequence of the replacement of 3'-hydroxyl group
thymidine, by an azido group (figure 1). We have in the
extensive and detailed PCILO investigation on AZT
correlation holds good for AZT or not.

2. Procedure

The method utilized in this study is the quantum-m
(Pullman and Saran 1976); the details of which can be
(Diner *et al* 1969a,b; Jordan *et al* 1969). The various tor
the conformation of AZT (figure 1) are defined (Sara
Saran 1976) as:

$$\chi_{CN} = O1' - C1' - N1 - C6,$$

$$\phi_{C4'-C5'} = C3' - C4' - C5' - O5',$$

PCILO energies have been computed as a fun
preselected values of $\phi_{C5'\text{-}O5'}$ at 30° intervals of the
two-dimensional conformational energy maps ha
presentation of the results on these maps has been
curves above the global minimum. For brevity, only
been presented in the text though the results of
discussed.

3. Results and discussion

Tables 1 and 2 list the global minima and low
1 kcal/mol for both molecules of AZT as well as tl

Table 1. Preferred conformation of C2'-endo,
thymidine.

Molecule	Map constructed with $\phi_{C5'\text{-}O5'}$	Glob χ_{CN}
AZT- molecule A	60	240 (syn)
(I = $-N-N \equiv N$)	180	330 (anti)
		60 (anti)
	300	180 (syn)
AZT-molecule A	60	240 (syn)
(II = $-N=N=N$)	180	330 (anti)
		60 (anti)
	300	180 (syn)
Thymidine	60	240 (syn)
	180	330 (anti)
		60 (anti)
	300	180 (syn)

along with their energies taking the energy of the lowest global mi[nimum to?]
be zero.

3.1 *AZT-molecule A (C2'-endo, C3'-exo)*

The most stable conformation for C2'-endo, C3'-exo AZT-molecule[...]
resonant structures I and II for the azido group is obtained with[...]
$\phi_{C5'-O5'} = 60°$. Figure 2 shows the conformational energy ma[p for?]
structure I and it can be seen that a highly localized global mi[nimum at?]
$\chi_{CN} = 240°$ (*syn*) and $\phi_{C4'-C5'} = 30°$ (*gg*). This global minimum is[...]
strong intramolecular hydrogen bonding between O5' of deoxyr[ibose and?]
thymine base through favourable orientation of HO5' (i.e. ϕ_{C5}[...]
intramolecular hydrogen bonding has been observed for a[...]
antibiotics having C2'-endo sugar pucker (see review by Saran[...]
identical conformational energy map has been obtained for the re[sonant structure?]
II. In fact, a glance at the results summarized in tables 1 and 2 ind[icates?]
no significant effect of the resonant structures I and II for the az[ido group on?]
conformational properties of AZT.
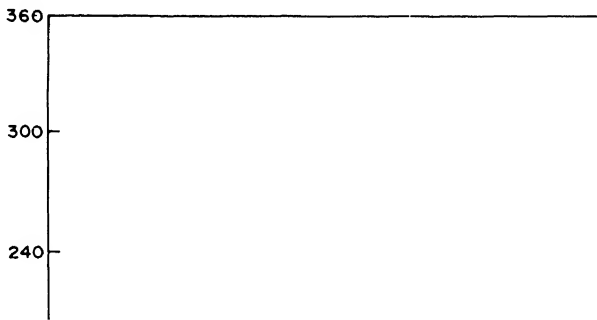
The conformational energy maps for AZT-mole[cule]
and II constructed with a preselection of $\phi_{C5'-O5'}$ [=]
figures 3 and 4. It can be observed from these [maps]
conformational flexibility as compared to the ve[ry]
figure 2. Both maps exhibit very similar confor[mation]
global minima having the same energy at $\chi_{CN} = 3$[0°]
of them are associated with the same $\phi_{C4'}$[-C5']
($\chi_{CN} = 150°-240°$) are about 2 to 4 kcal/mol hi[gher]
minima. In the preselection of $\phi_{C5'-O5'} = 180°$, HO[5']
therefore, there is no possibility of intramolecula[r]
atoms of the deoxyribose and the thymine base. [The]
results presented in figures 3 and 4 has been discu[ssed]

Figure 5 shows the conformational energy map [for]
structure I and $\phi_{C5'-O5'} = 300°$. The global minim[um]
$\phi_{C4'-C5'} = 150$ (gt). This map exhibits larger confo[rmation]
to that shown in figure 2. A very similar conforma[tion]
the resonant structure II showing the global minim[a]
those observed in the map of figure 5.
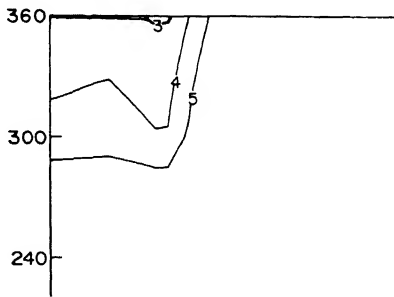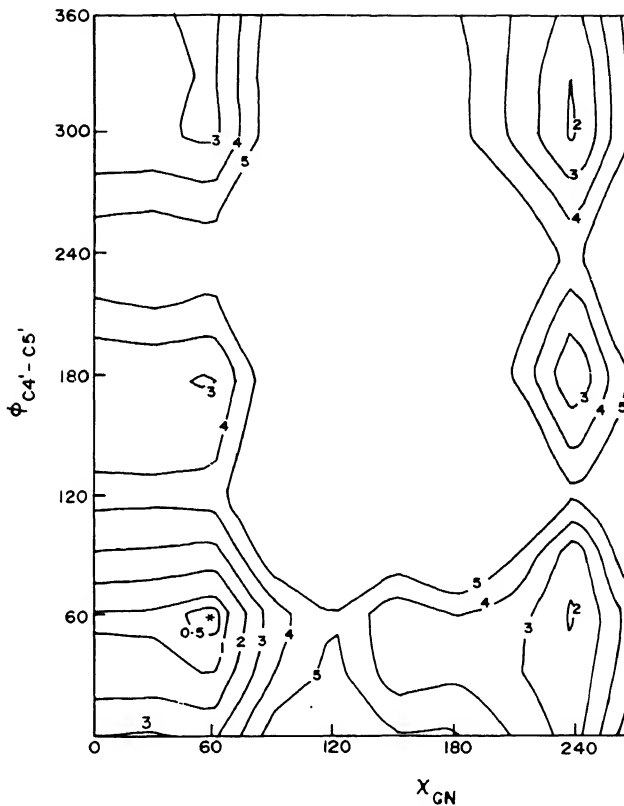
Figure 4. $(\chi_{CN}-\phi_{C4'\text{-}C5'})$ conformational energy map for AZT-mol (exo) with resonant structure II and $\phi_{C5'\text{-}O5'} = 180°$.
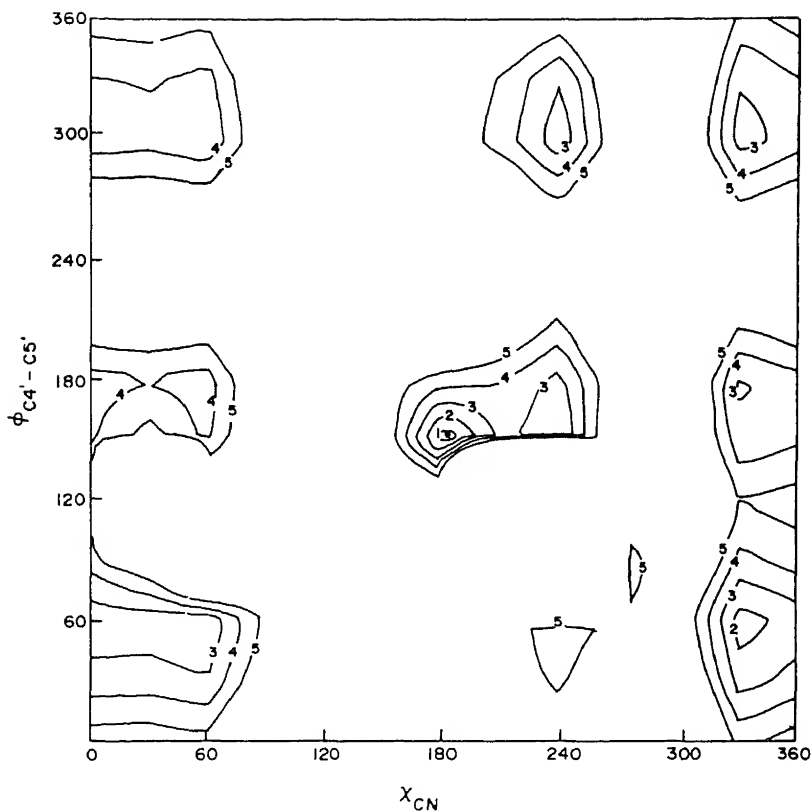
Figure 5. $(\chi_{CN} - \phi_{C4'\text{-}C5'})$ conformational energy map for AZT-molecule A (C2'-endo, C3'-exo) with resonant structure I and $\phi_{C5'\text{-}O5'} = 300°$.

3.3 AZT-molecule B (C3'-exo, C4'-endo)

The conformational energy maps constructed for C3'-exo, C4'-endo AZT-molecule B with both resonant structures I and II and with $\phi_{C5'\text{-}O5'} = 60°$ indicate a global minimum at $\chi_{CN} = 0°$ (*anti*) and $\phi_{C4'\text{-}C5'} = 60°$ (*gg*) (see table 2). In this sugar puckering there is no intramolecular hydrogen bonding between the atoms of deoxyribose and the base as that observed in the case of C2'-endo, C3'-exo AZT-molecule A (figure 2).

Figures 7 and 8 show the conformational energy maps for resonant structures I and II constructed with $\phi_{C5'\text{-}O5'} = 180°$. The two maps are very similar to each other and the global minimum occurs in both the maps at $\chi_{CN} = 0°$ (*anti*) and $\phi_{C4'\text{-}C5'} = 60°$ (*gg*). There is a low energy region within 1 kcal/mol above the global minimum in both the maps at $\chi_{CN} = 180°$ (*syn*) and $\phi_{C4'\text{-}C5'} = 120°$ (*gt*). The preselection of $\phi_{C5'\text{-}O5'} = 180°$ in these maps completely rules out the possibility of intramolecular hydrogen bonding and this has important biological implications (Saran 1981, 1987, 1989). This will be discussed in the next section.

It can be seen from table 2 that for $\phi_{C5'\text{-}O5'} = 300°$, both the resonant structures indicate a global minimum at $\chi_{CN} = 90°$ (*anti*) and $\phi_{C4'\text{-}C5'} = 120°$ (*gt*) and a low-
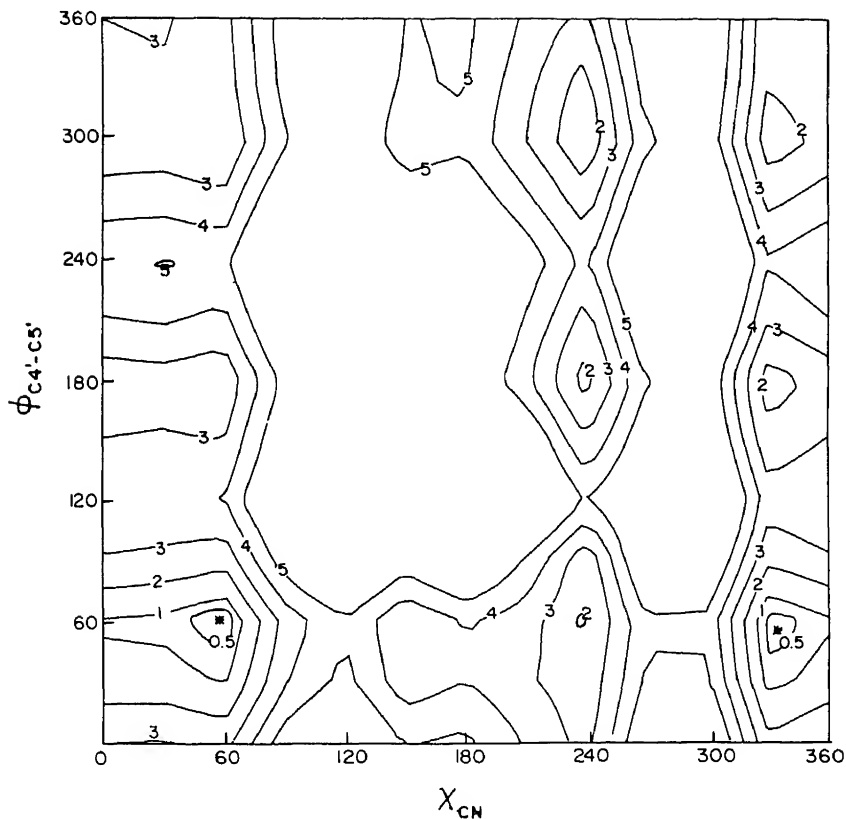
Figure 6. $(\chi_{CN}-\phi_{C4'-C5'})$ conformational energy map for thymidine (C2'-endo, C3'-exo) with $\phi_{C5'-O5'}$ 180°.

·gy region within 1 kcal/mol of the global minimum at $\chi_{CN} = 330°$ (*anti*) and ·° (*gt*). Both maps (not shown) have very similar conformational features ·cating that the two resonant structures of the azido group have an almost ·gnificant effect on the conformation of the molecule.

Thymidine (C3'-exo, C4'-endo)

·computations carried out for the parent nucleoside, thymidine, having C3'-exo, ·-endo sugar pucker indicate almost identical results to those for AZT-molecule ·ee table 2). The global and local minima observed for thymidine are identical to ·se for AZT-molecule B. Figure 9 shows the conformational energy map for ·midine constructed with a preselection of $\phi_{C5'-O5'} = 180°$ and it can be seen that ·results of this map are remarkably similar to those presented in figures 7 and 8. ·minimum occurs at $\phi_{CN} = 0°$ (*anti*) and $\phi_{C4'-C5'}$ (*gg*) similar to that in figures 7 ·8 for AZT-molecule B with the two resonant structures. A low energy region
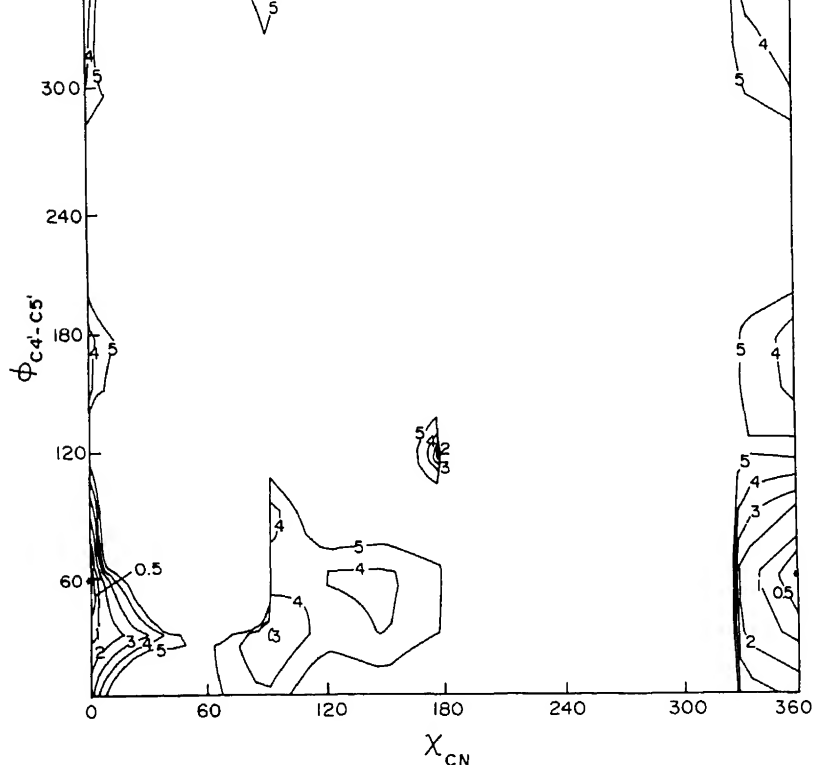
Figure 7. $(\chi_{CN}-\phi_{C4'-C5'})$ conformational energy map for AZT-molecule B (C3'-exo, C4'-endo) with resonant structure I and $\phi_{C5'-O5'} = 180°$.

4. Biological significance

The results presented in tables 1 and 2 and in figures 3, 4, 6, 7–9 clearly demonstrate that the AZT molecule either in C2'-endo, C3'-exo or in C3'-exo, C4'-endo sugar geometry has similar conformational preferences as those of the parent nucleoside: thymidine. This similarity is quite remarkable in the conformational energy maps constructed with $\phi_{C5'-O5'} = 180°$. Our earlier studies on a number of nucleoside antibiotics (Saran and Chatterjee 1980a, b, 1984; Saran and Patnaik 1981, 1982, 1986; Patnaik and Saran 1984; Saran 1988) have revealed that the aqueous solution situation is very successfully mimicked by carrying out theoretical computations with a preselection of $\phi_{C5'-OS} = 180°$. In this preselection there is no possibility of intramolecular hydrogen bonding between atoms of the sugar moiety and the base and this is the situation that prevails in aqueous solution because intermolecular hydrogen bonds with water molecules will be preferred to intramolecular hydrogen bonds. This point has been borne out by the excellent agreement between theoretical computations on 8-azadenosine (Saran et al 1978), tubercidin (Saran and Mitra 1979), cordycepin (Saran and Patnaik 1981),
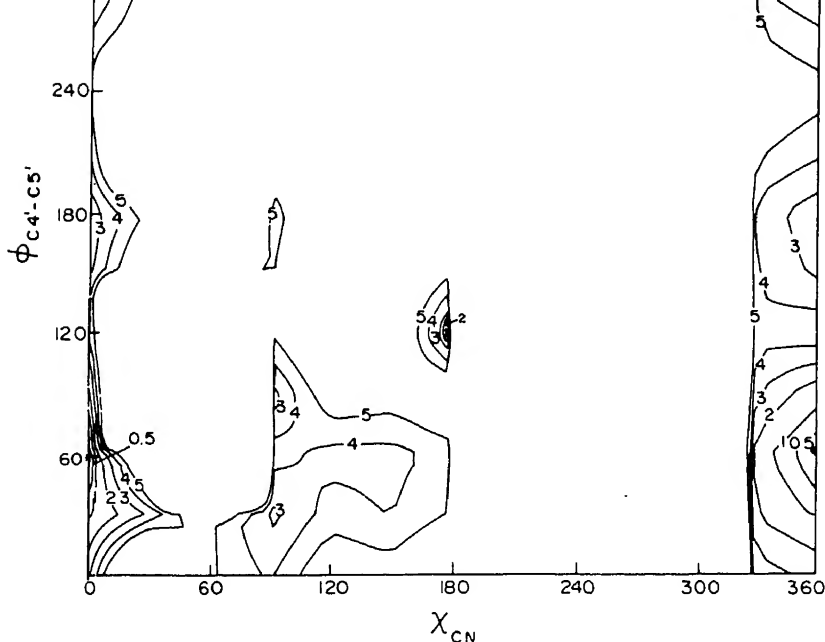
Figure 8. $(\chi_{CN} - \phi_{C4'-C5'})$ conformational energy map for AZT-molecule B (C3'-exo, C4'-endo) with resonant structure II and $\phi_{C5'-O5'} = 180°$.

propranolol, a β-adrenergic blocking drug (Kulkarni *et al* 1979) and the experimental NMR results in aqueous solution. The results of theoretical computations on 6-azauridine and 6-azacytidine (Mitra and Saran 1978) show exact correspondence with the results from ORD and CD studies in aqueous solution.

Since all biochemical reactions occur in aqueous medium, the results presented in tables 1 and 2 and figures 3, 4, 6 and 7–9 assume great biological significance. Because of the striking similarity in the conformational features, AZT molecules can successfully mimick thymidine and get incorporated in DNA in place of thymidine. Further, AZT molecules can readily get phosphorylated and mimick thymidylate in enzymatic reactions. These theoretical deductions are fully corroborated by the experimental evidence of St. Claire *et al* (1985) and Ono *et al* (1986). In order to explain the biological action of AZT, St. Claire *et al* (1985) proposed that AZT gets incorporated into viral DNA. Once AZT is incorporated into viral DNA, the termination of chain elongation follows because of the absence of 3'-OH functional group in AZT which has been replaced by an azido group. The experiments of Ono *et al* (1986) implicate the competitive binding of AZT with reverse transcriptase as compared to thymidylate binding.
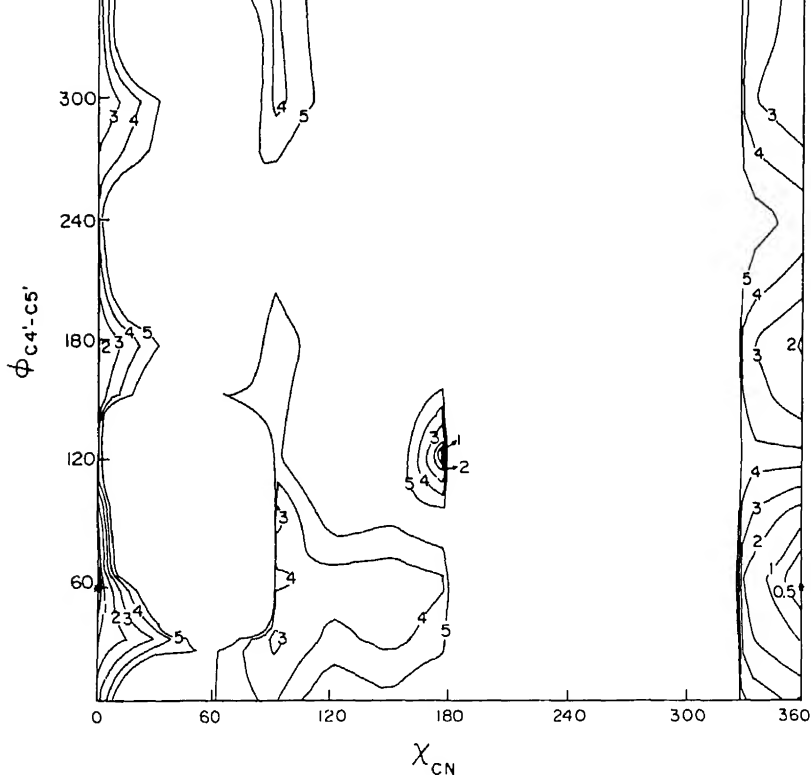
Figure 9. $(\chi_{CN}-\phi_{C4'-C5'})$ conformational energy map for thymidine (C3'-exo, C4'-endo) with $\phi_{C5'-O5'} = 180°$.

5. Conclusion

In conclusion, the results of the present investigation indicate that the conformational preferences of AZT are very similar to those of the parent nucleoside: thymidine. This similarity is remarkably striking in situations that prevail in the aqueous solution with the result that AZT molecules can very efficiently mimick thymidine and get incorporated in growing chains of viral DNA and terminate the chain elongation. The correlation obtained earlier for nucleoside antibiotics (Saran 1981, 1987, 1989), thus, holds true for AZT. It then becomes obvious to visualize the drug action of AZT.

Finally, it is relevant here to remark that as discussed earlier, the agreement between X-ray crystallographic results on AZT and the theoretical predictions presented in this paper is not to be expected at all. This is due to the fact that PCILO computations have been carried out on an isolated molecule *in vacuo* whereas the conformation observed in the solid state is dictated by many factors such as conditions for crystallization, crystal-packing forces, and environmental effects. However, when the computations have been carried out with $\phi_{C5'-O5'} = 180°$ mimicking the situation prevailing in the aqueous solution, the PCILO results on

$- 180$, which will be again in agreement with the molecular mechanics calculation of Herzyk et al (1987) and NMR solution studies of Swapna et al (1989).

References

Camerman N, Fawcett J K and Camerman A 1976 Molecular structure of deoxyribose-dinucleotide sodium thymidylyl-(5'-3')-thymidylate-(5') hydrate (pTpT) and a possible structural model for poly thymidylate; *J. Mol. Biol.* **107** 601–621

Camerman A, Mastropaolo D and Camerman N 1987 Azidothymidine: Crystal structure and possible functional role of the azido group; *Proc. Natl. Acad. Sci., USA* **84** 8239–8242

Diner S, Malrieu J P and Claverie P 1969a Localized bond orbitals and the correlation problem I. The perturbation calculation of the ground state energy; *Theor. Chim. Acta* **13** 1–17

Diner S, Malrieu J P, Jordan F and Gilbert M 1969b Localized bond orbitals and the correlation problems III. Energy up to the third-order in the zero-differential overlap approximation. Application to σ-electron systems; *Theor. Chim. Acta* **15** 100–110

Furman P A, Fyfe J A, St. Claire M H, Weinhold K, Rideout J L, Freeman G A, Lehrman S N, Bolognesi D P, Broder S, Mitsuya H and Barry D W 1986 Phosphorylation of 3'-azido-3'-deoxythymidine and selective interaction of the 5'-triphosphate with human immunodeficiency virus reverse transcriptase; *Proc. Natl. Acad. Sci., USA* **83** 8333–8337

Gallo R C, Salahuddin S Z, Popovic M, Shearer G M, Kaplan M, Haynes B F, Palker T J, Redfield R, Oleske J, Safai B, White G, Foster P and Markham P D 1984 Frequent detection and isolation of cytopathic retrovirus (HTLV-III) from patients with AIDS and at risk for AIDS; *Science* **224** 500–503

Herzyk P, Beveridge A and Neidle S 1987 Conformational properties of 3'-azido-3'-deoxy-thymidine (AZT): An inhibitor of HIV transcriptase; *Biochem. Biophys. Res. Commun.* **145** 1356–1361

Jordan F, Gilbert M, Malrieu J P and Pincelli U 1969 Localized bond orbitals and the correlation problems IV. Stability of the perturbation energies with respect to bond hybridization and polarity; *Theor. Chim. Acta* **15** 211–224

Kolata G 1987 Imminent marketing of AZT raises problems; *Science* **235** 1462–1463

Kulkarni V M, Vasantkumar N, Saran A and Govil G 1979 Structure and function of propranolol: A β-adrenergic blocking drug; *Int. J. Quantum Chem. Quantum Biol. Symp.* **6** 153–170

Lapatto R, Blundell T, Hemings A, Overington J, Wilderspin A, Wood S, Merson J R, Whittle P J, Danley D E, Geoghegan K F, Hawrylik S J, Lee S E, Scheld K G and Hobart P M 1989 X-ray analysis of HIV-1 proteinase at 2·7 Å resolution confirms structural homology among retroviral enzymes; *Nature (London)* **342** 299–302

Malim M H, Hauber J, Le S Y, Maizel J V and Cullen B R 1989 The HIV-1 rev transactivator acts through a structured target sequence to activate nuclear export of unspliced viral mRNA; *Nature (London)* **338** 254–257

Mitra C and Saran A 1978 Molecular orbital studies on the structure of nucleoside analogs II. Conformation of 6-azapyrimidine nucleosides; *Biochim. Biophys. Acta* **518** 193–204

Mitsuya H, Weinhold K J, Furman P A, St. Claire M H, Lehrman S N, Gallo R C, Bolognesi D, Barry D W and Broder S 1985 3'-azido-3'-deoxythymidine (BWA 5090): An antiviral agent that inhibits the infectivity and cytophathic effect of human T-lympotropic virus type III lymphadenopathy-associated virus in *vitro*; *Proc. Natl. Acad. Sci. USA* **82** 7096–7100

Mitsuya H and Broder S 1987 Strategies for antiviral therapy in AIDS; *Nature (London)* **325** 773–778

Ono K, Ogasawara M, Iwata Y, Nakane H, Fujii T, Sawai K and Saneyoshi M 1986 Inhibition of reverse transcriptase activity by 2'-3'-dideoxythymidine 5'-triphosphate and its derivatives modified on the 3'-position; *Biochem. Biophys. Res. Commun.* **140** 498–507

Pang S, Kayanagi Y, Miles S, Wiley C, Vinters H V and Chen I S Y 1990 High levels of unintegrated HIV-1 DNA in brain tissue of AIDS dementia patients; *Nature (London)* **343** 82–89

crystal structure of 3'-azido-3'-deoxy thymidine (AZT), an antiviral agent that inhibits HIV reverse transcriptase; *Biochem. Biophys. Rev. Commun.* **152** 351–358

Patnaik L N and Saran A 1984 Molecular orbital studies on nucleoside antibiotics VII. Conformation of 2'-amino-2'-deoxyguanosine; *J. Biol. Phys.* **12** 12–16

Pullman B and Saran A 1976 Quantum mechanical studies on the conformation of nucleic acids and their constituents; *Nucleic Acid Res. Mol. Biol.* **18** 215–322

Saran A 1981 Conformation of nucleoside antibiotics; *Int. J. Quantum Chem.* **20** 439–447

Saran A 1987 Nucleoside antibiotics: Conformation and biological activity; *Proc. Indian Acad. Sci. (Chem. Sci.)* **99** 119–128

Saran A 1988 Molecular orbital studies of nucleoside antibiotics IX: Conformation of 5-ethynyl and 5-vinyl-2'-deoxycytidines; *J. Mol. Struct. (Theochem.)* **179** 215–223

Saran A 1989 Correlation between the conformation of nucleoside antibiotics and their biological activity; *Int. J. Quantum Chem.* **35** 193–203

Saran A and Chatterjee C L 1980a Molecular orbital studies on nucleoside antibiotics III. Conformation of toyocamycin and sangivamycin; *Int. J. Quantum Chem. Quantum Biol. Symp.* **7** 123–136

Saran A and Chatterjee C L 1980b Molecular orbital studies on the structure of nucleoside analogs III. Conformation of 3-deazapyrimidine nucleosides; *Biochim. Biophys. Acta* **607** 490–502

Saran A and Chatterjee C L 1984 Molecular orbital studies on the structure of nucleoside analogs IV. Conformation of 3-deazapurine nucleosides; *Int. J. Quantum Chem.* **25** 743–752

Saran A and Mitra C 1979 Molecular orbital studies on nucleoside antibiotics II. Conformation virazole, tubercidin and conformycin; *Indian J. Biochem. Biophys.* **16** 304–309

Saran A, Mitra C K and Pullman B 1978 Molecular orbital studies on the structure of nucleoside analogs I. Conformation of 8-azapurine nucleosides; *Biochim. Biophys. Acta* **517** 255–264

Saran A and Patnaik L N 1981 Molecular orbital studies on nucleoside antibiotics IV. Conformation of 3'-deoxyadenosine (Cordycepin) and 3'-amino-3'-deoxyadenosine; *Int. J. Quantum Chem.* **20** 357–367

Saran A and Patnaik L N 1982 Molecular orbital studies on nucleoside antibiotics VI. Conformation of 5-vinyl- and 5-ethynyl-2'-deoxyuridines; *Int. J. Quantum Chem. Quantum Biol. Symp.* **9** 247–257

Saran A and Patnaik L N 1986 Molecular orbital studies on nucleoside antibiotics VIII. Conformation of 5-substituted uridines; *Int. J. Quantum Chem. Quantum Biol. Symp.* **13** 121–131

Saran A., Pullman B and Perahia D 1972 Molecular orbital calculations on the conformation of nucleic acids and their constituents IV. Conformation about the exocylic C(4')-C(5') bond; *Biochim. Biophys. Acta* **287** 211–231

St. Claire M H, Weinhold K, Richards C A, Barry D W and Furman P A 1985 *Proc. of 25th Interscience Conference on Antimicrobial Agents and Chemotherapy* (Washington D C: Am. Soc. Microbiol.) pp 439–441

Swapna G V T, Jagannadh B, Gurjar M K and Kunwar A C 1989 NMR investigation on the structure and conformation of 3'-azido-2'-3'-dideoxyribosylthymine (AZT), an inhibitor of the HIV (AIDS Virus); *Biochem. Biophys. Res. Commun.* **164** 1086–1092

Vogel J, Hinrichs S H, Reynolds R K, Luciw P A and Jay G 1988 The HIV tat gene induces dermal lesions resembling Kaposi's sarcoma in transgenic mice; *Nature (London)* **335** 606–611

Yarchoan R and Broder S 1987 Development of antiretroviral therapy of acquired immunodeficiency syndrome and related disorders: A progress report; *N. Engl. J. Med.* **316** 557–564

Yarchoan R, Mitsuya H and Broder S 1988 AIDS therapies; *Sci. Am.* **259** 88–97

Haemoglobin: A scavenger of superoxide radical

ASOKE MAL, ANURADHA NANDI and I B CHATTERJEE*

Department of Biochemistry, University College of Science, 35, Ballygunge Circular Road, Calcutta 700 019, India

Abstract. Superoxide is continuously generated in the erythrocytes, and oxyhaemoglobin from different animals including fish, amphibians, reptiles, birds, flying mammals, mammals and human beings acts as a scavenger of superoxide. The approximate rate constants of the reaction between superoxide and oxyhaemoglobin of different animals are $0.32–1.6 \times 10^7 \, M^{-1} \, s^{-1}$. Results obtained with anion ligands like CN^- and N_3^- indicate that superoxide preferentially reacts with anion ligand-bound deoxyhaemoglobin. Carbonmonoxyhaemoglobin and methaemoglobin are ineffective. Work with photochemically generated oxyradical indicate that oxyhaemoglobin may also act as a scavenger of singlet oxygen. The rate constant of the reaction between superoxide and human oxyhaemoglobin is $K_{app} = 6.5 \times 10^6 \, M^{-1} \, s^{-1}$, which is about three orders less than K_{SOD} ($2 \times 10^9 \, M^{-1} \, s^{-1}$). Thus, in the erythrocytes, oxyhaemoglobin would appear to act as a second line of defence. Oxyhaemoglobin appears to be as effective as superoxide dismutase for scavenging superoxide in the erythrocytes.

Keywords. Oxyhaemoglobin; deoxyhaemoglobin; methaemoglobin; ligand; superoxide; superoxide dismutase; erythrocyte.

1. Introduction

In our study on the assay of superoxide dismutase (SOD) activity in the Tsuchihasi extract of human erythrocyte haemolysate by the pyrogallol autoxidation method (Nandi and Chatterjee 1988), we observed that the SOD activity was about 1000–1100 units per g haemoglobin (Hb). On the other hand, when the untreated whole erythrocyte haemolysate was used, the apparent SOD activity was about 6000–8000 units per g Hb. Later, we observed that this high superoxide (O_2^-) scavenging activity of the whole haemolysate was present in the oxyhaemoglobin (HbO_2) isolated from the haemolysate by ion-exchange chromatography over phospho-cellulose (Mal and Chatterjee 1991). The O_2^- scavenging activity was also observed in HbO_2 isolated from erythrocytes of other animals including fish, amphibians, reptiles, birds and mammals. Scarpa *et al* (1984) have shown that O_2^- is continuously generated in human erythrocytes. Demma and Salhany (1977) demonstrated that O_2^- produced by photolytic dissociation of HbO_2 reattacks HbO_2 to produce methaemoglobin (MetHb) and H_2O_2. That O_2^- reacts with HbO_2 has also been shown by Sutton *et al* (1976), Lynch *et al* (1977) and Watkins *et al* (1985). We have also demonstrated that O_2^- produced during autoxidation of HbO_2, apparently by dissociation of $Hb^{3+}O_2^-$, reattacks HbO_2 to produce MetHb (Mal and Chatterjee 1991). In this communication, we present evidence indicating that HbO_2 is a

---

*Corresponding author.

bound deoxyhaemoglobin is the preferential form which reacts with O_2^-.

2. Materials and methods

2.1 *Chemicals*

Cellulose phosphate P-11 was purchased from Whatman, England. Xanthine, xanthine oxidase, bovine erythrocyte superoxide dismutase and riboflavin were obtained from Sigma Chemical Company, St. Louis, Mo, USA. Catalase (free of SOD) was purchased from the CSIR Centre for Biochemicals, New Delhi. All other chemicals and reagents used were of analytical grade. All solutions were made with double distilled water.

2.2 *Isolation and estimation of HbO_2*

The procedure for the isolation and estimation of haemoglobin has been described earlier (Mal and Chatterjee 1991).

2.3 *Quantitative determination of HbO_2 and MetHb*

These were done according to the method described by Mal and Chatterjee 1991.

2.4 *Assay of erythrocyte SOD*

SOD activity of erythrocyte haemolysate was measured in the Tsuchihasi extract (Crapo *et al* 1978) by the pyrogallol autoxidation method (Nandi and Chatterjee 1988) as described below.

2.5 *Assay of O_2^- scavenging activity of HbO_2*

This was done by the pyrogallol autoxidation method (Nandi and Chatterjee 1988). The assay system contained 1 mM DTPA, 40 μg catalase, 50 mM air-equilibrated Tris-cacodylate buffer, pH 8·5, and HbO_2 solution as needed, in a final volume of 2 ml. The reaction was initiated by the addition of 100 μl of freshly prepared 2·6 mM pyrogallol solution in 10 mM HCl to attain a final concentration of pyrogallol of 0·13 mM in the assay mixture. One unit of O_2^- scavenging activity of HbO_2 represents the amount of HbO_2 required to produce 50% inhibition in 3 ml assay mixture.

Results

Oxyhaemoglobin isolated from erythrocytes of different animals including fish, amphibians, reptiles, birds, flying mammals, mammals and human beings acts as a scavenger of O_2^- (table 1). The O_2^- scavenging activity has been assayed by the pyrogallol autoxidation method (Nandi and Chatterjee 1988). At the pH of the

Animal	Activity in unit/g Hb		
	Tsuchihasi extract (SOD)	HbO$_2$	$K_{app} \times 10^7 \, M^{-1} \, s^{-1}$
Fish			
Labeo rohita (6)	1,072[a]	6,525 ± 900[b]	0·34
Amphibians			
Toad[c] (*Bufo melanostictus*) (18)	1,144	13,452 ± 2000	1·60
Frog[c] (*Rana tigrina*) (18)	1,100	10,600 ± 2000	0·90
Reptiles			
Blood sucker[c] (*Caloter versicolor*) (18)	1,067	7,214 ± 950	0·56
Anjani (*Mabuya carinata*) (8)	1,050	10,884 ± 1000	1·28
Turtle (*Lissemys punctata*) (4)	1,014	4,471 ± 500	0·36
Common Indian monitor (*Varanus monitor*) (4)	1,050	8,071 ± 1000	0·68
Birds			
Pigeon (4)	1,007	6,731 ± 600	0·45
Chicken (4)	1,060	10,506 ± 1100	0·95
Flying mammals			
Indian fruit bat (4)	3,360	5,346 ± 500	0·32
Mammals			
Rabbit (4)	1,012	5,178 ± 450	0·47
Rat (12)	1,020	5,750 ± 550	0·48
Guinea pig (6)	1,550	5,102 ± 500	0·44
Goat (4)	1,029	5,146 ± 550	0·50
Cattle (4)	1,026	5,036 ± 400	0·39
Human (4)	1,074	7,692 ± 800	0·65

One unit represents the amount of HbO$_2$ required to produce 50% inhibition of the autoxidation of pyrogallol.

O$_2^-$ scavenging activity was assayed by the pyrogallol autoxidation method (Nandi and Chatterjee 1988). The assay system contained 1 mM DTPA, 40 μg catalase, 50 mM air-equilibrated Tris-cacodylate buffer, pH 8·5, and Hb solution and Tsuchihasi extract as needed, in a final volume of 2 ml. The reaction was initiated by the addition of 100 μl of freshly prepared 2·6 mM pyrogallol solution in 10 mM HCl to attain a final concentration of pyrogallol of 0·13 mM in the assay mixture. The details of the procedure are described elsewhere (Nandi and Chatterjee 1988). The final concentration of Hb in the assay mixture varied from 0·2 to 1 μM depending on the O$_2^-$ scavenging activity.

Numbers in parentheses indicate the number of animals used.

[a]Average values.

[b]Mean ± SD

[c]Each blood sample was pooled from 3 animals.

assay system used (pH 8·5), the autoxidation of pyrogallol is essentially fully inhibited by SOD and hence this method can be used as an effective assay for the determination of O$_2^-$ scavenging activity (Nandi and Chatterjee 1988; Màrklund and Marklund 1974; McCord *et al* 1977). The O$_2^-$ scavenging activity cannot be assayed by the xanthine-xanthine oxidase ferricytochrome c (cyt c^{3+}) method (McCord and Fridovich 1969) because as indicated in the previous paper (Mal and

Chatterjee 1991), HbO_2 directly reduces cyt c^{3+} to cyt c^{2+} at a very fast rate and about 79% of this reduction is insensitive to SOD. The direct reaction between HbO_2 and cyt c^{3+} has also been shown by Tomoda *et al* (1980). Also, the O_2^- scavenging activity of HbO_2 cannot be assayed by xanthine-xanthine oxidase-nitroblue tetrazolium (NBT) method (Beauchamp and Fridovich 1971) because we have observed that NBT directly oxidizes HbO_2 to MetHb. In the 2 ml assay system containing $2\,\mu M$ HbO_2, $0.1\,mM$ EDTA in $50\,mM$ potassium phosphate buffer, pH 6.8, $0.25\,\mu M$ NBT produced 15% MetHb in 10 min at 37°C.

In table 1 the O_2^- scavenging activities of HbO_2 isolated from different animals have been expressed in unit per g Hb. Since one unit of SOD also represents the amount of SOD needed to produce 50% inhibition of the autoxidation of pyrogallol, one unit of O_2^- scavenging activity of HbO_2 is apparently equivalent to one unit of SOD. Since the amount of SOD needed to produce 50% inhibition in the pyrogallol autoxidation system is about half of that needed to produce 50% inhibition in the xanthine-xanthine oxidase—ferricytochrome c system (Nandi and Chatterjee 1988), one unit of SOD in the pyrogallol system may be taken to be 165 ng of SOD. This is approximately equivalent to 2.58×10^{-9} M. Taking K_{SOD} to be equal to $2 \times 10^9\,M^{-1}\,s^{-1}$ (McCord *et al* 1977), the approximate rate constants of the reaction between HbO_2 and O_2^- in the pyrogallol system have been calculated for HbO_2 of different animals to be $0.32–1.6 \times 10^7\,M^{-1}\,s^{-1}$ (table 1).

Figure 1 shows the effect of variation of concentration of the human HbO_2 on the O_2^- scavenging activity. The graph is linear for about 24 to 75% inhibition. The O_2^- scavenging activities of HbO_2 and SOD are additive. When 0.5 unit equivalent of HbO_2 is added to the pyrogallol autoxidation system containing 0.5 unit of SOD, 50% inhibition of the autoxidation is obtained. When one unit equivalent of HbO_2 is added to the pyrogallol system containing one unit of SOD, the
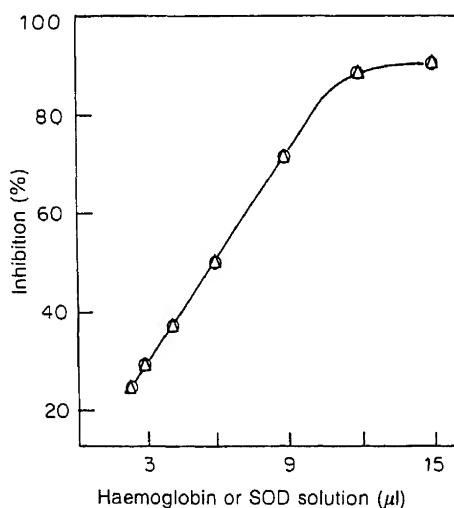
Figure 1. Per cent inhibition as a function of concentration in human HbO_2 solution/pure SOD solution.

O_2^- scavenging activity was assayed by the pyrogallol autoxidation method (Nandi and Chatterjee 1988). The detailed procedure is described under 'materials and methods'. ($\triangle$) and ($\bigcirc$) represent HbO_2 solution and SOD solution respectively.

system. In contrast to the erythrocyte SOD, the O_2^- scavenging property of HbO_2 is completely lost on treatment with heat (5 min at 65°), SDS (2%), H_2O_2 (50 μM) and chloroform-methanol mixture (Tsuchihasi procedure).

Figure 2 shows that in the pyrogallol autoxidation system, human HbO_2 undergoes oxidation to MetHb. An adequate amount of catalase is present in the system to prevent any oxidation of HbO_2 by H_2O_2. The formation of MetHb is completely inhibited in the presence of excess SOD (figure 2) indicating that in the pyrogallol autoxidation system the oxidation of HbO_2 is mediated by O_2^-. Pyrogallol or preoxidized pyrogallol does not oxidize HbO_2 to MetHb. At pH 6 autoxidation of pyrogallol is very slow and there is practically neither production of O_2^- nor oxidation of HbO_2.

Figure 3 shows that photochemically-generated reactive oxygen species oxidizes human HbO_2 to MetHb very fast as evidenced by the increase of A_{630} and decrease of A_{575}. However, this production of MetHb is not inhibited by SOD (15 μg). This would indicate that the active species is probably singlet oxygen rather than O_2^-, because irradiation of riboflavin is known to produce singlet oxygen (Hodgson and Fridovich 1976; Michelson 1977; Foote 1982). It was also observed that 2 mM NaN_3, a scavenger of singlet oxygen (Klebanoff and Rosen 1979), completely inhibited the oxidation of HbO_2 in the photochemical system.

Figure 4 shows that when HbO_2 is allowed to react with O_2^- generated in the xanthine-xanthine oxidase system, no MetHb is formed. However, MetHb is produced when HbO_2 is added to the xanthine-xanthine oxidase system containing 2 mM KCN (figure 4). A large excess of catalase was present to scavenge the H_2O_2 produced, which would otherwise oxidize HbO_2 to MetHb. The amount of catalase
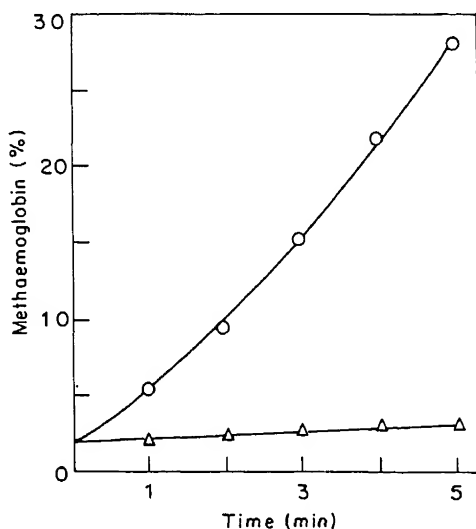
Figure 2. Oxidation of human HbO_2 to MetHb in the pyrogallol autoxidation method. Reaction mixture was the same as indicated in figure 1 except that the concentration of HbO_2 was 2 μM. (O) represents the oxidation of HbO_2 in the absence of SOD and ($\triangle$) represents the oxidation in the presence of SOD (10 μg).
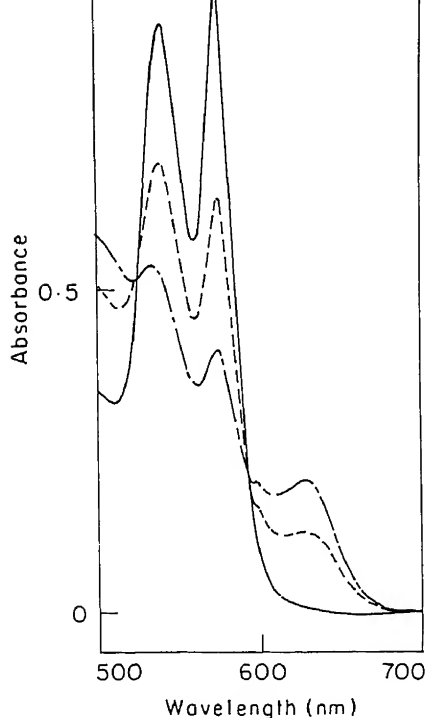
Figure 3. Spectral changes obtained during the oxidation of human HbO_2 to MetHb in the photochemical system.

Two ml reaction mixture contained $2\,\mu M$ HbO_2, $50\,mM$ potassium phosphate buffer, pH 6·8, 0·1 mM EDTA, catalase (80 μg), 1 μM riboflavin. The reaction mixture was illuminated 6 cm away by a 40 W fluorescence lamp. Spectra were obtained at 0, 5 and 10 min elapsed time.

used was over and above that which could be inhibited by CN^-. This would indicate that O_2^- reacts with $HbCN^-$. In other words, O_2^- reacts with anion ligand-bound deoxyhaemoglobin rather than HbO_2. Figure 5 shows the spectral changes obtained during the oxidation of $HbCN^-$ in the pyrogallol autoxidation system. That O_2^- reacts with anion ligand-bound deoxyhaemoglobin is also confirmed by the observation that in the presence of a large excess of catalase, HbN_3^- reacts with O_2^- to produce MetHb (figure 6). Figure 7 shows that oxidation of HbN_3^- is a function of O_2^- concentration. The rate of oxidation increases with the increased concentration of O_2^-.

While $HbCN^-$ and HbN_3^- react readily with O_2^-, HbCO is completely inactive both in the pyrogallol autoxidation system and the xanthine-xanthine oxidase system.

The product of the reaction of O_2^- with HbO_2 is MetHb. However, MetHb is ineffective as a scavenger of O_2^- either in the pyrogallol system or in the xanthine-xanthine oxidase system. We have observed that when MetHb (2–5 μM) from different sources (human bovine, toad) is allowed to react with O_2^- (4 nmol/min,
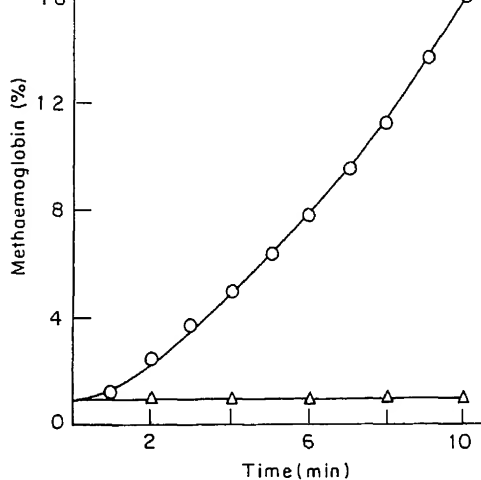
Figure 4. Oxidation of human HbO_2 by O_2^-

Two ml reaction Mixture contained $2\,\mu M$ HbO_2 preincubated with 2 mM KCN when needed, 50 mM potassium phosphate buffer, pH 7·4, 0·1 mM EDTA, catalase (100 μg), 0·4 mM xanthine and 4·5 mU (5 μl) xanthine oxidase. The amount of catalase was more than sufficient to scavenge the H_2O_2 produced in the presence of 2 mM KCN. The amount of O_2^- produced in this mixture was 2 nmol/min as determined by the reduction of ferricytochrome c (McCord and Fridovich 1969). ($\triangle$) represents oxidation of HbO_2 in the absence of KCN and ($\bigcirc$) represents oxidation in the presence of 2 mM KCN.

ed by the xanthine-xanthine oxidase system) there is no decrease of A_{630} or
e of A_{575}, indicating that MetHb does not react with O_2^-. However, the O_2^-
ging property is regained when MetHb is reduced to HbO_2 with sodium
ite (100 $\mu g/ml$ for 2 μM MetHb). Figure 8 shows that MetHb is also reduced
physiological concentration of ascorbic acid. The rate of reduction of MetHb
rbic acid is $K_{app} = 2\cdot64\ \text{min}^{-1}$.

cussion

tion, while providing numerous biochemical advantages, imposes the need
ra protection against free radical toxicity. This is needed at the very first
t when Hb binds O_2 in the erythrocytes, because part of the HbO_2
ates into MetHb and O_2^- (Misra and Fridovich 1972; Mal and Chatterjee
esulting in a continuous generation of O_2^- in the erythrocytes (Scarpa et al
The rate of formation of O_2^- in the erythrocytes has been calculated to be
0^{-8} M s^{-1} (Mal and Chatterjee 1991). This O_2^-, unless scavenged properly,
lead to irreversible oxidative damage of the red cells (Fridovich 1972, 1979;
and Fridovich 1977). There are present in the erythrocytes, scavengers of
mely, SOD (about $1\cdot63 \times 10^{-6}$ M; $K_{SOD} = 2 \times 10^9$ M^{-1} s^{-1}) and ascorbic
out 4×10^{-5} M; $K_{AH_2} = 8\cdot2 \times 10^7$ M^{-1} s^{-1}) (Nandi and Chatterjee 1987) as
scavengers of H_2O_2, namely, catalase and glutathione peroxidase. However,
sence of SOD and ascorbic acid need not necessarily mean that these
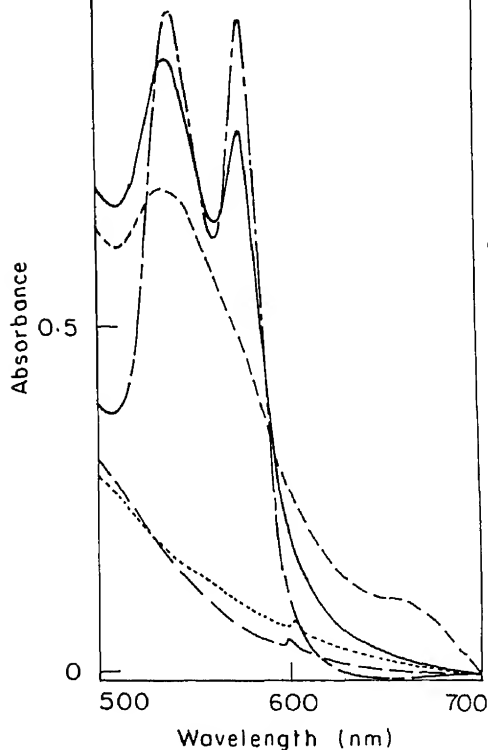
Figure 5. Spectral changes obtained during the oxidation of human HbO_2 in the pyrogallol autoxidation system in the presence of KCN.

Reaction mixture was the same as in figure 1 except that the concentration of HbO_2 was $2\,\mu M$, KCN $2\,mM$ and catalase $100\,\mu g$. Spectra were obtained at 0, 5 and 10 min elapsed time. Bottom lines represent the spectral changes of only pyrogallol in the absence of HbO_2 at 0 min and 10 min.
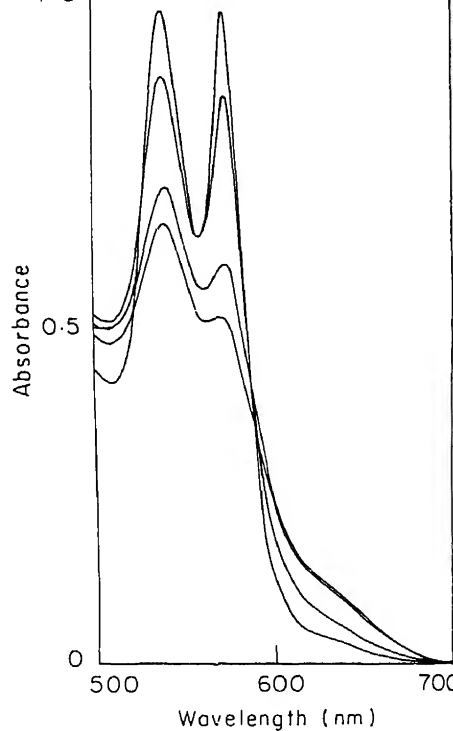
Figure 6. Spectral changes obtained during the oxidation of human HbO_2 by O_2^- generated in the xanthine-xanthine oxidase system in the presence of NaN_3.

Reaction mixture was the same as in figure 4 except that HbO_2 was preincubated with $2\,mM$ NaN_3 when needed instead of $2\,mM$ KCN. The amount of catalase was more than sufficient to scavenge the H_2O_2 produced in the presence of $2\,mM$ NaN_3. Spectra were obtained at 0, 5, 15 and 30 min elapsed time.

scavengers succeed totally. A fraction of the O_2^- generated in the erythrocytes may always escape and, if they do, they will cause oxidative damage to the red cells. Evidences presented in this communication indicate that in addition to SOD and ascorbic acid, HbO_2 is also a potential scavenger of O_2^-. The rate constant of the reaction between human HbO_2 and O_2^- in the pyrogallol system is approximately $6.5 \times 10^6\,M^{-1}\,s^{-1}$. Results obtained with $HbCN^-$ and HbN_3^- indicate that O_2^- preferentially reacts with anion ligand-bound deoxyhaemoglobin (HbL^-) rather than HbO_2. In the pyrogallol system also, pyrogallol presumably acts as an anion ligand to Hb. It has been shown that the hydrophobic cluster on the side of E_7 (distal histidine), which accommodates the heme-linked O_2, contains enough room beneath His E_7 for the entry of a heme ligand as large as n-butylisocyanide (Perutz 1979). However, under physiological conditions, only Cl^-, H_2O and OH^- appear to serve as anion ligands (Watkins et al 1985).

The reaction of HbL^- with O_2^- produces MetHb. However, MetHb is ineffective
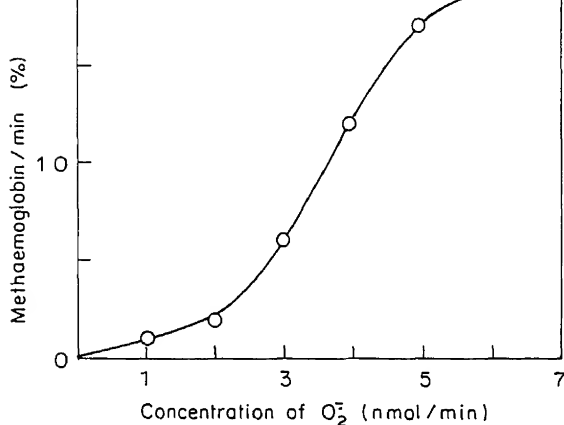
Figure 7. Oxidation of human HbO_2 as a function of O_2^- concentration in the presence of NaN_3.

Reaction mixture was the same as in figure 6 except that the increased concentration of O_2^- was obtained by using an increased amount of xanthine oxidase (5–15 μl).
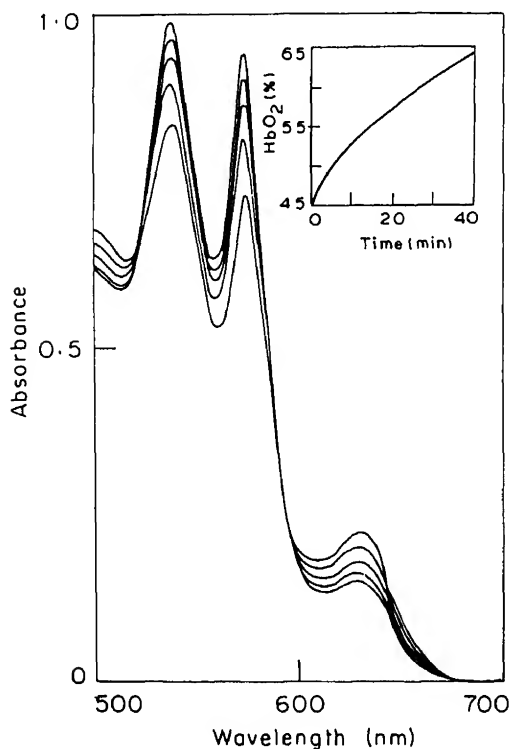
Figure 8. Spectral changes obtained during the reduction of human MetHb in the presence of ascorbic acid

Two ml reaction mixture contained 1·5 μM human MetHb, 50 mM potassium phosphate buffer, pH 6·8, 0·1 mM ascorbic acid and catalase (80 μg). The reaction was carried out at 37° using a temperature controlled cell holder. Spectra were obtained at 0, 10, 20, 30 and 40 min elapsed time. Inset of the figure represents the rate of reduction of MetHb.

HbO$_2$. *In vivo*, this reduction of MetHb is accomplished by erythrocyte NADH MetHb reductase as well as ascorbic acid (see figure 8) to achieve a steady state HbO$_2$ level, which is 0·5 to 1% in normal blood (Rodkey and O'Neal, 1974).

It has already been shown that the rate constant of the reaction between O$_2^-$ and human HbO$_2$ is $K_{app} = 6·5 \times 10^6$ M^{-1} s^{-1}, which is about three orders smaller than that of K_{SOD} (2×10^9 M^{-1} s^{-1}). Thus, in the erythrocyte, HbO$_2$ would appear to act as a second line of defence. However, the concentration of HbO$_2$ in the erythrocyte is approximately $4·65 \times 10^{-3}$ M (Mal and Chatterjee 1991) which is about three orders greater than that of SOD ($1·6 \times 10^{-6}$ M). Thus, considering both the rate constants and the concentrations, HbO$_2$ appears to be as effective as SOD for scavenging O$_2^-$ in the erythrocytes.

Acknowledgements

References

Beauchamp C and Fridovich I 1971 Superoxide dismutase: Improved assay and an assay applicable to acrylamide gel; *Anal. Biochem.* **44** 276–287

Crapo J D, McCord J M and Fridovich I 1978 Preparation and assay of superoxide dismutases; *Methods Enzymol.* **53** 382–393

Demma L S and Salhany J M 1977 Direct generation of superoxide anions by flash photolysis of human oxyhaemoglobin; *J. Biol. Chem.* **252** 1226–1231

Foote C S 1982 Light, oxygen and toxicity; in *Pathology of oxygen* (ed.) A P Autor (New York: Academic Press) pp 21–42

Fridovich I 1972 Superoxide radical and superoxide dismutase; *Acc. Chem. Res.* **5** 321–326

Fridovich I 1979 *Oxygen free radicals and tissue damage*, Ciba Foundation Symposium 65 (New Series) (Amsterdam: Excerpta Medica) pp 77–93

Hodgson E K and Fridovich I 1976 The mechanism of the activity dependent luminescence of xanthine oxidase; *Arch. Biochem. Biophys.* **172** 202–205

Kellog E W III and Fridovich I 1977 Liposome oxidation and erythrocyte lysis by enzymically generated superoxide and hydrogen peroxide; *J. Biol. Chem.* **252** 6721–6728

Klebanoff S J and Rosen H 1979 *Oxygen free radicals and tissue damage*, Ciba Foundation Symposium 65 (New Series) (Amsterdam: Excerpta Medica) pp 263–272

Lynch R E, Thomas J E and Lee G R 1977 Inhibition of methemoglobin formation from purified oxyhemoglobin by superoxide dismutase; *Biochemistry* **16** 4563–4567

Mal A and Chatterjee I B 1991 Mechanism of autoxidation of oxyhemoglobin; *J. Biosci.* **16** 55–70

Marklund S and Marklund G 1974 Involvement of the superoxide anion radical in the autoxidation of pyrogallol and a convenient assay for superoxide dismutase; *Eur. J. Biochem.* **47** 469–474

McCord J M, Crapo J D and Fridovich I 1977 Superoxide dismutase assays: A review of methodology; in *Superoxide and superoxide dismutase* (eds) A M Michelson, J M McCord and I Fridovich (New York: Academic Press) pp 11–17

McCord J M and Fridovich I 1969 Superoxide dismutase: An enzymic function of erythrocuprein (hemocuprein); *J. Biol. Chem.* **244** 6049–6055

Michelson A M 1977 Toxicity of superoxide radical anions; in *Superoxide and superoxide dismutase* (eds) A M Michelson, J M McCord and I Fridovich (New York: Academic Press) pp 245–255

Misra H P and Fridovich I 1972 The generation of superoxide radical during the autoxidation of hemoglobin; *J. Biol. Chem.* **247** 6960–6962

 and Chatterjee I B 1988 Assay of superoxide dismutase activity in animal tissues; *J. Biosci.* **13** 315

M F 1979 Regulation of oxygen affinity of hemoglobin: Influence of structure of the globin on the iron; *Annu. Rev. Biochem.* **48** 327–386

F L and O'Neal J D 1974 Effects of carboxyhemoglobin on the determination of methemoglobin ood; *Biochem. Med.* **9** 261

M, Viglino P, Contri D and Rigo A 1984 Generation of superoxide ion in the human red blood lysates; *J. Biol. Chem.* **259** 10657–10659

H C, Robert P B and Winterbourn C C 1976 The rate of reaction of superoxide radical ion with iaemoglobin and methaemoglobin; *Biochem. J.* **155** 503–510

a A, Tsuji A and Yoneyama Y 1980 Mechanism of hemoglobin oxidation by ferricytochrome c er aerobic and anaerobic conditions; *J. Biol. Chem.* **255** 7978–7983

s J A, Kawanishi S and Caughey W S 1985 Autoxidation reactions of hemoglobin A free from r red cell components: A minimal mechanism; *Biochem. Biophys. Res. Commun.* **132** 742–748.

Mechanism of autoxidation of oxyhaemoglobin

ASOKE MAL and I B CHATTERJEE*

Department of Biochemistry, University College of Science, 35, Ballygunge Circular Road, Calcutta 700 019, India

Abstract. Oxyhaemoglobins from erythrocytes of different animals including fish, amphibians, reptiles, birds, mammals and human beings have been isolated by ion-exchange chromatography over phosphocellulose and the comparative rates of autoxidation of oxyhaemoglobin studied. The mechanism of autoxidation *in vitro* has been elucidated using toad as well as human oxyhaemoglobin. Autoxidation is markedly inhibited by carbon monoxide as well as by anion ligands, namely, potassium cyanide, sodium azide and potassium thiocyanate. The inhibition by anions is in the same order as their strength as nucleophiles, indicating that it is the oxyhaemoglobin and not the ligand-bound deoxy species which undergoes autoxidation. The structure of oxyhaemoglobin is considered to be mainly $Hb^{3+}O_2^-$ and determination of the rate of autoxidation with or without using superoxide dismutase and catalase indicates that the initial process of autoxidation takes place by dissociation of $Hb^{3+}O_2^-$ to methaemoglobin and superoxide to the extent of 24%. The superoxide thus produced reattacks oxyhaemoglobin to produce further methaemoglobin and hydrogen peroxide. H_2O_2 is a major oxidant of oxyhaemoglobin producing methaemoglobin to the extent of 53%. A tentative mechanism of autoxidation showing the sequence of reactions involving superoxide, H_2O_2 and $OH^.$ has been presented.

Keywords. Oxyhaemoglobin; methaemoglobin; autoxidation; superoxide; superoxide dismutase; catalase; erythrocytes; animals; phyla.

1. Introduction

Superoxide radical (O_2^-) is continuously generated in human erythrocytes (Scarpa *et al* 1984). Several authors have produced evidence that this production of O_2^- can take place during autoxidation of oxyhaemoglobin (HbO_2) to methaemoglobin (MetHb) under certain conditions which can also occur *in vivo* (Misra and Fridovich 1972; Wever *et al* 1973; Wallace *et al* 1974a; Brunori *et al* 1975; Gotoh and Shikama 1976; Lynch *et al* 1976; Winterbourn *et al* 1976). The concentration of MetHb in normal human erythrocytes at any given moment is about 0·5 to 1% (Salvati and Tentori 1981). Apparently, the MetHb content results from an equilibrium between the rate of formation of MetHb and the rate of reduction to haemoglobin (Hb). Experiments on patients with hereditary methaemoglobinemia indicated the rate of MetHb production to be approximately 3% per day (Jaffe and Neumann 1964). While MetHb can lead to haemichrome formation, Heinz body formation and other changes, O_2^- has been implicated in lipid peroxidation resulting in irreversible damage and lysis of red cell membranes (Fridovich 1972, 1979; Kellog and Fridovich 1977). Since autoxidation of HbO_2 has profound influence on the normal

---

*Corresponding author.

autoxidation is extremely important.

The structure of HbO_2 has been considered to be mainly $Hb^{3+}O_2^-$ (Viale *et al* 1964; Weiss 1964; Peisach *et al* 1968; Misra and Fridovich 1972; Wittenberg *et al* 1970; Yamamoto *et al* 1973; Peisach 1975). Using shark HbO_2, Misra and Fridovich (1972) observed that direct dissociation of $Hb^{3+}O_2^-$ could account for the slow autoxidation of HbO_2 to MetHb and O_2^-. However, the detailed mechanism of autoxidation was not studied, probably because shark HbO_2 was unstable and the rate of autoxidation of shark HbO_2 was too fast (Misra and Fridovich 1972).

On the other hand, using human HbO_2 Wallace *et al* (1982) considered that direct dissociation of HbO_2 to MetHb and O_2^- was not probable. In studies on the effects of strong anionic nucleophiles, not normally found in red cells, namely, potassium cyanide (CN^-), sodium azide (N_3^-) and potassium thiocyanate (SCN^-), these authors proposed that the anion ligands were promoters of the autoxidation of haemoglobin and that the anions were increasingly effective as promoters in the same order as their strength as nucleophiles. These authors considered that the anion complex of haemoglobin (HbL^-) or a complex of protonated deoxy-heamoglobin species with anion $[Hb(H^+)(L^-)]$ reacted with molecular oxygen to produce O_2^- (Wallace *et al* 1982; Watkins *et al* 1985). In other words, these authors proposed that it was the ligand-bound deoxy rather than the oxy species which underwent autoxidation to MetHb. However, Wallace *et al* (1982) did not produce data of control experiments showing the rate of autoxidation of HbO_2 in the absence of any added ligand compared to that obtained in the presence of CN^-, N_3^- or SCN^-. Moreover, the production of O_2^- by the reaction of HbL^- with molecular oxygen was assumed on the basis of simultaneous reduction of ferricytochrome c (cyt c^{3+}) during autoxidation of HbL^- to $MetHbL^-$. On the contrary, we have observed that cyt c^{3+} is directly reduced by HbO_2 at a very fast rate and that about 79% of this reduction of cyt c^{3+} is insensitive to superoxide dismutase (SOD). We have further observed that while CN^- and N_3^- significantly inhibit the autoxidation of HbO_2, these enhance the reduction of cyt c^{3+}. In earlier studies, Tomoda *et al* (1980) demonstrated that cyt c^{3+} oxidized both human deoxy- and oxyhaemoglobin to MetHb and that the rate of oxidation was directly proportional to the concentration of cyt c^{3+} used. The direct reaction between Hb and cyt c^{3+} has also been reported by others (Brown 1961; Wallace and Caughey 1979). Wu *et al* (1972) have shown that MbO_2 directly reduces cyt c^{3+}.

It would thus appear that the detailed mechanism of autoxidation of HbO_2 is not clear and remains controversial. We have therefore carried out systematic experiments bearing on the mechanism of autoxidation of HbO_2 and the results are presented in this paper.

2. Materials and methods

2.1 *Chemicals*

Cellulose phosphate P-11 was purchased from Whatman, England. Cooma-ssie brilliant blue R, acrylamide, bovine erythrocyte SOD, epinephrine and

tochrome c were obtained from Sigma Chemical Company, St. Louis, Mo,
Catalase (free of SOD) was purchased from the CSIR Centre for
emicals, New Delhi; 2-deoxyribose from SRL, India; heparin from Biological
d. (India) and bisacrylamide from Koch-Light Laboratories, England.
rioxamine was a gift from CIBA-GEIGY, Basel, Switzerland. All other
als and reagents used were of analytical grade. All solutions were made with
-distilled water.

Collection of blood

from toad (*Bufo melanostictus*), frog (*Rana tigrina*), blood sucker (*Caloter*
lor), anjani (*Mabuya carinata*), common Indian monitor (*Varanus monitor*),
Lissemys punctata), rat, guinea pig, rabbit and Indian fruit bat was obtained
diac puncture. Chicken and pigeon blood was obtained from the subclavian
ish blood was collected from the caudal vein. The blood of goat and cattle
btained from jugular vein and collected from the slaughter house. We are
ed to Dr D K Bhattacharyya, Bhoruka Research Centre for Hematology and
Transfusion, Calcutta, India for supplies of fresh human blood. Blood
s were collected in heparin (100 units for about 5 ml blood).

Haemoglobin

lls were sedimented by centrifugation and washed three times with 0·15 M
The buffy coat was aspirated with each wash. Packed washed red cells were
in 19 volumes of cold distilled water. The ghosts were sedimented by
ugation at 17,000 g for 20 min in a Hitachi automatic high speed refrigerated
uge, model SCR 20BA. After adjustment of pH at 6·8, 10 ml of the
atant was applied to a phosphocellulose column ($6 \times 1·5$ cm) previously
rated with 10 mM sodium phosphate buffer, pH 6·8. The column was washed
nes with equilibrated buffer. The adsorbed Hb was eluted with 0·5 M sodium
ate buffer, pH 6·8. The Hb fraction was collected in 2 ml of buffer. The
ry of Hb from the haemolysate was 50 to 60%. All steps in the purification of
m blood were performed at 0–6° without delay. The eluted Hb solution was
SOD as assayed by polyacrylamide gel electrophoresis (Beauchamp and
ich 1971) and catalase as assayed by determining the rate of decrease in
ance at 240 nm of 22·5 mM H_2O_2 (Lynch *et al* 1977). The purity of the Hb
etermined by sodium dodecyl sulphate-polyacrylamide discontinuous gel
phoresis according to the method of Laemmli (1970). Hb eluted from the
nocellulose column was used without delay and without any chemical
ent for subsequent studies. Hb was estimated by the modified method of
in (Richteric 1969).

Determination of the rate of autoxidation of HbO₂ at 37°

te of autoxidation of HbO_2 was determined at 37° by measuring the decrease
ratio of absorbance at 575 : 500 nm (Salvati *et al* 1969), increase of absorbance
nm and by recording the change of visible spectra between 700 and 500 nm

Multi Temp. The reaction mixture (final volume 2 ml) contained 2 μm HbO_2, 50 mM potassium phosphate buffer, pH 6·8, 0·1 mM EDTA, incubated at 37°.

2.5 Co-oxidation of epinephrine

Superoxide produced during the autoxidation of HbO_2 was measured by the co-oxidation of epinephrine following the method of Misra and Fridovich (1972). The assay system contained 10 μm HbO_2, 50 mM aerated potassium phosphate buffer, pH 6·8, 0·1 mM EDTA and 0·6 mM epinephrine. The formation of adrenochrome was followed at 480 nm at 37°C using a temperature-controlled water-circulated cell holder.

Measurement of the production of OH·

Hydroxyl radical formed during the autoxidation of HbO_2 was measured by the method of deoxyribose degradation as described by Puppo and Halliwell (1988).

3. Results

3.1 Contents of oxy and met forms of haemoglobin isolated from different animals

Table 1 gives comparative values of the oxy and met forms of Hb isolated from fish, toad, frog, blood sucker, turtle, anjani, common Indian monitor, chicken, pigeon, Indian fruit bat, rat, rabbit, guinea pig, goat, cattle and human being. The results show that Hb isolated from different animals except fish contains 90 to 99% HbO_2. Hb isolated from fish contained only 79% HbO_2 and 21% MetHb. That fish HbO_2 loses it stability after purification has also been reported by Riggs (1981).

3.2 Rate of autoxidation of HbO_2 from different animals

Comparison of the rates of autoxidation of HbO_2 at 37°C from different animals indicate that the rate is very high in the case of fish and blood sucker. Table 2 shows the approximate pseudo-first-order rate constants observed during the autoxidation of HbO_2 of different animal species. The constants were determined by the method of Satoh and Shikama (1981).

3.3 Co-oxidation of epinephrine

Figure 1a shows the spectral changes obtained during autoxidation of toad HbO_2 in the presence of epinephrine. The figure indicates that autoxidation of HbO_2 to MetHb (increase of A_{630}) is accompanied by oxidation of epinephrine to adrenochrome (increase of A_{480}). The inset of figure 1a shows that the amount of adrenochrome formed ($\varepsilon_{480} = 4$ mM^{-1} cm^{-1}) and MetHb produced at any time during the autoxidation is in the molar ratio of approximately 1. The co-oxidation of epinephrine was almost completely inhibited by SOD and catalase (figure 1b). The possibility that the co-oxidation of epinephrine was mediated by any free iron was eliminated because addition of 20 μm desferrioxamine did not inhibit the co-oxidation of epinephrine.

3.4 Effects of SOD, catalase, thiourea and mannitol

SOD inhibits about 31% of the autoxidation of toad HbO_2 indicating that O_2^- is

Animal	HbO$_2$ (%)	MetHb (%)
Fish		
*Labeo rohita** (6)	79	21
Amphibians		
Toad (*Bufo melanostictus*) (18)	97	3
Frog (*Rana tigrina*) (12)	97	3
Reptiles		
Blood sucker (*Caloter versicolor*) (12)	97	3
Anjani (*Mabuya carinata*) (8)	98	2
Turtle (*Lissemys punctata*) (4)	90	10
Common Indian monitor		
(*Varanus monitor*) (2)	99	1
Birds		
Pigeon (2)	93	7
Chicken (4)	97	3
Flying mammal		
Indian fruit bat (4)	91	9
Mammals		
Rabbit (2)	99	1
Rat (12)	97	3
Guinea pig (6)	99	1
Goat (4)	99	1
Cattle (2)	99	1
Human (6)	99	1

Two ml of the assay mixture contained $2\,\mu M$ HbO$_2$, 0·1 mM EDTA, 50 mM potassium phosphate buffer, pH 6·8.

Numbers in parentheses represent the number of animals used.

The data are average values of HbO$_2$ and MetHb.

*Similar results were obtained with *Catla catla*, *Labeo calbasu* and *Cirrhina mrigala*.

ly produced but also involved in the further oxidation of Hb to MetHb. The dation is also inhibited about 53% by catalase indicating that H_2O_2 is ced during autoxidation and it is a major oxidant of HbO$_2$. Figure 2 shows e low concentration of H_2O_2 oxidizes HbO$_2$ to MetHb at a fast rate. The t of H_2O_2 used (2 nmol) was approximately three times that produced mol) during the autoxidation under the experimental conditions used. The t of H_2O_2 produced was calculated on the basis of catalase inhibition. The ion of HbO$_2$ by added H_2O_2 was completely inhibited by catalase. When and catalase were present together, the oxidation of HbO$_2$ was inhibited by 76%. This would indicate that about 24% of the MetHb formed was bly due to dissociation of $Hb^{3+}O_2^-$. The autoxidation of HbO$_2$ was also ted 50% by thiourea and 23% by mannitol, the scavengers of OH·, indicating OH· was also involved in the autoxidation. That OH· is produced during dation of HbO$_2$ has been demonstrated by the method of deoxyribose lation (Puppo and Halliwell 1988) as shown in table 3. The deoxyribose lation was inhibited about 98% by thiourea and 71% by mannitol.

observed during autoxidation of HbO$_2$ of different animals.

Animals	$K_{app} \times 10^3$ (min^{-1})
Blood sucker	25·0
Fish	19·0
Guinea pig	14·0
Toad	7·0
Frog	6·5
Goat	6·0
Common Indian monitor	4·5
Rat	2·0
Anjani	1·5
Chicken	1·5
Rabbit	1·5
Cattle	1·0
Human	0·7

Condition: 2 μM HbO$_2$ in 0·1 M potassium phosphate buffer, pH 6·8, 0·1 mM EDTA at 37°. The K_{app} (average) was calculated by the method of Satoh and Shikama (1981).
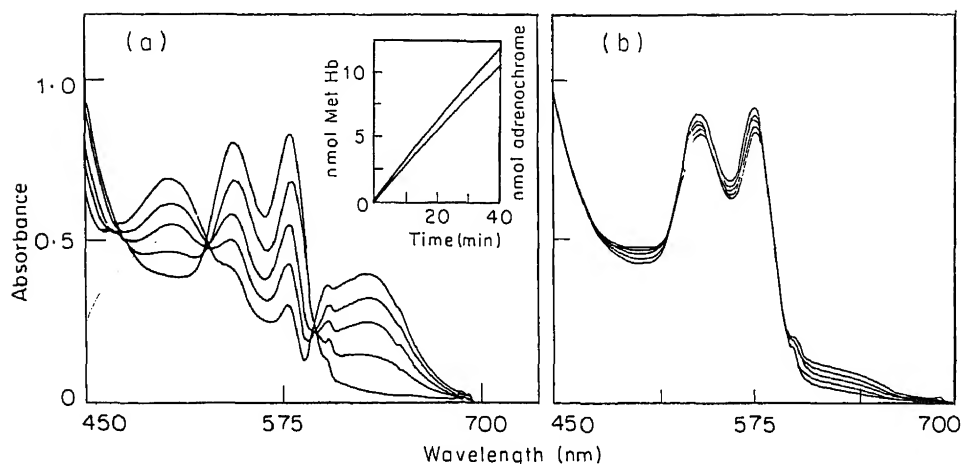
Figure 1. Autoxidation of HbO$_2$ in the presence of epinephrine.

(a) Control, containing aerated 50 mM potassium phosphate buffer, pH 6·8, 0·1 mM EDTA, 10 μM HbO$_2$, 0·6 mM epinephrine; (b) with 20 μg SOD plus 80 μg catalase. Spectra were obtained at 0, 10, 20, 30 and 40 min elapsed time. *Inset:* (1) nmol of adrenochrome formed ($\varepsilon_{480} = 4$ mM^{-1} cm^{-1}) and (2) nmol of MetHb produced during the co-oxidation of epinephrine.

3.5 Effect of pH

It has been observed that the rate of autoxidation is increased as the pH is decreased. The approximate rate constants at different pH are given in table 4. Similar observations were made with human HbO$_2$. Under the conditions used for toad HbO$_2$, the percentage of MetHb formed from human HbO$_2$ was 6 at pH 6·8
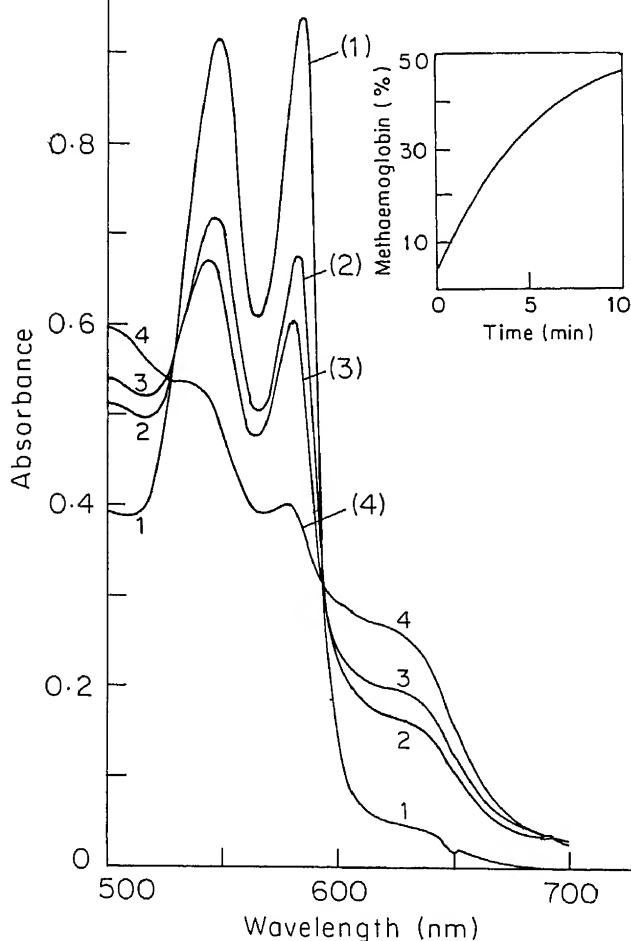
Figure 2. Spectral changes obtained during the oxidation of toad HbO in the presence of hydrogen peroxide.

Spectra at different time intervals are: (1) 0 min (control without H_2O_2), (2) 4 min, (3) 10 min, after addition of 2 μM H_2O_2. *Inset*: Increase of % MetHb against time. Graph 4 represents the spectrum obtained after 7 min incubation with 10 μM H_2O_2. The MetHb formed with 10 μM H_2O_2 was 74%. Other conditions are given under 'materials and methods'.

and 10 at pH 6·0 in 40 min. The increased rate of autoxidation was probably due to the increased rate of dissociation of $Hb^{3+}O_2^-$, because the rate of formation of MetHb in the presence of SOD and catalase increased as the pH was decreased (figure 3). The approximate rate constant $K \times 10^3$ (min^{-1}) observed in the presence of SOD and catalase were at pH 7·4, 0·5; pH 6·8, 1·7; pH 6·0, 2·4 and pH 5·5, 4·4. Nevertheless, the inhibition of autoxidation by SOD plus catalase was similar at different pH. The per cent inhibition was 76 at pH 6·8, 68 at pH 6·0 and 73 at pH 5·5.

determined by deoxyribose degradation.

Reagent added to reaction mixture	A_{532}	Inhibition of deoxy-ribose degradation (%)
None (complete reaction mixture)	0·048	0
Thiourea (10 mM)	0·001	98
Mannitol (40 mM)	0·014	71

Reaction mixture was incubated at 37° for 90 min. It contained the following reagents at the final concentrations stated: HbO_2 (50 μM), deoxyribose (5·6 mM) and KH_2PO_4/K_2HPO_4 buffer, pH 6·8 (50 mM in phosphate). After incubation colour was developed, extracted into butan-1-ol and measured at 532 nm as described (O'Connell et al 1986). Scavengers were added to the reaction mixture to give the final concentrations stated. Absorbances were read against respective blanks which contained everything but not incubated.

Table 4. Effects of pH, enzymes and oxyradical scavengers on the observed first order rate constant (K_{app}) of the autoxidation of toad HbO_2.

Variable factors	$K_{app} \times 10^3$ (min^{-1})
pH	
6·8	7·0
6·0	10·0
5·5	18·0
Enzymes[a]	
SOD	5·0
CAT	3·6
SOD+CAT	1·7
Hydroxyl radical scavengers	
Thiourea	3·9
Mannitol	5·8
Ligands[a]	
CO	0·1
CN$^-$	0·3
N$_3^-$	1·4
SCN$^-$	3·6

Reaction conditions: 2 μM HbO_2, 37°, 50 mM potassium phosphate buffer, pH 6·8 and 6·0, 50 mM sodium acetate buffer, pH 5·5, 20 unit SOD, 80 μg catalase, 20 mM mannitol, 10 mM thiourea, 2 mM CN$^-$, 2 mM N$_3^-$ and 2 mM SCN$^-$.
[a]All at pH 6·8.

3.6 Effect of CN^-, N_3^-, SCN^- and CO

Figure 4a shows the spectral changes obtained during the autoxidation of toad HbO_2 in the absence of any added ligand. Figure 4b-e shows that autoxidation is inhibited by CO as well as by anion ligands, namely, CN$^-$, N$_3^-$ and SCN$^-$ respectively. Further, the inhibition by the anion ligands is in the same order as their strength as nucleophiles. This would indicate that it is the oxy species, that is
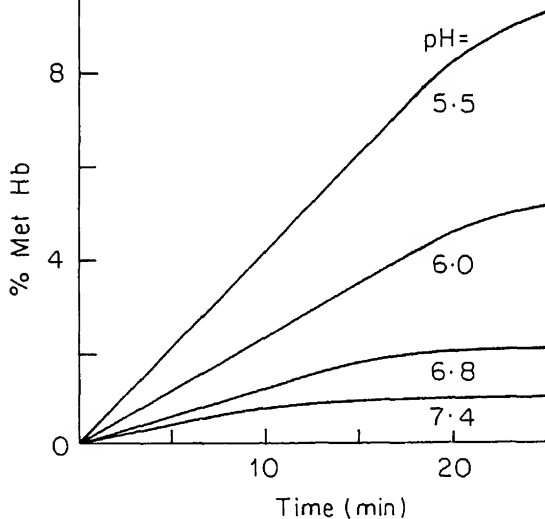
Figure 3. Rate of autoxidation of toad HbO_2 at different pH in the presence of SOD and catalase.

Two ml reaction mixture contained $2\,\mu M$ HbO_2, 0.1 mM EDTA, SOD ($20\,\mu g$) and catalase ($80\,\mu g$); pH 7.4, 6.8 and 6.0 were 50 mM potassium phosphate buffer and pH 5.5 was 50 mM sodium acetate buffer.

HbO_2, and not the ligand-bound deoxy species as presumed by Wallace *et al* (1982), which undergoes autoxidation. A similar result was obtained with human HbO_2. Although the rate of autoxidation of human HbO_2 was very slow, nevertheless, CN^- and N_3^- significantly inhibited autoxidation. In the absence of any ligand the percentage of MetHb formed was 7, whereas in the presence of CN^- and N_3^- MetHb% were 2 and 4 respectively. Wallace *et al* (1982) and Watkins *et al* (1985) assumed that protonated anion-ligands were effective as promoters of autoxidation of HbO_2. However, the marked inhibitory effect of CN^- was also observed when the pH was decreased (figure 5a, b).

3.7 *MetHb formation and ferricytochrome c reduction*

Figure 6a shows that the addition of ferricytochrome c (cyt c^{3+}) to a solution of toad HbO_2 results in the reduction of cyt c^{3+} to cyt c^{2+} as evidenced by the increase of A_{550}. The reduction of cyt c^{3+} is accompanied by oxidation of HbO_2 to MetHb as indicated by the increase of A_{630} and decrease of A_{575}. Figure 6a further shows that the initial rate of cyt c^{3+} reduction is very fast. In a reaction period of 10 min, about 78% of the cyt c^{3+} reduction takes place within the first 3.5 min. There is no stoichiometry between cyt c^{3+} reduction and MetHb formation. During the initial period of 1.5 min, the amount of cyt c^{3+} reduced is 1.14 nmol ($\varepsilon_{550} = 21$ mM^{-1} cm^{-1}) whereas the MetHb formed is only 0.1 nmol indicating a molar ratio of 11.4. The observed molar ratios in 2.5 min, 3.5 min and 4.5 min are 8, 7.3 and 6.5 respectively (inset of figure 6a). This would indicate that cyt c^{3+} reduction is not directly related to heme iron oxidation. This has been further
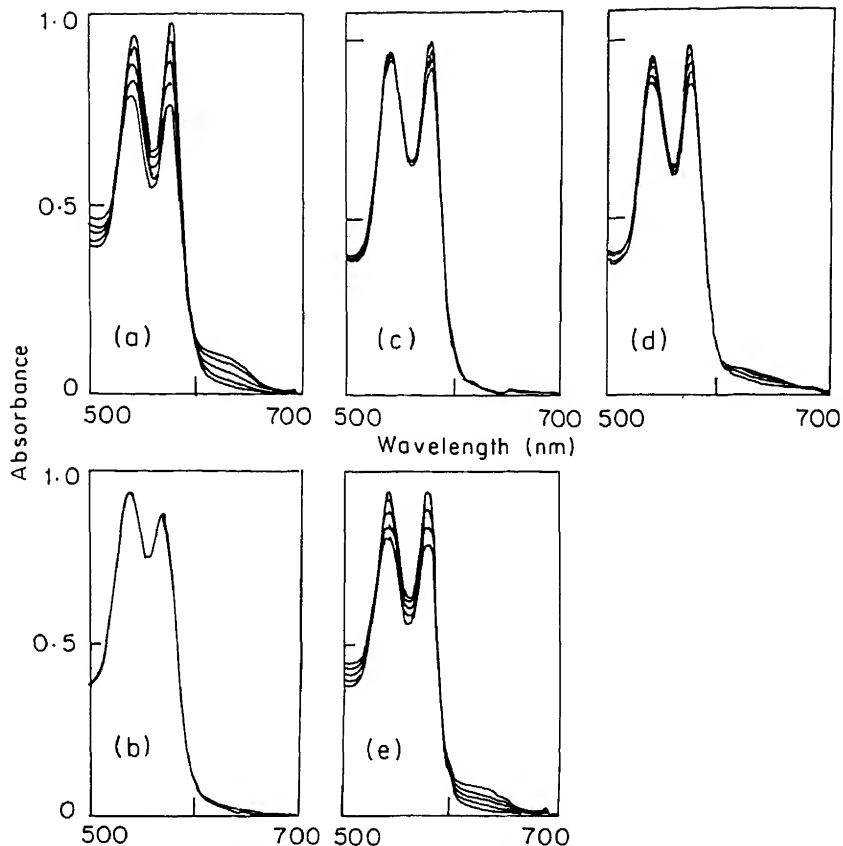
Figure 4. Spectral changes observed during the autoxidation of toad HbO_2 in the absence and presence of different ligands. The reaction mixture contained 50 mM potassium phosphate buffer, pH 6·8, 0·1 mM EDTA, 2 μM HbO_2. (a) Control; (b) 2 μM HbCO; (c) 2 mM cyanide; (d) 2 mM azide; (e) 2 mM thiocyanate. Spectra were obtained at 0, 10, 20, 30 and 40 min elapsed time.

evidenced by the fact that in the presence of CN^-, oxidation of heme iron is markedly inhibited whereas the reduction of cyt c^{3+} is rather enhanced (figure 6b). A similar observation has been made with N_3^- (figure 6c). Moreover, the reduction of cyt c^{3+} by HbO_2 is only 21% inhibited by SOD indicating that 79% cyt c^{3+} reduction is not related to O_2^- production. During a reaction period of 10 min, the amount of cyt c^{3+} reduced in the absence of SOD is 3·79 nmol, and that in the presence of 20 units of SOD, 3 nmol. Human HbO_2 also reduces cyt c^{3+}, but the rate of reduction is very slow compared to that observed with toad HbO_2. In 20 min and under the conditions used for toad HbO_2, the amount of cyt c^{3+} reduced by human HbO_2 was 0·95 nmol, whereas the amount of MetHb formed was 0·2 nmol, indicating a molar ratio of 4·5. The reduction of cyt c^{3+} by human HbO_2 was only 20% inhibited by SOD, confirming our results obtained with toad HbO_2, that cyt c^{3+} reduction by HbO_2 was neither directly related to heme iron oxidation, nor did it account for the O_2^- production.
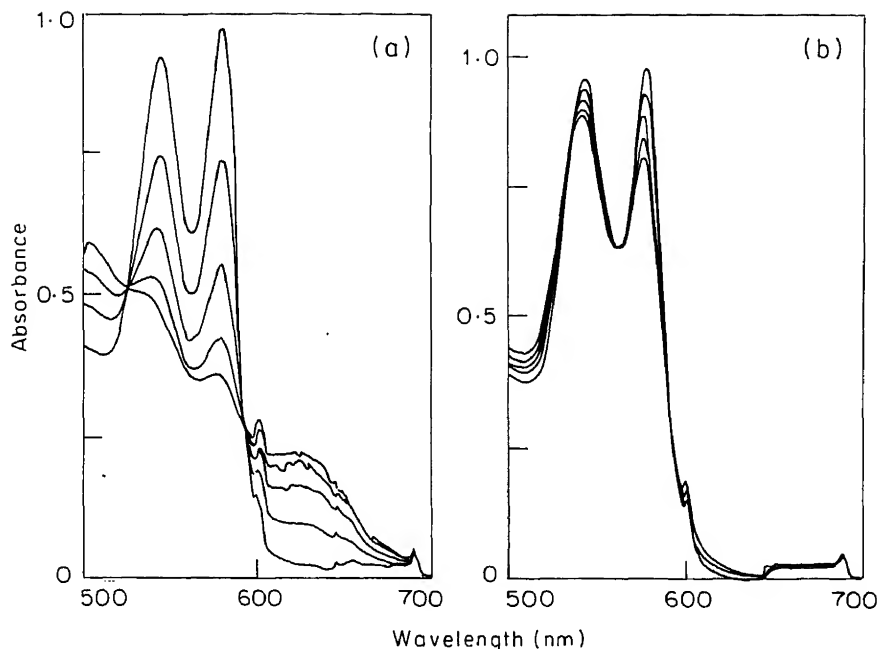
Figure 5. Spectral changes observed during the autoxidation of toad HbO_2 in the absence and presence of cyanide.

(a) 50 mM sodium acetate, pH 5·5, 0·1 mM EDTA, 2 μM HbO_2; (b) same as in figure 4c plus 2 mM cyanide. Spectra were obtained at 0, 10, 20, 30 and 40 min elapsed time.

4. Discussion

Elucidation of the detailed mechanism of autoxidation of HbO_2 needs a sample of HbO_2, the rate of autoxidation of which should be neither too fast like fish HbO_2 as used by Misra and Fridovich (1972) nor too slow like human HbO_2 as used by Wallace *et al* (1982). In this regard, toad HbO_2 appears to be a suitable sample for studying the sequence of reactions involved in the process of autoxidation. Perutz (1979) indicated that though haemoglobins of different species may vary in amino acid sequence depending on the position of the species on the evolutionary tree (Romero–Herrera 1973; Goodman 1975), the three-dimensional structure and function of the different haemoglobins are similar. Therefore, results obtained with toad HbO_2 may represent a general mechanism of autoxidation of HbO_2. We have also verified some of the results using human HbO_2.

Using the technique of co-oxidation of epinephrine for the estimation of O_2^- we have observed that during autoxidation of HbO_2, the adrenochrome formed and MetHb produced is in the molar ratio of 1. That the initial step of autoxidation is dissociation of $Hb^{3+}O_2^-$ into MetHb and O_2^- is also apparent from kinetic studies. Since epinephrine is an acceptor of O_2^-, the O_2^- produced by the dissociation of $Hb^{3+}O_2^-$ may be considered to be fully consumed by epinephrine. The rate of formation of MetHb in the presence of epinephrine would represent the rate of dissociation of $Hb^{3+}O_2^-$ in the presence of an acceptor of O_2^-. When SOD and catalase are added along with epinephrine, epinephrine can no longer act as an
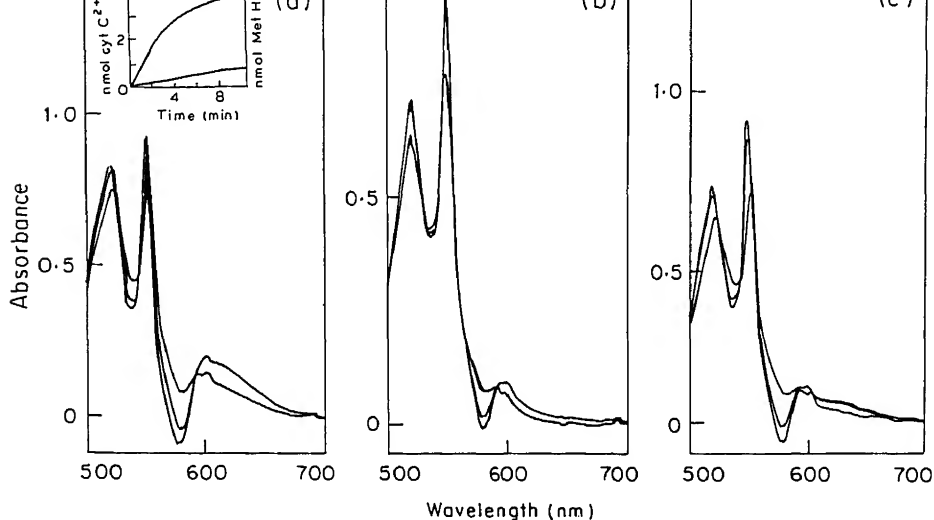
Figure 6. Spectral changes observed when toad HbO_2 was allowed to autoxidize in the presence of cyt c^{3+} with cyanide and azide.

(a) Control, containing 50 mM potassium phosphate buffer, pH 6·8, 2 μM HbO_2, 10 μM cyt c^{3+}; (b) in the presence of 2 mM cyanide; (c) in the presence of 2 mM azide. Spectra were obtained at 1·5, 6 and 11 min elapsed time. *Inset*: (1) nmol cyt c^{2+} formed ($\epsilon_{550} = 21$ mM^{-1} cm^{-1}) and (2) nmol MetHb produced during the autoxidation of HbO_2 in the presence of cyt c^{3+}.

acceptor of O_2^- and the rate of formation of MetHb represents the actual rate of dissociation of $Hb^{3+} O_2^-$. It is expected that the rate of dissociation should increase markedly in the presence of a O_2^- acceptor. In fact, the results show that when SOD and catalase are present along with epinephrine, only 1·6 nmol of MetHb are produced in 40 min. Whereas, when SOD and catalase are omitted, the amount of MetHb formed is 11·2 nmol. In other words, the rate of dissociation of $Hb^{3+} O_2^-$ increased about 7 times in the presence of epinephrine, an acceptor of O_2^-. Comparing the rate constant of the reaction observed in the presence of epinephrine along with SOD and catalase [$K_{app} = 2·1 \times 10^{-3}$ (min)$^{-1}$] and that in the absence of SOD and catalase [$K_{app} = 17 \times 10^{-3}$ (min)$^{-1}$], it would appear that the rate of dissociation of $Hb^{3+} O_2^-$ is increased about 8 times when an acceptor of O_2^- is present in the reaction mixture. Apparently, the rate of dissociation of $Hb^{3+} O_2^-$ is also increased as the pH is decreased. As mentioned before, the production of MetHb during autoxidation of HbO_2 in the presence of SOD and catalase would represent the actual dissociation of $Hb^{3+} O_2^-$.

The O_2^- produced during autoxidation of HbO_2 could not be measured by the method of cyt c^{3+} reduction because cyt c^{3+} is directly reduced by HbO_2. Stoichiometric studies indicate that the initial rate of cyt c^{3+} reduction is very fast compared to that of MetHb formation. The slow rate of heme iron oxidation compared to the fast rate of cyt c^{3+} reduction may be explained by the consideration that cyt c^{3+} cannot abstract an electron directly from the heme iron and the reaction apparently takes place on the outer surface of the haemoglobin

probably takes place by charge transfer in a relay system, the mechanism of which is yet to be known. That cyt c^{3+} reduction is not directly related to heme iron oxidation has been further proved by the fact that in the presence of CN^-, oxidation of heme iron is markedly inhibited, whereas the reduction of cyt c^{3+} is enhanced.

That it is the oxy form of haemoglobin and not the deoxy form which undergoes autoxidation is proved by the fact that anion ligands like CN^-, N_3^- and SCN^- markedly inhibit the autoxidation of HbO_2 and that inhibition by ligands is in the same order as their strength as nucleophiles.

Several studies have implicated the involvement of O_2^- and H_2O_2 on the autoxidation of HbO_2 (Wallace et al 1974a,b; Wallace and Caughey 1979; Winterbourn et al 1981). In an attempt to elucidate the mechanism of autoxidation of HbO_2, Watkins et al (1985) studied the effects of SOD, catalase and $OH\cdot$ scavenger at different pH. However, the data obtained were inconclusive and no stoichiometric involvement of O_2^-, H_2O_2 and $OH\cdot$ could be ascertained. Also, Watkins et al (1985) did not demonstrate the actual formation of $OH\cdot$ during autoxidation of HbO_2. The varied effect of SOD and catalase observed by Watkins et al (1985) is probably due to the fact that autoxidation of human HbO_2 is a very slow process and the authors have carried out the incubation for a prolonged period of 20 h at $37\cdot5°$, which affects the catalytic activities of SOD and catalase. Regarding the mechanism of O_2^- production during autoxidation of HbO_2, Watkins et al (1985) assumed that a complex of protonated deoxyhaemoglobin species with anions reacted with molecular oxygen to produce O_2^-. As indicated before, we have observed that it is the oxy species and not the ligand bound deoxy form which undergoes autoxidation and the initial step of autoxidation is dissociation of $Hb^{3+}O_2^-$ to MetHb and O_2^-.

Sutton et al (1976) and Lynch et al (1977) have shown that O_2^- oxidizes HbO_2 to MetHb with production of H_2O_2. Demma and Salhany (1977) demonstrated that HbO_2 dissociated into MetHb and O_2^- when flashed with low intensity white light. The authors observed that O_2^- produced by the dissociation reattacked a fresh molecule of HbO_2 to produce MetHb and H_2O_2 and they observed 23% inhibition of oxidation by SOD. We have also observed that autoxidation is 31% inhibited by SOD indicating that O_2^- produced by the dissociation of $Hb^{3+}O_2^-$ reattacks HbO_2. Autoxidation of HbO_2 is also 53% inhibited by catalase confirming the observations of others (Sutton et al 1976; Demma and Salhany 1977; Lynch et al 1977; Watkins et al 1985) that H_2O_2 is produced by the reaction of O_2^- with HbO_2 and that H_2O_2 further oxidizes HbO_2 to MetHb. Consideration of the rate constant ($K_{app} = 1\cdot6 \times 10^7\ M^{-1}\ s^{-1}$) of the reaction of toad HbO_2 with O_2^- (Mal et al 1991) and that ($K = 1\cdot0 \times 10^5\ M^{-1}\ s^{-1}$) of spontaneous dismutation of O_2^- (McCord et al 1977) would indicate that the source of H_2O_2 is rather a product of the reaction of HbO_2 with O_2^- than spontaneous dismutation of O_2^-. Autoxidation is also 50% inhibited by thiourea and 23% by mannitol indicating that $OH\cdot$ is also involved in autoxidation. The large extent of inhibition by thiourea is probably due to the fact that thiourea is not a specific inhibitor of $OH\cdot$ (Cederbaum et al 1979; Wasil et al 1987). HbO_2 is considered to be a biological Fenton reagent (Sadrzadeh et al 1984; Puppo and Halliwell 1988), so $OH\cdot$ is apparently formed by the reaction of HbO_2 with H_2O_2. Using the deoxyribose degradation method (Puppo and

$$HbO_2 \rightleftharpoons Hb^{3+}O_2^-, \tag{1}$$

$$Hb^{3+}O_2^- \rightarrow MetHb + O_2^-, \tag{2}$$

$$HbO_2 + O_2^- + 2H^+ \rightarrow MetHb + H_2O_2 + O_2, \tag{3}$$

$$HbO_2 + H_2O_2 \rightarrow MetHb + OH \cdot + OH^- + O_2, \tag{4}$$

$$HbO_2 + OH \cdot \rightarrow MetHb + OH^- + O_2. \tag{5}$$
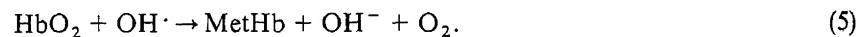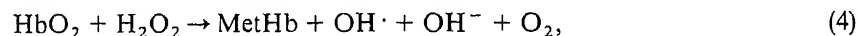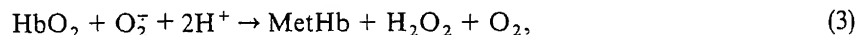
The overall reaction may be represented as

$$4HbO_2 + 2H^+ \rightarrow 4MetHb + 2OH^- + 3O_2. \tag{6}$$
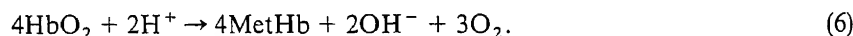
The aforesaid mechanism of autoxidation is also supported by the observed inhibition of autoxidation by the anion ligand (L^-) namely, CN^-, N_3^- and SCN^-. The anion ligands convert HbO_2 to HbL^- according to their strength as nucleophiles and consequently the formation of $Hb^{3+}O_2^-$ and its subsequent dissociation to MetHb and O_2^- is inhibited. Since formation of O_2^- is the rate-limiting step of autoxidation, the overall process is inhibited in the presence of anion ligands. A similar explanation may be given for HbCO.

We have observed that human erythrocytes contain per g Hb enough of SOD (1000 units), ascorbic acid (132 nmol) which is a chemical scavenger of O_2^- (Nandi and Chatterjee 1987) and catalase (100×10^3 units). These scavengers of reactive oxygen species will prevent reattack of HbO_2 by O_2^- and H_2O_2. Therefore, the dissociation of $Hb^{3+}O_2^-$ probably represents the main mechanism of the formation of MetHb and O_2^- *in vivo*. Our results indicate that this dissociation accounts for the *in vitro* formation of about 2·55% MetHb per hour. If the results obtained *in vitro* are extrapolated to *in vivo* conditions, the rate of formation of O_2^- in human erythrocytes may be roughly calculated as 6·5 nmol per g HbO_2 per min. Taking the average concentration of HbO_2 as 300 g per 1000 ml packed cell, the rate of O_2^- formation becomes $3·25 \times 10^{-8}$ M s^{-1}. This is nearer the value (2×10^{-8} M s^{-1}) calculated by Scarpa *et al* (1985) in the erythrocytes of healthy individuals. It remains a question if in the presence of scavengers of reactive oxygen species, this amount of O_2^- can produce any oxidative damage to the erythrocytes. However, no defence is perfect and some fraction of generated O_2^- may always escape. If they do so, they will produce injury to the erythrocyte membrane. This may be one of the causes of aging in erythrocytes.

Beauchamp C and Fridovich I 1971 Superoxide dismutase: Improved assay and an assay applicable to acrylamide gel; *Anal. Biochem.* **44** 276–287

Brown W D 1961 Chromatography of myoglobin on diethylaminoethyl cellulose columns; *J. Biol. Chem.* **236** 2238–2240

Brunori M, Falcioni G, Fioretti E, Giardina B and Rotilio G 1975 Formation of superoxide in the autoxidation of the isolated α and β chains of human hemoglobin and its involvement of hemichrome precipitation; *Eur. J. Biochem.* **53** 99–104

Cederbaum A I, Dicker E, Rubin E and Cohen G 1979 Effect of thiourea on microsomal oxidation of alcohols and associated microsomal functions; *Biochemistry* **18** 1187–1191

Demma L S and Salhany J M 1977 Direct generation of superoxide anions by flash photolysis of human oxyhemoglobin; *J. Biol. Chem.* **252** 1226–1231

Fridovich I 1972 Superoxide radical and superoxide dismutase; *Acc. Chem. Res.* **5** 321–326

Fridovich I 1979 Superoxide dismutases: defence against endogenous superoxide radical; in *Oxygen free radicals and tissue damage*, Ciba Foundation Symposium 65 (New Series) (Amsterdam: Excerpta Medica) pp 77–93

Goodman M, Moore W and Matsuda G 1975 Darwinian evolution in the genealogy of hemoglobin; *Nature (London)* **253** 603–608

Gotoh T and Shikama K 1976 Generation of the superoxide radical during autoxidation of oxymyoglobin; *J. Biochem. (Tokyo)* **80** 397–399

Jaffe E R and Neumann G 1964 A comparison of the effect of menadione, methylene blue and ascorbic acid on the reduction of methaemoglobin *in vivo*; *Nature (London)* **202** 607–608

Kellog E W III and Fridovich I 1977 Liposome oxidation and erythrocyte lysis by enzymically generated superoxide and hydrogen peroxide; *J. Biol. Chem.* **252** 6721–6728

Laemmli U K 1970 Cleavage of structural proteins during the assembly of the head of bacteriophage T_4; *Nature (London)* **227** 680–685

Lynch R E, Lee G R and Cartwright G E 1976 Inhibition by superoxide dismutase of methemoglobin formation from oxyhemoglobin; *J. Biol. Chem.* **251** 1015–1019

Lynch R E, Thomas J E and Lee G R 1977 Inhibition of methemoglobin formation from purified oxyhemoglobin by superoxide dismutase; *Biochemistry* **16** 4563–4567

Mal A, Nandi A and Chatterjee I B 1991 Haemoglobin: A scavenger of superoxide radical; *J. Biosci.* **16** 43–53

McCord J M, Crapo J D and Fridovich I 1977 Superoxide dismutase assays: A review of methodology; in *Superoxide and superoxide dismutase* (eds) A M Michelson, J M McCord and I Fridovich (New York: Academic Press) pp 11–17

Misra H P and Fridovich I 1972 The generation of superoxide radical during the autoxidation of hemoglobin; *J. Biol. Chem.* **247** 6960–6962

Nandi A and Chatterjee I B 1987 Scavenging of superoxide radical by ascorbic acid; *J. Biosci.* **11** 435–441

O'Connell M, Halliwell B, Moorhouse C P, Aruoma O I, Baum H and Peters T J 1986 Formation of hydroxyl radicals in the presence of ferritin and haemosiderin. Is haemosiderin formation a biological protective mechanism?; *Biochem. J.* **234** 727–731

Peisach J 1975 An interim report on electronic control of oxygenation of heme proteins; *Ann. N. Y. Acad. Sci.* **244** 187–202

Peisach J, Blumberg W E, Wittenberg B A and Wittenberg J B 1968 The electronic structure of protoheme proteins: Configuration of the heme and its ligands; *J. Biol. Chem.* **243** 1871–1880

Perutz M F 1979 Regulation of oxygen affinity of hemoglobin: Influence of the structure of the globin on the heme iron; *Annu. Rev. Biochem.* **48** 327–386

Puppo A and Halliwell B 1988 Formation of hydroxyl radicals from hydrogen peroxide in the presence of iron; *Biochem. J.* **249** 185–190

Richteric R 1969 Haemoglobin as cyanmethaemoglobin; in *Clinical chemistry* (Switzerland, Basel: S Karger) pp 333–335

Riggs A 1981 Preparation of blood haemoglobins of vertebrates; *Methods Enzymol.* **76** 5–13

Romero-Herrera A E, Lehmann H, Joysey K A and Friday A E 1973 Molecular evolution of myoglobin and the fossil record: A phylogenetic synthesis; *Nature (London)* **246** 389–395

Sadrzadeh S M H, Graf E, Panter S S, Hallaway P E and Eaton J W 1984 Hemoglobin: A biological fenton reagent; *J. Biol. Chem.* **259** 14354–14356

Ital. J. Biochem. **18** 1–18

Salvati A M and Tentori L 1981 Determination of aberrant haemoglobin derivatives in human blood; *Methods Enzymol.* **76** 715–731

Satoh Y and Shikama K 1981 Autoxidation of oxymyoglobin: A nucleophilic displacement mechanism; *J. Biol. Chem.* **256** 10272–10275

Scarpa M, Rigo A, Momo F, Isacchi G, Novelli G and Dallapiccola B 1985 Increased rate of superoxide ion generation in Fanconi anemia erythrocytes; *Biochem. Biophys. Res. Commun.* **130** 127–132

Scarpa M, Viglino P, Còntri D and Rigo A 1984 Generation of superoxide ion in human red blood cell lysates; *J. Biol. Chem.* **259** 10657–10659

Sutton H C, Robert P B and Winterbourn C C 1976 The rate of reaction of superoxide radical ion with oxyhaemoglobin and methaemoglobin; *Biochem. J.* **155** 503–510

Tomoda A, Tsuji A and Yoneyama Y 1980 Mechanism of hemoglobin oxidation by ferricytochrome C under aerobic and anaerobic conditions; *J. Biol. Chem.* **255** 7978–7985

Viale R O, Maggiora G M and Ingraham L L 1964 Molecular orbital evidence for Weiss's oxyhaemoglobin structure; *Nature (London)* **203** 183–184

Wallace W J and Caughey W S 1979 in *Biochemical and clinical aspects of oxygen* (ed.) W S Caughey (New York: Academic Press) pp 69–86

Wallace W J, Houtchens R A, Maxwell J C and Caughey W S 1982 Mechanism of autoxidation for hemoglobins and myoglobins: Promotion of superoxide production by protons and anions; *J. Biol. Chem.* **257** 4966–4977

Wallace W J, Maxwell J C and Caughey W S 1974a The mechanisms of hemoglobin autoxidation: Evidence for proton-assisted nucleophilic displacement of superoxide by anions; *Biochem. Biophys. Res. Commun.* **57** 1104–1110

Wallace W J, Maxwell J C and Caughey W S 1974b A role for chloride in the autoxidation of hemoglobin under conditions similar to those in erythrocytes; *FEBS Lett.* **43** 33–36

Wasil M, Halliwell B, Grootveld M, Moorhouse C P, Houtchison D C S and Baum H 1987 The specificity of thiourea, dimethylthiourea and dimethylsulphoxide as scavengers of hydroxyl radicals; *Biochem. J.* **243** 867–870

Watkins J A, Kawanishi S and Caughey W S 1985 Autoxidation reactions of hemoglobin A free from other red cell components: A minimal mechanism; *Biochem. Biophys. Res. Commun.* **132** 742–748

Weiss S S 1964 Nature of the iron-oxygen bond in oxyhaemoglobin; *Nature (London)* **202** 83–84

Wever R, Oudega B and Vangelder B F 1973 Generation of superoxide radicals during the autoxidation of mammalian oxyhemoglobin; *Biochim. Biophys. Acta* **302** 475–478

Winterbourn C C, McGrath B M and Carrell R W 1976 Reactions involving superoxide and normal and unstable haemoglobins; *Biochem. J.* **155** 493–502

Winterbourn C C, Williamson O, Vissers M C M and Carrel R W 1981 Unstable haemoglobin haemolytic crises: Contribution of pyrexia haemoglobins; *Br. J. Haematol.* **49** 111–116

Wittenberg J B, Wittenberg B A, Peisach J and Blumberg W E 1970 On the state of the iron and the nature of the ligand in oxyhemoglobin and neutrophil oxidant; *Proc. Natl. Acad. Sci. USA* **67** 1846–1853

Wu C S C, Duffy P and Brown W D 1972 Interaction of myoglobin and cytochrome c; *J. Biol. Chem.* **247** 1899–1903

Yamamoto T, Palmer G, Gill D, Salmeen I T and Rimai L 1973 The valence and the spin state of iron in oxyhemoglobin as inferred from resonance Raman spectroscopy; *J. Biol. Chem.* **248** 5211–5213

Altered kinetic properties of liver mitochondrial membrane-bound enzyme activities following paracetamol hepatotoxicity in the rat

S S KATYARE* and J G SATAV

Biochemistry Division, Bhabha Atomic Research Centre, Trombay, Bombay 400 085, India
*Present address: Department of Biochemistry, Faculty of Science, M S University of Baroda, Baroda 390 002, India

Abstract. The effects of treatment with subtoxic (375 mg/kg) and toxic (750 mg/kg) doses of paracetamol on NADH oxidase, succinoxidase and Mg^{2+}-ATPase activities in rat liver submitochondrial particles were examined. In the NADH oxidase system, treatment with subtoxic doses of paracetamol resulted in a 37% increase in activation energy in the high temperature range (E_1) while the phase transition temperature (Tt) for this system decreased by 9°C. Subtoxic doses caused a 43% decrease in E_1. For the succinoxidase system, Tt decreased by 2·4 to 3·4°C after paracetamol administration. E_2 increased by 42% only in the subtoxic-treatment group while E_1 remained unaltered in both paracetamol-treated groups. For the Mg^{2+}-ATPase system, subtoxic doses of paracetamol treatment did not change the values of E_1, E_2 and Tt whereas toxic dose treatment resulted in a 29% decrease in E_2 with a concomitant increase in Tt by 2·4°C without any change in the value of E_1. The results thus suggest that treatment with toxic and subtoxic doses of paracetamol results in possible differential alterations in the membrane lipid milieu.

Keywords. Paracetamol; hepatotoxicity; Arrhenius kinetics; NADH oxidase; succinoxidase; Mg^{2+}-ATPase.

Introduction

Acetaminophen (4-hydroxyacetanilide), commonly known as paracetamol, is a widely used analgesic drug (Mitchell *et al* 1973; Hinson *et al* 1981; Breen *et al* 1982; McClain 1982). It is considered to be safe at therapeutic doses, however, its overdoses are known to produce hepatic centrilobular necrosis associated with structural damage to the mitochondria (Mitchell *et al* 1973; Dixon *et al* 1975; Hinson *et al* 1981; Dixon 1984). Disruption of liver mitochondrial cristae structures and a transient increase in the succinate dehydrogenase activity followed by loss in this enzyme activity have been reported (Cobden *et al* 1982; Newton *et al* 1983; Dixon 1984). High doses of paracetamol are also known to increase the levels of transaminases in the serum (Dixon 1984).

Recently, we have shown impairment in the liver mitochondrial energy metabolism following paracetamol treatment of rats (Katyare and Satav 1989). Thus toxic doses (750 mg/kg) of paracetamol caused impairment in the coupled respiration rates with several substrates with concomitant decrease in the ADP-phosphorylation rates. In addition, this treatment also led to compositional defects

the dehydrogenase activities with an increase in the rate of succinate oxidation (Katyare and Satav 1989). Meyers et al (1988) have also shown the acetaminophen-induced inhibition of hepatic mitochondrial respiration in mice.

These observations on impairment in the hepatic mitochondrial oxidative energy metabolism (Katyare and Satav 1989), loss of hepatic mitochondrial integrity by paracetamol treatment (Dixon, 1984; Meyers et al 1988) and binding of paracetamol and its metabolites to hepatic mitochondria (Jallow et al 1973; Ginsberg and Cohen 1985) prompted us to examine the temperature-dependent changes in the mitochondrial respiratory enzymes such as NADH oxidase, succinoxidase and Mg^{2+}-ATPase. The results of such studies when examined in terms of Arrhenius plots would give information on possible alterations in phase transition temperature and activation energy (Raison 1972). These parameters are known to be affected by the integrity of cellular membranes and their lipid composition (Raison 1972; Hulbert et al 1976; Dave et al 1989); the respiratory enzymes presently examined are membrane-bound and require lipids for their activities (Raison 1972).

2. Materials and methods

2.1 Animals

Male albino rats of Wistar strain, weighing between 250 and 260 g, were used. Animals were fasted overnight and injected with paracetamol the next morning. Paracetamol solutions (35 mg/ml) were prepared in warm (40–50°C) saline. Rats were injected intraperitoneally with 375 or 750 mg/kg of paracetamol (Katyare and Satav 1989); these doses, hereafter, are referred to as 'subtoxic' and 'toxic' respectively. Control animals received an equivalent volume of warm saline. After injections, the animals had free access to food and water. They were killed after 24 h of paracetamol or saline administration for isolation of mitochondria and preparation of submitochondrial particles (SMP).

2.2 Isolation of mitochondria and SMP

Liver mitochondria were isolated as described previously (Satav and Katyare 1982; Katyare and Satav 1989), washed once and suspended in 0·25 M sucrose containing 10 mM Tris-HCl buffer, pH 7·4 (10 mg protein/ml). SMPs were isolated after sonication for 4 min (10 s sonication followed by 10 s rest interval) at 20 kHz in a 'Vibro-cell' ultrasonic disintegrator (Sonics and Materials Inc., USA) by following standard procedures, suspended in 0·25 M sucrose (6–8 mg protein/ml) and stored at −25°C. Temperature-dependent changes in enzyme activities were studied within 2–3 days of the preparation of SMP. In separate experiments, it was ascertained that under these storage conditions, the enzyme activities did not change for up to one week.

2.3a *NADH oxidase and succinoxidase activities*: NADH oxidase and succin-oxidase activities were measured employing a Clark-type oxygen electrode (Chance and Williams 1955; Katyare and Rajan 1988; Katyare and Satav 1989) in a respiration medium consisting of 225 mM sucrose, 10 mM potassium phosphate buffer, pH 7·4, 10 mM Tris-HCl buffer, pH 7·4, 5 mM $MgCl_2$ and approximately 1 mg of SMP proteins in a final volume of 1·3 ml (Satav and Katyare 1982; Katyare and Satav 1989). NADH (2 mM) and sodium succinate (10 mM) were used as substrates to start the reaction. Enzyme activities were measured over a temperature range of 10° to 46°C with a 4°C temperature increase at every step.

2.3b *Mg^{2+}-ATPase activity*: ATPase activities in SMP were examined in a medium (final volume: 1 ml) consisting of 50 mM Tris-HCl buffer, pH 7·4, 75 mM KCl, 0·4 mM EDTA, 6 mM $MgCl_2$ and 150–200 μg of SMP protein (Satav and Katyare 1982). After pre-incubation for 2 min, the reaction, started by adding ATP (neutralized to pH 7·4 with Tris base) in a final concentration of 6 mM, was carried out for 15 min for measurements of the enzyme activity. At the end of the incubation period, the reaction was stopped by adding 0·1 ml of 10% (w/v) sodium dodecyl sulphate (SDS) (Shallom and Katyare 1985) and the liberated inorganic phosphate was estimated following the method of Fiske and Subba Row (1925). The temperature employed ranged from 10° to 46°C with a 4°C temperature increase at every step.

2.3c *Kinetic analysis*: For kinetic analyses, the log-specific activities of the given enzyme system were plotted against the reciprocal of the absolute temperature to obtain Arrhenius plots. The activation energies in high and low temperature ranges (E_1 and E_2 respectively) were determined as reported earlier (Raison *et al* 1971; Raison 1972; Katyare and Rajan 1988). The phase transition temperature was determined from the Arrhenius plots.

Protein was estimated according to Lowry *et al* (1951) with crystalline bovine serum albumin as the standard. Serum levels of glutamate-oxaloacetate transaminase (GOT) were determined by colorimetric assay (Bergmeyer and Bernt 1963).

Results are given as mean ± SE of the number of experiments indicated. Statistical evaluation of the data was by Fisher's Z test.

2.4 *Chemicals*

Paracetamol (A.R.) was purchased from Aldrich Chemical Co., Milwaukee, WI, USA. Sodium salt of succinic acid, vanadium-free ATP and NADH were obtained from Sigma Chemical Co., St. Louis, Mo, USA. All other chemicals used were of analytical-reagent grade.

3. Results

The extent of hepatic damage in paracetamol-treated animals was ascertained by measuring the levels of GOT. The mean serum levels of GOT was 186 ± 15

respectively in animals which received the 'subtoxic' and 'toxic' doses of paracetamol indicating a moderate and severe hepatic damage in this experimental animal model of paracetamol hepatotoxicity.

The NADH oxidase activity in SMP obtained from control animals increased with temperature and reached a plateau around 46°C. A similar trend was also seen in the two paracetamol groups — subtoxic and toxic. However, in the latter group, the activity was low (15–30%) at all the temperature points examined. The succinoxidase activity showed a steady increase with temperature up to 46°C in all the groups, with the toxic-treatment group showing a significant higher activity at 46°C (data not shown). A more or less similar trend was noticed for Mg^{2+}-ATPase activity (data not shown).

The corresponding Arrhenius plots are given in figures 1 to 3 and the results on energies of activation (E_1 and E_2) and phase transition temperature (Tt) are summarized in table 1. It can be noted that the Arrhenius plots for the NADH oxidase, succinoxidase and Mg^{2+}-ATPase activities from control as well as from paracetamol-treated animals were biphasic in nature showing breaks (figures 1–3). Similar biphasic Arrhenius plots for many other mitochondrial enzyme systems have been reported by other workers (Raison 1972; Hulbert et al 1976; Katyare and Rajan 1988; Dave et al 1989).

The data in figure 1 and table 1 indicate that treatment with 'subtoxic' doses of paracetamol resulted in a 37% increase in the value of activation energy in the high temperature range (E_1) with a simultaneous decrease in the phase transition temperature by 9°C for the NADH-oxidase system. However, the activation energy

Figure 1. Arrhenius plots of temperature-dependent changes in NADH oxidase activity in rat liver SMP. (a) Control; (b) paracetamol: subtoxic dose; (c) paracetamol: toxic dose. Details of calculations for energies of activation and phase transition temperatures are as given in the text. Each point represents mean of 10 independent experiments. Activation energies are expressed as KJ/mol.
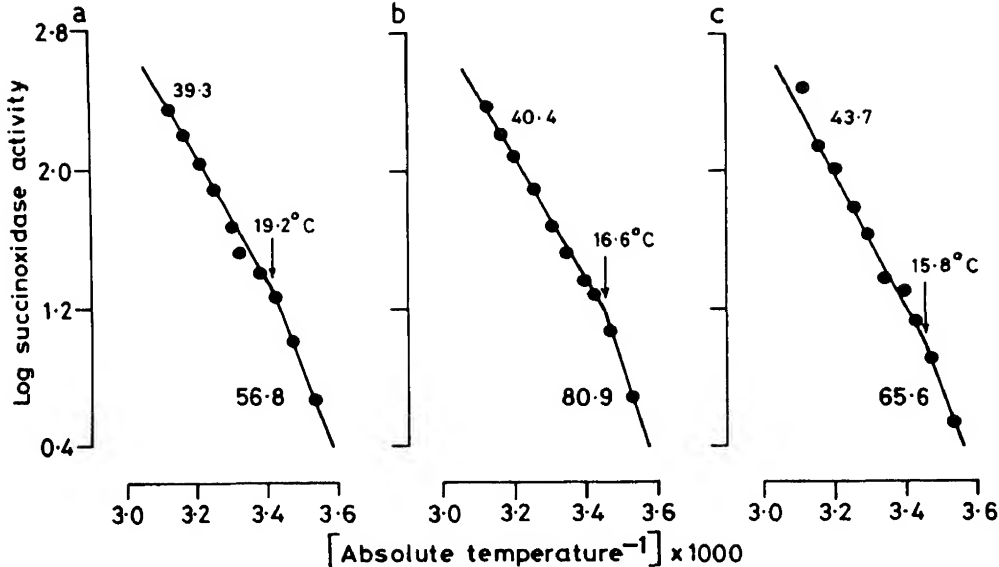
Figure 2. Arrhenius plots of temperature-dependent changes in succinoxidase activity in rat liver SMP. (a) Control; (b) paracetamol: subtoxic dose; and (c) paracetamol: toxic dose. The experimental details are as given in the text and figure 1. Each point represents mean of 9 independent experiments.

in the low temperature range (E_2) was not altered (table 1). In contrast, treatment with toxic doses of paracetamol caused a 43% decrease in E_1 without any effect on E_2 or Tt although the latter exhibited a tendency to decrease (2°C).

The results in figure 2 show the Arrhenius plots for succinoxidase activity and the values of E_1 and E_2 and Tt are summarized in table 1. It is clear that the subtoxic doses of paracetamol resulted in a 44% increase in the value of E_2 without any change in the value of E_1. However, Tt decreased by 2·4°C which was statistically significant (figure 2, table 1). Toxic doses of paracetamol resulted in a further decrease in Tt (3·4° decrease) without any change in the values of E_1 or E_2.

The Arrhenius plots for Mg^{2+}-ATPase activity are depicted in figure 3. It is apparent that the pattern was practically identical for the control and the subtoxic-dose-group. However, in the toxic-dose-group, the E_2 decreased by 29%, while Tt increased by 2·7°C (table 1).

4. Discussion

In the present studies we have shown that NADH oxidase activity in SMP decreased from 15 to 30% over the entire temperature range examined in the animals receiving toxic doses of paracetamol. The observed decrease in NADH oxidase activity correlates well with our earlier observations on generalized impairment in coupled respiration rates with NAD^+-linked substrates i.e. glutamate, β-hydroxybutyrate and pyruvate + malate (Katyare and Satav 1989). On the other hand, succinoxidase and Mg^{2+}-ATPase activities were generally in the
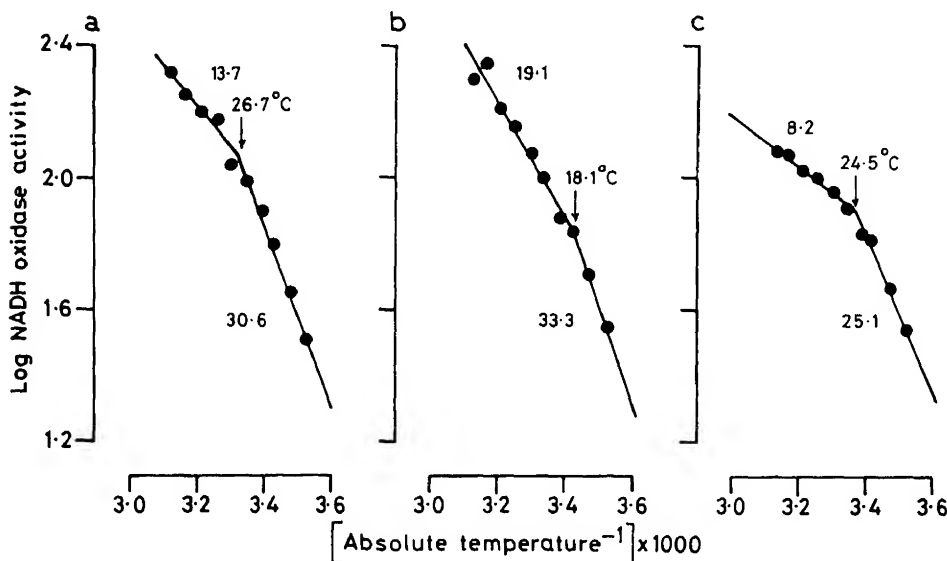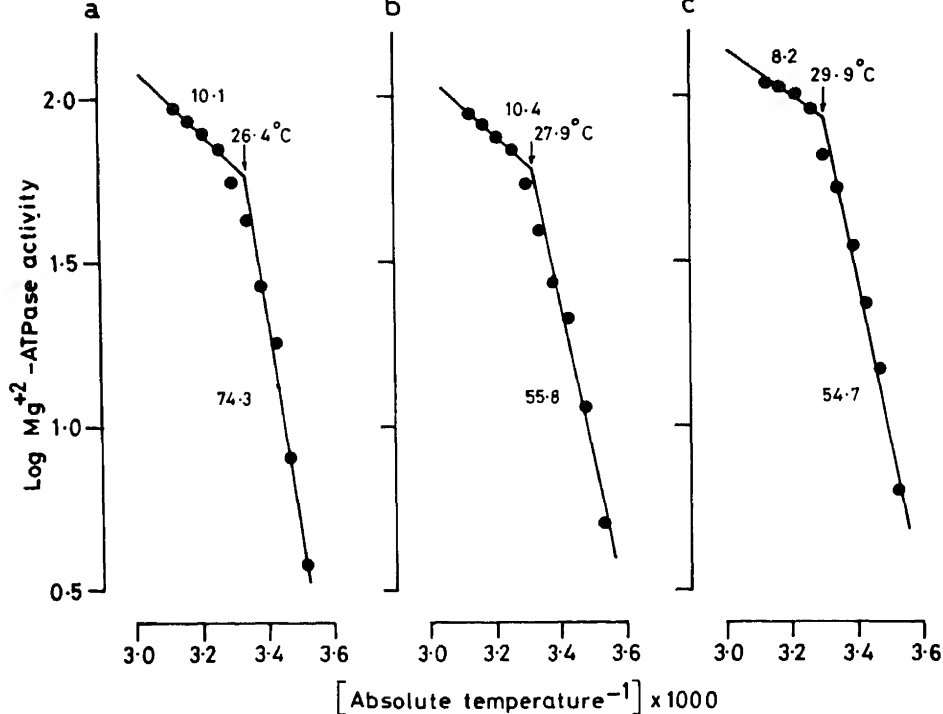
Figure 3. Arrhenius plots of temperature-dependent changes in Mg^{2+}-ATPase activity in SMP from rat liver. (a) Control; (b) paracetamol: subtoxic dose; (c) paracetamol: toxic dose. Other experimental details are as given in the text and figure 1. Each point represents mean of 10 independent experiments.

same range as in the control and the two paracetamol-treated groups (data not given), although the coupled (state 3) respiration rate with succinate had increased in the group receiving the subtoxic dose and decreased in those animals receiving toxic doses of paracetamol (Katyare and Satav 1989).

Arrhenius kinetic studies revealed that the subtoxic doses of paracetamol resulted in an increase in the energy of activation at high temperature range (E_1) for NADH oxidase with concomitant substantial lowering in the phase transition temperature (9°C). Subtoxic doses resulted in an increased value of E_2 in succinoxidase system with a decrease in Tt, while for the Mg^{2+}-ATPase activity all the above parameters were unaffected (table 1).

Toxic dose treatment, on the other hand, brought about a decrease in the values of E_1 only for the NADH oxidase activity and lowered the value of E_2 for Mg^{2+}-ATPase system. The phase transition temperature was lowered for succinoxidase, while its value increased for Mg^{2+}-ATPase. Thus, the effects of subtoxic and toxic doses of paracetamol were differential and sometimes of opposite nature depending upon the enzyme system under study and the dose of paracetamol employed.

The three respiratory enzymes which we have studied are membrane bound and require lipids for their activity (Raison 1972; Ashraf et al 1980; Tzagoloff 1982). It is now well recognized that the changes in lipid composition alter membrane fluidity and energies of activation of membrane-associated enzymes (Raison et al 1971;

Table 1. Effects of *in vivo* paracetamol treatment on kinetic parameters of NADH oxidase, succinoxidase and Mg^{2+}-ATPase activities in SMP from rat liver.

Enzyme	Treatment group	Phase transition temperature (Tt) (0°C)	Energy of activation (KJ/mol)	
			High temperature range (E_1)	Low temperature range (E_2)
NADH oxidase	Control (10)	27·3±0·98	13·9±1·11	30·9±1·54
	Subtoxic (10)	18·3±0·85****	19·1±1·02***	33·1±1·57NS
	Toxic (10)	25·5±1·69NS	8·0±0·74****	27·6±2·12NS
Succinoxidase	Control (9)	19·1±0·74	39·7±1·53	55·1±3·51
	Subtoxic (9)	16·7±0·63*	39·6±0·74NS	79·1±4·49****
	Toxic (9)	15·7±0·35****	43·9±2·10NS	64·4±3·19NS
Mg^{2+}-ATPase	Control (10)	27·0±0·99	11·9±0·90	74·5±7·25
	Subtoxic (10)	25·8±1·60NS	11·5±0·66NS	58·7±3·98NS
	Toxic (10)	29·7±0·61*	9·3±1·14NS	52·8±3·42**

The experimental details are as described in the 'materials and methods' section. Results are given as mean ±SE of number of independent experiments indicated in the parentheses.

$*P < 0.05$; $**P < 0.02$; $***P < 0.002$; $****P < 0.001$; NS not significant.

enzyme complexes studied could be due to alterations in lipid microdomains of these enzyme systems caused by paracetamol treatment. Drug-induced changes in lipid metabolism have been previously reported with imipramine and desipramine (Albouz *et al* 1982; Fauster *et al* 1983). It would therefore be of interest to examine if paracetamol intoxication also leads to alterations in membrane lipid composition.

The observed impairment in the mitochondrial energy-linked functions (Katyare and Satav 1989) and alterations in phase transition temperatures and activation energies could also be due to membrane lipid peroxidation, since lipid peroxidation has been suggested to be responsible for paracetamol-induced tissue damage (Wendel *et al* 1979). Paracetamol-induced lipid peroxidation would change the degree of unsaturation of fatty acids in the lipid domains of the membrane resulting in alterations in the membrane fluidity and activities of the membrane bound enzymes (Raison 1972). Alternatively, it is also possible that the two doses of paracetamol employed may have led to differential adduct formation with mitochondrial proteins and enzyme proteins (Hinson *et al* 1981; Dixon 1984). Interestingly, Potter *et al* (1974) have reported that a reactive metabolite of paracetamol, N-acetyl-*p*-benzoquinoneimine is generated by the hepatic mixed-function oxidase system in amounts sufficient to exceed its detoxification. This metabolite binds to critical macromolecules causing disturbed cellular homeostasis and eventual cell death (Potter *et al* 1974). In addition, paracetamol is known to alter the Ca^{2+} permeability, Ca^{2+} release and cause swelling of mitochondria (Beatrice *et al* 1984; Meyers *et al* 1988). Therefore, it is also likely that altered intracellular Ca^{2+} homeostatis may be responsible for impairment in the mitochondrial functions (Schanne *et al* 1979), however, we have not examined this possibility in the present studies.

The data presented here do not pinpoint which of the factors discussed above play a predominant role. More direct experiments will be necessary to ascertain these possibilities. Nevertheless, the present studies clearly show that the toxic and even the subtoxic doses of paracetamol bring about alterations in the kinetic properties of mitochondrial enzyme systems which are intimately associated with energy transduction processes.

References

Albouz S, Tocque B, Hauw J J, Boutry J M, Lesaux F, Bourden R and Baumann N 1982 Tricyclic antidepressant desipramine induces stereo-specific opiate binding and lipid modifications in rat glioma C_6 cells; *Life Sci.* 31 2549–2554

Ashraf J, Somasundaram T and Jayaraman J 1980 Assembly of succinic dehydrogenase complex into mitochondrial membrane in yeast; *Biochem. Biophys. Res. Commun* 97 263–269

Beatrice M C, Stiers D L and Pfeffer D R 1984 The role of glutathione in the relation of Ca^{2+} by liver mitochondria; *J. Biol. Chem.* 259 1279–1287

Bergmeyer H U and Bernt E 1963 Glutamate oxaloacetate transaminase; in *Methods of enzymatic analysis* (ed.) H U Bergmeyer (New York, London: Academic Press) vol 1, pp 837–845

Breen K J, Bury R W, Desmond P V, Forge H R, Mashford M L and Whelan G 1982 Paracetamol self-poisoning: Diagnosis, management and outcome; *Med. J. Aust.* 1 77–79

Chance B and Williams G R 1955 Respiratory enzymes in oxidative phosphorylation: Kinetics of oxygen utilization; *J. Biol. Chem.* 217 383–393

Cobden I, Record C O, Ward M K and Kerr D N S 1982 Paracetamol-induced acute renal failure in the absence of fulminant liver damage; *Br. Med. J.* 284 21–22

enzymes following experimental-thyrotoxicosis; *J. Biosci.* **14** 341-349

Dixon M F, Dixon B, Aparicio S R and Loney D P 1975 Experimental paracetamol-induced hepatic necrosis: A light and electron microscope and histochemical study; *J. Pathol.* **116** 17-29

Dixon M F 1984 Histopathological and enzyme changes in paracetamol-induced liver damage; in *Advances in inflammation research* (eds) K D Rainsford and G P Velo (New York: Raven press) pp 169 178

Fauster R, Honegger U and Wiesmann U 1983 Inhibition of phospholipid degradation and changes of the phospholipid pattern by desipramine in cultured human fibroblasts; *Biochem. Pharmacol.* **32** 1739-1744

Fiske C H and Subba Row Y 1925 The colorimetric determination of phosphorous; *J. Biol. Chem.* **66** 375-400

Ginsberg G L and Cohen S D 1985 Plasma membrane alterations and covalent binding to organelles after an hepatotoxic dose of acetaminophen; *Toxicologist* **5** 154

Hinson J A, Pohl L R, Monks T J and Gillette J R 1981 Acetaminophen-induced hepatotoxicity; *Life Sci.* **29** 107-116

Hulbert A J, Augee M L and Raison J K 1976 The influence of thyroid hormones on the structure and function of mitochondrial membrane; *Biochim. Biophys. Acta* **455** 597-601

Jallow D J, Mitchell J R, Potter W Z, Davis D C, Gillette J R and Brodie B B 1973 Acetaminophen-induced hepatic necrosis: II. Role of covalent binding *in vivo*; *J. Pharmacol. Exp. Ther.* **187** 195-202

Katyare S S and Rajan R R 1988 Enhanced oxidative phosphorylation in rat liver mitochondria following prolonged *in vivo* treatment with imipramine; *Br. J. Pharmacol.* **95** 914-922

Katyare S S and Satav J G 1989 Impaired mitochondrial oxidative energy metabolism following paracetamol-induced hepatotoxicity in the rat; *Br. J. Pharmacol.* **96** 51-58

Lowry O H, Rosebrough N J, Farr A L, and Randall R J 1951 Protein measurement with Folin-phenol reagent; *J. Biol. Chem.* **193** 265-275

McClain C J 1982 Late presentation of acetaminophen hepatotoxicity: An unresolved problem; *Dig. Dis. Sci.* **27** 375-376

Meyers L L, Beierschmit W P, Khairallah E A and Cohen S D 1988 Acetaminophen-induced inhibition of hepatic mitochondrial respiration in mice; *Toxicol. Appl. Pharmacol.* **93** 378-387

Mitchell J R, Jollow D J, Potter W Z, Davis D C, Gillette J R and Brodie B B 1973 Acetaminophen-induce hepatic necrosis 1. Role of drug metabolism; *J. Pharmacol. Exp. Ther.* **187** 185-199

Newton J F, Yoshimoto M, Bernstein J, Rush G F and Hook J B 1983 Acetaminophen nephrotoxicity in the rat. 2. Strain differences in nephrotoxicity and metabolism of P-aminophenol, a metabolite of acetaminophen; *Toxicol. Appl. Pharmacol.* **69** 307-318

Potter W Z, Thorgeirsson S S, Jallow D J and Mitchell J R 1974 Acetaminophen-induced hepatic necrosis. V. Correlation of hepatic necrosis, covalent binding and glutathione depletion in hamsters; *Pharmacology* **12** 129-143

Raison J K, Lyon J M and Thomson W W 1971 The influence of membrane on the temperature-induced changes in the kinetics of some respiratory enzymes of mitochondria; *Arch. Biochem. Biophys.* **142** 83-90

Raison J K 1972 The influence of temperature-induced phase changes on the kinetics of respiration and other membrane-associated enzyme system; *Bioenergetics* **4** 285-309

Satav J G and Katyare S S 1982 Effect of experimental thyrotoxicosis on oxidative phosphorylation in rat liver, kidney and brain mitochondria; *Mol. Cell. Endocrinol.* **28** 178-189

Schanne F A X, Kane A B, Young E E and Farber J L 1979 Calcium dependence of toxic cell death: A final common pathway; *Science* **206** 700-702

Shallom J M and Katyare S S 1985 Altered synaptozomal ATPase activiy in the rat brain following prologed *in vivo* treatment with nicotine; *Biochem. Pharmacol.* **34** 3445-3449

Tzagoloff A 1982 The mitochondrial adenosine triphosphatase; in *Mitochondria* (ed.) P Seikevitz (New York: Plenum press) pp 157-179

Wendel A, Feurstein S and Konz K H 1979 Acute paracetamol intoxication of starved mice leads to lipid peroxidation *in vivo*; *Biochem. Pharmacol.* **28** 2051-2059

Effect of thyroidectomy and subsequent treatment with triiodothyronine on kidney mitochondrial oxidative phosphorylation in the rat

J G SATAV and S S KATYARE*†

Biochemistry Division, Bhabha Atomic Research Centre, Trombay, Bombay 400 085, India
*Present address: Department of Biochemistry, Faculty of Science, M S University of Baroda, Baroda 390 002, India

Abstract. The effect of thyroidectomy (Tx) and subsequent treatment with triiodothyronine (T_3) on rat kidney mitochondrial oxidative phosphorylation was examined. Thyroidectomy resulted in lowering of state 3 respiration rates and cytochrome contents. Thyroidectomized animals administered with T_3 (20 μg/100 g body wt) resulted in the nonsynchronous stimulation of state 3 respiration rates in kidney mitochondria with glutamate, β-hydroxybutyrate, succinate and ascorbate + TMPD as substrates. Cytochrome contents were also elevated differentially. Increase in the state 4 respiration rates was transient and reversible. However, primary dehydrogenases were not generally altered in the Tx and T_3- treated Tx animals. The results thus indicate that the T_3-treatment to Tx animals brings about differential and nonsynchronous increase in the respiratory parameters and respiratory chain components of kidney mitochondria.

Keywords. Thyroidectomy; triiodothyronine; kidney mitochondria; respiratory parameters.

1. Introduction

Thyroid hormones influence multiple physiological functions such as cell growth and differentiation, protein synthesis and basal metabolic rate. Their effects, especially on the mitochondrial metabolic activities are well documented (Tata *et al* 1963; Tata 1964, 1966; Satav *et al* 1973; Rajwade *et al* 1975; Katyare *et al* 1977; Nunez 1988). Thus, hypothyroidism in general, results in decreased metabolic activities and the treatment of hypothyroid animals with physiologic doses of thyroid hormones restores these activities to an almost normal level (Tata *et al* 1963; Katyare *et al* 1970, 1977).

Earlier studies from our laboratory had shown that the thyroid hormone effects on mitochondrial metabolism were tissue-specific and brought out an interesting point that the kidney mitochondria were most sensitive to the hormonal action, whether it was thyroid deficiency (Rajwade *et al* 1975; Katyare *et al* 1977) or T_3-induced thyrotoxicosis (Satav and Katyare 1982). Additionally, it was also found that thyroid hormone deficiency caused a non-synchronous turnover of protein components in the kidney mitochondria (Rajwade *et al* 1975) i.e. the turnover of insoluble proteins and cytochrome c decreased without any changes being seen for the turnover of the 'other cytochromes' fraction (Rajwade *et al* 1975).

Since most of the earlier studies on thyroid hormone action on mitochondria reported in the literature deal with liver and muscle mitochondria (Tata 1964, 1966; Katyare *et al* 1970), it was of interest to examine the metabolic responses of kidney

assume importance in elucidating the tissue-specific action of thyroid hormone *e.g.*, the kidney nuclei possess practically the same number of binding sites for T_3 as the liver nuclei (Oppenheimer 1979), nevertheless, the response with respect to stimulation of phosphoenolpyruvate kinase is differential (Muller *et al* 1982; Sibrowski *et al* 1982; Muller and Seitz 1984).

Therefore, we have examined the time course of effects of a single injection of 3,3′,5-triiodothyronine (T_3) at physiologic dose (Satav and Katyare 1981) to thyroidectomized rats on various parameters of energy metabolism of kidney mitochondria.

2. Materials and methods

2.1 *Animals and T_3-treatment*

Weanling male albino rats of Wistar strain were surgically thyroidectomized (Katyare *et al* 1970; Satav *et al* 1973; Satav and Katyare 1981) and used after 8–10 weeks for further studies. Thyroidectomized (Tx) animals received a single injection of T_3 at a dose of 20 μg/100 g body weight as described earlier (Satav *et al* 1973). Control animals received only saline vehicle. The animals were killed at the end of 12, 24, 48 and 72 h after hormone/saline administration and kidney cortex mitochondria were isolated and washed once (Satav and Katyare 1982). State 3 and state 4 respiration rates were measured using Clark-type oxygen electrode as described by Katyare and Satav (1989). Substrates used were: glutamate, β-hydroxybutyrate, succinate and ascorbate + TMPD; with latter two substrates, 1 μM rotenone was also employed (Satav and Katyare 1982).

2.2 *Enzyme assays*

Succinate dehydrogenase and glutamate dehydrogenase activities were measured as described earlier (Rajwade *et al* 1975; Katyare and Satav 1989). β-hydroxybutyrate dehydrogenase activity was measured in sonicated mitochondria as described by Katyare and Satav (1989). Mitochondrial cytochrome contents were determined following the methods described earlier (Satav and Katyare 1982). Protein was estimated by the method of Lowry *et al* (1951).

Fine chemicals were purchased from sources described in an earlier communication (Katyare and Satav 1989).

3. Results

The results of the effects of thyroidectomy (Tx) and T_3-treatment of Tx animals on state of 3 respiration rates with various substrates are given in figure 1. Figure 1A gives the respiration rates as per cent of control while figure 1B shows these values as per cent of Tx. It is clear that the state 3 respiration rates in isolated kidney mitochondria from Tx animals decreased from 36 to 51% with four substrates used (figure 1A). After T_3-treatment to Tx animals, the respiration rates with glutamate and ascorbate + TMPD reached a value comparable to control on day 1 and then

Figure 1. Effect of T_3-treatment to thyroidectomized (Tx) animals on state 3 respiration rates in kidney mitochondria.

Tx animals were injected with 20 μg T_3/100 g body wt (s.c.) and were killed at various time intervals as indicated. Respiration rates are expressed as (**A**) per cent of control and (**B**) per cent of Tx. '0' time values represents the respiration rates in Tx. Substrates used: glutamate (○); β-hydroxybutyrate (●); succinate (×) and ascorbate+TMPD (△). Results and mean ± SEM of 10-18 observations. State 3 respiration rates in control for glutamate, β-hydroxybutyrate, succinate and ascorbate+TMPD were 40.2 ± 1.24; 30.81 ± 1.28; 119.43 ± 3.91 and 141.81 ± 17.78, nmol O_2/min/mg protein, respectively.

increased only slightly on day 2 and declined on day 3. For succinate, the control value was already reached within 24 h of T_3-treatment and at 72 h the value was still high as compared with control. For β-hydroxybutyrate the respiration was not affected up to 24 h, but reached the peak value comparable to control on day 2 and came back to Tx level on day 3. Thus, the patterns were quite different and specific for the substrate employed. These differences were further accentuated when the values were expressed as per cent of Tx. The profile for β-hydroxybutyrate was different as compared to the other substrates; a sharp peak on day 2 was seen with this substrate (figure 1B).

The pattern for state 4 respiration rates is shown in figure 2. When the respiration rates for various substrates were expressed as per cent of control (figure 2A), it was clear that the maximum stimulatory effect could be noted on day 1 after T_3 treatment; at 12 h post T_3-treatment respiration was stimulated only with glutamate and β-hydroxybutyrate. On day 2, the rates for these two substrates were still high (20 to 25% higher) compared to the controls but declined to about 80% of the
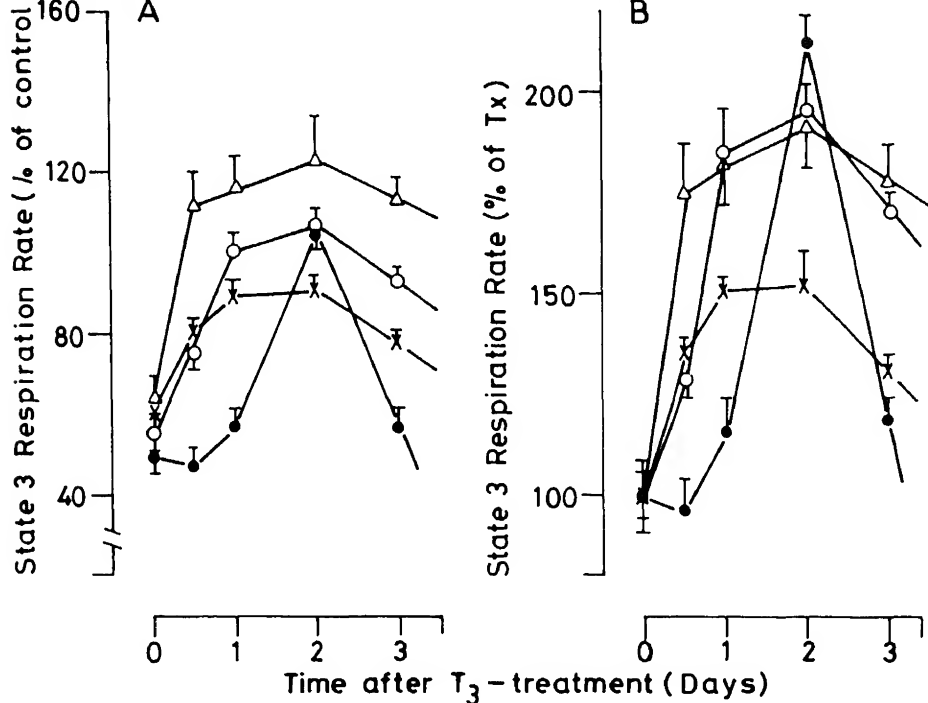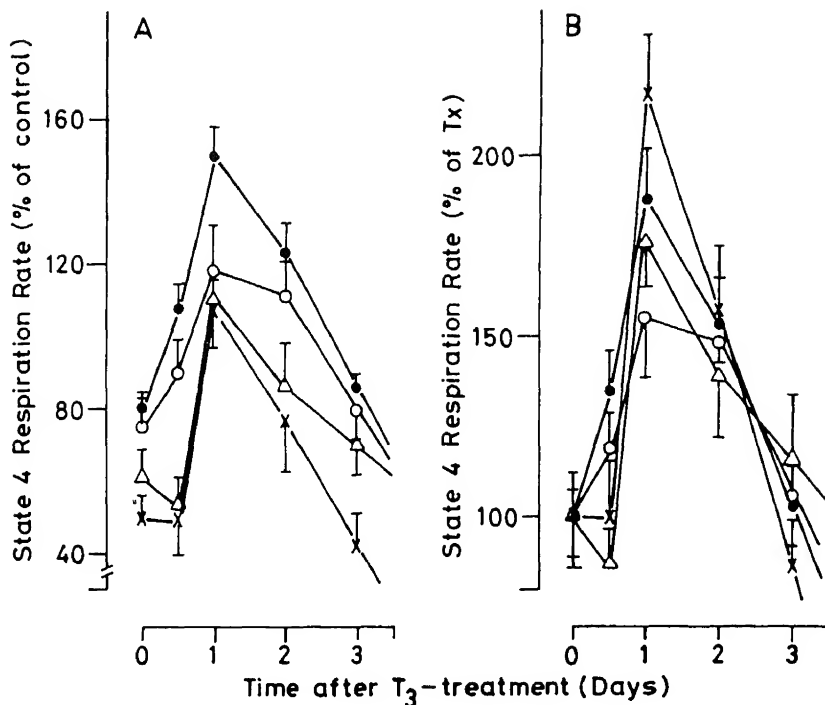
Figure 2. Effect of T_3-treatment to thyroidectomized (Tx) animals on state 4 respiration rates in kidney mitochondria.

Respiration rates are expressed as (A) per cent of control and (B) per cent of Tx. '0' time values represent the respiration rates in Tx animals. Results are given mean ± SEM of 10–20 observations. Other details are same as given in figure 1. Substrate used: glutamate (○); β-hydroxybutyrate (●); succinate (×) and ascorbate + TMPD (△). State 4 respiration rates in control mitochondria for glutamate, β-hydroxybutyrate, succinate and ascorbate + TMPD were 6·93 ± 0·74; 2·56 ± 0·59; 31·73 ± 2·80 and 52·71 ± 10·90, nmol O_2/min/mg protein, respectively.

control value by day 3. For succinate and ascorbate + TMPD, the rates had already decreased further to the basal Tx value by day 3 of the T_3 treatment. The effects were comparable even when expressed as per cent of Tx (figure 2B).

The results on mitochondrial cytochrome contents are given in table 1. Thyroidectomy brought about 52% and 66% decrease respectively in cytochrome aa_3, b and $c + c_1$ content which is consistent with our earlier findings (Katyare *et al* 1977). After T_3-treatment of the Tx animal, contents of cytochrome aa_3 and b increased as early as 12 h reaching the peak value on day 1 (figure 3A). These values then declined on day 2 and became comparable to those found at 12 h. The content of ·cytochrome b then decreased on day 3 considerably while the values of aa_3 remained more or less at the same level without further decrease. Cytochrome $c + c_1$ content increased marginally up to 24 h and reached a peak value on day 2 of T_3-treatment to subsequently decline on day 3. It was thus clear that the patterns of accretion and the turnover profiles were also specific for the given cytochrome species. In this context it is interesting to note that in T_3-treated thyroidectomized rats, the profile for cytochromes accretion in liver and skeletal muscle mitochondria

| Cytochrome | pmol of cytochrome/mg protein | | |
	Normal (7)	Tx (5)	Decrease (%)
aa_3	215 ± 11	103 ± 5*	52
b	273 ± 9	90 ± 30*	67
$c + c_1$	666 ± 26	229 ± 9*	66

Cytochromes were determined in Triton X-100 solubilized mitochondria from difference spectra of dithionite reduced minus ferricynide oxidized cytochromes.

Results are given as mean $\pm$ SEM of number of observations given in parentheses.

*$P < 0.001$ compared with normal.
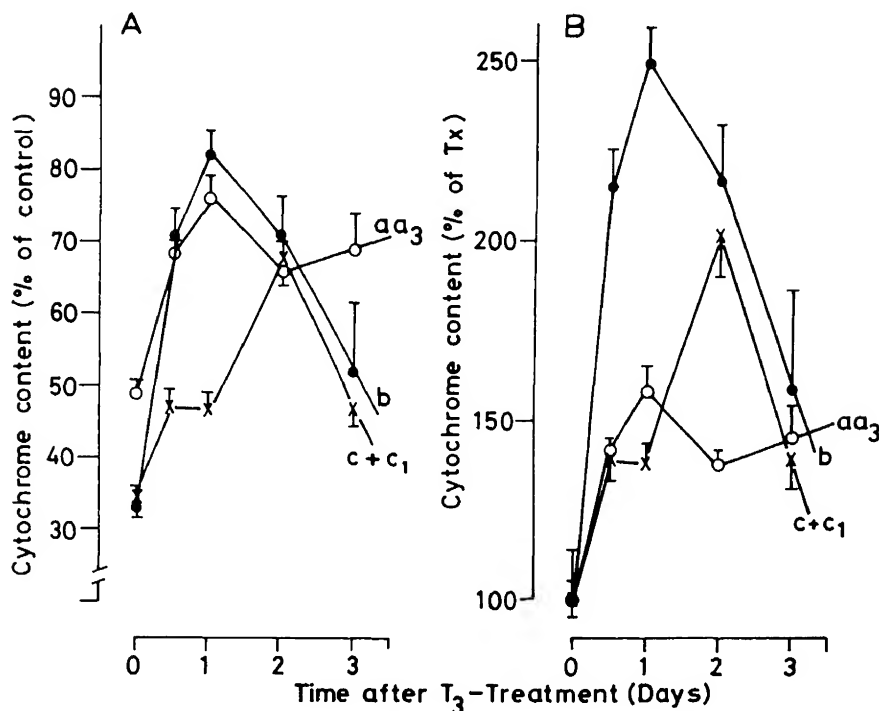
Figure 3. Changes in the cytochrome content of kidney mitochondria after T_3-treatment. Cytochromes were determined as described in the text. Results are given as (A) per cent of control and (B) per cent of Tx. '0' time values represents the cytochrome content in kidney mitochondria from Tx animals. Cytochrome aa_3 (O), b ($\bullet$) and $c + c_1$ ($\times$). Results are mean $\pm$ SEM of 6–8 independent observations.

from figure 3 that although the contents of all the cytochromes were elevated, the values were still 25–30% lower than the euthyroid controls. When the patterns were represented as per cent of Tx, it was apparent that the maximum stimulation was seen in cytochrome b synthesis followed by cytochrome $c + c_1$; synthesis of aa_3 was least stimulated amongst these cytochrome classes (figure 3B).
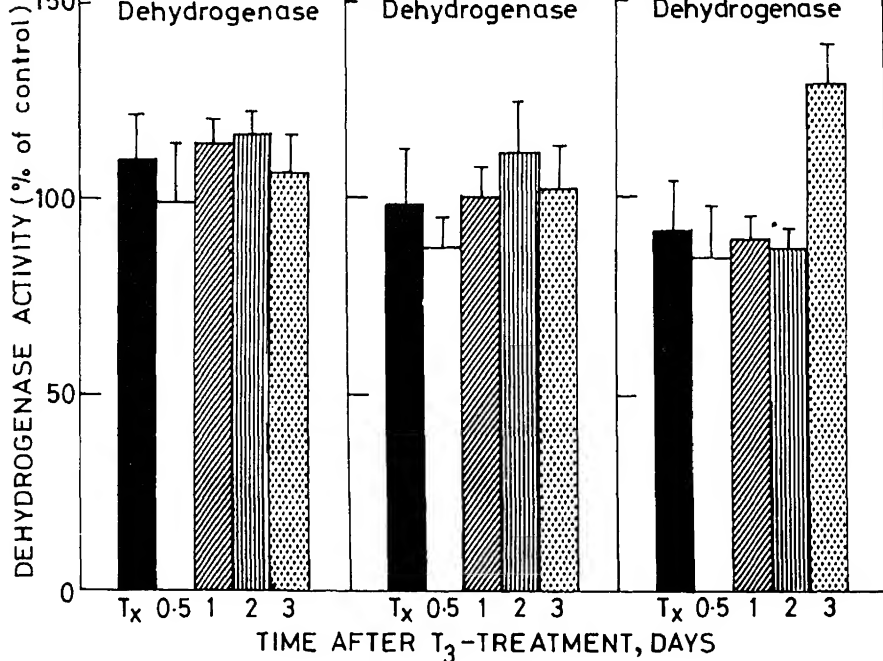
Figure 4. Changes in kidney mitochondrial dehydrogenases after T_3-treatment.

Enzyme activities were measured as described in text. Results are expressed as per cent of controls and are mean of 8 independent observations. 'Tx' represents the enzyme activities obtained in kidney mitochondria from thyroidectomized animals. Enzyme activities in control animals were: GDH : 52.47 ± 12.58 nmol NADH formed/min/mg protein; BDH : 219.74 ± 11.88 nmol NADH formed/min/mg protein; SDH : 55.29 ± 7.60 nmol DCIP reduced/min/mg protein.
*$P < 0.001$ compared with Tx or control.

We then examined the effects of thyroidectomy and T_3-treatment on the primary dehydrogenase activities. It is apparent that the dehydrogenase activities did not change significantly except in the case of succinate dehydrogenase which registered a small but reproducible increase at 72 h post T_3-treatment (figure 4).

4. Discussion

Since the early studies of Barker (1956) and Pittman *et al* (1961), the kidney has been recognized as a thyroid hormone responsive tissue with respect to oxygen consumption. This agrees well with the good correlation between the thyromimetic action of the hormone metabolites and nuclear receptor binding sites in the tissues reported earlier (Oppenheimer 1979, 1983). It has thus been reported that the number of T_3-binding sites which the kidney nuclei possesses is almost comparable to those of liver (Oppenheimer 1979, 1983; Muller and Seitz 1984). However, much of the work on thyroid hormone effects on the mitochondrial metabolism has been carried out either with liver or with skeletal muscle mitochondria rather than with kidney (Tata *et al* 1963; Tata 1964, 1966). Few scattered studies on the kidney are available which relate to thyroid hormone deficiency (Katyare *et al* 1977; Rajwade

(Hoch and Lipmann 1954; Maley and Lardy 1955; Satav and Katyare 1982) or thyroid powder was fed to animals (Kadenbach 1966). Besides, some of these studies deal mainly with kidney slices where a co-relationship between respiration and $Na^+ + K^+$-ATPase activity is sought (Somjen *et al* 1981). Occasionally, studies on thyroid-status dependent changes in $Na^+ + K^+$-ATPase activity are reported (Silva *et al* 1976).

Our interest in the thyroid hormone effects on kidney mitochondrial metabolism arose from our earlier observations that: (i) the kidney was the most sensitive tissue to the thyroid status (Rajwade *et al* 1975; Satav and Katyare 1982) and (ii) thyroid hormone deficiency caused a nonsynchronous turnover of kidney mitochondrial proteins (Rajwade *et al* 1975). Therefore it seemed most appropriate to find out in systematic studies if, as in the case of liver and skeletal muscle mitochondria (Gustafsson *et al* 1965; Gear 1970; Gross 1971; Rajwade *et al* 1975), thyroid hormones also constitute a factor for maintaining the synchrony of kidney mitochondrial functions.

The present results show that thyroid hormone deficiency resulted in impaired respiratory functions, but the effects were not uniform; rather they were substrate-specific (*e.g.* figures 1 and 2). Also, the contents of cytochromes decreased in a differential manner (table 1 and figure 3). Subsequently when the Tx animals were given T_3, the mitochondrial functions were restored more or less to normalcy, but once again the effects were differential and interestingly, non-synchronous. It would thus seem that the T_3-treatment triggered a series of non-synchronous events leading to a stimulation of respiration in kidney mitochondria. The results thus point out that the thyroid hormone effects on mitochondrial functions in the kidney are different from those described for liver and skeletal muscle mitochondria (Gustafsson *et al* 1965; Gear 1970; Gross 1971; Rajwade *et al* 1975). This observation is consistent with our earlier findings on nonsynchronous turnover of kidney mitochondrial protein components (Rajwade *et al* 1975). Such an observation is not altogether unexpected since thyroid hormone action is known to be tissue-specific (Katyare *et al* 1977; Nikodem *et al* 1981; Satav and Katyare 1981, 1982).

The tissue-specific action of thyroid hormones has been explained partly on the basis of the number of nuclear binding sites present in the responsive tissues (Oppenheimer 1979, 1983). Although, the mechanism of thyroid hormone action is not yet clearly understood, there exists a good correlationship between the number of nuclear T_3-receptors and thyromimetic action of hormone metabolites (Oppenheimer 1979, 1983; Muller *et al* 1982). It is believed that the early action of T_3 may be the regulation of synthesis of rapidly turning over mRNA (Seeling *et al* 1982) whose translational product secondarily exerts effects on DNA-dependent RNA polymerase, thus, regulating the synthesis of specific mRNA species (Muller and Seitz 1984; Mutvei and Nelson 1989). Recently, in a model system using rat liver nuclei, it has been shown that in thyroidectomized rats, 102 out of 500 proteins disappeared, but 13 reappeared at 6 h after thyroid hormone administration (Nikodem *et al* 1981; Muller and Seitz 1984); 67 additional proteins could be detected 24 h later (Nikodem *et al* 1981). Similar studies on mitochondrial proteins especially in the kidney should be interesting.

While the presence of nuclear receptors is well documented (Oppenheimer 1979, 1983), the thyroid hormone action at the target cell level seems to be pleiotypic

least binding sites in mitochondria, plasma membranes and cytosol has been reported (Oppenheimer 1983; Muller and Seitz 1984; Nunez 1988). Although the mitochondrial receptor is a controversial matter, it still deserves a comment. The presence of a specific binding site for thyroid hormones in mitochondria from various organs *i.e.* liver, kidney, intestine, heart, lung, skeletal muscle, etc. has been well described (Oppenheimer 1979; Hashizume and Ichikawa 1982; Muller and Seitz 1984; Nunez 1988). Interestingly, in kidney mitochondria, it has been reported that there are four and two binding sites, respectively, for the outer and inner mitochondrial membranes (Hashizume and Ichikawa 1982). Other workers, however, could demonstrate only non-specific binding sites on the outer membrane (Wahl *et al* 1977), while others failed to demonstrate a specific mitochondrial binding protein for T_3 (Greif and Sloane 1978). Interestingly, there is an isolated report by Shivakumar and Jayaraman (1986) claiming that the fish gill mitochondria have a T_4-specific receptor. The functional significance of the putative mitchondrial receptor is obscure, although it has been implicated in the early effects of thyroid hormones on mitochondrial respiration (Mutvei and Nelson 1989; Sterling 1986). Recently, Sterling (1986) has shown that T_3 at nM concentrations can stimulate respiration in mitoplasts from rat liver under *in vitro* conditions.

The earliest time point in the present studies was 12 h post T_3-treatment. Besides, physiological and not nM concentrations of T_3 were used in these studies. The effects we observed here are therefore not the early effects reported by others (Sterling 1986) but relate mostly to specific gene activation by thyroid hormones. In this connection the reported presence of totally six different binding sites for T_3 on kidney mitochondrial membranes seems to be interesting and deserves further elucidation (Hashizume and Ichikawa 1982).

Acknowledgement

References

Barker B S 1956 Metabolic action of thyroxine derivatives and analogs; *Endocrinology* **59** 548–554

Gear A R L 1970 Inner- and outer-membrane enzymes of mitochondria during liver regeneration; *Biochem. J.* **120** 577–587

Greif R L and Sloane D 1978 Mitochondrial binding sites for triiodothyronine; *Endocrinology* **103** 1899–1902

Gross N J 1971 Control of mitochondrial turnover under the influence of thyroid hormone; *J. Cell Biol.* **48** 29–40

Gustafsson R, Tata J R, Lindberg O and Ernster L 1965 The relationship between the structure and activity of rat skeletal muscle mitochondria after thyroidectomy and thyroid hormone treatment; *J. Cell Biol.* **26** 555–578

Hashizume K and Ichikawa K 1982 Localization of 3, 5, 3'-triiodothyronine receptor in rat kidney mitochondrial membranes; *Biochem. Biophys. Res. Commun.* **106** 920–924

Hoch F L and Lipmann F 1954 The uncoupling of respiration and phosphorylation by thyroid hormones; *Proc. Natl. Acad. Sci. USA* **40** 909–921

Kadenbach B 1966 Effect of thyroid hormones on mitochondrial enzymes; in *Regulation of metabolic processes in mitochondria* (eds) J M Tager, S Papa, E Quagliariello and E C Slater (Amsterdam: Elsevier) pp 508–517

and effects of triiodothyronine on their protein turnover; *Biochem. J.* **118** 111–121

Katyare S S, Joshi M V, Fatterpaker P and Sreenivasan A 1977 Effect of thyroid deficiency on oxidative phosphorylation in rat liver, kidney and brain mitochondria; *Arch. Biochem. Biophys.* **182** 155–163

Katyare S S and Satav J G 1989 Impaired mitochondrial oxidative energy metabolism following paracetamol-induced hepatotoxicity in the rat; *Br. J. Pharmacol.* **96** 51–58

Lowry O H, Rosebrough N J, Farr A L and Randall R J 1951 Protein measurement with the Folin phenol reagent; *J. Biol. Chem.* **193** 265–275

Maley G F and Lardy H A 1955 Efficiency of phosphorylation in selected oxidations by mitochondria from normal and thyrotoxic rat livers; *J. Biol. Chem.* **215** 377–388

Muller M J and Seitz H J 1984 Pleiotypic action of thyroid hormones at the target cell level; *Biochem. Pharamacol.* **33** 1579–1584

Muller M J, Thomsen A, Sibrowski W and Seitz H J 1982 3, 5, 3'-triiodothyronine induced synthesis of rat liver phosphoenolpyruvate carboxykinase; *Endocrinology* **111** 1469–1475

Mutvei A and Nelson D B 1989 The response of individual polypeptides of the mammalian respiratory chain to thyroid hormones; *Arch. Biochem. Biophys.* **268** 215–220

Nikodem U M, Trus B L and Rall J E 1981 Two-dimensional gel electrophoresis of rat liver nuclear proteins after thyroidectomy and thyroid hormone treatment; *Proc. Natl. Acad. Sci. USA* **78** 4411–4415

Nunez J 1988 Mechanism of action of thyroid hormone; in *Hormones and their actions* Part I (eds) B A Cooke, R J B King and Vander Molen (Amsterdam: Elsevier) pp 61–80

Oppenheimer J H 1979 Thyroid hormone action at the cellular level; *Science* **203** 971–979

Oppenheimer J H 1983 The nuclear receptor triiodothyronine complex: Relationship to thyroid hormone distribution, metabolism and biological action; in *Molecular basis of thyroid hormone action* (eds) J H Oppenheimer and H H Samuels (New York: Academic Press) pp 1–34

Pittman C S, Lindsay R H and Barker B S 1961 Specificity of T_4 action on oxygen uptake of kidney slices during prolonged incubation; *Endocrinology* **69** 761–768

Rajwade M S, Katyare S S, Fatterpaker P and Sreenivasan A 1975 Regulation of mitochondrial protein turnover by thyroid hormones; *Biochem. J.* **152** 379–387

Satav J G and Katyare S S 1981 Thyroid hormone and Cathepsin D activity in rat liver, kidney and brain; *Experientia* **37** 100–101

Satav J G and Katyare S S 1982 Effect of experimental thyrotoxicosis on oxidative phosphorylation in rat liver, kidney and brain mitochondria; *Mol. Cell. Endocrinol.* **28** 173–189

Satav J G, Rajwade M S, Katyare S S, Netrawali M S, Fatterpaker P and Sreenivasan A 1973 Significance of promitochondrial structures in rat liver for mitochondrial biogenesis; *Biochem. J.* **134** 687–695

Seeling S, Jump D B, Towle M C, Liaw C, Mariash C N, Schwartz H L and Oppenheimer J H 1982 Paradoxical effects of cycloheximide on the ultra-rapid induction of two hepatic mRNA sequences by triiodothyronine (T_3); *Endocrinology* **110** 671–673

Shivakumar K and Jayaraman J 1986 Salinity adaptation in Fish: Interaction of thyroxine with fish gill mitochondria; *Arch. Biochem. Biophys.* **245** 356–362

Sibrowski W, Muller M J, Thomsen A and Seitz M J 1982 Renal phosphoenolpyruvate carboxykinase turnover in hypo- and hyper-thyroid rat *in vivo*; *Biochim. Biophys. Acta* **717** 20–25

Silva P, Torretti J, Hayslett J P and Epstein F H 1976 Relation between $Na^+ + K^+$-ATPase and respiratory rate in the rat kidney; *Am. J. Physiol.* **230** 1432–1438

Somjen D, Ismail–Beigi F and Edelman I S 1981 Nuclear binding of T_3 and effect on QO_2, $Na^+ + K^+$-ATPase and α-GPDH in liver and kidney; *Am. J. Physiol.* **240** 146–154

Sterling K 1986 Direct thyroid hormone activation of mitochondria: The role of adenine nucleotide translocase; *Endocrinology* **119** 292–295

Tata J R 1964 Biochemical action of thyroid hormones at the cellular and molecular levels; in *Action of hormones on molecular processes* (eds) G Litwack and D Kritschevsky (New York: Wiley) pp 58–131

Tata J R 1966 The regulation of mitochondrial structure and function by thyroid hormone under physiological conditions; in *Regulation of metabolic processes in mitochondria* (eds) J M Tager, S Papa, E Quaglianello and E C Slater (Amsterdam: Elsevier) pp 489–507

Tata J R, Ernster L, Lindberg O, Arrhenius E, Pederson S and Hedman R 1963 The action of thyroid hormones at the cell level; *Biochem. J.* **86** 408–428

Wahl R, Geiseler D and Kallee E 1977 Absorption equilibria of thyroid hormones in liver cell; *Eur. J. Biochem.* **80** 25–33

Effect of naloxone on renal cortical microcirculation in haemorrhagic shock

R REGHUNANDANAN*, V REGHUNANDANAN and
R K MARYA

Department of Physiology, Medical College, Rohtak 124 001, India

Abstract. In order to assess the effect of opioid receptor antagonists, naloxone and noradrenaline, on renal cortical microcirculation, India ink infusion was made through the renal artery, one hour after treatment with each drug, in dogs subjected to haemorrhagic shock. Naloxone (1 mg/kg) treatment showed a dual beneficial effect of significant improvement ($P < 0.001$) in the mean arterial pressure without increasing the renal resistance as indicated by the presence of ink particles in about 75% of the cortical glomeruli. However, in the case of noradrenaline (2 μg/kg/min)-treated animals, although mean arterial pressure increased significantly ($P < 0.001$) only very few glomeruli (25%) in the cortical region showed ink particles, demonstrating severe vasoconstriction. In the control group infused only with saline, although most of the glomeruli (92%) were filled with ink particles, there was a significant decline in the mean arterial pressure ($P < 0.001$).

Keywords. Naloxone; renal microcirculation; haemorrhagic shock.

1. Introduction

Many laboratories have reported that haemorrhagic shock is associated with a decrease in the renal cortical blood flow (Carrier *et al* 1966; Logan *et al* 1971; Rector *et al* 1972). This decrease in outer cortical blood flow has been attributed to the enhanced sympathetic activity, increased release of catecholamines and diminished perfusion pressure. More recently a characteristic biphasic response in the renal nerve activity with an initial transient sympathetic activation followed by a more pronounced sympathetic inhibition during prolonged haemorrhagic shock has been reported by Skoog *et al* (1985) and Koyama *et al* (1988). The decrease in renal nerve activity during the later stages of hypovolemic shock appears to be mediated through opioid receptors (Burke and Dorward 1988). Endogenous opioid peptides released during haemorrhagic shock, play an important role in the cardiovascular suppression seen in haemorrhagic shock and the opioid receptor antagonist naloxone reverses these effects on the cardiovascular system (Holaday 1983). It is also reported from this laboratory (Reghunandanan *et al* 1988) that renal clearances are improved after administration of naloxone in haemorrhaged dogs. Schadt *et al* (1984) reported no significant change in the renal resistance after administration of naloxone in rabbits subjected to hypovolemic shock.

We have performed angiohistopathological studies on the renal cortex of dogs subjected to haemorrhagic shock, to determine whether the opioid antagonist

*Corresponding author.
Abbreviation used: MAP, Mean arterial pressure.

91

Twenty one Mongrel dogs of either sex were used for the present study. They were anaesthetized with Nembutal (sodium pento barbitone), 30 mg/kg intravenously (i.v.). Soft endotracheal tubes were inserted in the trachea after tracheostomy to make them breathe atmospheric air spontaneously. Femoral vessels of both sides were exposed and cannulated. The femoral artery of one side was connected to a polygraph for recording blood pressure while that of the other side was used for producing haemorrhage. The femoral vein of one side was used for infusion of drugs and saline. Renal vessels were exposed by a flank incision. After 30 min of surgery the animals were administered heparin (250 units/kg body weight) and bled over a period of 15 min until a mean arterial pressure (MAP) of 45 mm Hg was achieved (t_0). The MAP was maintained at this pressure for 1 h $(t_0 - t_{60})$ by adjusting the height of the bottle in which the shed blood was collected. The average loss of blood in each animal during this period was 43.5 ± 1 ml/kg body weight. After 1 h, i.e. at t_{60}, the reservoir was clamped and the drug treatment started for the different animal groups. Either naloxone as i.v. bolus in a dose of 1 mg/kg in 2 ml of saline or noradrenaline (2 μg/kg/min) as i.v. infusion in 0.5 ml of saline per min was administered. The control group of animals received only saline at 0.5 ml/min i.v.

After 1 h of treatment with drugs at t_{120} min India ink was infused through the renal artery under arterial pressure till it started coming out through the renal vein. Immediately the vessels were ligated and the kidneys removed before sacrificing the animals with overdosage of Nembutal. Since the saline-treated animals died before t_{120} in our previous experiment (Reghunandanan et al 1988), in the present case, the kidneys were removed from this group of animals just before death i.e. at t_{90}. Each of the kidneys was fixed in 10% formalin solution. Blocks from the cortical region of the kidney were made. Sections were cut and stained with haematoxilin and eosin after routine processing. Kidneys of three dogs without haemorrhage were also perfused with India ink and processed in the same way. Three hundred glomeruli were counted under high power objective (40 ×) from each kidney taken from various regions of the cortex. Statistical analysis was performed by using Student's paired t test and χ^2 test.

3. Results

MAP increased significantly $(P < 0.001)$ in both noradrenaline- and naloxone-treated groups of animals subjected to haemorrhagic shock (table 1). In the control group of animals infused only with saline the blood pressure deteriorated further $(P < 0.001)$. The section of the normal dog's kidney showed that almost all the glomeruli in the cortical region were completely filled with India ink particles (table 2). Only about 25% of the glomerular capillaries were partially filled with India ink in the renal cortex of the dogs subjected to haemorrhagic shock and treated with noradrenaline whereas about 75% of the glomeruli were partially filled with ink particles in the case of the naloxone group of animals (table 2). Statistical analysis

	A (Basal)	B (t_{60})	C (t_{120})	P value B vs C
Naloxone	118 ± 4.0	45 ± 2.2	81 ± 3.4	< 0.001
Noradrenaline	116 ± 6.8	45.5 ± 1.6	80 ± 6.0	< 0.001
Saline	112 ± 3.1	45.0 ± 0.5	30 ± 3.0	< 0.001

Values are mean $\pm$ SE. For saline group values at column C are taken at t_{90}. The number of animals in each group is 6.

Table 2. Status of the renal cortical glomerular perfusion after infusing India ink through renal artery in various groups of dogs.

Experimental group	Glomeruli counted	Glomeruli perfused	Perfusion (%)
Normal (no haemorrhage)	900	880	98
Naloxone	900	672	75
Noradrenaline	900	140	25
Saline	900	825	92

The number of animals in each group is 3.

of the data (χ^2 test) revealed that the difference between the two groups was highly significant ($P < 0.01$). In the control group of dogs, the kidneys taken just before death (t_{90}) showed ink particles in a majority of the glomeruli (92%).

4. Discussion

In the present study MAP deteriorated significantly ($P < 0.001$) from 45 ± 0.5 (t_{60}) to 30 ± 3 (t_{90}) in the control group of dogs subjected to haemorrhagic shock. At the same time it is interesting to note that there was a reduction in the renal resistance as indicated by the presence of ink particles in the majority of the glomeruli (92%) in the cortical region of the kidney perfused with India ink and removed just before the death of the animal at t_{90} min. These observations demonstrate a decrease in total peripheral and renal resistance. This might be due to sympathetic inhibition, as reported by Skoog *et al* (1985) and Koyama *et al* (1988), that increased renal nerve activity at the beginning of haemorrhage decreased significantly when the hypotension is prolonged. Endogenous opioid peptides released during shock may also be responsible for this effect (Burke and Dorward 1988).

On the other hand in noradrenaline (2 μg/kg/min)-treated dogs there was a severe vasoconstriction in the cortical region of the kidney as indicated by the observation that only very few glomeruli (25%) and its surrounding area of the cortex showed ink particles (table 2) at t_{120} min. This is in spite of the significant increase in the MAP from 45 mm Hg at t_{60} to 80 mm Hg at t_{120} (table 1). The increased renal vasoconstriction seen in this case is supported by reports that sympathetic fibers are found mainly in the renal cortex, and intrarenal infusion of noradrenaline produces

death (Mitchel 1951; Frank *et al* 1956; Carrier 1969).

In the group of animals treated with the opioid receptor antagonist naloxone, after haemorrhage, a majority (75%) of the glomerular capillaries in the cortical region were partially filled with ink particles (table 2). This histological picture is indicative of the partial patency of the majority of the vasculature in the cortical region even at the low flow state. There was also improvement in MAP in this case (table 1). A supporting and correlating observation for this change in the vasculature of the kidney with increased MAP is provided by the improvement in the renal clearances observed in the previous study (Reghunandanan *et al* 1988). Naloxone treatment while improving MAP in haemorrhagic shock also produces the dual benefit of not increasing total peripheral resistance (Lechner *et al* 1985), renal resistance (Schadt *et al* 1984) and preventing its decline in the later stages of shock. Endogenous opioid peptides released during haemorrhagic shock may limit the sympathetic activity including that of renal nerve activity (Burke and Dorward 1988; Koyama *et al* 1988). This may be responsible for the decreased norepinephrine release seen during haemorrhagic shock (Schadt and Gaddis 1984). Naloxone, by antagonizing this peptide-mediated effect, removes the limit and allows the sympathetic activity to continue. Alpha adrenergic receptors appear to mediate this effect as it is attenuated by phenoxy benzamine pretreatment (Bond *et al* 1985; Lechner *et al* 1985).

To conclude, the outcome of this study suggests that any drug which can improve both cardiovascular status and renal function without increasing renal resistance, can be of immense help in combating the circulatory derangements associated with haemorrhagic shock. In this context, naloxone seems to meet the requirements.

References

Bond R F, Bond C H, Peissner L C and Manning E S 1981 Adrenergic responses of gracillis arteries removal during hemorrhagic hypotension and shock; *Circ. Shock* **8** 411–423

Burk S L and Dorward P K 1988 Influence of endogenous opiates and cardiac afferents on renal nerve activity during hemorrhage in conscious rabbits; *J. Physiol.* **402** 9–27

Carrier S, Thorburn G D, Morchor C C O and Barger A L 1966 Intra renal distribution of blood flow in dogs during hemorrhagic hypotension; *Circ. Res.* **19** 167–179

Carrier S 1969 Effect of norepinephrine isoproterenol and adrenergic blockers upon intra renal distribution of blood flow; *Can. J. Physiol. Pharmacol.* **47** 199–208

Frank E D, Frank A H, Jood S, Veisel H A, Korman H and Fine J 1956 Effect of norepinephrine on circulation of the dog in hemorrhagic shock; *Am. J. Physiol.* **186** 74–75

Holaday J W 1983 Cardiovascular effects of endogenous opiate systems; *Annu. Rev. Pharmacol. Toxicol.* **23** 541–594

Koyama S, Aibiki M, Kanai K, Fiyiter T and Miyakawa K 1988 Role of central nervous system in renal nerve activity during prolonged hemorrhagic shock in dogs; *Am. J. Physiol.* **254** R761–769

Lechner R B, Gurll N J and Reynolds D G 1985 Role of autonomic nervous system in mediating response to naloxone in canine hemorrhagic shock; *Circ. Shock* **16** 279–295

Logan A, Jose G, Eisner J, Lilienfield F and Slotkoff L C 1971 Intra cortical distribution of renal blood flow in circulatory shock in dogs; *Circ. Res.* **29** 257–266

Mitchel C A G 1951 The intrinsic renal nerves; *Acta Anat.* **13** 1–15

Rector J B, Stein J H, Bay W H, Osgood R W and Ferris T F 1972 Effect of hemorrhage and vasopressor agents on distribution of renal blood flow; *Am. J. Physiol.* **222** 1125–1131

catecholamines on renal function and survival in hemorrhagic shock in dogs; *Indian J. Med. Res.* **87** 516–520

Schadt J C, McKown M D, McKown D P and Franklin D 1984 Hemodynamic effects of hemorrhage and subsequent naloxone treatment in conscious rabbits; *Am. J. Physiol.* **247** R497–508

Schadt J C and Gaddis R R 1985 Endogenous opioid peptides may limit norepinephrine release during hemorrhage; *J. Pharmacol. Exp. Ther.* **232** 656–660

Skoog P, Mason J and Thoren P 1985 Changes in the renal sympathetic outflow during hypotensive hemorrhage in rats; *Acta Physiol. Scand.* **125** 655–660

Instructions to authors

Authors should send papers to: The Editor, 'Journal of Biosciences', Indian Academy of Sciences, P. B. No. 8005, C. V. Raman Avenue, Bangalore 560 080.

Three copies of the paper must be submitted.

The papers must present results of original work. Submission of the manuscript will be held to imply that it has not been previously published and is not under consideration for publication elsewhere; and further, that if accepted, it will not be published elsewhere.

Authors are invited to suggest names and addresses of three experts who in their opinion can review the paper. The choice of referees will however remain with the editorial board.

Typescript

Papers must be typed (on one side only) double-spaced and with a 30 mm margin on all sides on *white bond paper (280 × 215 mm)*. This also applies to the abstract, tables, figure captions and the list of references each of which should be typed on separate sheets.

Title page

- The title of the paper must be brief and contain words useful for indexing. Serial titles are to be avoided.
- The names with initials of authors and the address of the institution where the work was carried out must be given.
  An abbreviated running title of not more than 50 letters (including spaces) must also be given.
  The address for communication (with telephone, telex and fax numbers, if available), should be given.

Abstract

Papers must have an abstract (typed on a separate page) of not more than 200 words summarizing the significant results reported.

Keywords

Three to six keywords must be provided.

Text

The paper must be divided into sections preferably starting with 'Introduction' and ending with 'Discussion'.
The main sections should be numbered 1, 2 etc., the sub-sections 1.1, 1.2, etc., and further sub-sections (if necessary) 1.1a, 1.1b, etc.
- All measurements should be given in SI units.
- Avoid numbers at the beginning of a sentence, but if you have to use them, spell them.
- Taxonomic affiliation such as phylum, order and Family as well as the common name of the main study organism should be given in the title or at the first mention unless such information is likely to be obvious to a broad range of biologists.
  The scientific names of genera and species are printed in italics and should be underlined in the typescript.
- Authority for names of taxa should be cited in the summary and at the first mention of a taxon in the text, but not elsewhere.
- Accepted common names of plants and animals (and other organisms) and of plant and animal or other diseases should neither be capitalized nor placed within quotation marks.
- Words and phrases not of English origin and not in common use (*e.g. in vitro, in situ*) are printed in italics and should therefore be underlined.

Tables

- All tables must be numbered consecutively in arabic numerals in the order of appearance in the text.
- Tables should be self-contained and have a descriptive title.
  Details of the experiment (not mentioned in the text) may be indicated below the table as a legend.

- *Please do not submit photographs of line drawings.*
- Good photocopies of all figures should accompany each copy of the typescript.
- Photographs should be numbered consecutively along with the figures in arabic numerals in the order of appearance in the text. They should be assembled together suitably to form one or more plates.
- Do not include line drawings and photographs in the same plate.
- Photographs should be sharp, of high contrast and on glossy paper with an indication of the scale.
- Xerox copies of photographs are unsatisfactory for refereeing; three prints of each photograph should be submitted, both black and white and colour photographs are welcome.

References

References should be cited in the text by author and year, not by number. If there are more than two authors, reference should be made to the first author followed by *et al* in the text. References at the end of the paper should be listed alphabetically by authors' names, followed by initials, year of publication, full title of the paper, name of the journal (abbreviated according to the World List of Scientific Periodicals, Butterworths, London), volume number, initial and final page numbers. References to books should include: name(s) of author(s), initials, year of publication, title of the book, edition if not the first, initials and name(s) of editor(s) if any, preceded by ed(s), place of publication, publisher, and pages referred to. References to these must include the year, the title of the thesis, the degree for which submitted and the university.

Examples

Mani A and Prabhu V K K 1986 Significance of critical development stage on starvation induced endocrine mediated precocious metamorphosis in *Oryctes rhinoceros* (Coleoptera: Scarabaeidae); *Proc. Indian Acad. Sci. (Anim. Sci.)* **95** 379–385

Zar J H 1974 *Biostatistical analysis* (New Jersey: Prentice Hall)

Samiwala E B 1987 *DNA cloning in Haemophilus influenzae*, Ph. D thesis, University of Bombay, Bombay.

Ramanna M S and Hermsen J H Th 1979 Genome relationships in tuber-bearing Solanums; in *Biology and taxonomy of Solanaceae* (eds) J G Hawkes, R N Lester and A G Skelding (London: Academic Press) pp 647–654

Abbreviations, symbols, units etc

The authors should follow *internationally agreed rules* especially those adopted by the IUPAC-IUB Commission on Biochemical Nomenclature (CBN). The journal will essentially follow the rules defined in the IUPAC *Manual of symbols and terminology for physico-chemical quantities and units* (Butterworths, London), 1970. Enzyme names may be abbreviated except on the first occasion, when the full name and abbreviation in parenthesis should be given.

Footnotes

Footnotes to the text should be avoided if possible but when essential should be numbered consecutively and typed on a separate sheet.

Proofs

Proofs sent to the authors together with a reprint order form must be returned to the editorial office within two days of their receipt (preferably by speed post or courier and definitely not by registered post). Delayed despatch of corrected proofs will delay publication. In order to minimize the corrections and alterations in the proof stage, authors are requested to prepare the manuscript carefully before submitting it for publication.

Reprints

100 reprints will be supplied free of charge.

Manuscripts not conforming to these specifications will be returned.

Direct correlation between the circadian sleep-wakefulness rhythm and time estimation in humans under social and temporal isolation

M K CHANDRASHEKARAN*, G MARIMUTHU, R SUBBARAJ,
P KUMARASAMY, M S RAMKUMAR and K SRIPATHI

Department of Animal Behaviour and Physiology, School of Biological Sciences, Madurai
Kamaraj University, Madurai 625 021, India

Abstract. Several bodily functions in humans vary on a 24 h pattern and most of these variations persist with a circadian period of *ca* 25 h when subjects are studied under conditions of social and temporal isolation. We report in this paper that the estimates of short time intervals (TE) of 2 h are strongly coupled to the circadian rhythm in sleep-wakefulness. There is a linear correlation between the number of hours humans stay awake (α) and their estimation of 2 h intervals. The coupling of TE to α appears to obtain only under conditions of physical well-being.

Keywords. Human circadian rhythms; sleep-wakefulness; temperature; freeruns; dissociation; biological oscillators and models.

1. Introduction

It is well established that almost all the bodily functions in the human organism show a 24 h (daily) variation and that these rhythms are in synchrony with sleep and wakefulness as well as with the alternation of day and night (Aschoff and Wever 1981). In subjects living in isolation without any time cues these rhythms persist, as they do in plants and in animals (Bünning 1973), with a circadian period of *ca* 25 h (Wever 1979). In the absence of entraining stimuli such as light/darkness and social cues, the rhythms freerun.

We have investigated the circadian rhythms in bodily functions of human subjects since November 1987 in a specially constructed and equipped 'human isolation facility' for periods of 15–35 days. So far experiments have been completed on 8 human subjects (6 men and 2 women) between the ages of 24 and 35 years. The social and temporal isolation of the subjects was total and rigorous. In two cases the subjects freeran impressively, their sleep-wakefulness cycles at times approximating circabidian periods of 48 h. We have reported in a recent paper (Chandrashekaran *et al* 1991) that a 24-year-old female subject experienced 22 subjective days while in isolation in the actual experimental duration of 35 calendar days. All experimental subjects stated on coming out of the isolation facility that they believed they had followed a 24 h schedule of sleep and wakefulness.

In spite of three decades of intense experimentation it is still not known how the passage of time is perceived by humans living in social isolation. We have investigated how human subjects in our isolation facility estimated 2 h intervals without the aid of watches or clocks. Aschoff (1985) first reported the correlation between estimation of duration of 1 h and the number of hours the subject stayed

TE (time estimates) of 2 h and hours of wakefulness (α). We found... different that TE are coupled with the circadian rhythm underlying sleep-wakefulness.

2. Materials and methods

The subjects lived in $25' \times 25'$ isolation quarters with fortified walls and no windows. Cool air was passed through a duct with sound muffles and the room was ventilated. A kitchenette, a bath room with toilet, refrigerator, bicycle ergometer, weighing scales, blood pressure (BP) monitor, books, writing materials, a video cassette player (with timer cut-off), beds, table, chairs and all facilities for cooking were available. The isolation facility was well lit by fluorescent tubes and the ambient lighting ranged from 1,300 to 1,800 l_x depending on the distance from the source of light. The subjects turned lights on and off at will and experienced darkness only during hours of sleep.

The subjects did not have access to clocks or any other cues to civil time but two of the subjects did have access to a stop-watch. All indications of measured activities were given by pressing the appropriate buttons on a panel which activated the writing stylets of an event recorder. Various channels of the event recorder (which was placed outside the isolation living quarters) were used for the different time series data on 2 h TE, breakfast, lunch, dinner, snacks, naps, toilet, to bed, wakeup, mental alertness tests, BP measurements etc. All our estimated TE readings were made by the subjects themselves, inevitably only during hours of wakefulness. The core (rectal) temperature and locomotor activity (wrist movements) were recorded continuously during sleep and wakefulness with a temperature probe and an ambulatory monitor connected to a Solicorder and Apple IIe set-up with an interface card which was replaced every 4–6 days. The data presented here on 2 h estimates (TE) represent 110 data points which were obtained from seven human subjects living in isolation for periods of 15–35 days. In practice, for TE of 2 h the human subjects pressed the appropriate button on the panel once every presumed 2 h.

3. Results

Humans almost always underestimate the passage of time when they live in isolation without external or societal time cues. In keeping with this tendency the sleep-wakefulness cycles also lengthen their period (τ). The TE of 2 h of six of our seven subjects 'contracted' and 'dilated' as a function of correspondingly shorter and longer spells of α in the same subject. The correlation between TE and α extended also to individual subjects as shown in table 1. Figure 1 illustrates how the 2 h TE are directly correlated with α. In the course of our experiments we could even predict how long the subject was likely to stay up that day on the basis of the first two or three TE readings at the beginning of that subjective day.

Figure 2 contains the TE data, which are random and independent of α, of a deviant subject, a 29-year-old male. It might be of general interest to note that this individual slept only for very short periods of 1·5–4·0 h in a sleep-wake cycle (as against the range of hours of sleep (ρ) values of 6·0–18 h of other subjects). Further, he contracted fever on day 4 of the experiment which was unfortunately detected

2	27	0·377	0·10
3	15**	0·902	<0·01
4	10	0·432	NS
5	15*	0·541	0·05
6	19**	0·613	<0·01
7	09	0·606	0·01

NS, Not significant.
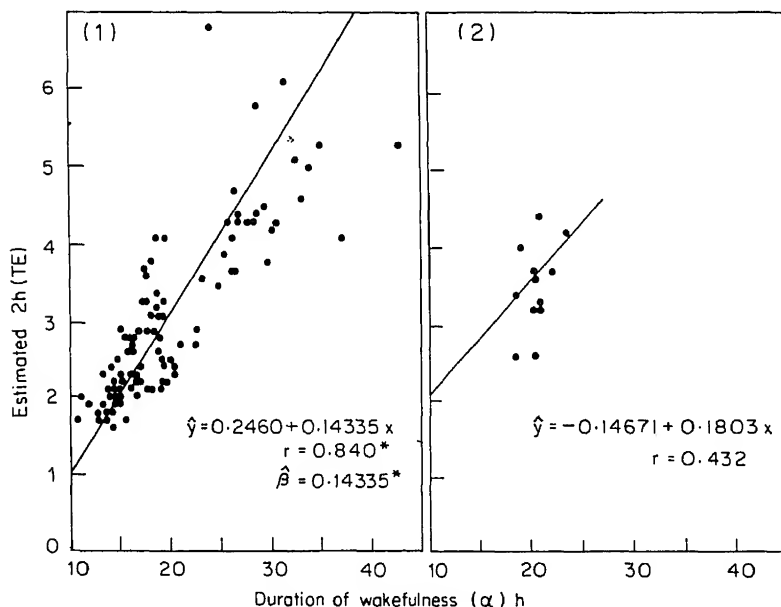
Figures 1 and 2. 1. The direct correlation between 2 h TE and α representing 110 data points made on seven human subjects living in social isolation for periods of 15–35 days. Each point represents the mean estimates of 5–7 readings made during one 'day' *Significant at $P < 0.01$. 2. The lack of correlation between 2 h TE and α in the human subject who showed curtailed sleep of 1·5–4·0 h per cycle and lived in isolation for 15 days.

only on day 15 from the printout data of our Solicorder when the experiment was prematurely terminated and the subject came out of isolation quarters.

4. Discussion

In reporting the dependence of 1 h time estimates on α Aschoff (1985) remarked "..... it must be admitted that a reconfirmation of the results reported here by other methods ... would be worthwhile". This is accomplished in the present report. It is worth pointing out that the first three participants were not aware of the dependence of TE on α nor of Aschoff's paper. No human subject studied so far

(1990) has made another interesting observation, namely that locomotor activity and α are negatively correlated in humans during isolation. It will be of considerable interest to further investigate if artificial shortening or lengthening of α will result in contracting and dilating TE and if locomotory activity will also show homeostatic adjustments in accordance with variations in α.

Aschoff (1985) found that short time estimates of 10, 20, 30 and 120 s are independent of the duration of α and claimed that "... somewhere between 120 s and 1 h the perception of time seems to change from being independent to being dependent on α". In contrast, we find a correlation of TE of 1 and 2 min with α values longer than 20 h (unpublished). It would appear from our findings on TE that it is difficult to precisely measure the interval at which TE switches from independence to dependence on α. The values of α seem to be more critical in the equation between TE and α. TE of 2 h of all our subjects show a strong correlation with α. We are unable to explain our finding that TE is a function of α in humans in isolation, a finding which suggests that the human mind 'knows' already at the time. of waking how long the day will last. The coupling of TE with the α of the circadian rhythm we are reporting, is reminiscent of the coupling of ultradian courtship song cycles of *ca* 1 min in *Drosophila melanogaster* with τ of the circadian rhythm in their locomotory activity (Konopka and Benzer 1971; Kyriacou and Hall 1980; Yu *et al* 1987).

All subjects adjusted meal timings in consonance with α so that the midday lunch was roughly midway through α, as was reported by Aschoff (1985). Although TE could be made only during α, the correlation between the two suggests that α and TE are coupled with the basic circadian rhythm underlying sleep and wakefulness. The circadian sleep-wakefulness rhythm and the circadian rhythm modulating core temperature dissociated only in one case in our studies. Data obtained by Aschoff (1985) and our own data from desynchronized rhythms clearly demonstrate that TE are not related to the circadian clock that controls the rhythms of autonomic functions such as body temperature. As we report in a recent communication (Chandrashekaran *et al* 1991) the menstrual cycle in a human female in isolation, contrary to TE, was not correlated with the circadian rhythm in sleep-wakefulness. These findings lend credence to models (Aschoff and Wever 1976) which postulate that the sleep-wakefulness rhythm and the body temperature rhythm are driven by two separate clocks. Since data of the kind obtained on our deviant subject and illustrated in figure 2 cannot be easily replicated, we speculate on the basis of existing data (which is not statistically significant) that the coupling of TE with α may be obtained only under conditions of physiological and physical harmony, and that under stressful conditions leading to discomfort and fever the coupling between the two might break down.

Arendt J, Minors D S and Waterhouse J M 1989 *Biological rhythms in clinical practice* (London: Wright)

Aschoff J 1985 On the perception of time during prolonged temporal isolation; *Human Neurobiol.* **4** 41–52

Aschoff J 1990 Interdependence between locomotor activity and duration of wakefulness in humans during isolation; *Experientia* **46** 870–871

Aschoff J and Wever R 1976 Human circadian rhythms: A multioscillator system; *Federation Proc.* **35** 2326–2332

Aschoff J and Wever R 1981 The circadian system of man; in *Handbook of behavioral neurobiology. Biological rhythms* (ed.) J Aschoff (New York: Plenum Press) vol 4, pp 311–331

Bünning 1973 *The Physiological clock* (London: English University Press)

Chandrashekaran M K, Geetha L, Marimuthu G, Subbaraj R, Kumarasamy P and Ramkumar M S 1991 The menstrual cycle in human female under social and temporal isolation is not coupled to the circadian rhythm is sleep-wakefulness; *Curr. Sci.* **60** 703–705

Konopka R J and Benzer S 1971 Clock mutants of *Drosophila melanogaster*; *Proc. Natl. Acad. Sci. USA* **68** 2112–2116

Kyriacou C P and Hall J C 1980 Circadian rhythm mutations in *Drosophila melanogaster* affect short-term fluctuations in the male's courtship song; *Proc. Natl. Acad. Sci. USA* **77** 6729–6733

Minors D S and Waterhouse J M 1981 *Circadian rhythms and the human* (London: Wright)

Wever R 1975 The circadian multioscillator system of man; *Int. J. Chronobiol.* **3** 19–55

Wever R 1979 *The circadian system of man* (New York: Springer)

Yu Q, Colot H V, Kyriacou C P, Hall J C and Rosbash M 1987 Behaviour modifications by *in vitro* mutagenesis of a variable region within the period gene of *Drosophila*; *Nature (London)* **326** 1082–1083

Why do ladybirds (Coleoptera: Coccinellidae) cannibalize?

B K AGARWALA*

Department of Biological Sciences, University of East Anglia, Norwich NR4 7TJ, England
*Present address: Department of Life Science, Tripura University, Agartala 799 004, India

Abstract. Cannibalism of eggs by larvae of *Adalia bipunctata*, an aphidophagous species of ladybirds, is important for survival when aphids are scarce. Ladybirds survive longer by eating eggs of their own species rather than aphids. Since it costs less, in terms of larval growth, to eat eggs rather than aphids, cannibalism has a strong advantage under conditions of prey scarcity.

Keywords. Ladybirds; aphidophagous coccinellids; cannibalism.

1. Introduction

Fox (1975) reviewed cannibalism in animals. Several studies have recognized that the predatory species of ladybirds show cannibalism of eggs and larvae (Banks 1956; Dixon 1959; Kaddou 1960; Brown 1972; Dimetry 1974; Osawa 1989; Agarwala and Dixon 1990).

Dixon (1959) considered egg cannibalism of ladybirds as an artifact of laboratory rearing and, therefore, of little ecological significance. Mills (1988), however, showed that density-dependent egg cannibalism of 6–30% occurred in *Adalia bipunctata* (L.) in the field. Osawa (1989) recorded that sibling and non-sibling cannibalism occurred throughout the oviposition period of *Harmonia axyridis* Pallas in the field.

The reproductive strategy of aphidophagous ladybirds has probably been adapted to the seasonality of aphid incidence. As a consequence, ladybirds are reproductively active for short periods when host plant quality favours population build-up of aphids (Hemptinne and Dixon 1991).

Ladybirds lay eggs in the vicinity of a high concentration of aphids (Dixon 1959) which enables the new born larvae to eat young aphids. Any interference in the form of intraspecific competition and/or population collapse of aphids may result in cannibalism in the larvae of ladybirds which are under tremendous pressure to complete development.

In this paper the conditions which favour cannibalism in ladybirds are examined.

2. Materials and methods

Adults of *A. bipunctata* were collected from the field in the summer of 1989 in eastern England and used for raising stock cultures in the laboratory at 20°C and a 16 h photoperiod. Rectangular plastic boxes (922 × 13 × 9 cu cm) were used to keep the adults and were provided with corrugated paper to facilitate the laying of eggs. Water-soaked tissue paper, fresh leaves of *Vicia faba* and plenty of fresh pea aphids, *Acyrthosiphon pisum* (Harris) were also provided. Pea aphids were obtained from a large culture developed on *Vicia faba* in the green house. A large culture of

Egg cultures were separated from the boxes at 2-day intervals and kept, one cluster each, in a 9 cm diameter Petri dish at 20°C and a 16 h photoperiod. New-born first instar larvae were transferred, 4–6 in number, to another 9 cm diameter Petri dish and offered adequate freshly obtained pea aphids at 2-day intervals until pupation.

Experiments were carried out in a clean, dry 5 or 9 cm Petri dish at 20°C and a 16 h photoperiod. Each of the experimental larvae was starved for 24 h prior to an experiment in order to induce the same level of hunger. Fourth instar and younger larvae of ladybirds were respectively offered fourth instar and second instar nymphs of aphids as food. Eggs of *A. bipunctata* were used as food wherever required. Fresh to dry weight conversion ratios were obtained by drying at 37°C for 6–10 days until constant weight.

2.1 *Do ladybirds eat eggs in the presence of prey?*

Two-day old fourth instar larvae were offered low (4), moderate (28) and high (44) quantities of fourth instar aphids. The choice of the number of aphids offered was tentative and approximately corresponded to the respective level of aphid infestation usually prevalent in the field. In addition, the ladybird larvae were provided with a cluster of 20 eggs (2-day old). Twenty of these larvae were tested at each aphid density. The number of eggs or aphids consumed was recorded after 1, 5 and 24 h.

2.2 *Do ladybirds differ in their daily feeding capacity on eggs and aphids?*

Two-day old first, second, third and fourth instar larvae were each offered an equal quantity of eggs (1–2-day old) and aphids (second instar nymph) by fresh weight. Twenty of these larvae of each instars were tested for 24 h to record the mean quantity of eggs and aphids eaten.

2.3 *Do ladybirds have the same duration of survival by eating either eggs or aphids?*

To determine this, individuals of similar age of each of the four larval instars of *A. bipunctata* were offered a fixed quantity of aphids (second instar nymphs) or eggs by fresh weight. Twenty of the larvae of each instars were tested and the length of time for which they survived after feeding was noted.

2.4 *Can larvae of A. bipunctata eat eggs and aphids with equal efficiency?*

This was determined by offering 2-day old fourth instar larvae an equal quantity of eggs (1–2-day old) or aphids (fourth instar nymphs) by fresh weight. Twenty such larvae were tested for the amount of eggs or aphids eaten.

2.5 *Relative nutritive values of eggs and aphids*

To determine this, 1-day old fourth instar larvae were fed a known weight of eggs

two foods needed to support similar growth rates were determined. The comparisons were made on a dry weight basis. Twenty of the fourth instar larvae were used to test the cost associated with eating aphids.

2.6 *Is cost the same by eating eggs of different age?*

To determine this, individual 1-day old first instar larvae were offered 1- or 4-day old eggs in a 5 cm diameter Petri dish in equal weights (0·40 mg). Twenty of the first instar larvae were tested for 24 h. Comparison was made on dry weight basis in terms of increase in weight of larvae.

3. Results

3.1 *Do ladybirds eat eggs in the presence of aphids?*

Egg cannibalism occurred at all aphid densities but was more pronounced at lower densities. The number of eggs eaten at aphid density 4 was significantly more than at 28 after 1, 5 and 24 h and one at 28 was significantly more than that at 44 after 24 h (table 1). Lower cannibalism at higher aphid density possibly resulted from a decline in the chances of encountering eggs as aphid density increased.

3.2 *Do ladybirds differ in their daily feeding capacity on eggs and aphids?*

Growing larvae of ladybirds show a gradual increase in their daily feeding capacity of aphids (Agarwala *et al* 1988).

In the present experiment the daily feeding capacity of all the four instars of larvae was significantly higher on aphids than eggs (table 2). Discernible variations were noticed between the larvae of different instars in their choice of eggs and aphids (figure 1). Older larvae ate proportionately more aphids than eggs compared to younger larvae.

Table 1. Mean number of eggs eaten at low (4), medium (28) and high (44) aphid densities by fourth instar larvae of *A. bipunctata* after 1, 5 and 24 h at 20°C.

Period after (h)	Mean no. of eggs eaten at aphid densities		df	t^*	P
	Low (4)	Medium (28)			
I	M SD	M SD			
1	2·45 ± 0·58	1·04 ± 0·25	38	4·0	< 0·001
2	8·57 ± 1·53	2·90 ± 0·96	38	7·87	< 0·001
24	17·95 ± 0·76	6·70 ± 1·37	38	22·90	< 0·001
II	Medium (28)	High (44)			
	M SD	M SD			
1	1·04 ± 0·25	0·87 ± 0·12	38	1·95	NS
5	2·90 ± 0·96	2·75 ± 1·01	38	0·30	NS
24	6·10 ± 1·37	5·20 ± 1·43	38	3·35	< 0·002

*t test for paired samples; NS, Not significant.

Larval instars	Mean quantity eaten (mg)		df	t*	P
	Eggs M SD	Aphids M SD			
I	0·403 ± 0·01	1·72 ± 0·26	19	12·65	< 0·001
II	0·979 ± 0·05	3·71 ± 0·86	19	9·76	< 0·001
III	2·465 ± 0·43	8·76 ± 1·02	19	11·51	< 0·001
IV	3·993 ± 0·78	12·13 ± 3·58	19	32·39	< 0·001

*t test for paired samples.
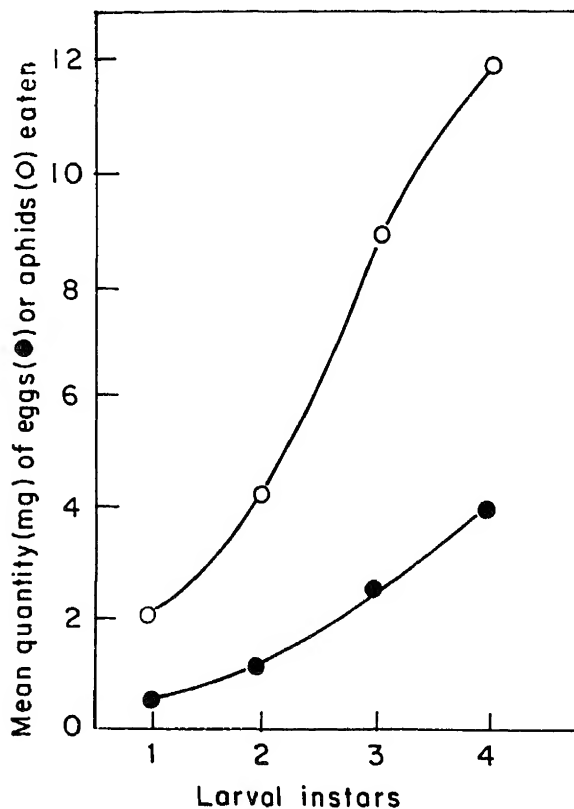
Figure 1. Variations in the choice of eggs and aphids eaten (Y) by the first (1), second (2), third (3) and fourth (4) instar larvae (X) of *A. bipunctata* after 24 h at 20°C.

3.3 *Do ladybirds have the same duration of survival by eating either eggs or aphids?*

Food affects the duration of developing larvae (Hukusima and Kouyama 1974). Duration of survival is linked to the nutrition value of the acceptable food.

Larvae of all the four instars survived significantly longer by feeding on eggs than aphids when given in equal quantities by fresh weights (table 3). This clearly indicates that eggs offer higher nutrition compared to aphids.

Food quantity	Mean duration of survival		df	t^*	P
	Eggs M ± SD	Aphids M ± SD			
1·4	6·15 ± 0·59	3·85 ± 0·87	19	9·114	<0·001
2·5	6·13 ± 0·91	4·80 ± 0·76	19	4·65	<0·001
4·0	5·85 ± 1·46	4·60 ± 0·94	19	3·10	<0·001
4·7	11·95 ± 1·05	5·75 ± 0·72	19	23·99	<0·001

or paired samples.

Table 4. The total quantity of aphids and eggs supplied, mean quantity eaten and not eaten by a fourth instar larva of *A. bipunctata* in 24 h at 20°C.

Food	Total quantity (mg)	Mean quantity (mg)	
		Eaten M ± SD	Not eaten M ± SD
Eggs	4·85	4·68 ± 0·72	0·17 ± 0·04
Aphids	4·91	4·17 ± 0·12	0·74 ± 0·03
df	19	19	19
t^*	1·09	4·74	6·03
P	NS	<0·001	<0·001

$^*t$ test for paired samples.

Can larvae of A. bipunctata eat eggs and aphids with equal efficiency?

g found that larvae of ladybirds show no inhibition in eating eggs it was
whether larvae can use aphids with equal efficiency.
r 24 h a fourth instar larva used a significantly higher quantity of eggs than
s (table 4). Most of the eggs were eaten in whole, and a few seem to have been
by the action of mandibles which possibly resulted in the loss of a little
nt of egg-yolk. In the case of aphids, the non-used amount consisted of
dages and, in some cases, head, including rostrum.

Relative nutritive value of eggs and aphids

birds do not lay unlimited eggs. Therefore, it was natural to know the cost
ated with eating eggs.
urth instar larvae required a much greater biomass of aphids than eggs for a
r growth rate (table 5). This clearly shows that it costs less to eat eggs in
of larval growth.

s cost of eating eggs of different age the same?

of *A. bipunctata* have an incubation period of 5–6 days at 20°C and a 16 h

| Food | Mean quantity given (mg) | Mean weight eaten (mg) | | Growth rate of larvae (mg/day) |
		Fresh weight M SD	Dry weight M SD	M SD
Aphids	48·0	43·6 ± 0·69	8·4 ± 0·15	1·7 ± 0·3
Eggs	16·56	15·7 ± 0·50	2·5 ± 0·10	1·7 ± 0·3
df		38	38	38
t*		69·4	77·0	0·1
P		< 0·001	< 0·001	NS

*t test for paired samples. NS, Not significant.

Table 6. Increase in fresh and dry weights of 1-day old first instar larvae of *A. bipunctata* after 24 h when provided with 1- and 4-day old eggs in equal quantity by weight.

| Age of eggs | Increase in weight (mg) | |
	Fresh weight M SD	Dry weight M SD
1-day old	0·31 ± 0·09	0·073 ± 0·012
4-day old	0·14 ± 0·05	0·048 ± 0·07
df	19	19
t*	6·79	4·12
P	<0·001	<0·001

*t test for paired samples.

photoperiod. First instar larvae, soon after hatching, are the potential predators to encounter eggs of different age.

There was a significantly higher increase in the dry weight of the first instar larva by eating 1-day old eggs than 4-day old eggs (table 6). This indicates that it costs more to eat older eggs containing embryos and, therefore, they are preferred less when compared to 1-day old eggs which largely contain the egg-yolk.

4. Discussion

The results reported here suggest that larvae of ladybirds will cannibalize eggs in the presence of aphids but the intensity of cannibalism is greater when aphids are scarce (table 1). This implies that the occurrence of cannibalism is possibly linked to the chances of encountering eggs in relation to aphids. At higher aphid density, less cannibalism is linked to a higher encounter of aphids than eggs which are immobile and defenceless.

Although the daily feeding capacity of eggs in all the four instars of ladybird larvae is much less compared to that on aphids (table 2), larvae show a higher duration of survival on eggs (table 3). Survival of new-born larvae of ladybirds is much dependent on the abundance of young aphids. Young larvae must complete development before aphid population collapses. In the event of aphid population collapse, larvae are under tremendous pressure to survive on alternate food.

itions favouring aphid scarcity also promote cannibalism in ladybirds. A
ibalizing larva not only improves its chances of survival but also eliminates
ntial competitors. Fresh eggs, being more nutritive, are preferred to the older
when conditions favour cannibalism (table 6).

though the level of egg cannibalism by ladybirds is low when aphids are
idant, nevertheless, cannibalism occurs in the field (Mills 1988; Osawa 1988). It
herefore, not surprising that a ladybird larva eats eggs more efficiently than
ds (table 4). Since it costs less to eat eggs than aphids in terms of larval growth
e 5), egg cannibalism would be a distinct advantage to ladybirds even at higher
density.

rcumstances which shape the attack strategy of ladybirds in the selection of
are little understood. Being predators, ladybirds are expected to orient their
k on target food by assessing its availability. One of the possibilities is to prefer
er and assured food supply for themselves and their offspring rather than to go
maller and unsure availability of eggs at higher prey density. This behaviour is
y to increase their fitness under natural conditions.

us, cannibalism is important for survival when aphids are scarce. Ladybirds,
ever, should first locate aphids to ensure adequate food availability for their
reproductive needs and their offspring.

rences

vala B K, Das S and Sen Chowdhuri M 1988 Biology and food relations of *Micraspis discolor* (F.):
aphidophagous coccinellid in India; *J. Aphidology* **2** 7–17
vala B K and Dixon A F G 1991 Cannibalism and interspecific predation by ladybirds; in *Ecology*
Aphidophaga (eds) A F G Dixon and I Hodek (Budapest: Academia) (in press)
C J 1956 Observations on the behaviour and mortality in Coccinellidae before dispersal from the
g shells; *Proc. R. Entomol. Soc. London* **A31** 56–60
n H D 1972 The behaviour of newly hatched coccinellid larvae (Coleoptera: Coccinellidae); *J.*
ntomol. Soc. South Afr. **35** 149–157
try N Z 1974 The consequences of egg cannibalism in *A. bipunctata* (Coleoptera: Coccinellidae);
ntomophaga **19** 445–451
A F G 1959 An experimental study in the searching behaviour of the predatory coccinellid beetle
dalia decempunctata (L.); *J. Anim. Ecol.* **28** 259–281
R 1975 Cannibalism in natural populations; *Annu. Rev. Ecol. Syst.* **6** 87–106
tinne J L and Dixon A F G 1991 Why ladybirds have generally been so ineffective in biological
ntrol; in *Ecology of Aphidophaga* (eds) A F G Dixon and I Hodek (Budapest: Academia) (in press)
sima S and Kouyama S 1974 Life histories and food habits of *Menochilus sexmaculatus* Fabricius
oleoptera: Coccinellidae); *Res. Bull. Fac. Agric. Gifu Univ.* **36** 19–20
ou I 1960 The feeding behaviour of *Hippodamia quinquesignata* (Kirby); *Univ. Calif. Publ. Entomol.*
181–232
N J 1988 Voracity, cannibalism and coccinellid predation; *Ann. Appl. Biol.* **101** 144–148
a N 1989 Sibling and non-sibling cannibalism by larvae of a ladybeetle *Harmonia axyridis* Pallas
oleoptera: Coccinellidae) in the field; *Res. Popul. Ecol.* **31** 153–160

Kairomones of *Heliothis armigera* and *Corcyra cephalonica* and their influence on the parasitic potential of *Trichogramma chilonis* (Trichogrammatidae: Hymenoptera)

T N ANANTHAKRISHNAN*, R SENRAYAN, S MURUGESAN and R S ANNADURAI

Entomology Research Institute, Loyola College, Madras 600 034, India

Abstract. Kairomones from moth scales tend to influence the parasitic potential by *Trichogramma chilonis* Ishii. Hexatriacontane, pentacosane, heptadecane, docosane and 2, 6, 10-dodecatrienal-3, 7, 11-trimethyl were identified from the active moth scale extract of *Heliothis armigera* Hubner (its natural host) and *Corcyra cephalonica* Stainton (a laboratory host). The significance of an array of compounds from moth scales with kairomonal activity for manipulating entomophagous insects in biological control programmes is discussed.

Keywords. Kairomones; *Heliothis armigera*; *Corcyra cephalonica*; *Trichogramma chilonis*; biological control of insects.

1. Introduction

Trichogramma chilonis is widely distributed in the Indian subcontinent and is responsible for large-scale mortality of the American boll worm *Heliothis armigera* in several crops and efficiently controls other lepidopteran and heteropteran insect pests (Manjunath *et al* 1985). Successful establishment, retention in target sites and manipulated behaviour of natural enemies are important components of a successful biological control programme (Gross *et al* 1975). Use of chemicals emanating from the host and its by-products which enhance the behavioural dynamics of entomophages increasing their effectiveness were advocated by Brown *et al* (1970), Whittaker and Feeny (1971) and Lewis *et al* (1975a). Lewis *et al* (1975b) showed that the efficiency of *Trichogramma* sp. released into the field was significantly improved by the application of the kairomone, tricosane. Studies by Gross *et al* (1975), Nordlund *et al* (1976, 1984), Lewis *et al* (1982), Elzen *et al* (1984) and Nordlund (1987) clearly suggest that kairomones originating from both the hosts and their food sources influence the searching, attacking and retention of entomophagous insects. This is an aspect of great interest in biological control programmes.

Shu and Jones (1989) observed the klinokinetic and orthokinetic behaviour of *Trichogramma nubilale* Ertle and Davis in response to kairomones from the scales of its host, *Ostrinia nubilalis* (Hubner), while Shu *et al* (1990), identified, isolated and synthesized 11, 15, 13, 7 and 15, 10-dimethyl nonatriacontanes as kairomonal substances that influenced the host-seeking behaviour and parasitism of *T. nubilale*. The pattern of kairomonal application both in laboratory and field is also an

important factor in the response elicited from *Trichogramma*, as evident from the investigations of Lewis *et al* (1975b).

In view of their potential importance to biological control programmes, an attempt was made in the present study to determine the nature and role of kairomones emanating from *H. armigera* scales on the parasitic potential of *T. chilonis*. This study also includes the evaluation of kairomones from *Corcyra cephalonica*, the factitious laboratory host of *T. chilonis*.

2. Materials and methods

2.1 *Insect cultures*

The eggs of *H. armigera* were obtained from the culture facility unit at the Entomology Research Institute, the alternate generations maintained on a standard semisynthetic diet and on a preferred host plant *Gossypium hirsutum* bolls (MCU 11). Adults were kept in mating cages (10 × 10") with *Cicer arietinum* L. plants for oviposition. Freshly laid eggs from the plants (mostly laid during the previous night) were removed every morning for experimental purposes. Eggs were washed in 0·1% sodium hypochloride to avoid possible viral contaminations. The larvae and adults were reared at 29°C ± 2°C under 12D:12L photoperiodic regimes. The eggs of *C. cephalonica* were obtained from the parasitoid culture unit of the Institute, especially for parasitoid colony maintenance. *C. cephalonica* larval cultures were maintained on a diet comprising pearlmillet and groundnut powder mixed in the ratio of 4:1.

2.2 *Moth scale collection and extraction*

Scales of *H. armigera* and *C. cephalonica* were collected from freshly emerged laboratory reared moths by immobilizing them at 0–2°C. The wings were removed from about 50 moths. Abdominal scales were obtained by placing immobilized moths in large test tubes and shaking them. The collected wings and abdominal scales were extracted by vigorous shaking for 2 h in 200 ml analytical grade hexane and heating for 20 min at 50°C. The hexane fraction was subsequently concentrated by vacuum evaporation at 40°C.

2.3 *Isolation and identification*

The hexane extracts of the moth scales are injected into a coupled gas chromatograph (Hewlett Packard 5890) with mass spectral detector, GC/MSD chemstation and a mass spectral library containing more than 40,000 compounds. Fused silica capillary column (10 × 0·2 m) with a cross-linked methyl silicon phase was used. Helium was used as the carrier gas. The temperature programme was 40° to 250°C at 5°C rise per min with a two min solvent delay. Injector transfer line and ion sources were set at 230° and 220°C respectively. Mass spectral data obtained during the assay were compared with the mass spectra of compounds available in the chemstation NBS 49K library.

Petri dishes in response to different treatments of *H. armigera* and *C. cephalonica* kairomones were made. The bottom of the 20 cm diameter Petri dish was covered with a filter paper (Whatman No. 1). In kairomone the treatments were restricted to egg sites herein referred to as stimulated egg surfaces (SES). UV-irradiated *H. armigera* eggs were arranged equidistant from one another in a circular ring. Hexane extract was applied at each egg site at the rate of 2 μl (total = 24 μl) using a syringe. In addition to spraying at random, in whole dish treatment, the entire surface was sprayed with 24 μl scale extracts. The bioassay of intact scales was performed by collecting from fresh immobilized moths and spraying over Petri dish surfaces. A control was maintained where only hexane was used. Eggs were glued to the respective egg site using a synthetic Fevibond adhesive. Two freshly emerged mated females of *T. chilonis* were introduced into each Petri dish and allowed to search for 4 h and the observations made during subsequent days for dark-coloured parasitized eggs. For each treatment, 10 observations were made and all the treatments conducted simultaneously in laboratory conditions.

2.5 *Bioassay of scale extracts in potted plants*

Twelve irradiated *H. armigera* eggs were placed on greenhouse grown cotton plants (approx. 1·5 feet in height). The three-scale extract treatment pattern includes (i) SES, (ii) random application and (iii) whole plant application. For random and whole plant application, scale extracts were sprayed using a chromatographic sprayer. Scale extract (15 ml) was used in various treatments in potted plant bioassay. To assess the moth scales, fresh scales were spread uniformly over the plant surfaces. Five mated *T. chilonis* females were introduced after covering the plant with a polythene sheet. The eggs were collected after a 6 h exposure to parasitoids and kept in small vials. Parasitized eggs were identified by their black colouration. Each treatment comprised ten replicates and all treatments conducted simultaneously. The data obtained in various treatments both in Petri dishes and potted plants were analysed by one-way ANOVA test (Zar 1974).

2.6 *Bioassay of scale extracts on parasitism rates in relation to parasitoid age*

Twenty fresh irradiated *H. armigera* eggs were glued to a paper strip. In experimental sets, the strips received a spray of scale extracts (*H. armigera*, *C. cephalonica* separately), while control strips received only hexane. The egg strips were placed in a test tube, to which a mated *T. chilonis* female was introduced. The egg strips were replaced everyday with fresh egg strips until the fifth day of the experiment. The number of dark coloured eggs was counted in each strip during all the five days. The experiments were conducted simultaneously and include 5 observations. The method of Nordlund *et al* (1976) was followed with a slight modification for this test. The data obtained in this investigation were analysed by Student *t* test analysis.

Figures 1 and 2 indicate the total ion chromatogram of scale extracts of *H. armigera* and *C. cephalonica* respectively. Comparison of the mass spectra obtained from various peaks matched with the standard kairomonal compounds in NBS 49K volatile chemical library in GC/MSD chemstation. The notable compounds identified were docosane, pentacosane, hexatriacontane, nonacosane, heptadecane 2, 6, 10, 15-tetramethyl etc. A list of compounds identified from the scales of *H. armigera* and *C. cephalonica* is provided in table 1 along with their matching
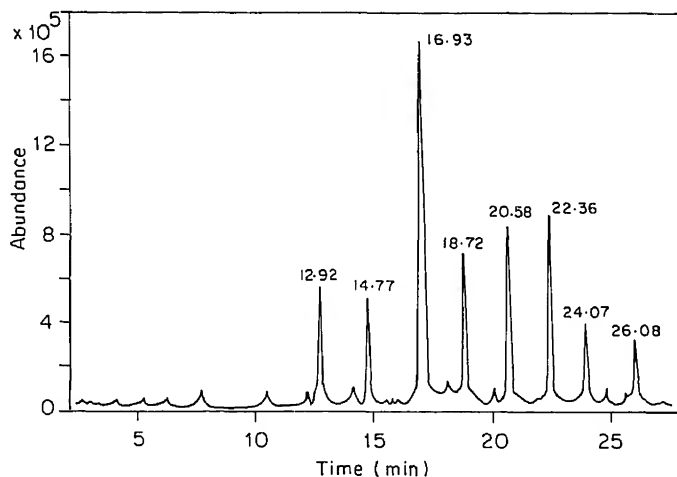
Figure 1.   Gas chromatogram of *H. armigera* scale extracts.
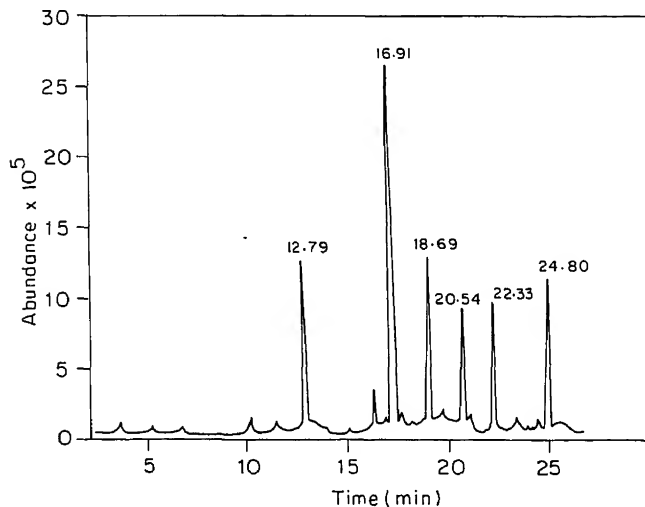
Figure 2.   Gas chromatogram of *C. cephalonica* scale extracts.

Kairomone source	Retention time	Identified* compound	Quality (%)
H. armigera scales	12·92	1, 2-Benzenedicarboxylic acid butyl octyl ester	64
	14·77	Docosane	88
	16·93	Hexatriacontane	94
	18·72	Tridecane, 1-iodo	89
	20·58	Hexatriacontane	96
	22·36	Heptadecane, 2, 6, 10, 15-tetramethyl	92
	24·07	Heptadecane, 2, 6, 10, 15-tetramethyl	93
	26·08	Heptadecane	88
	12·79	2, 6, 10-Dodecatrienal 3, 7, 11-trimethyl	88
C. cephalonica scales	16·91	Pentacosane	94
	18·69	Pentacosane	92
	20·54	Hexatriacontane	64
	22·33	Nonacosane	54
	24·80	Hexadecane	84

*Mass spectra of respective compounds are compared with NBS 49K library compounds for percentage matchability.
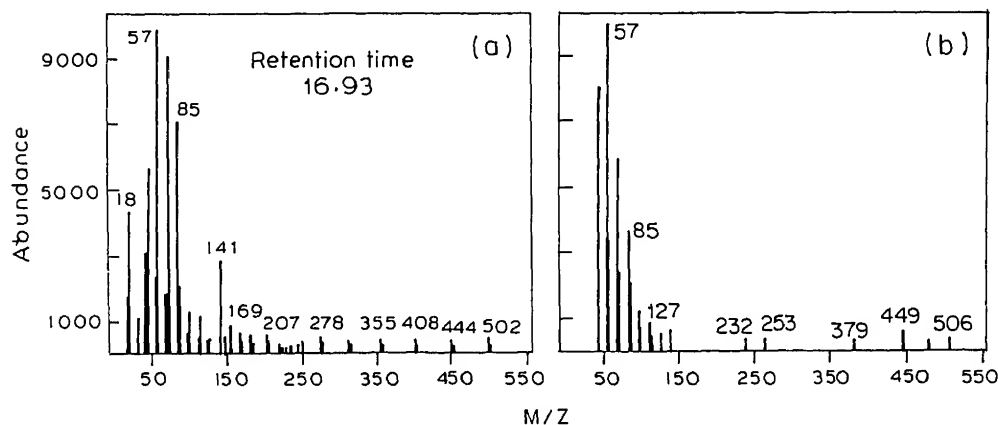
Figure 3. Mass spectrum of (a) isolated compound (b) standard hexatriacontane.

percentage with standard compounds. Figure 3 and 4 provide the mass spectra of authentic hexatriacontane and pentacosane compounds respectively along with compounds obtained in GC separation.

3.2 Petri dish bioassay

The results on Petri dish bioassays indicated highest parasitization ($\bar{X} = 83·4$) when the whole filter paper had been treated with *H. armigera* scale extracts followed by SES ($\bar{X} = 74·6$) as compared to random treatment. *C. cephalonica* moth scale extracts also increased parasitism rates when the entire surface ($\bar{X} = 68·5$) was treated
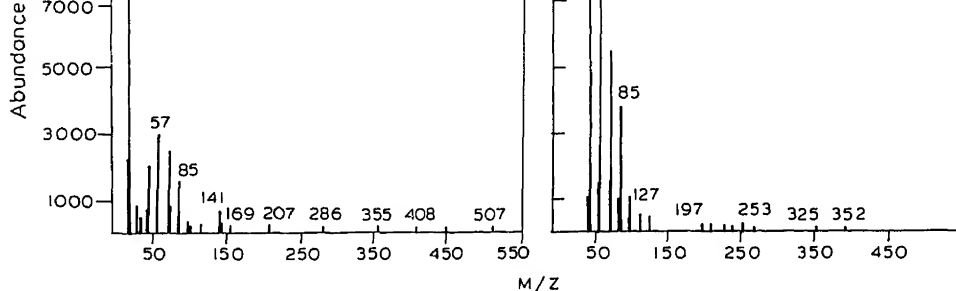
Figure 4. Mass spectrum of (a) isolated compound (b) standard pentacosane.

Table 2. Petri dish bioassay of moth scale extracts on parasitism rates on *T. chilonis* on *H. armigera* eggs.

| | Percentage parasitism | |
| | Scale extracts of | |
Treatment	*H. armigera*	*C. cephalonica*
Control	38·3 ± 1·77	38·3 ± 1·77
SES	74·6 ± 4·32	55·3 ± 2·99
Random	64·4 ± 3·32	54·3 ± 3·33
Whole dish	83·4 ± 5·17	68·5 ± 3·90
Scales	65·0 ± 3·34	53·5 ± 3·02
CD at 5% level	2·7	2·5

Data subjected to ANOVA ($P > 0.05$).

followed by SES ($\bar{X} = 55.3$). Egg surfaces treated with fresh scales of *H. armigera* and *C. cephalonica* increased parasitism rates of *T. chilonis* and the values were 65 and 53·5% respectively. A comparison of data clearly demonstrate that parasitism by *T. chilonis* was significantly enhanced in moth scale extract treatments compared to control ($\bar{X} = 38.3$) (table 2). The pattern of scale extract treatment exhibited a significant difference in the parasitism rates of *T. chilonis*.

3.3 *Potted plant bioassay*

Higher parasitism was recorded in plants treated completely with *H. armigera* and *C. cephalonica* moth scale extracts as compared to control ($\bar{X} = 58.4$ and $\bar{X} = 47.7$ respectively). SES form the next treatment to record higher parasitism and the values were 50·5 and 37·0% for *H. armigera* and *C. cephalonica* respectively compared to control ($\bar{X} = 12.4\%$). Random treatment of scale extracts as well as scales evoked lesser response among *T. chilonis* females compared to other treatment patterns (table 3).

| Treatment | Scale extracts of | |
	H. armigera	C. cephalonica
Control	13.97 ± 1.13	13.97 ± 1.13
SES	50.5 ± 2.68	37.0 ± 1.94
Random	41.3 ± 2.11	40.6 ± 2.28
Whole dish	58.4 ± 3.27	47.7 ± 2.46
Scales	45.4 ± 2.59	47.1 ± 2.97
CD at 5% level	1.15	1.12

Data subjected to ANOVA ($P > 0.05$).
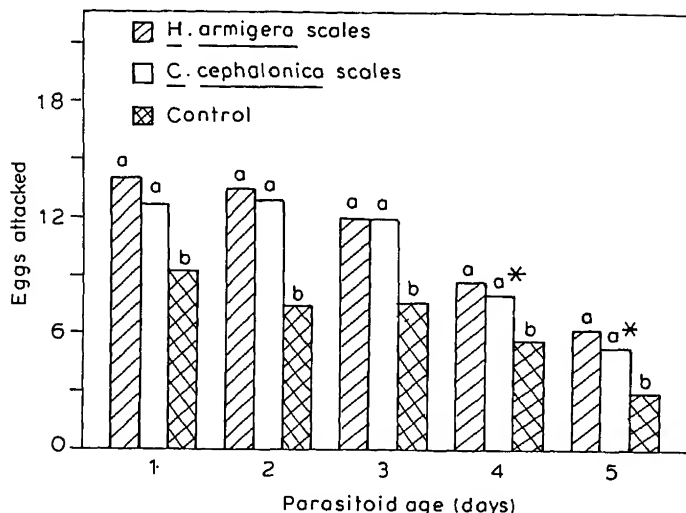
Figure 5. Parasitism by *T. chilonis* in moth scale treated and untreated egg cards at different parasitoid ages.
Data subjected to Students '*t*' test ($P > 0.05$).
Columns followed by same alphabet letters and a* and b are not significantly different.

3.4 *Parasitism rates in relation to parasitoid age*

Figure 5 demonstrated that egg cards treated with *H. armigera* and *C. cephalonica* moth scale extracts increased parasitism rates of *T. chilonis* in relation to parasitoid age. The mean per cent parasitization was significantly different in *H. armigera* moth scale extract treated egg cards compared to control. The degree of parasitism in *C. cephalonica* moth scale treated egg cards was significantly different from control during the second and third day and no significant difference was noted during subsequent days.

4. Discussion

The present results indicate that kairomonal compounds from *H. armigera* and *C.*

parasitoid systems (Lewis *et al* 1975a, b; Elzen *et al* 1984; Nordlund *et al* 1984; Nordlund 1987; Shu *et al* 1990). An analysis of *H. armigera* and *C. cephalonica* moth scales for possible kairomonal substances using gas chromatography indicated the presence of hexatriacontane, nonacosane, docosane, pentacosane and heptadecane. The significance of these kairomonal substances in behavioural manipulation of entomophagous insects was earlier emphasized and' reviewed by Lewis *et al* (1976).

The data presented here strongly indicate the role of moth scale extracts in enhancing the parasitization rate of *T. chilonis* on *H. armigera* eggs. Our results fully corroborate those of Jones *et al* (1973) who implicated the compounds such as tetracosane, docosane, tricosane and pentacosane from *H. zea* moth scales as a kairomone that influenced parasitization by *T. evanescens*. Gross *et al* (1975) and Lewis *et al* (1975a) demonstrated the role of tricosane as a kairomone to *T. evanescens* and *T. achaea* Nagarajan and Nagarkatti. The compounds from *H. virescens* scales, 11-methylhentriacontane, 16-methyldotriacontane and 11, 13-methyltriacontane were reported to act as kairomones and influence parasitism rates by *Cardiochiles nigriceps* Viereck. The treatment pattern of kairomones plays a major role in activating the natural enemies as is evident from this study. Lewis *et al* (1975b) attributed this differential parasitoid response to various kairomone treatment patterns to continuous behavioural stimulus available to parasitoids in target sites.

Laboratory observations on parasitism rates by *T. chilonis* in response to scale extract treatments reveal the importance of kairomones from moth scales. Similar observations by Nordlund *et al* (1976) in *T. pretiosum* Riley support our study on the role of kairomones in improving parasitism. Kairomone compounds from *H. armigera* and *C. cephalonica* moth scales in the manipulation of parasitoid activity could play a major role in future biological control programmes, since large cultures of moths are available in parasitoid breeding laboratories for efficient extraction and use of kairomones.

Acknowledgement

References

Brown W L Jr, Eisner T and Whittaker R H 1970 Allomones and kairomones: Transpecific chemical messengers; *BioScience* **20** 21–22

Elzen G W, Williams H J and Vinson S B 1984 Isolation and identification of cotton synomones mediating searching behaviour by parasitoid *Campoletis sonorensis*; *J. Chem. Ecol.* **19** 1251–1264

Gross H R Jr, Lewis W J, Jones R L and Nordlund D A 1975 Kairomones and their use for management of entomophagous insects: II Stimulation of *Trichogramma achaea, T. pretiosum* and *Microplitis croceipes* with host seeking stimuli at time of release to improve parasitization efficiency; *J. Chem. Ecol.* **1** 431–438

Jones R L, Lewis W J, Beroza M, Bierl B A and Sparks A N 1973 Host seeking stimulants (kairomones) for the egg parasite *Trichogramma evanescens*; *Environ. Entomol.* **2** 593–596

of entomophagous insects I. Evaluation for increasing rates of parasitization by *Trichogramma* spp. in the field: *J. Chem. Ecol.* **1** 343–347

ris W J, Jones R L, Nordlund D A and Gross H R Jr 1975b Kairomones and their use for management of entomophagous insects II. Mechanisms causing increase in rate of parasitization by *Trichogramma* spp. *J. Chem. Ecol.* **1** 349–360

ris W J, Jones R L, Gross H R Jr and Nordlund D A 1976 The role of kairomones and other behavioural chemicals in host findings by parasitic insects: *Behav. Biol.* **16** 267–289

ris W J, Nordlund D A, Gueldner R C, Teal P E A and Tumlinson J H 1982 Kairomones and their use for management of entomophagous insects. XIII kairomonal activity for *Trichogramma* spp. of abdominal tips, excretion, and a synthetic sex pheromone blend of *Heliothis zea* (Beddie) moths; *J. Chem. Ecol.* **8** 1323–1331

njunath T M, Bhatnagar V S, Pawar C S and Sithanantham S 1985 Economic imoprtance of *Heliothis* spp. in India and an assessment of their natural enemies and host plants; in *Proc. Workshop on Biol. Control. of Heliothis*, New Delhi, India, pp 197–228

dlund D A 1987 Plant produced allelochemics and their involvement in the host selection behaviour of parasitoids; in *Insects-plants* (eds) V Labeyrie, G Fabres and D Lachaise (Dordrecht: Dr W Junk Publishers) pp 103–114

dlund D A, Lewis W J, Jones R L and Gross H R Jr 1976 Kairomones and their use for management of entomophagous insects. IV Effects of kairomones on productivity and longevity of *Trichogramma pretiosum* Riley (Hymenoptera: Trichogrammatidae); *J. Chem. Ecol.* **2** 67–72

dlund D A, Chalfant R B and Lewis W J 1984 Response of *Trichogramma pretiosum* females to extracts of two plants attacked by *Heliothis zea*; *Agric. Ecosys. Environ.* **12** 127–133

S and Jones R L 1989 Kinetic effects of a kairomone in moth scales of European corn borer on *Trichogramma nubilale* Ertle and Davis (Hymenoptera: Trichogrammatidae); *J. Insect Behav.* **2** 123–31

S, Swedenborg P D and Jones R L 1990 A kairomone for *Trichogramma nubilale* (Hymenoptera: Trichogrammatidae): Isolation identification and synthesis; *J. Chem. Ecol.* **16** 521–529

ttaker R H and Feeny P O 1971 Allelochemics: chemical interaction between species; *Science* **171** 57–770

J H 1974 *Biostatistical analysis* (New Jersey: Prentice Hall)

Phosphoenolpyruvate-succinate-glyoxylate pathway in the filarial parasite *Setaria digitata*

M MOHAMED RAFI and R KALEYSA RAJ*

Department of Biochemistry, University of Kerala, Kariavattom, Trivandrum 695 581, India

Abstract. *Setaria digitata*, a filarial parasite of cattle possesses certain unique characteristics like cyanide insensitivity, and lack of cytochromes. In the present study, we have shown that the parasite has an incomplete tricarboxylic acid cycle with the absence of activities of isocitrate dehydrogenase, α-ketoglutarate dehydrogenase and succinyl-CoA synthase. However the parasite showed the existence of glyoxylate cycle and phosphoenolpyruvate-succinate pathway. The widely used antifilarial drug diethyl-carbamazine caused general inhibition of all enzymes of phosphoenolpyruvate-succinate pathway and glyoxylate cycle except that of fumarase and isocitrate lyase. The results may pave the way for new targets for chemotherapy in the control of filarial parasites.

Keywords. Filariae; *Setaria digitata*; mitochondriae; tricarboxylate cycle; phosphoenol-pyruvate-succinate pathway; glyoxylate cycle.

1. Introduction

All helminths examined are capable of utilizing glucose and consume oxygen under appropriate conditions (Saz 1972). Filarial parasites are reported to be homolactate fermenters (Barrett 1981; Saz 1981). However there is no evidence that any parasitic helminth exhibits homolactate fermentation in the strict sense of the term (Bryant 1989). There is considerable evidence now suggesting aerobic respiration in filarial parasites (Bryant and Behm 1989). Studies using mitochondrial isolates from *Brugia pahangi* and *Dipetalonema viteae* have shown the oxygen uptake to be completely inhibited by cyanide, while rotenone and antimycin A suppress it by about 80% (Barrett 1983).

Setaria digitata is a filarial parasite of cattle recommended as a model system by the WHO, due to its similarity to the human filarial parasites *Wuchereria bancrofti* and *Brugia malayi* (Hawking 1978). *S. digitata* possesses rare characteristics such as cyanide insensitivity, hydrogen peroxide production, absence of cytochrome, lipid peroxidation and substrate-dependent oxygen uptake (Kaleysa Raj *et al* 1988). A distinct difference was observed between *S. digitata* and those of *B. pahangi* and *D. viteae* in their sensitivity to cyanide (Barrett 1983; Kaleysa Raj *et al* 1988). The occurrence and formation of quinones Q_6 and Q_8 was reported recently by Santhamma and Kaleysa Raj (1990). They also showed generation of H_2O_2 (Santhamma and Kaleysa Raj 1991a) in *S. digitata*. These prompted a detailed study of the activities of enzymes connected with the tricarboxylic acid (TCA) cycle and PEP-succinate pathway in the parasite.

---

*Corresponding author.

2. Materials and methods

Adult *S. digitata* were collected from the peritoneal cavity of freshly-slaughtered cattle. The worms were washed well to remove host material and incubated for 2 h at 37°C in Tyrode solution (composition: w/v sodium chloride 0·8%, potassium chloride 0·02%, calcium chloride 0·02%, magnesium chloride 0·01%, sodium bicarbonate 0·015%, disodium hydrogen phosphate 0·05% and glucose 0·5%). The incubated worms were minced and homogenized in ice-cold 0·25 M sucrose solution and the homogenate was subjected to differential centrifugation. The pellet collected between 800 and 12000 g was used for the studies. The experimental fraction was termed mitochondria-like particulate fraction (MLP) as described by Kaleysa Raj *et al* (1988) and used for the assay of mitochondrial enzymes. The supernatant collected after removing MLP was used for the study of the cytosolic enzymes (PMS).

Enzyme assays were carried out by the following methods: pyruvate dehydrogenase (EC 1·2·4·1, Sumegi and Alkomyi 1983), citrate synthase (EC 4·1·3·7, Shephard and Garland 1966), aconitase (EC 4·2·1·3, Racker 1950), isocitrate dehydrogenase (ICDH) (EC 1·1·1·41, Chen and Plaut 1963), α-ketoglutarate dehydrogenase (KDH) (EC 1·2·4·2, Sanadi 1969), succinyl-CoA synthase (EC 6·2·1·4, Ramaley *et al* 1967), succinate dehydrogenase (SDH) (EC 1·3·99·1, Susheela and Ramasarma 1971), fumarase (EC 4·2·1·2, Kanarek and Hill 1964), malate dehydrogenase (MDH) (EC 1·1·1·37, England and Siegel 1969), malic enzyme (EC 1·1·1·40, Ochoa 1955), fumarate reductase (EC 1·3·1·6, Holwerda and Zwaan 1959), malate synthase (EC 4·1·3·2, Dixon and Kornberg 1959), pyruvate carboxylase (EC 6·4·1·1, Seubert and Weicker 1969), pyruvate kinase (EC 2·7·1·40, Bucher and Pfleiderer 1955), phosphoenolpyruvate carboxykinase (EC 4·1·1·32, Ward *et al* 1969), glucose-6-phosphatase (EC 3·1·3·9, Shull *et al* 1956), fructose-1, 6-diphosphatase (EC 3·1·3·11, Shull *et al* 1956), citrate lyase (EC 4·1·3·8, Srere 1959), isocitrate lyase (EC 4·1·3·1, Dixon and Kornberg 1959), and lactate dehydrogenase (EC 1·1·1·27, Kornberg 1955). The protein content of the preparations was determined after trichloroacetic acid precipitation by the method of Lowry *et al* (1951). Assays were carried out in a Shimadzu UV-240 spectrophotometer.

The effect of diethylcarbamazine (DEC) on the activities of selected enzymes was studied by preincubating the enzyme preparation with neutralized aqueous solution of DEC under different concentrations.

3. Results and discussion

The activities of ICDH, KDH and succinyl-CoA synthase were not detected in MLP under the experimental conditions. The activities of citrate synthase, aconitase, SDH, fumarase, malate dehydrogenase (MDH), isocitrate lyase, malic enzyme, malate synthase and fumarate reductase are given in table 1.

Thus *S. digitata* apparently has an incomplete TCA cycle. This is not in agreement with the information available in the case of certain other filarial parasites such as *B. pahangi* and *D. viteae* (Bryant and Behm 1989). These parasites are reported to have low levels of TCA cycle enzymes, in agreement with the cyanide sensitivity shown by them (Barrett 1983). Another filarial parasite *Litomosoides carinii* also behaved like *B. pahangi* (Ramp *et al* 1985). *S. digitata* is

Enzymes	Specific activity* (nmol/min/mg protein)
Pyruvate dehydrogenase	ND
Citrate synthase	19 ± 1
Aconitase	5 ± 0.3
Isocitrate dehydrogenase	ND
α-ketoglutarate dehydrogenase	ND
Succinyl-CoA synthase	ND
Succinate dehydrogenase	366 ± 12
Fumarase	757 ± 18
Malate dehydrogenase	820 ± 18
Isocitrate lyase	85 ± 3
Malate synthase	81 ± 6
Fumarate reductase	58 ± 4
Malic enzyme	135 ± 8

ND, Not detected.
*Average of 6 independent experiments.

In the context of the observed incomplete TCA cycle, the presence of glyoxylate cycle enzymes complete the cycle of events from acetate to oxaloacetate. In addition, the absence of ICDH and KDH indicates the absence of carbon loss as CO_2. Thus there is a possibility of complete conservation of the carbons of acetyl CoA entering the TCA cycle.

The findings that the activity of aconitase was very low suggest that it may be the rate-limiting step. It is also of significance because oxygen deficiency greatly reduced the activity of aconitase (Hirsch 1952). The reduction of fumarate to succinate catalysed by NADH-dependent fumarate reductase was also detected in mitochondrial isolates from *S. digitata*. The ratio of SDH to fumarate reductase was 6.3. This ratio is in agreement with the values reported for facultative anaerobes (Prichard and Schofield 1968).

Malate formed by fumarase action can be decarboxylated to pyruvate by malic enzyme. Malate may be converted by mitochondrial MDH to oxaloacetate which condenses with acetyl-CoA to form citrate by citrate synthase. Since the activity of pyruvate dehydrogenase complex is absent, the source of acetyl-CoA is from oxidation of fatty acids and catabolism of amino acids. Isocitrate lyase cleaves the isocitrate formed from citrate into succinate and glyoxylate. Glyoxylate condenses with acetyl-CoA to form malate and the net result is the condensation of two acetyl-CoA to yield a molecule of succinate. Recent studies from this laboratory showed continuous production of H_2O_2 by isolated mitochondria of *S. digitata* with either succinate or fumarate (Santhamma and Kaleysa Raj 1991a) with generation of ATP (Santhamma and Kaleysa Raj 1991b), indicating a cyclic reaction taking place involving SDH, fumarate reductase and fumarase system.

The activities of certain cytosolic enzymes (table 2) clearly suggest the presence of PEP-succinate pathway in *S. digitata*. Based on the observations, a scheme for substrate and product shuttling between the cytosol and mitochondria involving the glyoxylate cycle and PEP-succinate pathway is shown in figure 1. Such a pathway is reported in many parasites such as *Ascaris lumbricoides, Onchocerca voluvlus,*

Enzymes	Specific activity* (nmol/min/mg protein)
Pyruvate kinase	103 ± 6
PEP-carboxykinase	94 ± 4
Pyruvate carboxylase	57 ± 8
ATP-citrate lyase	66 ± 4
Lactate dehydrogenase	89 ± 3
Glucose-6-phosphatase	ND
Fructose-1,6-diphosphatase	57 ± 2

ND, Not detected.

*Average of 6 independent experiments.
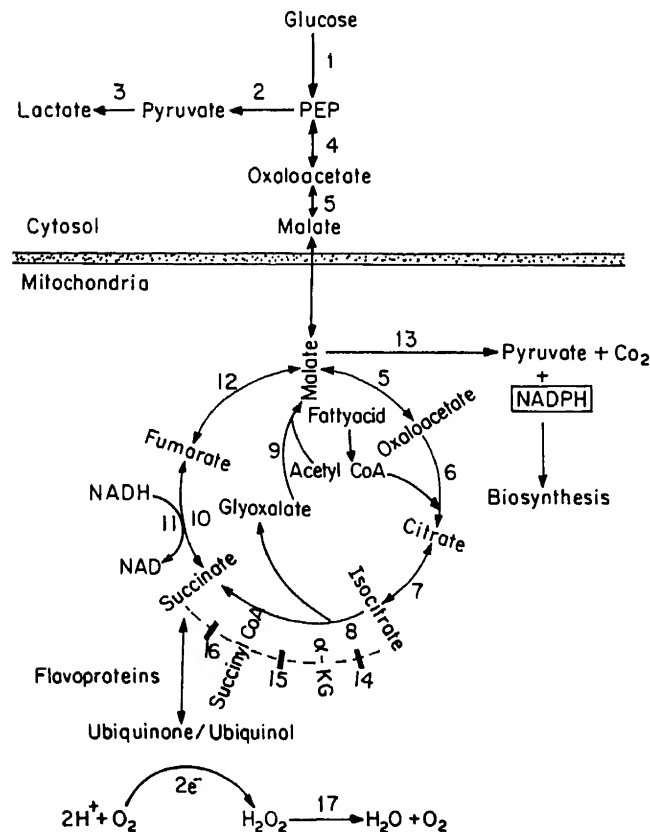
Figure 1. Proposed PEP-succinate-glyoxylate pathway in *S. digitata*.

1. Glycolytic enzymes; 2, pyruvate kinase; 3, lactate dehydrogenase; 4, PEP-carboxy kinase; 5, malate dehydrogenase; 6, citrate synthase; 7, aconitase; 8, isocitrate lyase; 9, malate synthase; 10, succinate dehydrogenase; 11, fumarate reductase; 12, fumarase; 13, malic enzyme; 14, isocitrate dehydrogenase; 15, α-ketoglutarate dehydrogenase; 16, succinyl-CoA synthase; 17, catalase.
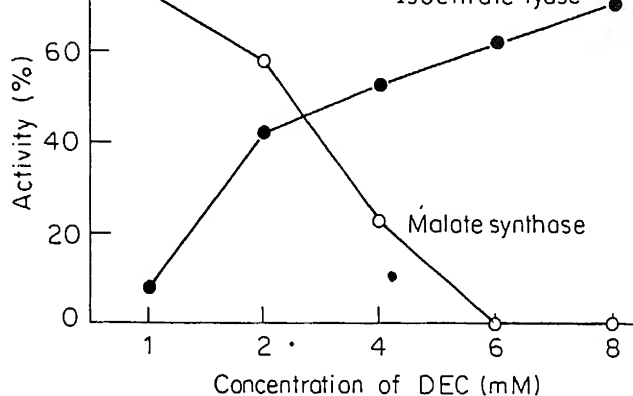
Figure 2. Effect of DEC on glyoxylate cycle enzymes.

Schistosoma mansoni, *Hymenolepis diminuta* and *Fasciola hepatica* (Behm and Bryant 1976) and also in *S. cervi* (Hussain *et al* 1990). However in none of these parasites, is glyoxylate cycle reported and many of them are entirely or partially cyanide sensitive.

The effect of DEC, a widely used antifilarial drug, when tested against the *Setaria* system, showed a generalized inhibition of the activities of enzymes of the PEP-succinate pathway, except that of fumarase (unpublished results). DEC showed a differential effect on glyoxylate cycle enzymes. It stimulates the activity of isocitrate lyase and inhibits the activity of malate synthase. This result is presented in figure 2. Because of this, lesser amounts of malate will be available for generating oxaloacetate and fumarate for the continuation of the cycle and a resultant decrease in the generation of ATP will lead to paralysis of the parasite.

Since *S. digitata* possesses electron transport system associated with two quinones Q_6 and Q_8, a unique feature of this parasite (Santhamma and Kaleysa Raj 1990), cyanide insensitivity (Kaleysa Raj *et al* 1988), incomplete TCA cycle, glyoxylate cycle and PEP-succinate pathway (present study), inhibitors specific to at least one of these systems may prove very effective targets of attack for controlling filariasis.

Acknowledgement

References

Barrett J 1981 *Biochemistry of parasitic helminths* (London and Basingstoke: Macmillan)

Barrett J 1983 Biochemistry of filarial worms; *Helminthol. Abstr.* **A52** 1–18

Behm C A and Bryant C 1976 *Biochemistry of parasites and host parasite relationships* (ed.) H Vanden Bosche (Amsterdam: North Holland and Elsevier)

Bryant C 1989 *Comparative biochemistry of parasitic helminths* (eds) E M Bannet, C A Behm and C Bryant (London: Chapman and Hall)

Bucher T and Pfleiderer 1955 Pyruvate kinase from muscle; *Methods Enzymol.* **1** 435–440

Chen R F and Plaut G W E 1963 Activation and inhibition of DPN-linked isocitrate dehydrogenase of heart by certain nucleotides; *Biochem. J.* **2** 1023–1032

Dixon G H and Kornberg H L 1959 Assay methods for key enzymes of the glyoxylate cycle; *Biochem. J.* **72** 3P

Englard S and Siegel L 1969 Mitochondrial L Malate dehydrogenase of beef heart; *Methods Enzymol.* **13** 99–106

Hawking F 1978 WHO/ONCHO/78.142.1

Hirsch H M 1952 A comparative study of aconitase, fumarase and DPN-linked isocitrate dehydrogenase in normal and respiratory deficient yeast; *Biochim. Biophys. Acta* **9** 674–686

Holewerda A D and De Zwaan A 1980 On the role of fumarate reductase in anaerobic carbohydrate catabolism of *Mytilus edulis*; *Comp. Biochem. Physiol.* **B67** 447–453

Hussain H, Shukla O P, Ghatak S and Kaushal N A 1990 Enzymes of PEP-succinate pathway in *Setaria cervi* and effect of anthelmintic drugs; *Indian J. Exp. Biol.* **28** 871–875

Kaleysa Raj R, Puranam R S, Kurup C K R and Ramasharma T 1988 Oxidative activities in mitochondria-like particles from *Setaria digitata*, a filarial parasite; *Biochem. J.* **256** 559–564

Kanarek L and Hill R L 1964 The preparation and characterization of fumarase from swine heart muscle; *J. Biol. Chem.* **239** 4202–4206

Kornberg A 1955 Lactate dehydrogenase of muscle; *Methods Enzymol.* **1** 441–443

Lowry O H, Roseborough N J, Farr A L and Randall R J 1951 Protein measurement with the folin phenol reagent; *J. Biol. Chem.* **193** 265–275

Ochoa S 1955 Malic enzyme from pigeon liver and wheat germ; *Methods Enzymol.* **1** 739–748

Prichard R K and Schofield P J 1968 A comparative study of tricarboxylic acid cycle enzymes in *Fasciola hepatica* and rat liver; *Comp. Biochem. Physiol.* **25** 1005–1019

Racker E 1950 Spectrophotometric measurements of the enzymatic formation of fumaric and cis-aconitic acids; *Biochim. Biophys. Acta* **4** 211–214

Ramaley R F, Briger W A, Moyer R W and Boyer P D 1967 The preparation, properties and reactions of succinyl CoA synthetase and its phosphorylated form; *J. Biol. Chem.* **242** 4287–4298

Ramp T, Bachmann R and Köhler P 1985 Respiration and energy conservation in the filarial worm, *Litoroosoides carinii*; *Mol. Biochem. Parasitol.* **15** 11–20

Sanadi D R 1969 α-ketoglutarate dehydrogenase from pig heart; *Methods Enzymol.* **13** 52–55

Santhamma K R and Kaleysa Raj R 1990 Quinone mediated ATP production in the filarial parasite *Setaria digitata*; *Biochem. Biophys. Res. Commun.* **167** 568–574

Santhamma K R and Kaleysa Raj R 1991a Quinone mediated electron transport system in the filarial parasite *Setaria digitata*; *Biochem. Biophys. Res. Commun.* **174** 386–392

Santhamma K R and Kaleysa Raj R 1991b Oxidative phosphorylation coupled to electron transfer in the filarial parasite *Setaria digitata*; *Biochem. Biophys. Res. Commun.* (in press)

Saz H J 1972 *Comparative biochemistry of parasites* (ed.) Van den Bossche (New York: Academic Press)

Saz H J 1981 *Energy metabolism of parasitic helminths*; *Annu. Rev. Physiól.* **43** 323–341

Seubert W and Weicker H 1969 Pyruvate carboxylase from pseudomonas; *Methods Enzymol.* **13** 258–262

Shephard D and Garland P G 1966 Citrate synthase from rat liver; *Methods Enzymol.* **13** 11–16

Shull K H, Ashmore J and Mayer J 1956 Hexokinase, glucose-6-phosphatase and phosphorylase levels in heriditarily obese, hyperglycemic mice; *Arch. Biochem. Biophys.* **62** 210–216

Srere P A 1959 The citrate cleavage enzyme distribution and purification; *J. Biol. Chem.* **234** 2544–2549

Sumegi B and Alkomyi I 1983 Elementary step in the reaction of pyruvate dehydrogenase complex from pig heart; *Eur. J. Biochem.* **136** 347–353

Susheela L and Ramasharma T 1971 Activation of succinate dehydrogenase by 2, 4-dinitrophenol—a complete competitive inhibition; *Biochim. Biophys. Acta* **242** 532–540

Ward C W, Castro C A and Fairbairn D 1969 Carbondioxide fixation and phosphoenol pyruvate metabolism in *Trichinelli spiralis* larvae; *J. Parasitol.* **55** 67–71

Diketopinic acid–a novel reagent for the modification of arginine[§]

C S PANDE[†], K D BASSI*, NEENA JAIN, A DHAR and J D GLASS**

Department of Chemistry, Himachal Pradesh University, Shimla 171 005, India
*IRS, ONGC, Chandkhera, Ahmedabad 380 005, India
**Medical Research Center, Brookhaven National Laboratory, Upton, NY 11973, USA

Abstract. Diketopinic acid has been synthesized and shown to be a reagent of choice for specific, reversible modification of the guanidine groups of arginine residues. Diketopinic acid is a yellow crystalline substance and the carboxyl group of the reagent is a convenient handle for attachment to other molecules. The adducts of diketopinoyl derivatives with the guanidine group are cleaved by 0·2 M o-phenylenediamine at pH 8–9. The modification and regeneration of arginine and of arginyl residues in soyabean trypsin inhibitor and insulin are presented as demonstrations of the use of the reagent. The use of diketopinoyl resin in the separation of oxidized A and B chains of insulin has been discussed.

Keywords. Diketone; reversible modification of arginine residues; aminopolymer; diketopolymer.

1. Introduction

Tremendous progress has been made in the development of protecting groups for various functionalities in proteins and amino acids. Protection of functional groups is not only important in the synthesis of polypeptides, but in the form of modification of amino acid residues in proteins it offers a useful technique of selective chemical and enzymatic cleavage of large protein molecules. Modification of specific residues in biologically active proteins may render them inactive or alter their activity and are useful probes for the active sites. Efforts have been directed to develop new amine or carboxyl-protecting groups, which can be introduced and cleaved under natural conditions *e.g.* neutral or near neutral pH, lower temperatures and physiological conditions. The choice is very limited in the selection of protecting groups for the protection of the guanidine function of arginine. Pande *et al* (1980) successfully introduced a new, bifunctional reagent, camphorquinonesulphonic acid for the protection of the guanidino group of arginine in peptides and proteins. Camphorquinonesulphonylnorleucine was found to be a reagent of choice when the work had to be carried out with larger peptides and proteins. The sulphonic acid gave it a high solubility in water, but there were limited ways to activate the group and the isolation and purification of the reagent was cumbersome.

Continuing our work on the development of 1,2-diketones with a suitable handle,

---

The adduct of DKPA is quite stable and resistant to hydrolysis by acid or base. The carboxylic group of the reagent serves as a handle for attachment on to a polymeric support and the 1,2-diketo group specifically protects the guanidino side chain of arginine. The modification is done at pH 7·5–7·8 in borate buffer and is removed by 0·2 M o-phenylenediamine.

2. Materials and methods

d-Camphor-10-sulphonic acid was purchased from Aldrich. Soyabean trypsin inhibitor (STI) and insulin were purchased from the Sigma Chemical Co., St. Louis, Mo, USA. Solvents were purified by standard methods before use. Thin-layer chromatography (TLC) was carried out on silica gel-G plates. Quantitative estimation of amino acids was carried out on a Beckman 121 automatic amino acid analyser. Hydrolysis of proteins was carried out with 6 N HCl at 110° for 22 h in sealed evacuated tubes.

2.1 *Preparation of d-camphor-10-sulphonyl chloride*

Chloride of d-10-camphorsulphonic acid was prepared using phosphorous pentachloride according to the method reported by Sutherland and Shriner (1936). The white material was washed several times with cold water. The crude product melted at 81–83°C (yield 80%) and was used as such in the next step.

2.2 *Preparation of ketopinic acid*

Ketopinic acid was prepared by the action of potassium permanganate on d-10-camphorsulphonyl chloride following the method of Bartlett and Knox (1939). Crude ketopinic acid has a melting point (mp) 233–235°C, yield 20%. The product was recrystallized from hot water.

2.3 *Preparation of DKPA*

Ketopinic acid (1·82 g, 0·01 mol) was dissolved in 20 ml of dioxane. SeO_2 (1·42 g, 0·011 mol) was added and the mixture was refluxed gently for 72 h. Precipitated selenium was filtered and the dioxane solution was concentrated on a rotary evaporator. The oily residue was dissolved in aqueous methanol and SO_2 was passed for 24 h. Colloidal red selenium was removed with the help of celite filter aid. Most of the methanol was removed on a rotavapor. The aqueous solution was extracted with ether several times. The combined extracts were dried over anhydrous sodium sulphate and the solvent was removed to give a yellow solid. This solid was dissolved in sodium bicarbonate solution, the solution washed with ether and the product reprecipitated by acidifying the solution. The solid was recrystallized from ethanol-water. An oil which separated, crystallized on cooling. The crystalline solid was purified by column chromatography on a column of silica

gel. The narrow yellow-coloured band was eluted with chloroform and the product was recrystallized from ethanol-water (yield 51·0%, mp 233–235°C). The homogeneity of the compound was checked on TLC in EtOAc: C_6H_6: AcOH in the ratio of 10:10:0·2 (R_f, 0·57) and CHCl$_3$: CH$_3$OH: AcOH, 20:1:0·5 (R_f, 0·83)

IR /cm^{-1}: 2640–2720 (COOH, b), 1710 (COOH, s), 1760 (CO, s), 1385 and 1370 (gem-dimethyl).

^{1}H NMR (CDCl$_3$) δ/ppm: 0·95 (s, 3H, CH$_3$); 1·15 (s, 3H, CH$_3$); 2·25 (d, 2H, CH$_2$), 2·75 (t, 2H, CH$_2$); 3·3 (d, 1H, −CH); 9·1 (s, 1H, COOH)

Anal: Calculated for $C_{10}H_{12}O_4$: C, 61·22; H, 6·12.
Found: C, 61·17; H, 6·21.

2.4 *Preparation of dicyclohexylamine salt of DKPA*

DKPA (10 mg) was dissolved in solvent ether. To this was added an etheral solution of dicyclohexylamine (DCHA). Crystals started forming soon afterwards. These were collected by filtration and washed with ether.

Anal: Calculated for $C_{22}H_{35}NO_4$: C, 70·03; H, 9·28; N, 3·71
Found: C, 70·14; H, 9·38; N, 3·75.

2.5 *Arginine binding with DKPA*

Borate buffer was prepared by dissolving a 12·367 g of boric acid in 100 ml of 1 N NaOH solution in one litre of water (sodium tetraborate 0·05 M). The pH of this solution was adjusted to 7·8 by the addition of the required amount of 0·1 N HCl.
    To 2 ml of borate buffer in a 50 ml round-bottomed flask, arginine hydrochloride (2·1 mg, 0·01 mmol) and DKPA (2·94 mg, 0·015 mmol) were added. The contents were stirred for 20 h on a magnetic stirrer and the reaction was monitored by TLC in BuOH: AcOH: H$_2$O (4:1:1) and spraying with ninhydrin. After two hours the adduct started showing up. In 20 h all the arginine had disappeared from the reaction mixture. The adduct of arginine and DKPA had an R_f 0·08.

2.6 *Specificity of DKPA for arginine*

A solution containing 2·5 μm each of the 18 amino acids in dilute HCl (calibration mixture for amino acid analysis) was evaporated to dryness. The residue was dissolved in 2 ml of water containing 0·2 ml of triethylamine and lyophilized. The lyophilized residue was taken in 2 ml of 0·2 M sodium borate buffer, pH 9 and the pH was readjusted to 9. Samples (0·7 ml each) of this stock solution were withdrawn. The first sample was treated with 0·3 ml of a solution of DKPA (10 mg/ml) in sodium borate buffer at pH 9. The second sample was added to 0·3 ml

2.7 Reversal of DKPA-modification of arginine with o-phenylenediamine

The solution of DKPA-arginine adduct from the experiment described earlier was subjected to preparative TLC. The band containing the DKPA-arginine adduct was scrapped and the material was eluted with warm water. The solution was lyophilized and the residue was taken in 2 ml of 0·2 M solution of o-phenylenediamine at pH 8·5. The solution was held at 37°C and analysed at time intervals by TLC after spraying with ninhydrin. The regeneration of arginine from starting material in o-phenylenediamine was 75% complete after 4 h. After overnight incubation, the starting material had completely vanished and the only ninhydrin-positive spot corresponded to arginine.

2.8 Modification of STI with DKPA

STI (20 mg) was added to a solution of DKPA (10 mg) in 4 ml of 0·2 M sodium borate buffer, pH 9. The solution was incubated at 37°C for 24 h in dark. It was then dialysed (3500 molecular weight cut-off membrane) against water (4 × 2 l) at 4°C and lyophilized. A few mg of modified STI were treated with o-phenylenediamine (0·2 M, pH 8·5) for 20 h in dark. The solution was then dialysed, filtered and lyophilized. Native STI, DKPA-STI and o-phenylenediamine treated DKPA-STI were subjected to gel electrophoresis on 15% polyacrylamide slabs at pH 8·6 in Tris/borate buffer, pH 9, and a constant current of 35 mA. The protein band was stained with Commassie blue G-250 in 6% (wt/vol) $HClO_4$. The DKPA-

Table 1. Effect of DKPA incubation of standard amino acid mixture.

Amino acid	Control	DKPA treated
Asp	1·00	1·00
Thr	1·00	0·95
Ser	1·00	0·95
Glu	1·00	1·00
Pro	1·00	1·00
Gly	1·00	0·93
Ala	1·00	1·00
Cys	0·50	0·50
Val	1·00	1·00
Met	1·00	0·96
Ile	1·00	1·00
Leu	1·00	1·00
Tyr	1·00	0·90
Phe	1·00	1·00
Lys	1·00	0·98
His	1·00	0·98
$(NH_4)_2SO_4$	1·00	0·93
Arg	1·00	0·07

2.9 Modification of insulin by DKPA

Bovin insulin (10 mg) was added to a solution of DKPA (10 mg) in 4 ml of 0·2 M sodium borate buffer, pH 9. The solution was incubated at 37°C for 24 h in the dark, then dialysed (3500 molecular weight cut-off membrane) against water (four times, 2 litres each) at 4°C and lyophilized.

Modified insulin (10 mg) was dissolved in 5 ml of 0·2 M phosphate buffer, pH 7 and was treated with 0·5 mg of trypsin in 0·5 ml of the same buffer. A control experiment was run with native insulin under the same conditions. After 2 h at 25°C, the solutions were· dialysed against aqueous acetic acid (2 ml/1) and lyophilized.

Samples of lyophilized powder were hydrolyzed and subjected to amino acid analysis. The trypsin-treated native insulin showed a significant loss of Phe, Thr and Lys, whereas the trypsin-treated DKPA-modified insulin had almost the same amino acid composition as the native insulin itself (table 2).

2.10 Preparation of diketopinoyl chloride

DKPA (570 mg, 5 mmol) was treated with thionyl chloride (2 ml) in dimethyl-formamide (DMF) (2 ml) in a 50 ml round-bottomed flask in an ice bath. The mixture was stirred under exclusion of moisture for 2 h at ice bath temperature and for 1 h at room temperature. The product was freed of thionyl chloride by adding dry benzene and removing the azeotrope on a rotavapor repeatedly and was used without further purification.

Table 2. Amino acid composition of modified insulins.

Amino acid	Native bovine insulin	Trypsin treated insulin	Trypsin treated DKPA-insulin
Asp	2·97	2·89	2·90
Thr	1·00	0·10	0·92
Ser	2·95	2·87	2·88
Glu	6·81	6·90	6·83
Pro	0·88	0·05	0·85
Gly	3·90	2·88	3·88
Ala	2·95	1·85	2·12
Val	5·00	5·00	4·88
Ile	0·98	0·88	0·98
Leu	6·00	6·00	6·00
Tyr	3·82	2·68	3·85
Phe	2·96	0·91	2·87
Lys	0·86	0·00	0·83
His	1·91	1·85	1·83
Arg	0·88	0·87	0·87

Cross-linked polyacrylamide (Biogel P4, 200–400 mesh) 10 g, was treated with 50 ml of sodium hypochlorite "Chlorox" in a cylindrical glass vessel having a sintered disc at the bottom further connected to a stopcock. The reaction was allowed to run with a stream of nitrogen bubbling through the bottom which kept the polymer well-stirred under inert atmosphere. The reaction was allowed to run for 6 h at 4°C after which the polymer was filtered and thoroughly washed under nitrogen. It gave a positive test with Kaiser reagent. This resin was stored under nitrogen.

2.12 Preparation of diketopinoyl cross-linked polyacrylamine

Cross-linked polyacrylamine (5 g) was suspended in an alkaline solution of sodium bicarbonate (pH 8·5). Diketopinoyl chloride (589 mg, 3 mmol) was dissolved in dioxane and added to the polymer. The reaction mixture was stirred vigorously for 5 h on a magnetic stirrer after which it was thoroughly washed with aqueous dioxane and water. The resulting polymer had a yellow colour.

2.13 Oxidation of insulin

Performic acid was prepared by adding 0·1 ml of 30% H_2O_2 to 1·9 ml of 99% formic acid and allowing the solution to stand in a stoppered flask at room temperature for 2 h. In another flask 10 mg of insulin was dissolved in 1 ml of 99% formic acid. The insulin and performic acid solutions were cooled to 0°C and mixed slowly. Reaction was allowed to proceed for 3 h at the same temperature. The formic acid was then partly removed on a rotavapor at 20°C. Cold water (5 ml) was added to the reaction mixture, the solution was shell frozen at once and lyophilized.

Table 3. Amino acid composition of bovine insulin chains.

Amino acid	Oxidized A chain (calculated)	Oxidized B chain (calculated)	Fraction A	Fraction B
Cysteic acid	4·00	2·00	3·95	1·84
Asp	2·00	1·00	1·88	0·98
Thr		1·00		0·90
Ser	2·00	1·00	1·98	0·89
Glu	4·00	3·00	3·85	2·88
Pro		1·00		0·97
Gly	1·00	3·00	0·95	3·01
Ala	1·00	2·00	0·93	2·00
Val	2·00	3·00	1·8	2·98
Ile	1·00		1·01	
Leu	2·00	4·00	2·00	4·00
Tyr	2·00	2·00	1·89	1·88
Phe		3·00		2·99
Lys		1·00		0·93
His		2·00		1·85
Arg		1·00		0·88

The diketopinoyl-polyacrylamine beads (5 g) were packed in a 20 cm column in 0·2 M sodium borate buffer, pH 8·5. Oxidized insulin dissolved in 5 ml of the same buffer was allowed to pass slowly through the column, which was then eluted with the same borate buffer. The eluate (50 ml) was dialysed in a dialysis bag (2000 molecular weight cut-off) against $4 \times 1\,1$ distilled water and lyophilized (fraction A).

The column was then eluted with 0·2 M o-phenylenediamine (100 ml) in borate buffer pH 9. The eluate was dialysed in a dialysis bag (2000 molecular weight cut-off) against $5 \times 1\,1$ distilled water, filtered from a little particulate matter and lyophilized (fraction B).

The fractions were hydrolysed and subjected to amino acid analysis. Amino acid composition of fraction A matched with that of oxidized A chain. Fraction B had the same amino acid composition as that of oxidized B chain (table 3).
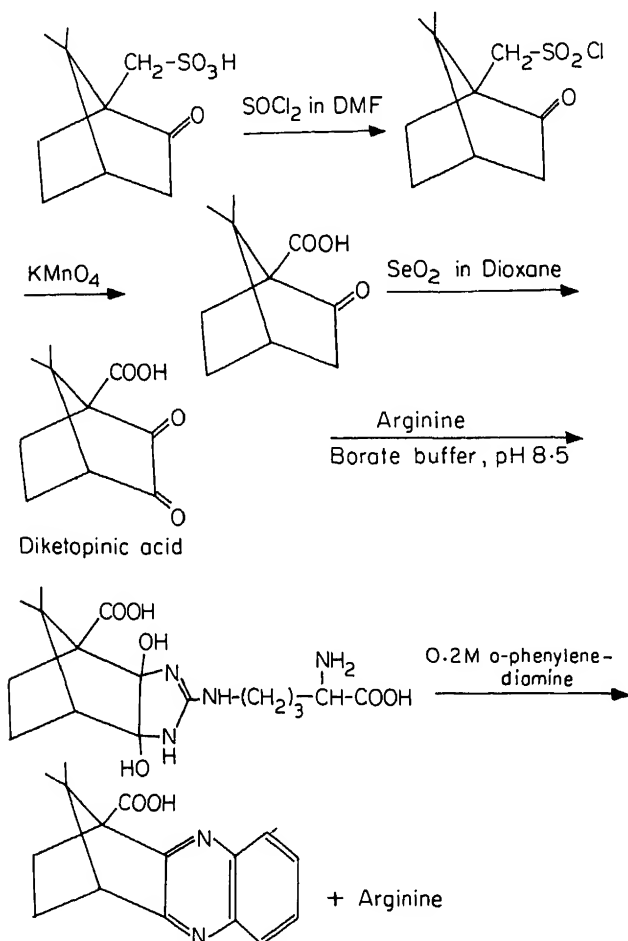
Scheme 1.

3. Results and discussion

DKPA synthesized from camphor-10-sulphonic acid in three steps has been found to be a promising reagent for the reversible protection of the guanidino group of arginine or arginine containing peptides (scheme 1). DKPA like the camphor-quinonesulphonic acid is a bifunctional reagent, the diketo moiety of which offers reversible protection to arginine. The carboxyl function of the reagent serves as a handle for covalent attachment to an insoluble support. DKPA reacted only with arginine from a standard mixture of amino acids in borate buffer. Insulin was modified at its arginine residue and the product resisted proteolysis with trypsin. STI was modified with DKPA as evidenced from the alteration of its electrophoretic mobility. Treatment with o-phenylenediamine removed the protection. The regenerated STI had the same electrophoretic mobility as the native STI.

Cross-linked polyacrylamine was prepared by the reaction of sodium hypochlorite on cross-linked polyacrylamide under nitrogen. During this reaction, the carboxamide groups of the polymer were converted into amino groups on a matrix which is compatible with aqueous media. Amino functions of this polymer were acylated with DKPA through its chloride. The derivatized polymer which
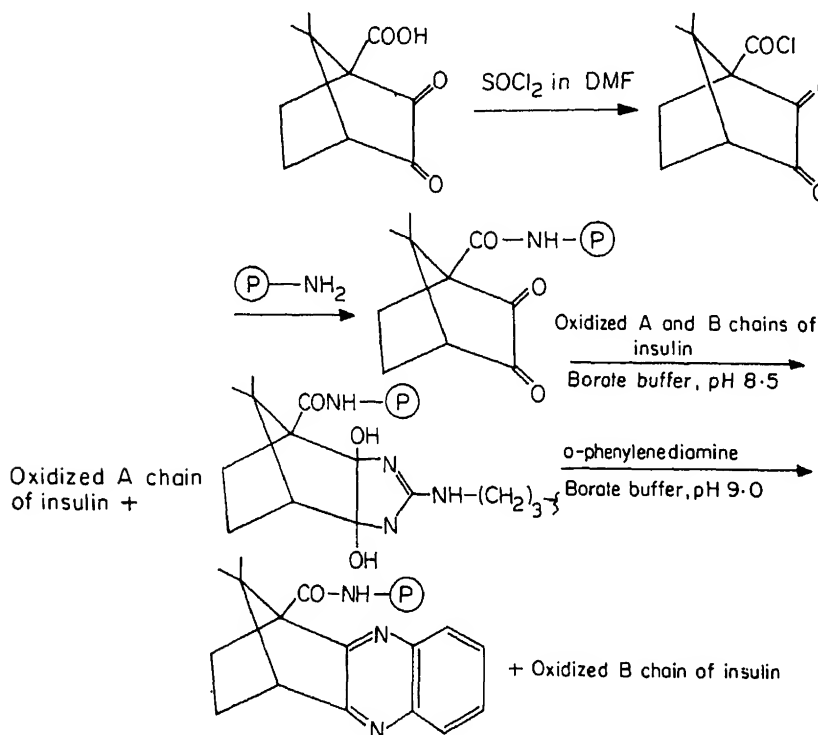
arginine from a mixture of amino acids passing through it. Furthermore, when
ixture of oxidized A and B chains of insulin in borate buffer, pH 8·5 was passed
ough the column, it retained only the B chain by reacting with its arginine
due. The A chain which did not contain arginine passed through the column
etarded. The column was then eluted with o-phenylenediamine at pH 9.
dized B chain was released in 98% yield (scheme 2). A column of this kind is,
refore, useful in batch type seperation of peptides with arginine residues from
se which do not possess arginine.

nowledgement

erences

e C S, Pelzig M and Glass J D 1980 Camphorquinone-10-sulfonic acid and derivatives, convenient
eagents for reversible modification of arginine residues; *Proc. Natl. Acad. Sci. USA* **77** 895–899
erland H and Shriner R L 1936 Anamalous mutarolation of salts of Reychler acid IV; *J. Am. Chem.*
oc. **58** 62–63
ett P D and Knox L H 1939 Bicyclic structures prohibiting the Walden inversion; *J. Am. Chem. Soc.*
1 3184–3192

Chloroquine delivery to erythrocytes in *Plasmodium berghei*-infected mice using antibody-bearing liposomes as drug vehicles*

SUBHASH CHANDRA, AJAY K AGRAWAL and C M GUPTA[†]

Divisions of Membrane Biology and Parasitology, Central Drug Research Institute, Lucknow 226 001, India

Abstract. Suitability of anti-erythrocyte $F_{(ab')2}$-bearing liposomes as vehicles for chloroquine in the treatment of chloroquine resistant *Plasmodium berghei* infections in mice has been examined. Free chloroquine or chloroquine encapsulated in antibody-free liposomes failed to show much effect on the resistant infections, but the same doses of this drug after being encapsulated in antibody-bearing liposomes exhibited a significant inhibitory effect on this infection. These results indicate that chloroquine delivery in antibody targeted liposomes may help in the successful treatment of the chloroquine resistant malarial infections.

Keywords. Drug targeting; liposomes; antibody; erythrocyte; malaria; drug-resistant infection; mice.

1. Introduction

Antibody-bearing liposomes are useful as carriers in drug targeting to specific cells in experimental animals (Agrawal *et al* 1987; Bankert *et al* 1989; Hospenthal *et al* 1989; Hughes *et al* 1989). We have previously shown (Singhal and Gupta 1986) that liposome binding to erythrocytes can be markedly increased by covalently attaching anti-erythrocyte $F_{(ab')2}$ to the liposome surface. Also, it has been demonstrated that these liposomes could serve a useful purpose in drug homing to erythrocytes during malarial infections (Agrawal *et al* 1987). To further evaluate the usefulness of these liposomes as drug homing devices in malaria, we have now studied the efficacy of the liposomized chloroquine (chq) against both chq-sensitive and chq-resistant *Plasmodium berghei* infections in mice.

2. Materials and methods

2.1 *Materials*

Egg phosphatidylcholine (PC), egg [^{14}C] PC and gangliosides were prepared as described earlier (Singhal *et al* 1986). Chloroquine diphosphate, sodium cyanoborohydride and pepsin were purchased from the Sigma Chemical Company

St. Louis, Mo, USA. Na $[^{125}I]$ (carrier-free) was obtained from the Bhabha Atomic Research Centre, Bombay.

2.2 *Liposomes*

Liposomes were prepared from egg PC (20 μmol), cholesterol (20 μmol) and gangliosides (4 μmol) in 0·8 ml of borate-buffered saline (10 mM borate, 60 mM NaCl, pH 8·4) containing chloroquine diphosphate (350 μmol) by sonication (Kumar and Gupta 1985) and fractionated by centrifugation (Kumar and Gupta 1983). Free chq from drug entrapped liposomes was removed by gel filtration over Sephadex G-50 (Gupta and Bali 1981). The mean outer diameter of these liposomes, as determined by molecular sieve chromatography (Kumar and Gupta 1985) was about 45 nm. The amount of chq entrapped in liposomes was about 170 ± 3 μg/μ mol lipid P.

2.3 *Chq estimation*

Chq was estimated by measuring its absorbance at 342 nm as described earlier (Agrawal *et al* 1987).

2.4 *Anti-mouse erythrocyte $F_{(ab')2}$ bearing liposomes*

Anti-mouse erythrocyte antibodies were raised in rabbits and isolated from anti-serum following the procedure of Singhal *et al* (1986). The $F_{(ab')2}$ fragments from the antibody were prepared, purified and covalently attached to the liposome surface as described earlier (Singhal *et al* 1986). The liposomes were passed through a millipore filter (pore size, 0·22 μm) prior to their use in animal experiments. The protein-to-lipid ratio (Singhal *et al* 1986) in the liposomes was about 90 μg protein/μmol lipid P.

2.5 *Animals*

Randomly bred Swiss mice were obtained from the animal house of our institute. Male mice (8–10 weeks old) of 20 ± 2 g weight were used. The animals were kept in plastic cages and given a diet of pellets (Hindustan Lever Limited) and water *ad libitum.*

2.6 *Parasites*

P. berghei parasites were obtained from the National Institute of Communicable Diseases, New Delhi, and maintained in the Swiss mice through serial blood passage. The strain was fully sensitive to chq; the ED 90 being 15 mg/kg × 4 days (i.p.). Parasitaemia was determined by counting 10^3 red cells in thin blood smear stained with Giemsa, and expressed as number of parasitized cells/100 erythrocytes.

2.7 *Development of chq-resistance*

Chq-resistance was developed by the relapse technique, as described earlier

erythrocytes and on the same day, a single dose (60 mg/kg, i.p.) of chq was administered. After the animals developed about 2% parasitaemia, the infected blood from these animals was transfused into healthy animals which were also given chq (60 mg/kg, i.p.) simultaneously. The above operation was repeated several times till the infection was rendered resistant to chq (50 mg/kg × 4 days, i.p.).

The chq-resistant *P. berghei* strain used in this study was developed about 4 years ago by us using the above technique, and has since been regularly maintained in mice under constant drug pressure. The strain retained its chq-resistant character for about a year even after withdrawing the drug pressure.

2.8 *Drug treatment*

Swiss mice (4–5 animals/group) were infected on day zero with about 10^6 erythrocytes infected with chq-sensitive or chq-resistant *P. berghei* strains. These animals were given a single intravenous dose of chq, chq loaded in non-targeted liposomes (free of $F_{(ab')2}$) or chq encapsulated in targeted liposomes (bearing $F_{(ab')2}$) on day 4 after the infection when parasitaemia was 0·01–0·10%. Parasitaemia was determined regularly from day 5. The per cent suppression of parasitaemia in animals treated with drug-laden liposomes was calculated by comparing the parasitaemias in these animals with those treated with an identical dose of free chq or buffer.

3. Results

Liposomes were formed from PC, cholesterol and gangliosides both in the presence and absence of chq by sonication and fractionated by ultracentrifugation. Most of the chq (over 90%) loaded in liposomes were found to reside in the liposomes internal aqueous phase rather than the lipid bilayer. Targeted liposomes were prepared by covalently attaching anti-mouse erythrocyte $F_{(ab')2}$ to the non-targeted liposomes surface. Mice infected with chq-sensitive or chq-resistant *P. berghei* strains were given only one dose of free or liposomized chq by intravenous route on day 4 after the infection. This administration of liposomes did not induce hemolysis, as judged by the measurement of haemoglobin levels in plasma of the injected animals (data not shown).

Erythrocyte surface structure and properties are altered during malarial infection (Howard 1982). It may thus be argued that the targeted liposome preparation used in this study could have an altered erythrocyte binding in infected mice as compared to the normal animals. To examine this possibility, we have determined the tissue distributions of liposomes before and after infecting the animals with *P. berghei*. Figure 1 shows that this distribution was not much affected by the infection, suggesting that the erythrocyte binding capacity of targeted liposomes was not influenced by infecting the animals with *P. berghei* (0·01–0·10% parasitaemia).

Efficacy of chq against malarial infections was examined at its various doses in mice infected with chq-sensitive *P. berghei*. Free and liposomized chq were administered to the separate groups of infected animals, and the efficacy of this treatment was determined by comparing parasitaemias in these animals with those treated with saline. Table 1 shows that the efficacy of chq against malarial infection
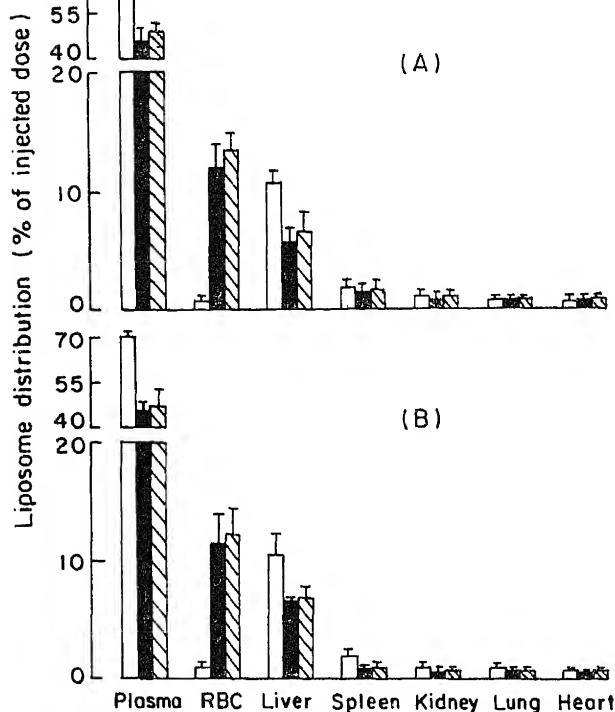
Figure 1. Distribution of liposomes in various tissues. Values shown are mean of 4 animals ± SD. (A) Normal mice. (B) *P. berghei*-infected mice. Tissue distributions were determined 15 min after injecting the liposomes, essentially as described earlier (Singhal and Gupta 1986). The non-targeted liposomes were radio-labelled by incorporating traces of egg [^{14}C] PC in their bilayers, while the targeted liposomes besides having egg [^{14}C] PC in their bilayers also contained [^{125}I] labelled $F_{(ab')2}$ on their surface. (□), Non-targeted liposomal [^{14}C]; (■), targeted liposomal [^{14}C]; (▧), targeted liposomal [^{125}I].

Table 1. Efficacy of chq against chq-sensitive *P. berghei* infection in mice after encapsulation in targeted liposomes.

Treatment	Dose (mg/kg)	Efficacy on day 6		Efficacy on day 11	
		Parasitaemia inhibition (%)	Survival	Parasitaemia inhibition (%)	Survival
Free Chq	5	64·6 ± 5·4	9/10	43·4 ± 7·7	5/10
	2·5	43·1 ± 3·0	8/10	31·5 ± 2·7	3/10
Liposomized Chq	5	95·2 ± 0·8	10/10	83·0 ± 2·7	9/10
	2·5	87·3 ± 3·9	9/9	62·3 ± 5·1	7/9

Treatments were given on day 4 after the infection. Values are mean ± SE.

was considerably increased by delivering it in targeted liposomes; both the per cent survival and per cent parasitaemia suppression were high in the liposomized chq-treated animals as compared to those treated with free chq. This result is in agreement with earlier studies (Agrawal *et al* 1987).

the chq-resistant malarial infections also, we evaluated the efficacy of free and liposomized chq in mice which were infected with chq-resistant *P. berghei*. The parasites were made resistant to chq as described earlier in §2. The chq resistance was ascertained after treating the infected animals with chq. While this drug failed to eliminate the resistant infections even at $50 \text{ mg/kg} \times 4$ days (i.p) dose, it completely cured the chq-sensitive infections at a much lower dose ($15 \text{ mg/kg} \times 4$ days, i.p.).

Table 2 shows that parasitaemias in chq-resistant *P. berghei*-infected mice after treatment with free chq were similar to those observed in saline or drug-free liposome-treated animals. However, the same doses of chq were very effective in controlling the chq-resistant infections when delivered in targeted liposomes (table 2). A 5 mg/kg dose of the liposomized chq appeared optimal, as the antimalarial effect did not significantly improve by increasing the drug dose (data not shown). This dose (5 mg/kg) of the liposomized chq was very effective in suppressing the parasitaemias at least up to day 12 after the infection (figure 2). Also, it considerably prolonged the survival time of the treated animals, when compared to the animals which were given chq in free form (figure 3).

4. Discussion

This study demonstrates that efficacy of chq against the malarial infection is markedly increased by delivering this drug in anti-erythrocyte $F_{(ab')2}$-bearing liposomes. The liposomized chq is effective in controlling not only the chq-sensitive infections but also the infections that were resistant to free chq. The latter effect of the liposomized chq appears to be related to the ability of our liposomes to concentrate the drug in erythrocyte, as chq encapsulated in nontargeted liposomes failed to exhibit any effect against the resistant infections (table 2).

Although the targeted liposomes used in this study were derived by covalently attaching anti-mouse erythrocyte $F_{(ab')2}$ to the liposome surface, their ability to specifically recognize erythrocytes *in vivo* was not altered by the malarial infection (figure 1). This may be attributed to the wider specificity of our antibodies, the low degree of infection or both.

Table 2. Efficacy of chq against chq-resistant *P. berghei* infection in mice after encapsulation in targeted liposomes.

Treatment	Chq dose (mg/kg)	Parasitaemia on day 8 (%)	Survival on day 13
Saline	—	2.9 ± 0.8	0/4
Drug-free non-targeted liposomes	—	2.5 ± 0.4	0/4
Drug-free targeted liposomes	—	2.0 ± 0.2	1/4
Chq-laden non-targeted liposomes	5.0	2.5 ± 0.5	1/4
Chq-laden targeted liposomes	2.5	1.1 ± 0.2	2/4
	5.0	0.25 ± 0.04	3/4
Free Chq	2.5	2.1 ± 0.3	0/4
	5.0	1.9 ± 0.9	0/4

Treatments were given on day 4 after the infection. Values are mean ± SE.
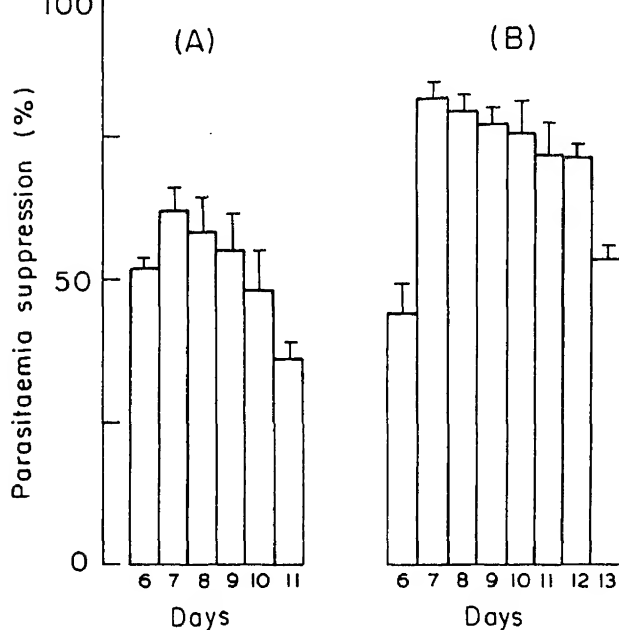
Figure 2. Efficacy of chq-laden targeted liposomes against chq-resistant *P. berghei* infection on various days after the treatment. The treatments were given on day 4 after the infection. Parasitaemia suppression was calculated by using the parasitaemias in free chq-treated animals as the control values (A) chq at 2·5 mg/kg dose. (B) chq at 5 mg/kg dose. Values are means ± SE. The number of animals used in each group was ten.
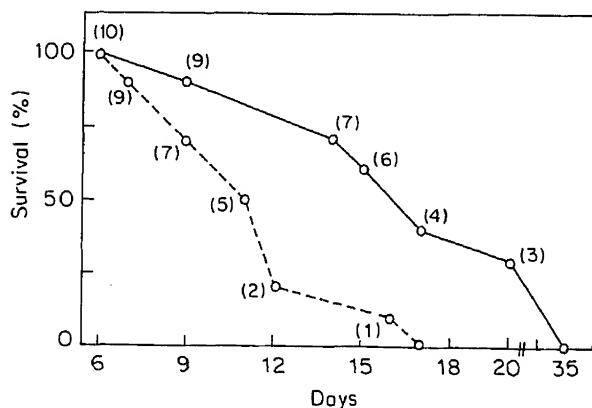
Figure 3. Effect of chq treatment before (broken line) and after (solid line) encapsulating the drug in targeted liposomes, on long-term survival of animals infected with chq-resistant *P. berghei*. The treatments (5 mg/kg dose of chq) were given on day 4 after the infection. Numbers in parentheses denote the number of animals surviving on a given day after the infection.

resistant *P. berghei* infections showed that encapsulation of chq in liposomes (non-targeted) increased not only the maximal tolerable dose from 0·8 to 10 mg chq/animal when given intraperitoneally but also the drug effectivity against the infections. A dose of 8 mg chq/mouse/day for three consecutive days was found to be the most effective. Although we have given only a single intravenous dose (5 mg/kg) of chq in targeted liposomes, which was much smaller than that used by these workers (2–8 mg/mouse), the antiparasitic effect observed by us against the chq-resistant infections was still quite significant. This finding clearly suggests that chq delivery in targeted liposomes could be successful in curing the chq-resistant infections, using low drug doses.

The demonstrated biologic response of chq-laden targeted liposomes against the chq-resistant malarial infections is not optimal, and may further be improved by using an infected erythrocyte-specific antibody rather than the nonspecific antibody, as used in this study. Also, the response may increase by changing the route of administration, and increasing the dose number. Finally, the intracellular concentration of chq in erythrocytes infected with chq-resistant *P. berghei* strain may be increased by encapsulating an appropriate Ca^{2+}-channel inhibitor along with chq in targeted liposomes, which in turn should increase the antimalarial activity (Martin *et al* 1987).

Acknowledgements

References

Agrawal A K, Singhal A and Gupta C M 1987 Functional drug targeting to erythrocytes *in vivo* using antibody bearing liposomes as drug vehicles; *Biochem. Biophys. Res. Commun.* **148** 357–361

Bankert R B, Yokota S, Ghosh S K, Mayhew E and You Y H 1989 Immunospecific targeting of cytosine arabinonucleoside containing liposomes to the idiotype on the surface of a murine B-cell tumor *in vitro* and *in vivo*; *Cancer Res.* **49** 301–309

Gupta C M and Bali A 1981 Carbamyl analogs of phosphatidylcholines: Synthesis, interaction with phospholipases and permeability behaviour of their liposomes; *Biochim. Biophys. Acta* **663** 506-515

Hospenthal D, Grentzinger K and Rogers A 1989 Treatment of murine model of systemic candidiasis with liposomal Amphotericin-B bearing antibody to *Candida albicans*; *J. Med. Microbiol.* **30** 193–197

Howard R J 1982 Alterations in the surface membrane of red blood cells during malaria; *Immunol. Rev.* **61** 67–107

Hughes B J, Kennel S, Lee R and Hwang L 1989 Monoclonal antibody targeting of liposomes to mouse lung *in vivo*; *Cancer Res.* **49** 6214–6221

Kumar A and Gupta C M 1983 Effect of altered polar head of phosphatidylethanolamines on transbilayer aminophospholipid distribution in sonicated vesicles; *Biochim. Biophys. Acta* **730** 1–9

Kumar A and Gupta C M 1985 Transbilayer phosphatidylcholine distribution in small unilamellar sphingomyelin-phosphatidylcholine vesicles. Effect of altered polar head-group; *Biochemistry* **24** 5157–5163

Martin S K, Oduola A M J and Milhous W K 1987 Reversal of chloroquine resistance in *Plasmodium falciparum* by Verapamil 1987; *Science* **235** 899–901

liposomes in the chemotherapy of murine malaria; *Parasitology* 93 301–306

Singhal A and Gupta C M 1986 Antibody-mediated targeting of liposomes to red cells *in vivo*; *FEBS Lett.* **201** 321–326

Singhal A, Bali A and Gupta C M 1986 Antibody-mediated targeting of liposomes to erythrocytes in whole blood; *Biochim. Biophys. Acta* **880** 72–77

Warhurst D C and Folwell R O 1968 Measurement of the growth rate of the erythrocytic stages of *Plasmodium berghei* and comparisons of the potency of inocula after various treatments; *Ann. Trop. Med. Parasitol.* **62** 349–360

Molecular cloning, characterization and expression of a nitrofuran reductase gene of *Escherichia coli*

AJIT N KUMAR[†] and R JAYARAMAN[*]

School of Biological Sciences, Madurai Kamaraj University, Madurai 625 021, India
[†]Present address: Department of Tropical Public Health, Harvard School of Public Health, Boston, MA 02115, USA

Abstract. Mini-mu derivatives carrying plasmid replicons can be used to clone genes *in vivo*. This method was adopted to generate phasmid clones which were later screened for their ability of restore nitrofurantoin sensitivity of a nitrofuran-resistant host by eliciting nitroreductase activity. One phasmid-derived clone (pAJ101) resulted in considerable increase in nitroreductase activity when introduced into a nitrofurantoin-resistant mutant of *Escherichia coli* with reduced nitroreductase activity. Subsequently, a 1·8 kb fragment obtained from pAJ101 by partial digestion with *Sau*3'A, was subcloned into pUC18 to yield pAJ102. The nitroreductase activity attributable to pAJ102 was capable of reducing both nitrofurantoin and nitrofurazone. The polypeptides encoded by pAJ102 were identified by the minicell method. A large, well-defined band corresponding to 37 kDa and a smaller, less-defined band corresponding to 35 kDa were detected. Tn1000 mutagenesis was used to delineate the coding segment of the 1·8 kb insert of pAJ102. A 0·8 kb stretch of DNA was shown to be part of the nitroreductase gene. The gene was mapped at 19 min on the *Escherichia coli* linkage map.

Keywords. Molecular cloning; nitrofurans; nitrofuran reductase.

1. Introduction

Nitrofurans are synthetic antimicrobial agents extensively used in human and veterinary medicine (reviewed by Grunberg and Titsworth 1973). The discovery of antibacterial activity in the 5-nitro derivatives of some 2-substituted furans (Dodd and Stillman 1944) led to the development of a series of such compounds with varying degrees of biological activity, many of which were put to clinical use. Although the subsequent discovery of side-effects such as pulmonary toxicity (Taskinen *et al* 1977; Holmberg and Bowman 1981), hepatic damage (Goodman and Gillman 1975; Black *et al* 1980), peripheral neuritis (Paul and Paul 1964) etc., led to a re-evaluation of their chemotherapeutic effectiveness *vis-a-vis* safety, a number of compounds have remained in use. Nitrofurazone (as a topical antiseptic), nitrofurantoin (in urinary tract infections) and furazolidone (for gastrointestinal infections in cattle and poultry) are some of the nitrofurans still in use.

Central to the biological activity of these drugs is their metabolic activation by a class of enzymes called nitroreductases (reviewed by Kedderis and Miwa 1988). These enzymes activate nitrofurans by mediating the reduction of their nitro group. The existence of nitroreductases and the constitutivity of expression of the corresponding genes in many bacteria are obviously responsible for the broad

---

[*]Corresponding author.

spectrum of antibacterial activity of these drugs. However, the normal physiological role of these enzymes is not known. Despite the large body of evidence relating nitroreductase activity with nitrofuran sensitivity of bacteria, the individual steps in the mode of activation have not been studied in detail. Development of resistance to a nitrofuran is usually attributed to mutations which result in the loss of nitroreductase activity (Asnis 1957; McCalla et al 1970, 1975, 1978; Bryant et al 1981). In Escherichia coli, oxygen-sensitive (type II) and oxygen-insensitive (type I) nitroreductase activities have been identified (Asnis 1957; McCalla et al 1970, 1975, 1978). The oxygen-insensitive activity consists of major and minor components (McCalla et al 1978), the genes for which have been designated nfsA and nfsB, respectively. The minor nitroreductase activity has been shown to consist of two independent entities (Bryant et al 1981). The genes coding for the oxygen-insensitive nitroreductases have been broadly mapped to the lac-gal region (McCalla et al 1978). The precise map positions were however not identified. Two-step nitrofurazone-resistant mutants (see below) were shown to have lost the major nitroreductase activity and one of the two minor activities (McCalla et al 1978). Taking advantage of the correlation between nitrofurantoin resistance and loss of nitroreductase activity, we used a nitrofurantoin-resistant mutant as a host to isolate potential nitroreductase clones by screening for restoration of nitroreductase activity and drug sensitivity. In the present communication we report the cloning of a 1·8 kb fragment carrying the nitroreductase gene, identification of the encoded polypeptide and mapping of the cloned nitroreductase gene.

2. Materials and methods

2.1 Bacterial strains and plasmids

The E. coli strains and the plasmids used are listed in table 1.

2.2 Chemicals

All chemicals were obtained commercially and were of analytical grade. ^{35}S methionine was obtained from Amersham, England through Bhabha Atomic Research Centre, Bombay. ATP and NADPH were from Boehringer-Mannheim, Germany. Enzymes and other chemicals used during DNA manipulations were obtained from New England Biolabs, USA, Amersham, England and BRL, USA. The concentrations (μg/ml) of the antibiotics used were as follows: ampicillin, 100; tetracycline, 20; kanamycin, 40 and chloramphenicol, 6. Nitrofurantoin (Sigma Chemical Co., USA) was used at varying concentrations depending on the experiment.

2.3 Isolation of nitrofurantoin resistant mutants

Spontaneous nitrofurantoin-resistant mutants were isolated by plating approxima-tely 10^7 cells of AB1157 on L-plates containing 10 μg/ml of the drug and incubating the plates at 37°C. Putative mutants were patched on to fresh L-plates containing the same concentration of nitrofurantoin. The stability of the mutation was assessed by growing these mutants for several cycles in non-selective L-medium and plating

Strain	Relevant genotype	Source/construction
Broda 8	*Hfr relA1 spoT1 metB1*	P Broda *via* B J Bachmann
HfrC	*Hfr relA1 spoT1*	L Cavalli–Sforza *via* B J Bachmann
KL208	*Hfr relA1? spoT1?*	K B Low *via* B J Bachmann
AB1157	F⁻ *thr1 leuB6 proA2 hisG4 argE3 thi1 rpsL31*	E A Adelberg *via* B J Bachmann
AB3027	F⁻ *thr1 leuB6 proA2 hisG4 argE3 thi1 polA20*	P Howard Flanders *via* B J Bachmann
S1316	*araD139* △ *(argF-lac)* 169 *zbh-428*::Tn10 *relA1 rpsL150 hisC9*::Mu *cts deoC1?*	A Campbell *via* B J Bachmann
RW1230	△ (*gpt-proA*) 62 *zbj-1230*::Tn10 *hisG4 thi1*	R Kadner *via* B J Bachmann
MM383	*lacZ53 thyA36 rpsL151 polA12*(Ts)	M Monk *via* B J Bachmann
DS410	*azi-8? tonA2? minA1 minB2 rpsL135*	J N Reeve *via* B J Bachmann
RE103	*proA23 lac28 cmlA1 trp 30 his-51 rpsL101*	E C R Reeve *via* B J Bachmann
NFR502	AB1157 but *nfsA nfsB*	D R McCalla *via* B J Bachmann
Xph43 Mu *cts*	F⁻ △ (*argF-lac*)U169 *trp* △ (*brnQ phoA phoC phoB phoR*) Mu *cts*	M Casadaban
RJ101	△ (*lac-pro*) Rif^r *recA*::Cm	Laboratory collection
AJ101	One-step nitrofurantoin resistant mutant of AB1157	This work
AJ102	AJ101::Mu *cts*	This work
AJ212	Higher level nitrofurantoin resistant mutant (two-step mutant?) of AJ102	This work
AJ251	AB1157::Mu *cts*	This work
AJ301	MM383 with pAJ102 on the chromosome by integrative recombination	This work
AJ302	AB3027, Amp^r	This work
AJ321	MM383 with pAJ103 on the chromosome by integrative recombination	This work
AJ322	AB3027, Amp^r, Kan^r	This work
Plasmids:		
pEG5005	10·2-kb, pBCO::Mu d5005 Kan^r, Amp^r	M Casadaban
pUC18	2·7-kb, derivative of pBR322 Amp^r	J Messing
pKU602	4·6-kb, pUC18 carrying ApH gene from Tn5 Kan^r, Amp^r	K Dharmalingam
pAJ101	ca. 24-kb, phasmid-based nitroreductase clone, Kan^r	This work
pAJ102	4·5-kb, nitroreductase subclone, Amp^r	This work
pAJ103	6·4-kb, pAJ102 with Kan^r cartridge in nitroreductase gene Amp^r, Kan^r	This work

suitable dilutions on L-nitrofurantoin and L-streptomycin plates. A mutant (AJ101) which fulfilled the criterion of matching titres on both types of plates was lysogenized with Mu *cts*62 to give AJ102. A two-step mutant AJ212 was obtained from AJ102 as before but by spreading the cells on L-plates containing 70 μg/ml nitrofurantoin.

AB1157 was lysogenized with Mu *cts*62 phage to give AJ251 which in turn was transformed to kanamycin resistance with pEG5005 isolated from Xph43Mu *cts* harbouring the phasmid. The lysate, obtained from pEG5005/AJ251 by heat induction, was used to transduce AJ212 to kanamycin resistance according to the protocol of Groisman and Casadaban (1986). The kanamycin-resistant trans-ductants were screened for loss of ampicillin resistance to select for phasmids with an included chromosomal fragment (Groisman *et al* 1984). The kanamycin-resistant, ampicillin-sensitive transductants were gridded on to L-nitrofurantoin (70 and 30 μg/ml) and L-kanamycin plates. Since interpretation of nitrofurantoin resistance/sensitivity is often obscured by cell density, care was taken to make thin and broad patches while gridding. The transductants which showed no (or least) growth on L-nitrofurantoin plates were later assayed for nitroreductase activity.

2.5 *Nitroreductase assays*

2.5a *Reduction of nitrofurantoin by whole cells*:   Strains were grown overnight in L-medium, diluted 1:100 in fresh medium and aerated at 30°C till mid-log phase. Appropriate antibiotics were included in the growth medium in the case of plasmid-bearing strains. The cells were collected, washed with M/15 phosphate buffer (pH 7·2) and the absorbance at 600 nm was adjusted to 0·4. Glucose was added to 0·2% and the suspension was aerated at 30°C for 30 min. Nitrofurantoin was added to a concentration of 20 μg/ml and aeration continued. Three ml aliquots were removed at intervals, centrifuged in a microfuge for 3 min and the absorbance of the supernatant was measured at 372 nm (the absorption maximum of nitrofurantoin). Rate of nitrofurantoin reduction by whole cell suspensions was expressed as nmol reduced/ml. A decrease of 0·06 units in absorbance was taken to correspond to the reduction of 10 nmol of nitrofurantoin. Each value was obtained as an average of three independent experiments.

2.5b *Reduction of nitrofurantoin and nitrofurazone by cell-free extracts*:   The cells were grown as above, collected, washed with M/15 phosphate buffer (pH 7·2) and resuspended in the same buffer at 1/20 the original volume. The cells were lysed by sonication in a Labline ultrasonic system, with several 30s pulses at 100 W with 1-min intervals, the cells being kept cold on ice. The lysate was clarified at 100,000 g for 1 h at 4°C and the organelle-free supernatant was assayed for nitroreductase activity. The assay mixture contained: 300 μg NADPH, enzyme extract, nitro-furantoin (0·25 μmol) or nitrofurazone (0·3 μmol) and M/15 phosphate buffer (pH 7·2) in a total volume of 3 ml. The assay mixture was preincubated at 25°C without NADPH for 10 min and the reaction was initiated by the addition of NADPH. The reduction was monitored at 372 nm (nitrofurantoin) or 375 nm (nitrofurazone). The amount of drug reduced was calculated as follows: reduction of 10 nmol of nitrofurantoin and nitrofurazone results in a decrease of 0·06 and 0·05, respectively, at the respective absorption maximum. Each value was obtained as the average of three independent experiments. Protein was estimated by the method of Lowry *et al* (1951). Reductase activity was expressed as nmol of nitrofuran reduced/min/mg protein.

DNA manipulations were carried out according to the protocols outlined by Silhavy *et al* (1984). Subcloning of the nitroreductase gene was accomplished by digesting pAJ101 (see 'results') with different concentrations of *Sau*3A and ligating the digest containing the maximum number of fragments in the 1·8–2·4 kb range, into the *Bam*HI site of pUC18. The ligated mixture was used to transform AJ212 to ampicillin resistance.

Cartridge mutagenesis with the 1·9 kb *Bam*HI fragment from pKU602, carrying the kanamycin resistance gene, was performed by ligating the *Bam*HI fragment into the *Bgl*II site within the nitroreductase gene (see 'results').

2.7 *Genetic techniques*

P1 transductions and conjugational crosses were carried out according to Miller (1972) and Silhavy *et al* (1984), respectively. Integrative recombination of pAJ102 and pAJ103 was achieved essentially by the protocol of Cunningham and Weiss (1985). However, immediately after transformation the plates were incubated at 30°C. The transformants were pooled and grown in L-medium for a few generations at 30°C before the culture was subjected to alternating temperature shifts from 30° to 42°C and *vice versa*.

2.8 *Mutagenesis with Tn1000*

RJ101 carrying F′128 was transformed to ampicillin resistance with pAJ102. One of the transformants was used as donor in a cross with AJ212 (as recipient) and ampicillin-resistant transconjugants were obtained. The ampicillin-resistant transconjugants were screened for nitrofurantoin sensitivity/resistance by gridding on L-nitrofurantoin plates (30 μg/ml) and were also subjected to restriction analysis (see 'results').

2.9 *Identification of plasmid-encoded polypeptides*

Plasmid-encoded polypeptides were identified by the minicell method of Komai *et al* (1982). The minicell-producing strain DS410 was transformed to ampicillin resistance with pUC18 (control) and pAJ102 separately. Minicells were isolated on discontinuous sucrose gradients and labelled with ^{35}S methionine. The labelled minicells were mixed with sample buffer, kept in a boiling water bath for 3 min and the proteins were electrophoresed according to Laemmli (1970). The gel was fluorographed with PPO as the scintillant according to the method of Bonner and Laskey (1974), dried under vaccum and exposed to Indu X-ray film at −70°C.

2.10 *Monitoring the response of AJ212 and AJ212/pAJ102 to nitrofurantoin challenge*

Overnight cultures of AJ212 in L-medium, and AJ212 harbouring pAJ102, in L-medium containing ampicillin, were diluted 1:100 in fresh L-medium and grown to a density of approximately 5×10^7 cells/ml. Nitrofurantoin was added to both cultures at 20 μg/ml and aeration continued. The kinetics of killing was monitored

The plates were incubated at 30 C for 24 h to score for the survivors.

3. Results

3.1 *Isolation of nitrofurantoin-resistant mutants*

A stable mutant (AJ101) which satisfied the criterion of matching titres on media with and without nitrofurantoin was isolated as described under experimental procedures. It was found to tolerate up to 40 μg/ml nitrofurantoin although it was isolated on an L-plate containing 10 μg/ml nitrofurantoin. AJ101 was lysogenized with Mu *cts*62 to give AJ102. Whole cell suspensions of AJ102 displayed very low levels of nitroreductase activity (figure 1). Subsequently, a two-step mutant, AJ212, was isolated from AJ102. However, in the case of the two-step mutant, the high level of resistance was not stably maintained. Immediately after isolation the strain tolerated the drug up to a concentration of 100 μg/ml but on prolonged storage followed by growth in drug-free media the level of resistance dropped considerably. In any case, the level of resistance was greater than that of the parent strain, AJ101. The nitroreductase levels of the one- and two-step mutants were however the same (figure 1). In the light of these observations the nature of the second level nitrofurantoin resistance mutation in AJ212 is uncertain.

3.2 *Cloning of the nitroreductase gene*

The cloning strategy involved the generation of a phasmid-based library of a
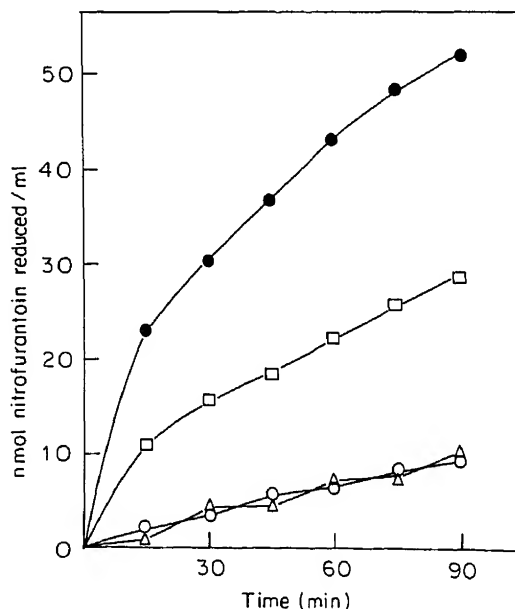
Figure 1. Nitroreductase activities of whole-cell suspensions.
($\bullet$), AJ212 carrying pAJ102; ($\square$) AJ212 carrying pAJ101; ($\bigcirc$), AJ102; ($\triangle$), AJ212.

resistant strain and selecting a clone in which nitroreductase levels and drug sensitivity are restored. The phasmid-based clones obtained as described under experimental procedures were used to transduce AJ212 to kanamycin resistance. Approximately 5000 kanamycin-resistant transductants were screened initially for sensitivity to ampicillin and the ampicillin-sensitive clones were screened for nitrofurantoin sensitivity. Ten potential nitroreductase clones were isolated based on the extent of their growth on L-plates containing 70 and 30 μg/ml of nitrofurantoin and the levels of nitroreductase activity in whole-cell suspensions. However, only one of the isolates displayed stable nitrofurantoin sensitivity. The presence of the phasmid (pAJ101) in this clone resulted in a substantial increase in nitroreductase activity in whole cell suspensions (figure 1). There was a corresponding increase in the activity in cell-free extracts (table 2).

3.3 Subcloning and restriction analysis of the nitroreductase gene

The nitroreductase gene was subcloned into pUC18. In an earlier report by McCalla et al (1978) the sizes of the major and minor nitroreductases were estimated to be 56 and 38 kDa respectively. Therefore random fragments in the 1·8–2·4 kb size range, obtained by partial digestion of pAJ101 DNA with Sau3A, were ligated with BamHI linearized pUC18 and used to transform AJ212 to ampicillin resistance. The transformants were screened for nitrofurantoin sensitivity and assayed for nitroreductase activity. One of the transformants displayed enhanced nitroreductase activity and carried a recombinant plasmid (pAJ102) with a 1·8 kb insert. Assays of the nitroreductase activities attributable to pAJ101, pAJ102 and the mutant host AJ212, both in vivo (figure 1) and in vitro (table 2) clearly demonstrate that pAJ102 includes the nitroreductase gene. The higher level of reductase activity due to pAJ102 can be attributed to the copy number of the plasmid. The possession of pAJ102, renders the cell hypersensitive to nitrofurantoin (see below). Since nitroreductases are known to activate a variety of nitrofurans, the activity was assayed with both nitrofurantoin and nitrofurazone as substrates (table 2). It is apparent that the activity is not restricted to nitrofurantoin but extends to atleast one other nitrofuran.

The presence of convenient restriction sites on the vector facilitated restriction analysis of the 1·8 kb insert. A partial restriction map of the 1·8 kb insert is depicted in figure 2a.

3.4 Mutagenesis of pAJ102 with Tn1000 ($\gamma\delta$)

In order to delineate the segment coding for nitrofuran reductase within the 1·8 kb

Table 2. Nitrofuran reductase activities in vitro.

Source of enzyme extract	Specific activity[a] with nitrofurantoin	Specific activity[a] with nitrofurazone
AJ212	3·7	3·7
AJ212 harbouring pAJ101	463	564
AJ212 harbouring pAJ102	686	813

[a] nmol of drug reduced/min/mg protein.
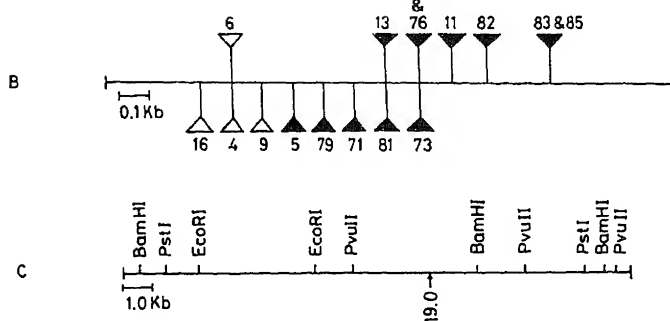
Figure 2. (A) Partial restriction map of insert in pAJ102.
(B) Location of Tn1000 on the 1·8 kb insert of pAJ102.
Tn1000 in $\gamma\delta$ (∇, $\blacktriangledown$) and $\delta\gamma$ ($\triangle$, $\blacktriangle$) orientation, not affecting (∇, $\triangle$) and inactivating ($\blacktriangledown$, $\blacktriangle$) nitroreductase.
(C) Partial restriction map of the chromosomal insert in pAJ101. The arrow indicates 19th min of the *E. coli* genetic map.
   The left and right ends of the figure correspond to the *Hind*III and *Eco*RI ends of the multiple cloning site of *pUC*18. Scale (A) and (B), 1 cm = 0·1 kb. (C) 1 cm = 1·0 kb.

insert of pAJ102, Tn1000 mutagenesis was carried out. The plasmid was first introduced into an F'-bearing strain (RJ101) and subsequently mobilized into a nitrofurantoin-resistant recipient (AJ212) selecting for amp^r transconjugants. F-mediated mobilization of non-conjugal plasmids involves transposition of the $\gamma\delta$ (Tn1000) element on to the plasmid, cointegrate formation, transfer through the F-conjugal system and resolution of the cointegrate in the recipient. Transposition of Tn1000 could result in insertional inactivation of gene function. Since pAJ102 harbours an insert coding for nitroreductase, insertions into the coding segments could be picked up by screening for loss of enzyme activity. The recipient (AJ212) is deficient in nitroreductase and is resistant to nitrofurantoin (see above). Introduction of a plasmid containing an insertionally-inactivated nitroreductase gene would not affect the resistance status of the host while introduction of a functional gene would. Screening for the persistence of nitrofuran resistance of the recipient would allow the detection of clones inheriting the insertionally- inactivated gene. However, loss of resistance would not distinguish between insertions on the vector and those in regions of the insert not coding for nitroreductase. Therefore the amp^r transconjugants were also subjected to restriction analysis which revealed sixteen insertions within the 1·8 kb insert of pAJ102. Using the known restriction maps of pUC18 and Tn1000 the orientations of Tn1000 in each of the insertions were also determined. Figure 2b presents the data. It can be seen from figure 2b that Tn1000 insertions in 0·5 kb of DNA at the left end of the 1·8 kb insert do not inactivate the nitroreductase gene (insertion nos ·4, 6, 9 and 16). Insertions in the next 0·8 kb of DNA (nos 5, 11, 13, 71, 73, 76, 79, 81, 82, 83, 84 and 85) inactivated the gene.·For reasons not known we did not get insertions in the last 0·5 kb of the insert. Therefore the maximum stretch of DNA available in the 1·8 kb insert for encoding the nitroreductase enzyme is 1·3 kb. Accordingly the size of the encoded

region.

3.5 *Identification of plasmid-encoded polypeptides*

The minicell producing strain DS410 was transformed to ampicillin resistance with pUC18 (control) and pAJ102. The minicells were isolated on discontinuous sucrose gradients, labelled with ^{35}S methionine and the proteins were solubilized with sample buffer. The plasmid-encoded polypeptides were identified by SDS-PAGE followed by autoradiography (figure 3). Two additional polypeptides were observed in minicells harbouring pAJ102 (figure 3, lane 2): a major band corresponding to 37 kDa and a minor band corresponding to 35 kDa. The major band was well-defined whereas the minor band was somewhat fuzzy and ill-defined. Considering the stretch of DNA in the 1·8 kb insert identified to constitute the nitroreductase gene (described above), the 37 kDa polypeptide should be the nitroreductase protein while the 35 kDa polypeptide can be attributed to degradation or processing of the 37 kDa polypeptide.

3.6 *Kinetics of survival of AJ212 and AJ212 harbouring pAJ102 upon nitrofurantoin challenge*

Since there is a direct correlation between nitrofuran reductase activity and nitrofuran sensitivity, an enhancement in nitroreductase activity would lead to increased nitrofuran sensitivity. The effect of nitrofurantoin on the viability of AJ212 (control) and AJ212 harbouring pAJ102 was monitored at different time intervals after exposure to nitrofurantoin. At a concentration of 20 μg/ml, nitrofurantoin drastically affected the survival of AJ212 harbouring the nitroreductase clone (figure 4). Within 30 min of addition of the drug, the number of survivors decreased more than 100-fold. (At earlier intervals, there was inhibition of colony-forming ability. On prolonged incubation in the absence of the drug, cells did grow to form colonies). In the case of normal, plasmid-free, nitrofuran-sensitive cells it takes approximately 7 h to obtain the same level of killing under identical conditions (D N Simha and R Jayaraman, unpublished results). The presence of pAJ102 did not affect the growth of AJ212 in the absence of nitrofurantoin (data not shown).

3.7 *Mapping of the nitroreductase gene*

A previous report (McCalla *et al* 1978) had indicated only the approximate map locations of the nitroreductase genes. In order to map the location of the gene that we had cloned, two approaches were followed. In one, the plasmid carrying the cloned gene was forced to integrate into the chromosome. This resulted in the transfer of plasmid-borne drug resistance marker to a chromosomal locus, homologous to the insert carried on the plasmid. The drug resistance marker was then utilized to map the locus of integration by conventional methods. Since DNA polymerase I is essential for the replication and maintenance of *col*EI replicons,
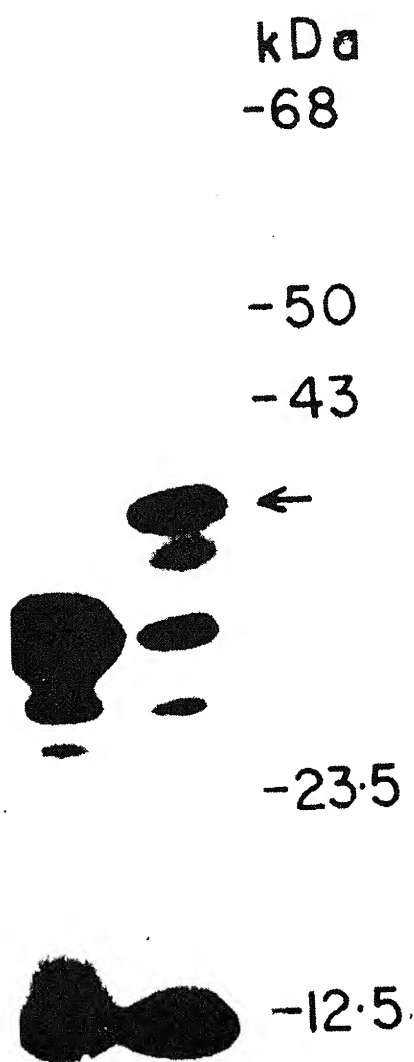
Figure 3. Detection of plasmid-encoded polypeptides by the minicell method. DS410 was transformed separately with pUC18 (control) and pAJ102. The minicells were isolated on discontinuous sucrose gradients and labelled with ^{35}S methionine. The plasmid-encoded polypeptides were identified by PAGE followed by autoradiography.
Lane 1: pUC18 encoded polypeptides. Lane 2: pAJ102 encoded polypeptides. Arrow indicates position corresponding to 37 kDa.

selection for drug resistance under conditions which rendered the enzyme inactive would yield derivatives with the plasmid integrated into the chromosome. Towards this end a *pol*A ts strain (MM383) was transformed with pAJ102 and the ampicillin-resistant transformants were subjected to alternate cycles of growth at 30° and 42°C. In another experiment a drug resistance marker was first introduced into the
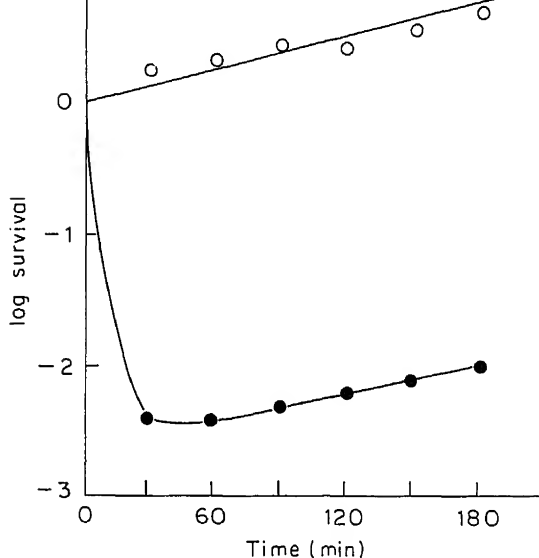
Figure 4. Response of AJ212 and AJ212 harbouring pAJ102, to nitrofurantoin challenge. (O), AJ212; (●), AJ212 harbouring pAJ102.

nitroreductase gene as follows. Since the *Bgl*II site lies within the gene (see above) a 1·9 kb *Bam*HI fragment from pKU602 carrying the gene for kanamycin resistance was ligated into it (cartridge mutagenesis). The resultant plasmid pAJ103 was used to transform MM383. Chromosomal integration of pAJ103 was achieved as described above for pAJ102.

The kanamycin and ampicillin resistance markers (due to integrated pAJ103 and pAJ102) from two derivatives of MM383 (AJ321 and AJ301), were transduced into AB3027. The nitroreductase activities of whole-cell suspensions of a kanamycin resistant transductant (AJ322) and an ampicillin-resistant transductant (AJ302) were determined as before. It is apparent from figure 5 that integration of pAJ102 led to a slight increase in nitroreductase activity whereas integration of pAJ103 did not. This can be explained by the fact that integration of pAJ102 which has an intact nitroreductase gene would give rise to two functional copies of the gene whereas integration of pAJ103 would still have only one functional copy of the gene. The duplication of the nitroreductase gene as a result of integration of pAJ102 leads to an increase in nitroreductase activity (figure 5).

Conjugational crosses between AJ322 (as the recipient) and various Hfrs showed that a good proportion of *gal*⁺ recombinants lost kanamycin resistance (table 3) suggesting that the cloned gene could lie in the vicinity of the *gal* locus. Subsequently, the kanamycin resistance marker of pAJ103 and the ampicillin resistance marker of pAJ102 were mapped by transduction of tetracycline resistance from strains carrying Tn10 insertions close to the *gal* locus and screening the *tet*ʳ transductants for the loss of kanamycin and ampicillin resistance, respectively. Reciprocally, the kanamycin resistance marker of AJ322 was transduced into RW1230 and the *kan*ʳ transductants were screened for loss of tetracycline resistance.
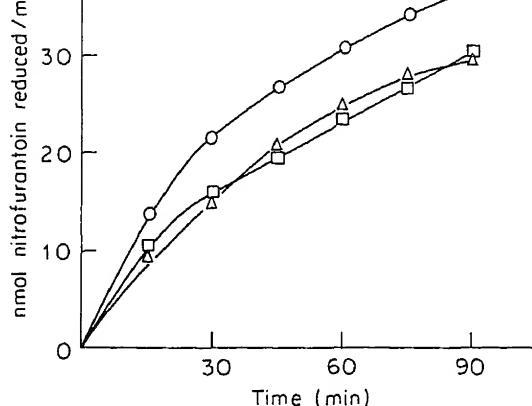
Figure 5. Nitroreductase activities of whole-cell suspensions of AJ302 (○), AB3027 (△) and AJ322 (□).

Table 3. Conjugational crosses between AJ322 and various Hfrs.

Donor	Origin (min) and direction of transfer	Selected marker	Unselected marker	Unselected/ selected (%)
Broda 8	9·5/cc	His$^+$	Kan^s	10·4 (11/106)
HfrC	13/c	Pro$^+$	Kan^s	— (0/112)
HfrC	13/c	Thr$^+$ Leu$^+$	Kan^s	— (0/116)
Broda 8	9·5/cc	Gal$^+$	Kan^s	42·9 (72/168)
KL208	30/c	Gal$^+$	Kan^s	70·5 (93/132)

c: Clockwise; cc: counter clockwise.

Table 4. Transductional mapping of the nitroreductase gene.

Donor	Recipient	Selected marker	Unselected marker	Cotransduction frequency (%)
RW1230	AJ322	Tet^r	Kan^s	1·13 (13/1147)
S1316	AJ322	Tet^r	Kan^s	3·95 (14/354)
RW1230	AJ302	Tet^r	Amp^s	0·97 (5/517)
AJ322	RW1230	Kan^i	Tet^s	0·98 (8/813)
AJ322	RE103	Kan^r	Cml^s	98·19 (163/166)

The results of the transductional analyses are presented in table 4. It can be seen that the nitroreductase locus is cotransducible with the Tn10 insertions in RW1230 and S1316 at a low frequency (1–4%). This observation suggests that the gene could lie between the loci of the two Tn10 insertions (17–19 min). Calculation of the map distances using Wu's formula (Wu 1966; taking L = 2·3) would place the position of the nitroreductase gene between 18·5 and 19·1 min on the linkage map. Table 4 also shows that the nitroreductase locus is very highly cotransducible with *cmlA* (18·8 min). Thus the transductional analyses suggest that the nitroreductase gene could be located at 18·8 min.

1987) in the region indicated by genetic methods were compared. The restriction map of the E. coli chromosome at a location close to 19 min (18·8–19·1 min; kilobase coordinates approximately 895 to 915) matches precisely with the restriction map of the insert in pAJ101. The gene can therefore be placed at 19 min. The PvuII site within the nitroreductase gene facilitated the identification of the map position. The slight discrepancy between the map positions obtained by the two methods can be ascribed to the relative imprecision of conventional genetic methodologies.

4. Discussion

In this report we have presented data on the cloning and characterization of a gene from E. coli coding for nitrofuran reductase. Since nitrofuran resistance and nitroreductase activity bear an inverse correlation we isolated a nitrofurantoin-resistant mutant with low levels of nitroreductase activity and used this to screen phasmid-based clones for restoration of enzyme activity and drug sensitivity. A 1·8 kb fragment of the chromosomal insert of one such clone obtained this way (pAJ101) was subcloned into pUC18, to give pAJ102. The observation that the nitroreductase activity of the host strain was very low in whole cell suspensions as well as cell-free extracts showed that the mutation inactivated the nitroreductase gene rather than creating a simple permeability barrier to nitrofurantoin. The restoration of nitroreductase activity by pAJ101 and pAJ102 in whole cells as well as cell-free extracts showed that the plasmids contain the gene coding for the enzyme. Possession of pAJ101 and pAJ102 renders AJ212, a nitrofurantoin-resistant mutant, highly sensitive to the drug. Although an earlier report (Herrlich and Schweiger 1976) suggested that unreduced nitrofurantoin can also have biological activity, our results demonstrate the need for reductive activation.

The identity of the cloned gene with nfsA or nfsB genes defined by McCalla et al (1978) can be deduced from the size of the encoded polypeptide, map position of the gene and level of enzyme activity due to a single copy of the gene. From the size of the coding segment of the insert (≤ 1·3 kb, as determined by Tn1000 mutagenesis) and the size of the polypeptide (37 kDa) identified in minicells, it is probable that the cloned gene could be nfsB. However the map location of the gene is at variance with that reported by McCalla et al (1978). Although the authors had not reported precise map positions, they had suggested that the order of loci in the relevant region could be lac (8 min) nfsB (?) galK (17 min) nfsA (?). That is, nfsB lies before 17 min on the E. coli linkage map. Our mapping data presented herein place the cloned gene at 19 min. However, a careful and critical analysis of the genetic data reported by McCalla et al (1978) does show that the more probable order could be lac gal nfsB nfsA. If this were so, nfsB would fall in the same position as reported herein. McCalla et al (1978) had isolated a two-step nitrofurazone-resistant mutant (NFR 502) which lacked both the major and minor nitroreductases. When this strain was transduced to kanamycin resistance using P1 propagated on AJ322 (see 'results') the nitroreductase activity was restored to only 10% of wild type levels (unpublished results). It could be recalled that AJ322 contains two copies of the nitroreductase gene, only one of which is functional and the other inactivated by

resistance using AJ522 as donor, in effect, introduces a single functional copy of the nitroreductase gene. The observation that enzyme activity is restored only to 10% of normal levels suggests that the cloned gene codes for the minor nitroreductase. The major and minor nitroreductases have been reported to differ in their sensitivity to 2 M urea. While McCalla *et al* (1978) showed that the minor enzyme was sensitive, Breeze and Obeseiki–Ebor (1983) have shown exactly the opposite. We have partially purified the enzyme encoded by the insert carried on pAJ102, by affinity chromatography on Sepharose CL-6B and found the partially purified enzyme to be relatively insensitive to urea (25% loss of activity after 45 min exposure to 2 M urea at 37°C; unpublished results). In view of the existence of mutually contradictory reports, urea sensitivity is not a satisfactory criterion to establish the identity of nitrofuran reductases. However, based on other criteria reported herein we believe that the gene we have cloned is *nfs*B. Thus, this work has established the precise map position of one of the genes involved in nitrofuran toxicity. Watanabe *et al* (1989, 1990) have reported the cloning of a nitroreductase · gene of *Salmonella typhimurium*. The size of the corresponding polypeptide was found to be 28 kDa. Since several enzymes are known to be involved in the metabolism of nitroheterocycles, it is difficult to say whether the gene cloned by Watanabe *et al* (1989, 1990) is analogous to the one reported herein.

pAJ102 can be exploited as a cloning vector since insertion of extraneous DNA into the nitroreductase gene will inactivate it and thereby permit direct selection when transformed into a nitrofurantoin-resistant host. This is currently being assessed.

References

Asnis R E 1957 The reduction of furacin by cell free extracts of furacin resistant strains of *Escherichia coli*; *Arch. Biochem. Biophys.* **66** 208–216

Black M, Rabin L and Schatz N 1980 Nitrofurantoin-induced chronic active hepatitis; *Ann. Intern. Med.* **92** 62–64

Bonner W M and Laskey R A 1974 A film detection method for tritium-labelled proteins and nucleic acids in polyacrylamide gels; *Eur. J. Biochem.* **46** 83–88

Breeze A S and Obaseiki–Ebor E E 1983 Nitrofurantoin reductase in nitrofurantoin-resistant strains of *Escherichia coli* K12: Some with chromosomally determined resistance and other carrying R- plasmids; *J. Antimicrob. Chemother.* **12** 543–547

Bryant D W, McCalla D R, Leekshma M and Laneuville P 1981 Type I nitroreductases of *Escherichia coli*; *Can. J. Microbiol.* **27** 81–86

Dodd M C and Stillman W B 1944 The *in vitro* bacteriostatic action of some simple furan derivatives; *J. Pharmacol. Exp. Ther.* **82** 11–18

Goodman L S and Gilman A 1975 *The pharmacologic basis of therapeutics* 5th edition (New York: Macmillan) pp 1008–1009

Groisman E A and Casadaban M J 1986 Mini-Mu bacteriophage with plasmid replicons for *in vivo* cloning; *J. Bacteriol.* **168** 357–364

Groisman E A, Castilho B A and Casadaban M J 1984 *In vivo* DNA cloning and adjacent gene fusing with a mini-Mu-*lac* bacteriophage containing a plasmid replicon; *Proc. Natl. Acad. Sci. USA* **81** 1480–1483

Grunberg E and Titsworth E H 1973 Chemotherapeutic properties of heterocyclic compounds: monocyclic compounds with five-membered rings; *Annu. Rev. Microbiol.* **27** 317–346

Herrlich P and Schweiger M 1976 Nitrofurans, a group of synthetic antibiotics with a new mode of action. Discrimination of specific messenger RNA classes; *Proc. Natl. Acad. Sci. USA* **73** 3386–3390

Holmberg L and Bowman G 1981 Pulmonary reactions to nitrofurantoin; *Eur. J. Respir. Dis.* **62** 180–189

Kedderis, G L and Miwa G T 1988 The metabolic activation of nitroheterocyclic therapeutic agents; *Drug Metab. Rev.* **19** 33–62

Kohara Y, Akiyama K and Isono K 1987 The physical map of the whole *E. coli* chromosome: application of a new strategy for rapid analysis and sorting of a large genomic library; *Cell* **50** 495–508

Komai N, Nishizawa T, Hayakawa Y, Murotsu T and Matsubara K 1982 Detection and mapping of six miniF-encoded proteins by cloning analysis of dissected miniF fragments; *Mol. Gen. Genet.* **186** 193–203

Laemmli U K 1970 Cleavage of structural proteins during the assembly of the head of bacteriophage T4; *Nature (London)* **227** 680–685

Lowry O H, Rosebrough N J, Farr A L and Randall R J 1951 Protein measurement with the Folin phenol reagent; *J. Biol. Chem.* **193** 265 275

McCalla D R, Reuvers A and Kaiser C 1970 Mode of action of nitrofurazone; *J. Bacteriol.* **104** 1126–1134

McCalla D R, Olive P L, Tu Y and Fan M L 1975 Nitrofurazone-reducing enzymes in *E. coli* and their role in drug activation *in vivo*; *Can. J. Microbiol.* **21** 1484–1491

McCalla D R, Kaiser C and Green M H L 1978 Genetics of nitrofurazone resistance in *Escherichia coli*; *J. Bacteriol.* **133** 10–16

Miller J H 1972 *Experiments in Molecular Genetics* (Cold Spring Harbor: Cold Spring Harbor Laboratory)

Paul H E and Paul M F 1964 The nitrofurans: Chemotherapeutic properties; in *Experimental chemotherapy* (ed.) R J Schnitzer (New York: Academic Press). Vol.2, part 1, pp 307–370

Silhavy T J, Berman M L and Enquist L W 1984 *Experiments with gene fusions* (Cold Spring Harbor: Cold Spring Harbor Laboratory)

Taskinen E, Tukainen P and Sovijarvi A R 1977 Nitrofurantoin-induced alterations in pulmonary tissue; *Acta Pathol. Microbiol. Scand.* **85** 713–720

Watanabe M, Ishidate M Jr and Nohmi T 1989 A sensitive method for the detection of mutagenic nitroarenes: Construction of nitroreductase overproducing derivatives of *Salmonella typhimurium* strains TA98 and TA100; *Mutat. Res.* **216** 211–220

Watanabe M, Ishidate M Jr and Nohmi T 1990 Nucleotide sequence of *Salmonella typhimurium* nitroreductase gene; *Nucleic Acid Res.* **18** 1059

Wu T T 1966 A model for three point analysis of random general transduction; *Genetics* **54** 405–410

Replication, maturation and physical mapping of bacteriophage MB78 genome

SAEED A KHAN[†], S S MURTY, MANZOOR A ZARGAR and M CHAKRAVORTY*

Molecular Biology Unit, Institute of Medical Sciences, Banaras Hindu University, Varanasi 221 005, India
[†]Present address: C/o Philip Serwar, Department of Biochemistry, University of Texas, Health Sciences Centre at San Antonio, Texas 78284, USA

Abstract. Bacteriophage MB78 is a virulent phage of *Salmonella typhimurium*. The viral DNA is 42 kb in size and seems to be circularly permuted. We show that viral DNA replication is through concatemeric DNA formation which is subsequently converted into full length DNA through headful packaging. A restriction map of MB78 DNA for six restriction endonucleases e.g. *BglII*, *PvuII*, *EcoRI*, *ClaI*, *SalI* and *SmaI* has been constructed. The yield of certain fragments in less than molar amount is explained in terms of permutation and the headful mechanism of packaging. The packaging site (pac site) has been suggested.

Keywords. Bacteriophage MB78; *Salmonella* phage; restriction map; DNA packaging; 'pac' site.

1. Introduction

Bacteriophage MB78 isolated in our laboratory (Joshi *et al* 1982) is one of the few virulent phages of *Salmonella typhimurium*. It is morphologically, serologically and physiologically different from other virulent and temperate phages of the same host. The phage MB78 possesses many interesting properties. It cannot grow on rifampicin-resistant mutants of the host but can be helped to some extent by phage P22 (Verma and Chakravorty 1985). Further, it restricts the development of other *Salmonella* phages. The physical characterization and mapping of the phage DNA have been reported in this communication, which would help in the understanding of the interaction of the MB78 phage with its host and other viruses at the molecular level.

2. Materials and methods

2.1 *Bacterial and phage strains*

S. typhimurium (LT2) and the clear mutant of phage P22 (C_1) were originally obtained from M Levine of the Department of Human Genetics, University of Michigan, Ann Arbor, Michigan, USA . The phage MB78 was isolated in our laboratory (Joshi *et al* 1982).

---

*Corresponding author.

161

Restriction endonucleases, like *Eco*RI, *Bgl*II, *Pvu*II, *Hind*III, *Sal*I, *Sma*I and *Cla*I were purchased from Pharmacia United Limited, Bangalore, India, New England Biolab, USA, Bethesda Research Laboratories, USA and the CSIR Centre for Biochemicals. One kb ladder was obtained from Bethesda Research Laboratory USA. [³H] thymidine, γ-[³²P] ATP, α-[³²P] dCTP, ³²PO₄ (carrier-free) were obtained from the Bhabha Atomic Research Centre, Bombay, and Amersham, UK. All other chemicals used were either of analytical or molecular biology grade.

2.3 *Growth media and preparation of phages*

The *S. typhimurium* cells were grown in M9 and M9CAA media (Smith and Levine 1964). The phages were propagated, purified and the DNA was isolated as described earlier (Verma *et al* 1986). [³²P] and [³H] labelled phages were prepared as described by Botstein (1968).

2.4 *Nuclease digestions*

Digestion of purified DNA with restriction endonucleases was carried out according to the instructions of the supplier. All digests were heated at 65°C for 5 min and immediately cooled on ice just prior to loading on agarose gels.

2.5 *Agarose gel electrophoresis*

Agarose (0·5 and 0·8% horizontal slab gels, 20 × 15 cm) were prepared in buffer (pH 8·2) containing 90 mM Tris base, 90 mM boric acid and 2·5 mM EDTA. Electrophoresis was carried out at 100 volts for 8 h at room temperature. Reaction mixtures to be electrophoresed were mixed with 1/10 volume of a solution composed of 0·5% bromophenol blue, 0·05 M EDTA and 10% glycerol. To visualize the DNA fragments, the gels were soaked in electrophoresis buffer containing ethidium bromide (1 μg/ml) and photographed with a polaroid land camera using an orange filter and polaroid type 667 film.

In some cases the restriction fragments were eluted from the gels by the freeze squeeze method (Thuring *et al* 1975), further purified and digested with other restriction endonucleases and analysed as above. Molecular weights of fragments were estimated from the mobilities of fragments after comparison with the mobilities of DNAs of known sizes. The convention used by Smith and Nathans (1973) was used to name the DNA fragments generated by different restriction endonucleases.

2.6 *Southern blotting and DNA-DNA hybridization*

[³²P] labelled probes were prepared to a very high specific activity (∼ 10⁸ cpm/μg) following the method of Rigby *et al* (1977). [³²P] and [³H] labelled phage DNAs were isolated as reported earlier (Verma *et al* 1986). DNA from the gels after

following the technique of Southern (1975) and hybridized according to Denhardt (1966). At the end of hybridization the filters were removed, washed under stringent conditions, dried and either counted in the LKB Rackbeta liquid scintillation counter or exposed to X-ray films.

2.7 *Preparation of lysate for sedimentation analysis*

Wild type LT2 cells were grown in M9 medium (Smith and Levine 1964). When the cells reached a density of 2.5×10^8/ml they were infected with MB78 at a multiplicity of infection (m. o. i.) of 10. After 20 min, the infected cells were labelled by incubating for 2 min with [^{3}H] thymidine ($\sim$10–20 μCi/ml; specific activity 18.8 Ci/mmol). The labelling was stopped by adding an excess of cold thymidine (2 mg/ml). Samples (0.5 ml) were withdrawn at desired times and lysed by adding an equal volume of lysis mixture containing 0.1 M Tris-HCl, pH 8; 0.01 M EDTA; 0.01 M sodium azide, 20 μg/ml lysozyme (freshly prepared in 0.25 M Tris-HCl, pH 8) as described by Botstein (1968).

For confirming the formation of concatemeric DNA and determining the size of the concatameric DNA, lysates were also prepared by repeated freezing (in liquid nitrogen) and thawing (at 50° C) of the infected cells.

2.8 *Sucrose density gradient centrifugation*

Labelled phages or infected cell lysates were analysed by velocity sedimentation in neutral as well as alkaline 5–20% (w/v) sucrose gradients. Gradients were prepared following either the compositions described by Ray *et al* (1984) or Botstein (1968). According to Ray *et al* (1984) the sucrose solutions were made in 0.02 M Tris-HCl pH 7.6; 0.01 M EDTA and 1 M NaCl. Following the method of Botstein (1968) for alkaline sucrose gradient the sucrose solutions were prepared in 0.01 M EDTA 1 M NaCl and 0.1% Sarkosyl and the pH was adjusted to 12.1 with 10 N NaOH. For neutral sucrose gradients the composition of the solution was the same except that the pH was adjusted to 7.6 with 0.02 M Tris-HCl. Gradients (4.5 ml) were prepared in nitrocellulose tubes over a cushion of 70% Angio Conray in 80% sucrose. Lysate (100 μl) was loaded on the gradient 45 min prior to ultracentrifugation at 30,000 rpm for 2 h at 15°C in Beckman SW 50.1 rotor. Fractions (4 to 5 drops) were collected on whatman 3 MM filters as described by Botstein (1968) and the radioactivity was measured in the LKB Rackbeta liquid scintillation spectrometer. In some experiments, fractions (150 μl) were collected in tubes and precipitated with cold 10% trichloroacetic acid. The precipitates were collected on Whatman GF/A filters, washed with 5% cold trichloroacetic acid followed by 70% alcohol, dried and the radioactivity measured. The molecular weights of mature phage DNA and replicative intermediates were estimated from their relative positions in the gradient at the end of the run, using [^{32}P] labelled P22 or MB78 DNA as markers as described by Sengupta *et al* (1985).

2.9 *Deproteinization of fast sedimenting complex*

Deproteinization of the fast sedimenting complex was carried out by treatment

3. Results

3.1 *Restriction enzyme analysis*

To characterize MB78 DNA and to facilitate physical mapping, purified phage DNA was digested with different restriction enzymes. Results of such digestion (figure 1) revealed that both *Bgl*II and *Pvu*II produced fragments of two sizes only (figure 1, lanes 1 and 2). Experiments with double digestions (figure 2) confirmed
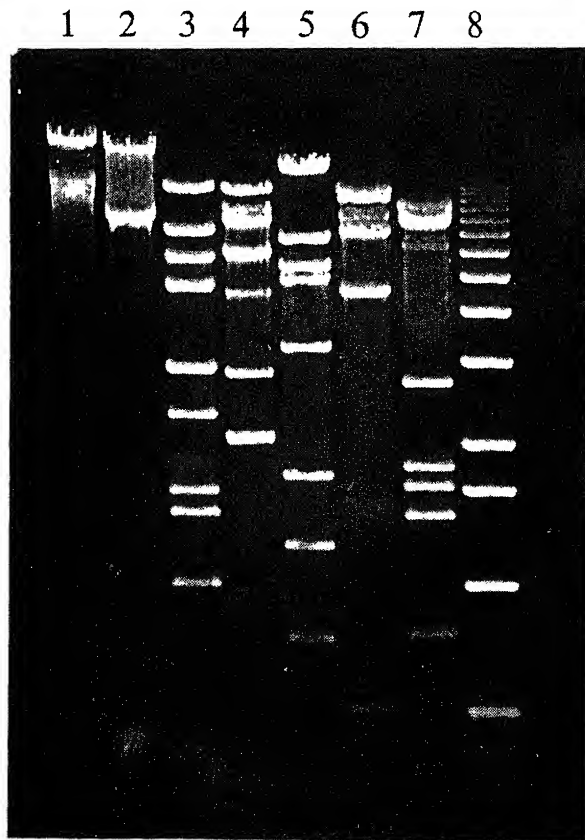
Figure 1. Restriction endonuclease digestion pattern of MB78 DNA.
    MB78 DNA (2 µg) was digested with various restriction endonucleases for 3 h at 37°C and the digestion products were analysed on 0·7% agarose gel. Lanes 1–7 represent the digestion patterns obtained with *Bgl*II, *Puv*II, *Eco*RI, *Sal*I, *Cla*I, *Sma*I and *Hind*III respectively: Lane 8 1 kb ladder (BRL).
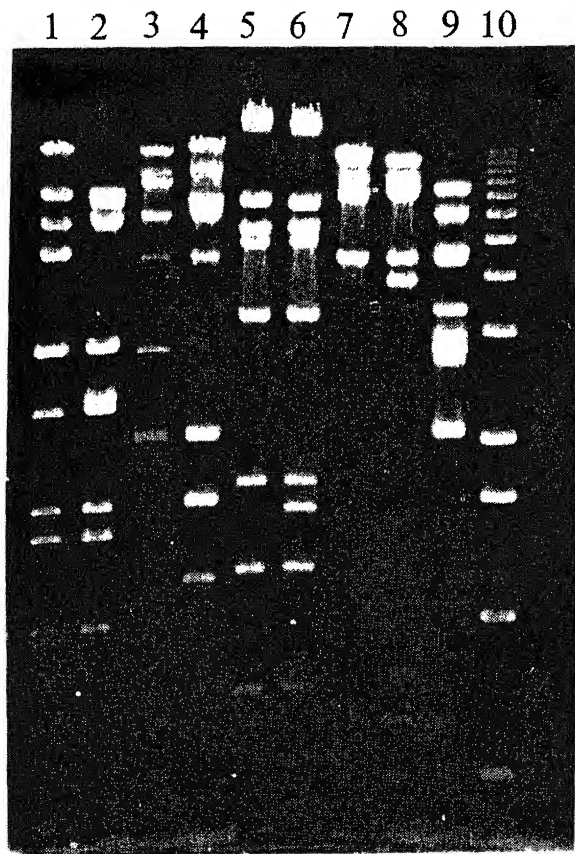
Figure 2. Agrose gel electrophoresis of MB78 DNA after digestion with either *Pvu*II alone or in combination with other enzymes.

MB78 DNA (2 μg) was digested with *Pvu*II and other restriction endonucleases at 37°C for 3 h and analysed on 0·7% agarose gel. (1) *Eco*RI; (2) *Puv*II + *Eco*RI; (3) *Sal*I; (4) *Sal*I + *Pvu*II; (5) *Cla*I; (6) *Pvu*II + *Cla*I; (7) *Sma*I; (8) *Puv*II + *Sma*I; (9) *Sal*I + *Sma*I; (10) 1 kb ladder (BRL).

that *Pvu*II has two sites, one in *Eco*RI A and the other in *Eco*RI D (compare lanes 1 and 2, figure 2). Enzymes, such as *Eco*RI, *Sal*I, *Sma*I and *Hind*III produced some fragments which are not in equimolar amounts (figure 1). Such fragments as *Eco*RI G, *Sal*I E, *Sma*I F and *Hind*III B and E will be referred to as submolar fragments. *Eco*RI E seemed to be a doublet from fragments which was confirmed from other experiments (data not provided).

3.2   *Physical map of MB78 DNA*

A physical map of phage MB78 DNA was constructed for *Bgl*II, *Pvu*II, *Eco*RI, *Cla*I, *Sal*I and *Sma*I (figure 3). The arrangement of various fragments was determined from the analysis of fragments after partial digestion, double digestion
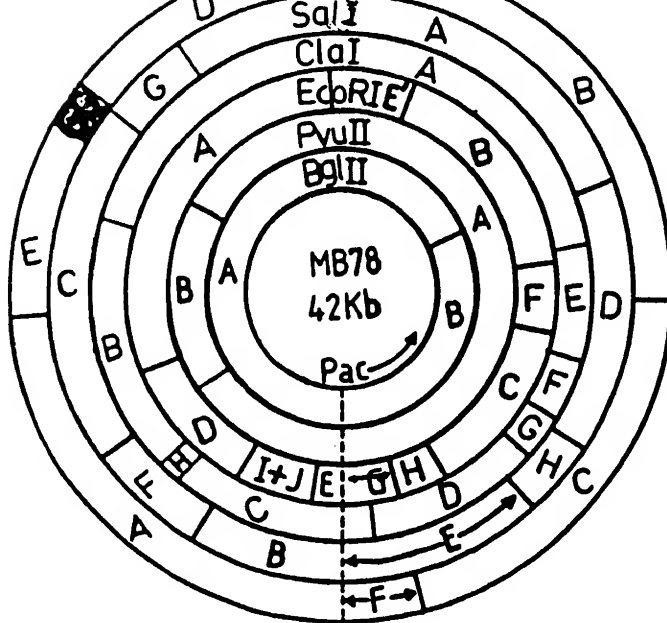
Figure 3. A circular physical map of MB78 genome

The construction of the maps has been described in the text. The map has been drawn to scale. The packaging initiation (pac) site and the direction of packaging (counter clockwise) are also indicated. The dotted line represents the 'pac' initiation site and the arrow indicates the direction of packaging.

map of MB78 DNA for *Bgl*II, *Pvu*II, *Eco*RI and *Cla*I was constructed which was later used as a reference map for assigning the positions of other restriction enzyme fragments. For confirmation, isolated purified fragments were nick translated and used as probes to hybridize with different restriction endonuclease digested fragments. Results of a few typical experiments have been presented. When nick translated *Eco*RI D fragment was hybridized with different endonuclease digestion fragments it hybridized with *Eco*RI D, *Cla*I B, C and H, and *Sma*I A (figure 4a). Similarly *Eco*RI F hybridized with *Eco*RI F, *Cla*I E and *Sma*I B and C (figure 4b). *Eco*RI J hybridized with *Eco*RI J, *Cla*I C and *Sma*I A (figure 4c). When labelled *Cla*I A was used as a probe, it hybridized with *Eco*RI A, B and E, *Cla*I A and *Sma*I B, D, E and G (figure 4d). When *Cla*I F was used as probe it hybridized with *Eco*RI C, *Sal*I D, *Sma*I C and *Cla*I F (figure 4e). A large number of similar experiments were carried out to confirm the physical map. When submolar fragments were used as probes the results yielded much more information which has been described under location of 'pac' site.

3.3 *Circular permutation in MB78 DNA and location of 'pac' site*

While constructing a physical map of MB78 DNA, terminal labelling with γ-[^{32}P] ATP or digestion with *Bal*31 was carried out to identify the end fragments of DNA.
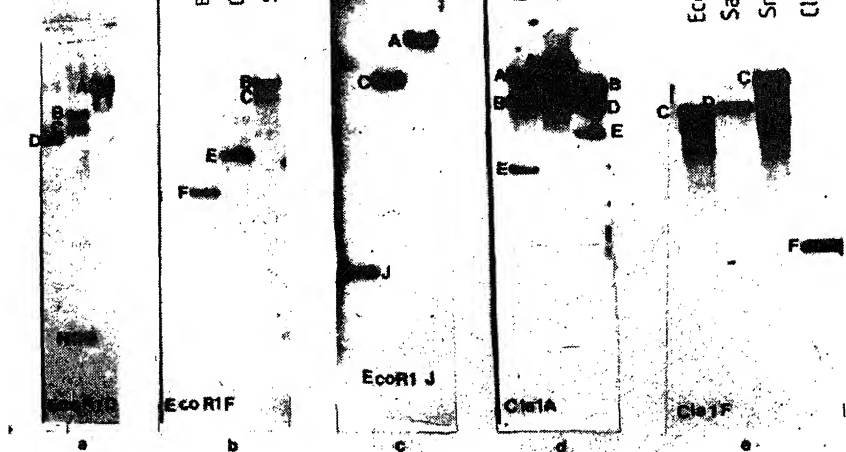
Figure 4. Hybridization of *Eco*RI D, F, J and *Cla*I A and F with different restriction fragments.

MB78 DNA (2 µg) was digested with different restriction endonucleases, *Eco*RI, *Cla*I and *Sma*I. The digested samples were loaded in five similar sets, electrophoresed and Southern blotted as mentioned under 'materials and methods'. The blotted samples were hybridized with nick-translated restriction fragment *e.g.* either *Eco*RI D or *Eco*RI F etc., as shown at the bottom of the figure. The autoradiogram of the gel after hybridization is shown in the figure. The bands hybridized have been marked.

When 5′ end-labelled MB78 DNA was digested with any of the enzymes *Hind*III, *Sal*I, *Sma*I and *Cla*I, run on agarose gel and autoradiographed, the submolar fragments of these enzyme digests were heavily labelled, suggesting that the submolar fragments were at the ends (figure 5B). Besides the submolar fragments, some other fragments were also moderately labelled which suggested that the DNA populations were not homogeneous as far as their termini are concerned and those moderately labelled fragments were at the ends of some molecules which could have arisen as a result of circular permutation. As a control, when λ DNA which is not circularly permuted was digested after 5′ end labelling it did not show any other fragment labelled except the end fragments (data not provided). Further, when MB78 DNA treated with *Bal*31 for 45 min, was digested with different restriction enzymes, *Hind*III B and E, *Sal*I B and E, and *Sma*I A, C and D disappeared completely and the intensity of some of the other fragments decreased considerably (figure 5A). This result also suggested that the DNA population was not homogeneous with respect to their termini. In other words, phage MB78 DNA is circularly permuted. The preferential loss in the intensities of only some of the fragments rather than all of them simultaneously suggested that the permutation in phage MB78 DNA is restricted. If the DNA is randomly permuted, then all fragments should have an equal probability to be at the end and the relative intensities of fragments produced by restriction enzyme cleavage of *Bal*31 treated DNA should have remained unaltered. The restricted permutation in phage MB78 DNA explains the presence of submolar bands in complete digests of some of the restriction enzymes (figure 1).
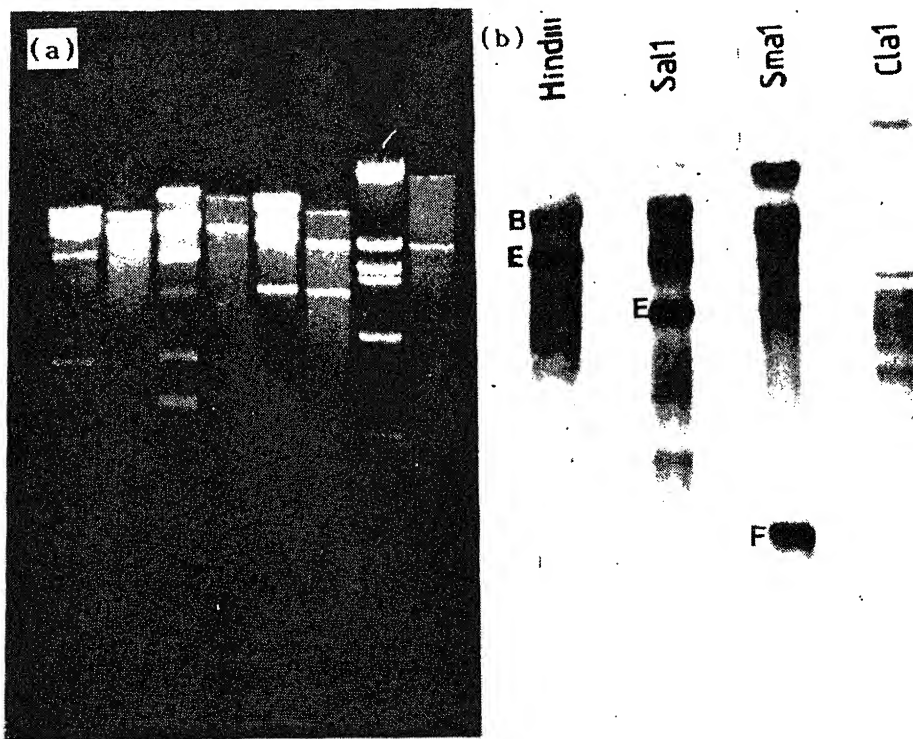
Figure 5. Determination of the ends of MB78 DNA.

MB78 DNA (5 μg) was labelled at 5' ends with γ-[^{32}P] ATP and T4 polynucleotide kinase and in another case 20 μg of MB78 DNA (unlabelled) was treated with Bal 31 at 30°C for 45 min. After end labelling or Bal 31 treatment as the case may be, the DNA samples were digested with restriction endonucleases and loaded in an alternate fashion on 0.7% agarose gel. After electrophoresis the gel was stained with ethidium bromide to locate or identify the missing fragments, if any. It was then dried and exposed to X-ray film for autoradiography.

(a) Ethidium bromide stained gel.

Lanes 1 and 2 *Hind*III; lane 3 and 4 *Sal*I; lane 5 and 6 *Sma*I; lane 7 and 8 *Cla*I; lanes 1, 3, 5 and 7 show the digestion patterns of end labelled MB78 DNA and lanes 2, 4, 6 and 8 show the digestion patterns of Bal 31 treated MB78 DNA.

(b) Autoradiogram of the gel shown in **a**.

It is to be noted that only lanes 1, 3, 5 and 7 which represent the results of end labelled DNA could be seen.

3.4 *Location of 'pac' site*

As discussed before, phage MB78 DNA upon digestion with certain enzymes always produced some fragments in submolar amounts such as *Eco*RI G, *Sal*I E, *Hind*III B and E and *Sma*I F (figure 1). From the reports in the literature (Jackson *et al* 1978; Johnson and Schilievert 1983; Sengupta *et al* 1985; Guidolin and Manning 1988) it was assumed as a working hypothesis that these submolar fragments come from the first piece of DNA to be packaged ('pac' fragment) or the last piece of fragment

the well-defined fragments as a result of limited circular permutation. In other words these submolar fragments are the subsets of well-defined fragments. No such anomaly is reported in the case of λ DNA (Thomas and Davis 1974) which is not circularly permuted. According to the working hypothesis stated above all such submolar fragments should come from one end of the DNA molecule which then should hybridize with each other and also with the fragments of which they are a part. To test this directly, all these submolar fragments were isolated individually and used as a probe to find out the hybridization pattern. For example, when EcoRI G was used as a probe it always hybridized with EcoRI E, of which it is a part and to all the submolar fragments produced by other enzymes and the fragments of which these submolar fragments are a part (figure 6). To test whether EcoRI G is really a part of EcoRI E, EcoRI E was also used as a probe and it was found to hybridize with all those fragments with which EcoRI G hybridized (figure 6). Since EcoRI E is a doublet, it hybridized with some additional fragments confirming again that EcoRI E is a doublet (figure 6). When similar experiments were carried out with other submolar fragments, results were in accordance with the above hypothesis (data not given).

Further, as reported by Guidolin and Manning (1988) a smeared signal was observed when submolar fragments were used as probes. This suggested that these
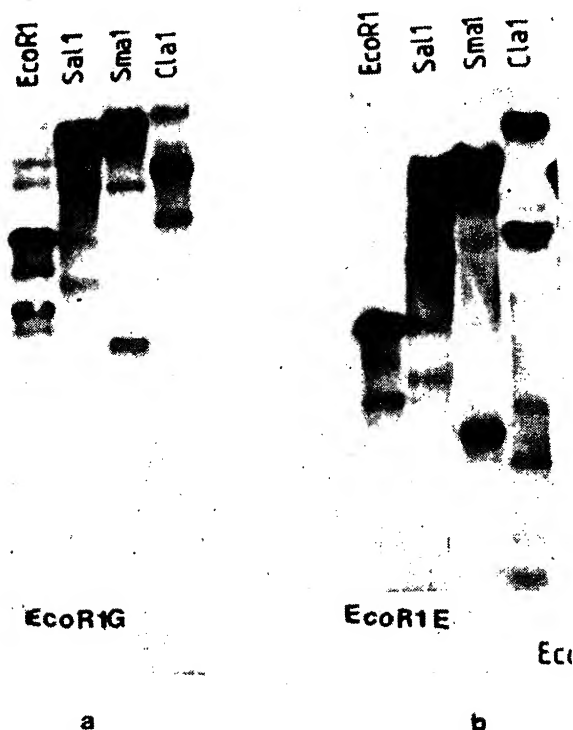
Figure 6. Hybridization of EcoRI G and E fragments with different restriction fragments. Experimental conditions were as described for figure 4. except digestion with SmaI was also carried out in addition to other enzymes and either EcoRI G subset (a) of EcoRI E (subset (b)) were used as probes after nick translation.

packaging.

In the light of the above observation the location of the 'pac' site was determined as shown in figure 3. The analysis of the results presented in figure 6 and of a number of similar experiments (data not presented) revealed that submolar fragments always hybridized with a number of other fragments in their vicinity located in the counter clockwise direction and not clockwise direction (see the physical map; figure 3). This observation suggested that the mature phage length DNA is more than genomic length and the direction of packaging is counter clockwise; as a result, some of these fragments also became the end fragments of a certain population of DNA molecules.

3.5 *Replicative intermediates*

All the above observations suggested that phage MB78 has circularly permuted DNA and such permutation is not random but restricted. Further, such heterogeneous DNA population can arise through headful packaging of DNA from a concatemeric DNA. Thus formation of concatemeric DNA is a prerequisite for such packaging. To study whether MB78 DNA synthesis actually proceeds through concatemer formation or not, the intermediates of DNA synthesis were investigated. The cells in the log phase were infected with phage MB78 at an m.o.i. of 10 and after 20 min of infection the cells were pulse labelled with [³H] thymidine for 2 min. The labelled DNA was then chased for different times, the samples were removed and lysed as described in §2. To resolve the intermediates of replicating DNA the lysates were analysed on both neutral and alkaline 5 to 20% (w/v) sucrose gradients as described in §2. The pattern of distribution of the replicating DNA in alkaline and neutral sucrose density gradients were the same. Hence the result of only neutral sucrose gradient analysis has been presented (figure 7). After 22 min of infection the majority of the pulse labelled DNA was detected with the fast sedimenting membrane complex marked as 'intermediate I' as well as with the concatemeric DNA or 'intermediate II' (figure 7). The size of the concatemeric DNA was calculated according to the following equation (Abelson and Thomas 1966; Burgi and Hershy 1963).

$$D_2/D_1 = (M_2/M_1)^X,$$

where, M is molecular weight, D is the distance travelled and $X = 0.35$ for neutral sucrose gradient.

The length of the concatemer was calculated to be 3 to 5 times the length of mature phage DNA. With time (after chasing) both forms I and II are converted to phage length DNA. To determine the size of the concatemeric DNA, lysis of the infected cells and centrifugation of the lysate in neutral sucrose density gradient was also carried out as described by Ray *et al* (1984). The sedimentation profile was not much different from that presented in figure 7.

3.6 *Association of the replicating DNA with the membrane complex*

To confirm that the fast sedimenting complex is a DNA-cell membrane complex, the
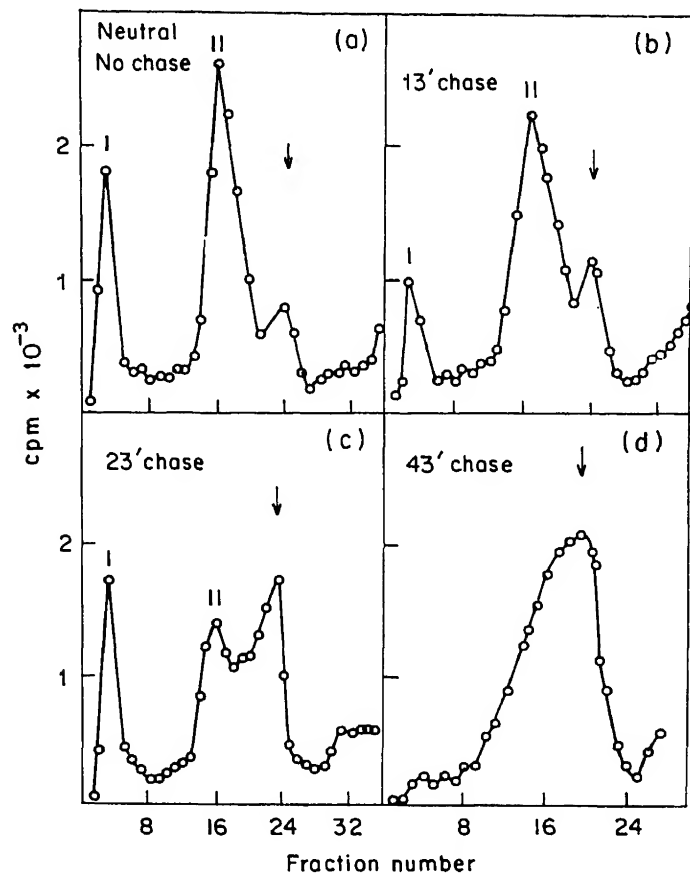
Figure 7. The fate of pulse labelled phage MB78 DNA in LT2 cells: Neutral sucrose gradient analysis.

Exponentially growing LT2 cells were infected with phage MB78 (m.o.i. = 10). The infected cells were pulsed for 2 min with [³H] thymidine (20 µCi/ml: 18·8 Ci/mmol) after 20 min of infection. It was followed by the addition of cold thymidine at a final concentration of 2 mg/ml (chasing). Samples (0·5 ml) were collected at different times as indicated in the figure and immediately lysed as per Botstein (1968). Lysates from such samples (chased for different lengths of time) were loaded on 5–20% neutral sucrose gradients as described in 'materials and methods'. [³²P] labelled MB78 DNA was used as a marker. The sedimentation is from right to left. The arrow indicates the position where marker DNA sedimented. I, represents the intermediate I or membrane complex and II, represents the intermediate II or concatemeric DNA.

fast sedimenting complex was collected under similar conditions as in figure 7a, with the exception that instead of Angio Conray, 1·3 g CsCl/ml of 40% sucrose was used. This complex was then dialyzed and deproteinized as described in §2. It was then subjected to 5–20% neutral sucrose density gradient centrifugation. The gradient was prepared following Ray *et al* (1984). Results presented in figure 8 clearly indicate that the DNA from the fast sedimenting complex can be released after proteinase K treatment confirming that the fast sedimenting complex is DNA-cell membrane protein complex. From the sedimentation pattern it appears that most of
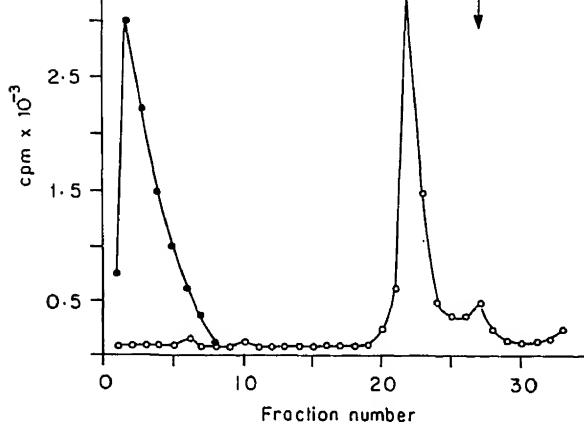
Figure 8. Neutral sucrose gradient centrifugation of deproteinized DNA-membrane complex.

The fast sedimenting complex as in figure 7a was dialysed against 10 mM Tris-HCl pH 7·8, 5 mM EDTA for 15 h at 4°C. It was then treated with proteinase K (500 μg/ml) for 12 h. Gradient was prepared as per Ray *et al* (1984).

(●), Untreated sample: (○), treated with proteinase K (500 μg/ml) for 12 h. The arrow denotes the position where mature phage DNA sediments.

the released DNA is a multimer (approximately 4–5 mer) of the mature phage length DNA.

4. Discussion

To understand the molecular organization of phage MB78 genome, phage DNA was analysed with a number of restriction endonucleases, namely, *Bgl*II, *Pvu*II, *Eco*RI, *Cla*I, *Sal*I and *Sma*I. From the analysis of restriction enzyme digestion fragments, the molecular weight of the phage DNA was estimated to be 28×10^6 Dalton or 42 kb. Our results demonstrate that the replication of the phage DNA proceeds through concatemer formation in association with the cell membrane. Some of the restriction endonucleases generated submolar fragments and by analogy with the cases reported in literature we believe that the submolar fragments are obtained as a result of limited circular permutation. Direct demonstration of the existence of concatemeric DNA supports the idea that submolar amounts of some restriction fragments are produced as a result of limited circular permutation of the phage genome while packaging more than genomic length DNA into the phage head, a mechanism common with many other phages.

Unpublished observations from our laboratory with bacteriophage 9NA, another virulent phage of *S. typhimurium* (Wilkinson *et al* 1972) indicate that phage 9NA also replicates in a similar way through the formation of concatemeric DNA (data not presented). It is interesting to note that bacteriophages P22, MB78 and 9NA of the same host replicate through the concatemeric DNA formation.

probable location of 'pac' site is within the *Eco*RI E, *Sal*I B or *Sma*I A fragments. It is quite interesting to note that the hybridization of Southern blotted restriction endonuclease digestion fragments with fragments derived from the region to the right of the 'pac' site as shown in figure 3 showed smeared background signal in contrast to the fragments derived from the left. The fragments which gave clear signals must be away from the ends which are circularly permuted. As the fragments to the right of the 'pac' site produced smeared signals it is strongly felt the packaging is in the anticlockwise direction. The final circular map, including the location of the 'pac' site and the direction of packaging is shown in figure 3. The order of *Eco*RI I and J fragments in the physical map and the position of *Sma*I G fragment, is located but could not be exactly defined. The presence of *Sma*I G fragment can be anywhere within 1 kb region as represented by the hatched area. A tentative position for *Sma*I G fragment has been assigned from the results of Southern blotting and hybridization of different restriction enzyme-digested fragments with *Sma*I G fragment (used as probe). In one of the previous communications (Verma *et al* 1986) there was difficulty in assigning the positions of *Eco*RI C and D, which were then decided on the basis of complementation studies of the *ts* mutants with cloned fragments. At that time we did not realize that *Eco*RI E was a doublet which is now evident from the analysis of various double digestion products.

The position of *Eco*RI C and D has also been changed on the basis of their double digestion patterns. *Eco*RI G was shown to be a subset of *Eco*RI A on the basis of hybridization of *Eco*RI G with *Eco*RI A (a false conclusion derived probably due to contamination somewhere). The Southern blotting and hybridization of different restriction enzyme digested fragments with individual submolar fragments used for physical characterization has never shown *Eco*RI A being hybridized with any of them. On the contrary, the submolar fragments always hybridized with other submolar fragments and the fragments of which they are a part of, namely, *Sal*I B, *Sma*I A, *Cla*I C and D and *Eco*RI E. Since all these fragments are overlapping and the location of 'pac' site in *Eco*RI E fragment can explain the generation of other submolar fragments, the physical map presented in this report, an improvement over the previous map, should be regarded more accurate and explanatory.

Acknowledgements

References

Abelson J and Thomas C A Jr 1966 The anatomy of T5 bacteriophage DNA molecule; *J. Mol. Biol.* **18** 262–291

Burgi E and Hershey A D 1963 Sedimentation rate as a measure of molecular weight of DNA; *Biophys. J.* **3** 309–321

Denhardt D T 1966 A membrane filter technique for the detection of complementary DNA; *Biochem. Biophys. Res. Commun.* **23** 641–646

Guidolin A and Manning P A 1988 Molecular analysis of the packaging signal in bacteriophage CP-Ti of *Vibrio Cholerae*; *Mol. Gen. Genet.* **212** 514–521

Jackson E N, Jackson D A and Deans R J 1978 *Eco*RI analysis of bacteriophage P22 DNA packaging; *J. Mol. Biol.* **118** 365–388

Johnson L P and Schlievert P M 1983 A physical map of the group A *Streptococcal* genome; *Mol. Gen. Genet.* **189** 251–255

Joshi A, Siddiqui J Z, Rao G R K and Chakravorty M 1982 MB78, a virulent bacteriophage of *Salmonella typhimurium*; *J. Virol.* **41** 1038–1043

Ray P, Sengupta A and Das J 1984 Phosphate repression of phage protein synthesis during infection by choleraphage ϕ 149; *Virology* **136** 110–124

Rigby P W J, Dieckman M, Rhodes C and Berg P 1977 Labelling deoxyribonucleic acid to high specific activity *in vitro* by nick translation with DNA polymerase I; *J. Mol. Biol.* **113** 237–251

Sengupta A, Ray P and Das J 1985 Characterization and physical mapping of choleraphage ϕ149 DNA; *Virology* **140** 217–229

Smith H O and Levine M 1964 Two sequential repressors of DNA synthesis in the establishment of lysogeny by phage P22 and its mutants; *Proc. Natl. Acad. Sci. USA* **52** 356–363

Smith H O and Nathans D 1973 A suggested nomenclature for bacterial host modification and restriction systems and their enzymes; *J. Mol. Biol.* **81** 419–423

Southern E M 1975 Detection of specific sequences among DNA fragments separated by gel electrophoresis; *J. Mol. Biol.* **98** 503–517

Thomas M and Davis R N 1975 Studies on the cleavage of bacteriophage lamda DNA with *Eco*RI restriction endonuclease; *J. Mol. Biol.* **91** 315–328

Thuring R W J, Sanders J P M and Borst P 1975 A freeze squeeze method for recovering long DNA from agarose gel; *Anal. Biochem.* **66** 213–220

Verma M and Chakravorty M 1985 Hybrid between temperate phage P22 and virulent phage MB78; *Biochem. Biophys. Res. Commun.* **132** 42–48

Verma M, Rao A S M K and Chakravorty M 1986 Isolation of temperature sensitive mutants, correlation of physical and genetic maps of bacteriophage MB78; *Virology* **151** 274–285

Wilkinson R G, Gemski P J and Stocker B A D 1972 Non smooth mutants of *Salmonella typhimurium*: Differentiation by phage sensitivity and genetic mapping; *J. Gen. Microbiol.* **70** 527–554

Instructions to authors

Authors should send papers to: The Editor, 'Journal of Biosciences', Indian Academy of Sciences, P. B. No. 8005, C. V. Raman Avenue, Bangalore 560 080.

Three copies of the paper must be submitted.

The papers must present results of original work. Submission of the manuscript will be held to imply that it has not been previously published and is not under consideration for publication elsewhere; and further, that if accepted, it will not be published elsewhere.

Authors are invited to suggest names and addresses of three experts who in their opinion can review the paper. The choice of referees will however remain with the editorial board.

Typescript

Papers must be typed (on one side only) double-spaced and with a 30 mm margin on all sides on *white bond paper (280 × 215 mm)*. This also applies to the abstract, tables, figure captions and the list of references each of which should be typed on separate sheets.

Title page

The title of the paper must be brief and contain words useful for indexing. Serial titles are to be avoided.

● The names with initials of authors and the address of the institution where the work was carried out must be given.
An abbreviated running title of not more than 50 letters (including spaces) must also be given.
● The address for communication (with telephone, telex and fax numbers, if available), should be given.

Abstract

Papers must have an abstract (typed on a separate page) of not more than 200 words summarizing the significant results reported.

Keywords

Three to six keywords must be provided.

Text

● The paper must be divided into sections preferably starting with 'Introduction' and ending with 'Discussion'.
● The main sections should be numbered 1, 2 etc., the sub-sections 1.1, 1.2, etc., and further sub-sections (if necessary) 1.1a, 1.1b, etc.
● All measurements should be given in SI units.
● Avoid numbers at the beginning of a sentence, but if you have to use them, spell them.
● Taxonomic affiliation such as phylum, order and Family as well as the common name of the main study organism should be given in the title or at the first mention unless such information is likely to be obvious to a broad range of biologists.
The scientific names of genera and species are printed in italics and should be underlined in the typescript. ·
● Authority for names of taxa should be cited in the summary and at the first mention of a taxon in the text, but not elsewhere.
Accepted common names of plants and animals (and other organisms) and of plant and animal or other diseases should neither be capitalized nor placed within quotation marks.
Words and phrases not of English origin and not in common use (*e.g. in vitro, in situ*) are printed in italics and should therefore be underlined.

Tables

All tables must be numbered consecutively in arabic numerals in the order of appearance in the text. Tables should be self-contained and have a descriptive title.
Details of the experiment (not mentioned in the text) may be indicated below the table as a legend.

- Photographs should be numbered consecutively along with the figures in arabic numerals in the order of appearance in the text. They should be assembled together suitably to form one or more plates.
- Do not include line drawings and photographs in the same plate.
- Photographs should be sharp, of high contrast and on glossy paper with an indication of the scale.
- Xerox copies of photographs are unsatisfactory for refereeing; three prints of each photograph should be submitted, both black and white and colour photographs are welcome.

References

References should be cited in the text by author and year, not by number. If there are more than two authors, reference should be made to the first author followed by *et al* in the text. References at the end of the paper should be listed alphabetically by authors' names, followed by initials, year of publication, full title of the paper, name of the journal (abbreviated according to the World List of Scientific Periodicals, Butterworths, London), volume number, initial and final page numbers. References to books should include: name(s) of author(s), initials, year of publication, title of the book, edition if not the first, initials and name(s) of editor(s) if any, preceded by ed(s), place of publication, publisher, and pages referred to. References to these must include the year, the title of the thesis, the degree for which submitted and the university.

Examples

Mani A and Prabhu V K K 1986 Significance of critical development stage on starvation induced endocrine mediated precocious metamorphosis in *Oryctes rhinoceros* (Coleoptera: Scarabaeidae); *Proc. Indian Acad. Sci. (Anim. Sci.)* **95** 379–385

Zar J H 1974 *Biostatistical analysis* (New Jersey: Prentice Hall)

Samiwala E B 1987 *DNA cloning in Haemophilus influenzae*, Ph. D thesis, University of Bombay, Bombay.

Ramanna M S and Hermsen J H Th 1979 Genome relationships in tuber-bearing Solanums; in *Biology and taxonomy of Solanaceae* (eds) J G Hawkes, R N Lester and A G Skelding (London: Academic Press) pp 647–654

Abbreviations, symbols, units etc

The authors should follow *internationally agreed rules* especially those adopted by the IUPAC-IUB Commission on Biochemical Nomenclature (CBN). The journal will essentially follow the rules defined in the IUPAC *Manual of symbols and terminology for physico-chemical quantities and units* (Butterworths, London), 1970. Enzyme names may be abbreviated except on the first occasion, when the full name and abbreviation in parenthesis should be given.

Footnotes

Footnotes to the text should be avoided if possible but when essential should be numbered consecutively and typed on a separate sheet.

Proofs

Proofs sent to the authors together with a reprint order form must be returned to the editorial office within two days of their receipt (preferably by speed post or courier and definitely not by registered post). Delayed despatch of corrected proofs will delay publication. In order to minimize the corrections and alterations in the proof stage, authors are requested to prepare the manuscript carefully before submitting it for publication.

Reprints

100 reprints will be supplied free of charge.

Manuscripts not conforming to these specifications will be returned.

Purification and characterization of a DNA synthesis inhibitor protein from mouse embryo fibroblasts

S SRINIVAS*, T NAGASHUNMUGAM** and G SHANMUGAM†

Cancer Biology Division, School of Biological Sciences, Madurai Kamaraj University, Madurai 625 021, India
Present address: *The Salk Institute, San Diego, California 92138, USA
**The Wistar Institute, Philadelphia, Pennsylvania 19104, USA

Abstract. A DNA synthesis inhibitor protein was purified from the conditioned medium of cycloheximide treated mouse embryo fibroblasts. This protein has a molecular weight of 45,000 as determined by gel filtration and polyacrylamide gel electrophoresis. The levels of the [^{35}S] methionine labelled 45 kDa protein in the medium and matrix were monitored across two cell cycles in synchronized cultures. The 45 kDa protein was present in higher levels in the medium of non-S-phase cells depicting a peak between the two S-phases. The DNA synthesis inhibitor protein was immunologically related to a chicken DNA-binding protein which showed similar cell cycle specific variations at the intracellular level. The purified 45 kDa protein inhibited DNA synthesis in murine and human cells. In mouse embryo fibroblasts, the DNA synthesis was inhibited to an extent of 86% by 0·25 μg/ml of the inhibitor, while higher amounts of the inhibitor were required to arrest DNA synthesis in human skin fibroblasts; in these cells, 4 μg/ml of the inhibitor inhibited DNA synthesis to an extent of 50%. The high levels of the 45 kDa protein in the medium of non-S phase cells and its DNA synthesis inhibitory potential suggest that this protein may be involved in the regulation of DNA synthesis during the cell cycle.

Keywords. DNA synthesis inhibitor; variations in cell cycle.

1. Introduction

The molecular mechanisms of regulation of cell growth by the endogenous proteins of the cell are of increasing interest. The role of autocrine growth factors in the stimulation of cell proliferation has been studied in detail (James and Bradshaw 1984; Heldin and Westermark 1984). However, much less is known about the role of endogenous growth inhibitor proteins on cell growth. A number of growth inhibitory proteins have been purified and characterized from various types of cells (Holley *et al* 1980; Harel *et al* 1985; Hsu and Wang 1986; Stein and Atkins 1986; Feltham *et al* 1987; Ervin *et al* 1989). Recently, transforming growth factor β was shown to act as a bifunctional modulator of cell growth (Roberts *et al* 1985). A secreted protein of molecular weight (M_r) 48,000 identified as plasminogen activator inhibitor-1 was suggested to be involved in the regulation of cell proliferation (Nagashunmugam *et al* 1989; Srinivas *et al* 1990).

We have recently shown that the conditioned media of non-S-phase fibroblast cultures contained large quantities of a 45 kDa protein, and this conditioned medium inhibited DNA synthesis (Nagashunmugam and Shanmugam 1987). In studies described here, the 45 kDa protein was purified from the conditioned medium of mouse embryo fibroblasts (MEF). The purified protein was shown to

---

†Corresponding author.
Abbreviations used: MEF, Mouse embryo fibroblasts; HOU, hydroxyurea; CH, cycloheximide.

45 kDa protein across two cell cycles and its immunological relatedness to a chicken DNA binding protein (Matsuhashi *et al* 1987) that showed similar cell cycle specific variations are also described.

2. Materials and methods

2.1 *Synchronization of Cells*

Primary cultures of Swiss MEF were grown in Eagle's minimal essential medium (MEM) (Flow Labs., UK) containing 10% bovine serum (Flow Labs, UK) and gentamycin (50 μg/ml) at 37°C. Cells from the fourth passage onwards (secondary cultures) were used for experiments. Sub-confluent monolayers were synchronized by a double block method first at quiescence by growing for 48–72 h in 0·5% serum-containing medium and then at G1/S junction by treatment with 1 mM hydroxyurea (HOU) in MEM containing 10% bovine serum for 16 h. The human skin fibroblasts (LN 9 cells) were obtained from Dr M Digweed, and these cells were also synchronized as above. Cells were relieved of HOU arrest by washing the monolayers thrice with phosphate buffered saline followed by incubation in 10% serum-containing medium.

2.2 *Protein purification*

Quiescent monolayers in rollers were first treated with cycloheximide (3 μg/ml) for 15 h and then maintained for 1 h in serum-free MEM. One hundred ml of conditioned medium were concentrated to 0·5 ml by ultrafiltration using a 10 kDa cut-off Millipore membrane. The concentrated sample was fractionated in a LKB HPLC system using size-exclusion column (7·5 × 600 mm, TSK G-3000). The proteins were eluted with 20 mM Tris-HCl pH 7·2 and 1 mM EDTA at a flow rate of 0·2 ml/min and 0·5 ml fractions were collected. The molecular weights of the eluted proteins were estimated using proteins of known molecular weights. The peak fractions were pooled, lyophilized and dissolved in phosphate buffered saline (PBS). The protein solution was then filter-sterilized and assayed for DNA synthesis inhibitory activity. The protein concentration was determined according to Lowry *et al* (1951).

2.3 *Inhibitor assay*

DNA synthesis inhibitory activity was assayed using MEF and LN9 cells grown in 24 well plates. Each well contained 2×10^4 cells in 0·5 ml of growth medium. Cells were synchronized by HOU treatment as mentioned earlier. The HOU arrested MEF and LN9 cells were washed thrice with PBS and maintained in fresh growth medium in the presence or absence of purified DNA synthesis inhibitor protein. The DNA synthesis was monitored by labelling the cells with 5 μCi/ml [^{3}H] thymidine for 30 min after 2 h of release from HOU arrest. At the end of labelling, the cells in the wells were washed thrice with cold PBS and acid precipitable radioactivity was determined (Russell *et al* 1984).

The HOU arrested and stimulated monolayers (25 cm²) were washed twice with PBS and labelled with 25 µCi of [^{35}S] methionine for 30 min in 2 ml of Hanks balanced salt solution. The radioactivity was later chased for 30 min in serum-free medium. The secreted and the extracellular matrix proteins were isolated as described earlier (Nagashunmugam *et al* 1989), electrophoresed in 5–18% polyacrylamide gradient gels containing sodium dodecyl sulphate (SDS) and fluorographed (Nagashunmugam *et al* 1989). The relative amounts of the 45 kDa protein was deduced by laser densitometry of the fluorograms.

3. Results

In our previous studies, we have identified a group of early growth response proteins in MEF (Subramaniam and Shanmugam 1985, 1986a, 1987, 1988). One of these, the 45 kDa protein was present in large amounts in the growth medium of non-S-phase cells. Of all the secreted proteins of MEF, the 45,000 dalton protein was super-induced by cycloheximide treatment (figure 1). For these studies, quiescent cells were treated with cycloheximide (CH) (3 µg/ml) for 15 h after which the CH containing medium was removed and the cells were labelled with [^{35}S] methionine for 30 min. The radioactivity was then chased for different periods in serum-free chase-medium. Figure 1 shows the fate of the labelled 45 kDa protein at different periods of chase. The 45 kDa protein was the major secreted protein in the medium of CH treated cells in the first 1 h of chase. Other proteins started to accumulate in the medium from 2 h onwards.

3.1 *45 kDa protein levels in synchronized cells*

When the DNA synthesis of synchronized cells that were released from HOU-arrest was monitored by labelling with [^{3}H] thymidine, two peaks of DNA synthesis (one at 3 h and the other at 24 h after release) were observed (figure 2). The levels of the 45 kDa protein was quantitated at various periods after release from HOU-arrest by labelling the cells with [^{35}S] methionine and analysing the labelled secreted proteins present in the chase-medium. In our previous studies we observed a decline in the level of the 45 kDa secreted protein as the cells entered into peak DNA synthesis (Nagashunmugam and Shanmugam 1987). Here, we report a second decrease in the level of the 45 kDa protein at the beginning of the second S-phase; this decline continued up to the peak of DNA synthesis of the second S-phase (figure 2). When the levels of the 45 kDa protein were quantitated by laser densitometry, a 3-4-fold decrease in its level was observed at the first and second S-phase peaks, in comparison to its level in the culture media of non-S-phase cells 12–18 h after release from HOU arrest.

3.1a *45 kDa protein is a component of extracellular matrix*: Some of the secreted proteins like fibronectin and vitronectin are extracellular matrix components. These proteins were shown to have important roles in cell adhesion and cell-cell communication. Therefore, we looked for the presence of the 45 kDa protein in the
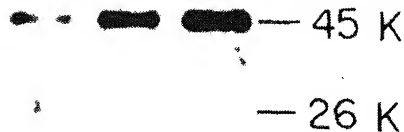
Figure 1. Secreted proteins of cycloheximide treated cells. Quiescent MEF were incubated with CH (3 μg/ml) containing medium for 15 h. At the end of incubation. CH-containing medium was removed, cells were washed and then labelled with [^{35}S] methionine for 30 min. After this pulse-labelling, the radioactive medium was removed, cells were washed and then incubated for different periods in serum free chase-medium. The labelled proteins secreted into the medium were analysed by electrophoresis in 5 to 18% polyacrylamide gradient gels containing SDS. The protein bands were visualized by fluorography. The numbers at the top of the lanes indicate hours of incubation of labelled cells in the chase-medium.

extracellular matrix and the results are shown in figure 3. Maximum levels of the 45 kDa protein were observed in both the matrix and medium at 12 h after release from HOU arrest; at this time, the DNA synthesis declined to background levels. When the DNA synthesis went up in the second S-phase (20 h onwards), the amount of the matrix-associated 45 kDa protein also declined. The major component of the extracellular matrix of MEF is a 48 kDa protein identified as plasminogen activator inhibitor (Nagashunmugam *et al* 1989), this protein did not show any spectacular variation across the cell cycle as that exhibited by the 45 kDa protein. However, a slight decrease in the level of the 48 kDa protein at 12 h after release of cells from HOU arrest was observed (figure 4); at this time (12 h after HOU release), the cells were expected to be at mitosis and the cells had a rounded shape. The decreased level of the protease inhibitor at the time of mitosis may correlate with increased pericellular proteolytic activity which results in the disruption of anchorage of these cells enabling them to become round and loosely attached to the substratum.
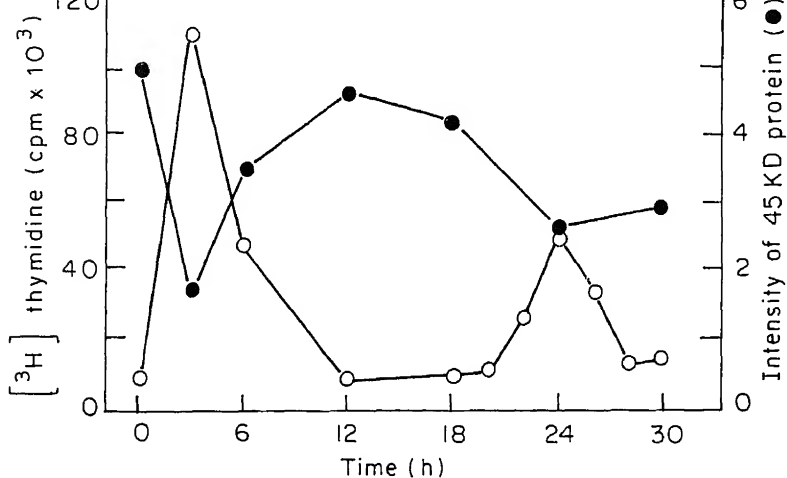
Figure 2. Levels of 45 kDa protein in the growth medium across two S-phases.

One set of MEF that were released from HOU-arrest were pulse-labelled for 30 min with $[^{35}S]$ methionine at the indicated periods after release. Another set was labelled for 30 min with $[^3H]$ thymidine under the same conditions. $[^3H]$ thymidine incorporation into DNA was estimated from TCA-insoluble counts. $[^{35}S]$ methionine-labelled secreted proteins were isolated and electrophoresed in polyacrylamide gradient gels as described under § 2·4. $[^{35}S]$ methionine incorporation into the secreted 45 kDa protein is represented as the intensity of the radioactive 45 kDa protein. The intensity was quantitated by laser densitometry of the 45 kDa protein bands of the fluorograms of gels in which the proteins were electrophoresed.

3.2 *45 kDa protein is related to P28 DBP*

Matsuhashi *et al* (1987) have shown that a 45 kDa protein present in serum-stimulated NIH 3T3 cells reacted with a monoclonal antibody raised against a chicken DNA binding protein called P28. The P28 protein was shown to be synthesized in the cells during late G1 and the synthesis of this protein ceased at the S-phase (Matsuhashi *et al* 1987). To establish the relatedness of these proteins, the 45 kDa DNA synthesis inhibitor protein secreted by MEF was reacted with monoclonal antibody against P28 antigen. Figure 4 shows the electrophoretic profile of immunoprecipitated proteins of medium and matrix. The electrophoretic pattern shows a 45 kDa protein as the sole labelled protein of the immunoprecipitate, indicating that the 45 kDa protein is related to the P28 antigen.

3.3 *DNA synthesis inhibition by purified 45 kDa protein*

For the purification of the 45 kDa protein, cells were grown in roller bottles and treated with cycloheximide for 15 h; the first hour conditioned media of these cultures were collected, clarified and concentrated by ultrafiltration. The concentrated medium was chromatographed in TSK 3000 HPLC column. Figure 5 shows the elution profile of the 45 kDa protein which coincides with the ovalbumin
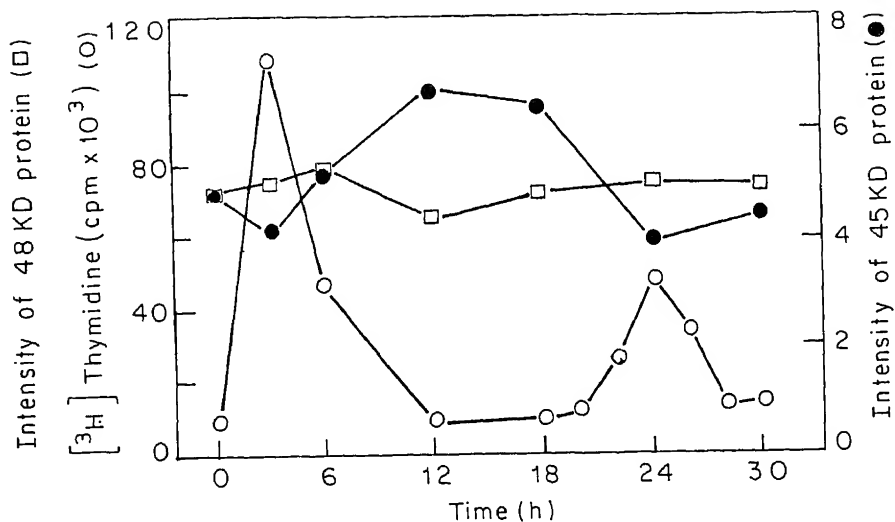
Figure 3. Levels of 45 kDa protein in the extracellular matrix across two S-phases.
One set of MEF that were released from HOU-arrest were pulse labelled for 30 min with [^{35}S] methionine. Labelled cells were removed at the indicated periods after release and the extracellular matrix proteins were isolated as described in §2·2. The labelled proteins were resolved by 5–18% PAGE and fluorographed. A 48 kDa protein identified previously as plasminogen activator inhibitor and the 45 kDa protein were the predominant components of the extracellular matrix. The intensities of the labelled 48 and 45 kDa protein bands were quantitated by laser densitometry. Another set of MEF were labelled for 30 min with [^{3}H] thymidine under the same conditions, and the thymidine incorporation into DNA was determined from TCA-insoluble radioactivity.

retention time. The 45 kDa protein fractions were pooled, lyophilized and dissolved in PBS. After filter sterilization, the protein was used in DNA synthesis inhibition assays.

Cells synchronized in G1/S border by the double block method were released by the addition of medium containing 20% foetal calf serum, in the presence or absence of column fractions. No inhibition of DNA synthesis was observed with fractions lacking the 45 kDa protein. Figure 6a shows the inhibition of DNA synthesis in MEF in the presence of various concentrations of the 45 kDa protein. Maximum DNA synthesis inhibition was observed at and above 0·25 µg/ml of inhibitor in MEF (figure 6a). The DNA synthesis inhibitory activity was found to be dose-dependent, and the half maximal inhibitory activity, calculated from figure 6a, was at 0·15 µg/ml of the 45 kDa protein. No DNA synthesis inhibitory activity was observed at this concentration in LN9 human fibroblasts. However, at higher concentration of the inhibitor, the DNA synthesis in these cells was also inhibited. In human fibroblasts, maximum inhibition of DNA synthesis (53%) was achieved with 4 µg/ml of the inhibitor protein and half maximum inhibition was observed with 1 µg/ml of the inhibitior (figure 6b).

Maximum inhibition of DNA synthesis was observed at 2 h after addition of the inhibitor in cells released from HOU arrest (figure 7). DNA synthesis was inhibited
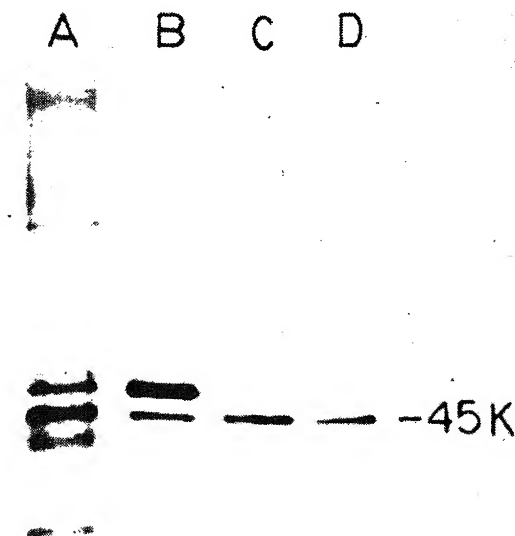
Figure 4. Immunoprecipitation of 45 kDa protein.

MEF 12 h after release from HOU arrest were labelled with [^{35}S] methionine for 30 min. Following a 30 min chase incubation, the labelled medium and extracellular matrix proteins were isolated as described in §2.4. For immunoprecipitation, antibodies to P28 protein provided by Dr K Hori was used and the method described by Srinivas *et al* (1990) was followed. The immunoprecipitates were analysed by SDS-PAGE and fluorographed. (A), secreted proteins of conditioned medium; (B), extracellular matrix proteins; (C), immunoprecipitate of proteins from conditioned medium; (D), immunoprecipitate of proteins from extracellular matrix. In each case proteins derived from one 75 cm^2 monolayer was used.

treated cells was observed which reached a maximum at 7 h after release from HOU arrest. During this period, only a basal level of DNA synthesis was observed in control cells that were released from HOU arrest in the absence of inhibitor protein. The growth inhibition after 7 h of release from HOU arrest was 56% of the maximum incorporation observed in control cells 3 h after release from HOU arrest. The decrease in the inhibitory activity of the protein after its presence for longer periods in the medium may be due to the inactivation of the protein. The DNA synthesis inhibitory activity was destroyed by heating the inhibitor protein at 60°C for 1 h.

4. Discussion

The results presented here show that secondary cultures of MEF secrete a growth inhibitory protein whose secretion is regulated during the cell cycle. The amount of the 45 kDa protein in the conditioned medium of S-phase cells was about one-fourth of that observed at G2 and other phases, suggesting an inverse correlation
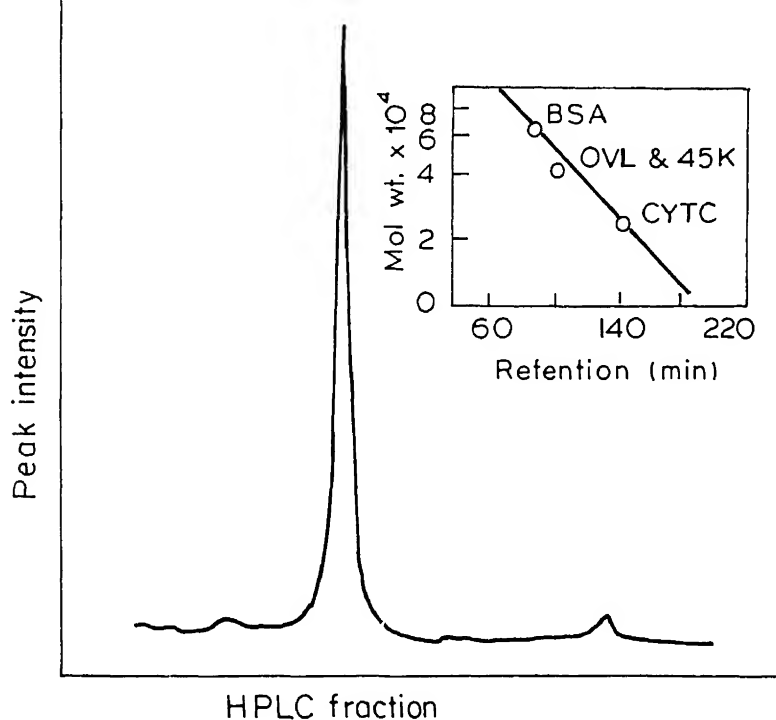
Figure 5. Purification of 45 kDa protein.

Conditioned media from cycloheximide treated MEF were concentrated by ultrafiltration (see §2·2) and chromatographed in a size exclusion (TSK 3000) HPLC column. The main figure shows the elution profile of the 45 kDa protein while the inset dipicts molecular weight calibration in which the retention times of standard marker proteins and the 45 kDa protein were ploted against log molecular weight.

quiescent and senescent human fibroblasts (Feltham *et al* 1987) and from the 3T3 cell plasma membranes (Whittenberger and Glaser 1977). Low molecular weight polypeptide inhibitors of DNA synthesis have been identified in the medium of mouse fibroblasts (Wells and Mallucci 1983). A 45,000 dalton protein called inhibitory diffusible factor (IDF) has been purified from the conditioned medium of density arrested NIH 3T3 cells and the N-terminal amino acid sequence of this protein has been determined (Blat *et al* 1989). Bohmer *et al* (1987) have shown that antibodies raised against bovine mammary derived growth inhibitor react with mouse fibroblast growth inhibitor.

Subramaniam and Shanmugam (1985, 1987, 1988) have shown that quiescent MEF secrete several proteins upon serum-stimulation. The results presented here show that among the secreted proteins, the 45 kDa protein alone is superinduced by cycloheximide treatment. The superinduction of the 45 kDa protein by CH suggests that the synthesis of this protein may be under the control of a labile repressor protein. Similar conclusion was also arrived at for the other CH-inducible proteins (Kruijer *et al* 1984; Makino *et al* 1984; Subramaniam and Shanmugam 1986b). The inhibition of extracellular levels of the 45 kDa protein by actinomycin-D (Subramaniam and Shanmugam 1988) shows that the synthesis and secretion of

45 KD protein (μg /ml)
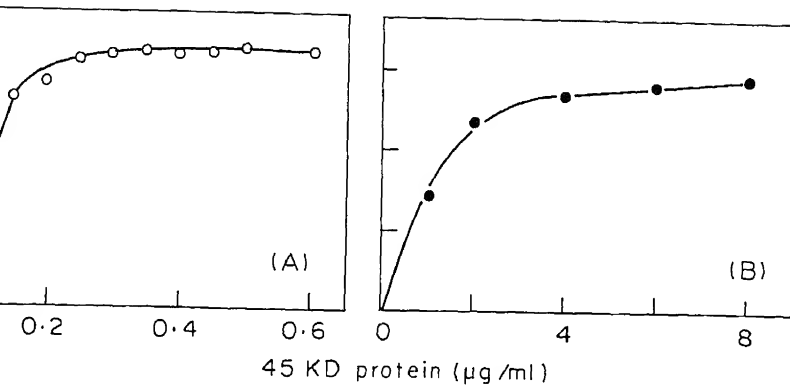
e 6. (A) Effect of purified 45 kDa protein on DNA synthesis in MEF.
e growth of MEF were arrested at Gl/S junction by HOU treatment for 15 h. At the
of this period, HOU was removed, cell monolayers were washed and incubated for
in fresh growth medium containing the indicated amounts of 45 kDa protein after
they were incubated another 30 min with [³H] thymidine. HOU released control
players were similarly incubated for 2·5 h in fresh medium followed by 30 more min in
um containing [³H] thymidine. Per cent inhibition of DNA synthesis was determined
the TCA insoluble radioactivities of control and 45 kDa protein treated monolayers.
ffect of purified 45 kDa protein on DNA synthesis in LN9 human fibroblasts. The
col followed for this study is identical to that described above for MEF.

Time (h)
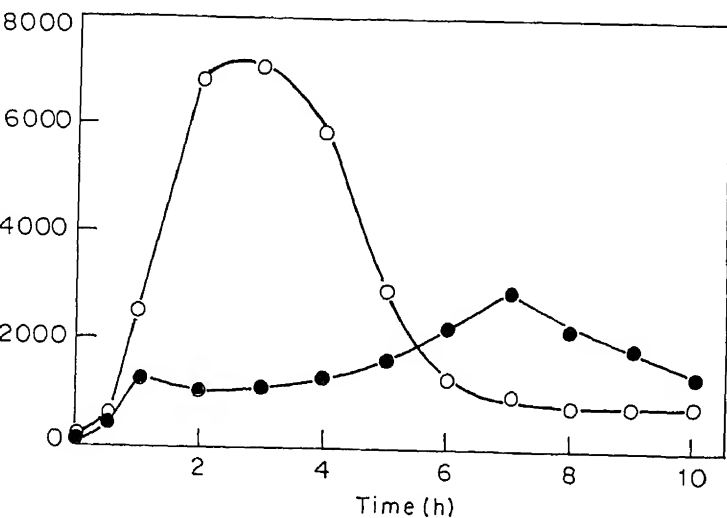
7. Time course of inhibition of DNA synthesis by the 45 kDa protein.
nolayers of MEF were labelled for 30 min with [³H] thymidine (5 μCi/ml) at the
ed periods after release from HOU arrest in the presence or absence of the 45 kDa
(0·3 μg/ml). DNA synthesis was monitored by determining TCA insoluble
ctivity. The X-axis indicates time (in hours) after release of cells from HOU arrest. In
se of control, the cells were released from HOU arrest by using fresh medium
ning foetal calf serum. To monitor DNA synthesis in the presence of the inhibitor,
s were released from HOU arrest using fresh medium containing foetal calf serum and
kDa protein; these cultures were later labelled with [³H] thymidine. (○), DNA
is in control cells; ( ), DNA synthesis in 45 kDa protein-treated cells.

...ase incubation of pulse-labelled cells. Since high extracellular levels of the 45 ...protein were observed in the conditioned medium within an hour of CH ...ent, this antibiotic was used to enrich this protein selectively for purification ...ses.

...racellular matrix proteins like fibronectin, vitronectin, collagen and laminin ...mportant roles in cell substrate adhesion and cell-cell interaction by binding ...t specific cell surface receptors (Kleinman *et al* 1981; Hasegawa *et al* 1985; ...da *et al* 1985; Laptin 1986; Hynes 1987). One of the 45 kDa secreted proteins ...3 cells was a glycoprotein associated with extracellular matrix (Santaren and ...1987). In our studies, the matrix associated 45 kDa protein showed ...ions across cell cycle, while the major matrix protein (PAI-1) showed little ...ion (figure 4).

...tsuhashi *et al* (1987) identified a 45 kDa protein in NIH 3T3 cells whose ...ellular level was regulated during cell cycle; the synthesis of this protein ...l during S-phase. A monoclonal antibody (P28) raised against a chicken DNA ...ig protein reacted with the intracellular 45 kDa protein of NIH 3T3 cells ...uhashi *et al* 1987). Here, we show that the secreted and the matrix associated ...Da proteins of MEF, are immunologically related to the 45 kDa protein of ...3T3 cells. Also the 45 kDa DNA synthesis inhibitory factor described here is ...r in molecular weight and mode of action to the IDF 45 described by Harel *et* ...85). Further characterization of this protein is necessary to confirm its ...ty with IDF 45. Experiments are underway for sequencing this protein.

...eral mechanisms may be postulated for the inhibitory action of 45 kDa ...n on DNA synthesis. The protein may inhibit the transport of $[^3H]$ thymidine ...plete the intracellular nucleotide pool. Also it is not known whether the 45 ...protein is internalized by specific receptors or by other mechanisms. The ...ng studies in our laboratory are aimed at unravelling the mechanism of action ...s protein on the inhibition of DNA synthesis.

...e 45 kDa DNA synthesis inhibitor protein might be one among the negative ...h regulators that control the proliferation of cells triggered by positive growth ...ators such as mitogens (Stocker 1973; Stocker and Piggolt 1974). Future ...ions of these studies include raising of antibodies and DNA clones to the 45 ...protein and its gene to understand the role of this protein in cell proliferation. ...ninary studies showed reduced levels of this protein in rapidly proliferating ...ene (*myc*-ras) transformed rat cells (M V V S Varaprasad and G Shanmugam, ...blished results). Higher amounts of the 45 kDa protein in normal cells may ...a negative control in these cells and regulate the rate of cell division.

References

Bohmer F D, Sun Q, Pepperle M, Muller T, Eriksson U, Wang J L and Grosse R 1987 Identification of a polypeptide growth inhibitor from bovine mammary gland; *Biochem. Biophys. Res. Commun.* **148** 1425–1431

Blat C, Bohlen P, Villaudy J, Chatelain G, Golde A and Harel L 1989 Isolation and amino-terminal sequence of a novel cellular growth inhibitor (Inhibitory Diffusible Factor 45) secreted by 3T3 fibroblasts; *J. Biol. Chem.* **264** 6021–6024

Ervin P R, Kaminski M S Jr, Cody R L and Wicha M S 1989 Production of mammastatin, a tissue-specific growth inhibitor by normal human mammary cells; *Science* **244** 1585–1587

Feltham N, Fahey D and Knight E Jr 1987 A Growth inhibitory protein secreted by human diploid fibroblasts; *J. Biol. Chem.* **262** 2176–2179

Harel L, Blat C and Chatelain G 1985 Regulation of cell proliferation. Inhibitory and stimulatory factors diffused by 3T3 cultured cells; *J. Cell Physiol.* **123** 139–143

Hasegawa T, Hasegawa E, Chen W-T and Yamada K M 1985 Characterization of a membrane-associated glycoprotein complex implicated in cell adhesion to fibronectin; *J. Cell Biochem.* **28** 307–318

Heldin C H and Westermark B 1984 Growth factors: mechanism of action and relation to oncogenes; *Cell* **37** 9–20

Holley R W, Bohlen P, Fava R, Baldwin J H, Kleeman G and Armour R 1980 Purification of kidney epithelial cell growth inhibitors; *Proc. Natl. Acad. Sci. USA* **77** 5989–5992

Hsu Y M and Wang J L 1986 Growth control in cultured 3T3 fibroblasts. V. Purification of an M_r 13000 polypeptide responsible for growth inhibitory activity; *J. Cell Biol.* **102** 362–369

Hynes R O 1987 Integrins: a family of cell surface receptors; *Cell* **48** 549–554

James R and Bradshaw R A 1984 Polypeptide growth factors; *Annu. Rev. Biochem.* **53** 259–292

Kleinman H J, Klebe R J and Martin G R 1981 Role of collagenous matrices in the adhesion and growth of cells; *J. Cell Biol.* **88** 473–485

Kruijer W, Cooper J A, Hunter T and Verma I M 1984 Platelet-derived growth factor induces rapid but transient expression of c-*fos* gene and protein; *Nature (London)* **312** 711–716

Leptin M 1986 The fibronectin receptor family; *Nature (London)* **321** 728–730

Lowry O H, Rosebrough N J, Farr A L and Randall R J 1951 Protein measurement with the Folin phenol reagent; *J. Biol. Chem.* **193** 265–275

Makino R, Hayashi K and Sugimura T 1984 c-*myc* transcript is induced in rat liver at very early stage of regeneration or by cycloheximide treatment; *Nature (London)* **310** 697–698

Matsuhashi S, Watanabe T and Hori K 1987 An antigen expressed in proliferating cells at late G1-S Phase; *Exp. Cell Res.* **170** 351–362

Nagashunmugam T and Shanmugam G 1987 S-phase mouse embryo fibroblasts secrete varying amounts of a 45000 dalton protein; *Cell Biol. Int. Rep.* **11** 147–155

Nagashunmugam T, Srinivas S and Shanmugam G 1989 Effect of dimethyl sulfoxide on mouse embryo fibroblasts: inhibition of plasminogen activator deposition and interference with early events of serum-stimulated growth; *Biol. Cell* **66** 307–315

Roberts A B, Anzano M A, Wakfield L M, Roche N S, Stern D F and Sporn M B 1985 Type B transforming growth factor: A bifunctional regulator of cellular growth; *Proc. Natl. Acad. Sci. USA* **82** 119–123

Russell W E, Van Wyk J J and Pledger W J 1984 Inhibition of the mitogenic effects of plasma by a monoclonal antibody to somatomedin C; *Proc. Natl. Acad. Sci. USA* **81** 2389–2392

Santaren J F and Bravo R 1987 Immediate induction of a 45 K secreted glycoprotein by serum and growth factors in quiescent mouse 3T3 cells; *Exp. Cell Res.* **168** 494–506

Srinivas S, Nagashunmugam T and Shanmugam G 1990 Translocation of plasminogen activator inhibitor-1 during serum stimulated growth of mouse embryo fibroblasts; *J. Biosci.* **15** 351–359

Stein G H and Atkins L 1986 Membrane-associated inhibitor of DNA synthesis in senescent human diploid fibroblasts: Characterization and comparison to quiescent cell inhibitor; *Proc. Natl. Acad. Sci. USA* **83** 9030–9034

Stocker M G P and Piggott D 1974 Shaking 3T3 cells: further studies on diffusion boundary effects; *Cell* **3** 207–215

Subramaniam M and Shanmugam G 1985 Intracellular and secreted proteins of density-inhibited serum-arrested and proliferating mouse embryo cells; *Cell Biol. Int. Rep.* **9** 51–60

Subramaniam M and Shanmugam G 1986a Effect of cycloheximide and growth factors on gene expression in quiescent mouse embryo fibroblasts; *J. Cell. Physiol.* **126** 47–52

Subramaniam M and Shanmugam G 1986b A serum-induced 29 kD protein of mouse embryo fibroblasts is tightly bound to the chromatin; *Cell Biol. Int. Rep.* **10** 323–329

Subramaniam M and Shanmugam G 1987 Secreted proteins of quiescent serum-stimulated and over-confluent mouse embryo fibroblasts; *J. Biosci.* **12** 281-287

Subramaniam M and Shanmugam G 1988 Effects of serum cycloheximide and actinomycin D on protein secretion by quiescent mouse embryo fibroblasts; *Mol. Biol. Rep.* **13** 133–138

Wells V and Mallucci L 1983 Properties of a cell growth inhibitor produced by mouse embryo fibroblasts; *J. Cell. Physiol.* **117** 148–154

Whittenberger B and Glaser L 1977 Inhibition of DNA synthesis in cultures of 3T3 cells by isolated surface membranes; *Proc. Natl. Acad. Sci. USA* **74** 2251–2255

Yamada K M, Akiyama S K, Hasegawa T, Hasegawa E, Humphries M J, Kennedy D W, Nagata K, Urushihara H, Olden K and Chen W-T 1985 Recent advances in research on fibronectin and other cell attachment proteins; *J. Cell. Biochem.* **28** 79–97

...ction enzyme digestion of heterochromatin in *Drosophila nasuta*

P K TIWARI*† and S C LAKHOTIA

Cytogenetics Laboratory, Department of Zoology, Banaras Hindu University,
Varanasi 221 005, India

*Present address: School of Studies in Zoology, Jiwaji University, Gwalior 474 011, India

Abstract. *In situ* digestion of metaphase and polytene chromosomes and of interphase nuclei in different cell types of *Drosophila nasuta* with restriction enzymes revealed that enzymes like AluI, EcoRI, HaeIII, Sau3a and SinI did not affect Giemsa-stainability of heterochromatin while that of euchromatin was significantly reduced; TaqI and SalI digested both heterochromatin and euchromatin in mitotic chromosomes. Digestion of genomic DNA with AluI, EcoRI, HaeIII, Sau3a and KpnI left a 23 kb DNA band undigested in agarose gels while with *TaqI*, no such undigested band was seen. The *AluI* resistant 23 kb DNA hybridized *in situ* specifically with the heterochromatic chromocentre. It appears that the digestibility of heterochromatin region in genome of *Drosophila nasuta* with the tested restriction enzymes is dependent on the availability of their recognition sites.

Keywords. *Drosophila*; heterochromatin: restriction enzyme digestion.

...roduction

...tantial amount of the genome of *Drosophila nasuta* is present as large ...tromeric blocks of heterochromatin on all the three pairs of larger ...osomes, occupying nearly 40% of the length of the mitotic chromosomes ...tia and Kumar 1978). Earlier cytological studies revealed these different ...of heterochromatin of *D. nasuta* to be remarkably similar in their various ...es such as C- and fluorescence banding patterns (Lakhotia and Kumar ...oalescing together to form a single compact chromocentre in interphase and ...e nuclei (Lakhotia and Kumar 1978; Kumar and Lakhotia 1977), containing ...etric A-T rich DNA sequence (Lakhotia *et al* 1979) and effects of DNA ...like Hoechst 33258, Distamycin A and Netropsin (Lakhotia and Roy 1981, ...These features suggested that the different heterochromatin regions in the ...e of *D. nasuta* shared similar asymmetric A-T rich DNA sequences. A single ...h satellite DNA, present on all the heterochromatin blocks, is reported to ...t for only 7–8% of total nuclear DNA of *D. nasuta* (Ranganath *et al* 1982). ...ture of other sequences constituting rest of the heterochromatin is not

...cent years, *in situ* digestion of aceto-methanol fixed or unfixed chromosomes ...striction endonucleases has been found to result in diverse banding patterns ...allows analysis of molecular organization of DNA sequences present in ...t regions (Lima-de Faria *et al* 1980; Miller *et al* 1983; Bianchi *et al* 1985; ...otte 1986; Mezzanotte *et al* 1986; Babu 1988; Burkholder 1989; Lopez-...dez *et al* 1989; Miller and Miller 1990). Restriction enzyme digestion of fixed

---

...onding author.

may appear similar in other cytological features (Miller *et al* 1985; Mezzanotte 1986; Mezzanotte *et al* 1986; Babu 1988).

With a view to know if the different heterochromatic regions in *D. nasuta* differ in their cytological organization, we examined effects of different restriction enzymes on cytological preparations of several cell types of *D. nasuta*. Our results showed that, in keeping with the earlier noted cytological uniformity, no difference was found between the different blocks of heterochromatin in chromosomes of *D. nasuta* with respect to sensitivity to restriction enzyme digestion *in situ*. Satellite as well as other non-satellite (presumably highly repetitive) sequences present in the different heterochromatin blocks thus appear to be deficient in recognition sites for enzymes like AluI.

2. Materials and methods

A wild type strain of *D. nasuta*, maintained in laboratory on standard food at $20° \pm 1°C$, was used.

2.1 *Restriction enzyme digestion of cytological preparations*

Metaphase chromosome preparations from brain ganglia of late third instar larvae were made by the air-dry method as described by Lakhotia and Kumar (1978). Polytene chromosome squashes were obtained from salivary glands of late third instar larvae in the usual manner except that the aceto orcein/carmine staining step prior to squashing was omitted. In addition, squash preparations of aceto-methanol (1:3) fixed interphase cells from early embryos (~ 4 h post-oviposition), brain ganglia of late third instar larvae, pupae and adults and the ovarian follicle and nurse cells of adult females were also made in 50% acetic acid. Coverslips of squash preparations were flipped off with a razor blade after the preparations were stored at $-70°C$ for 5 to 16 h. The slides were rinsed in absolute ethanol and air-dried.

Chromosome preparations of larval brain ganglia were digested with the following restriction endonucleases. AluI, EcoRI, HaeIII, Sau3a, SalI, SinI and TaqI (Amersham, UK). All other cytological preparations were digested only with AluI. For digestion of the cytological preparations with restriction endonucleases, 20–25 μl of appropriate reaction buffer containing 10–30 units of the enzyme was put on the slide, covered with a coverslip and incubated at 37°C (65°C in case of TaqI) for 16–20 h. After completion of digestion, the slides were washed in 5 mM EDTA, dehydrated through ethanol grades and air-dried. Parallel control slides were incubated only in the respective buffer without the enzyme. Finally the preparations were stained with 5% Giemsa, mounted with DPX mountant and examined by bright-field microscopy.

2.2 *Hoechst 33258 staining of ovarian nurse and embryonic cells*

To localize the chromocentric heterochromatin, cytological preparations of ovarian nurse and follicle cells and blastoderm cells from 4 h old embryos (after egg laying)

MPV-3 cytophotometer (using a 100 W ultra high pressure mercury burner, a 50X NPL-Fluotar oil immersion objective and the B filter block-UV-violet excitation).

2.3 Restriction digestion of genomic DNA

Genomic DNA from adult male flies was purified by the usual procedure involving SDS-Proteinase-K lysis, Phenol-chloroform extraction, ethanol precipitation and RNase treatment. Each DNA preparation was checked on agarose gels for possible shearing and only unsheared DNA preparations were used for restriction digestion. DNA samples were digested with excess (5–10 units/μg DNA) AluI, EcoRI, HaeIII, Sau3a, KprI or TaqI restriction enzymes for about 16 h using appropriate reaction buffers and other conditions. The digested DNA samples were fractionated on standard 0·8% agarose gels containing ethidium bromide (Maniatis et al 1983). HindIII digested λ-DNA was used as the size marker.

2.4 Electroelution of AluI-resistant high molecular weight DNA

The 23 kb genomic DNA band left undigested by AluI (see §3) was electroeluted from preparatory 0·8% agarose gels. After completion of the gel run, the bright band at 23 kb position was cut with a sharp razor blade and the DNA electroeluted following Maniatis et al (1983).

2.5 In situ hybridization

The electroeluted AluI DNA was nick-translated using ^{3}H-dNTPs (all four labelled dNTPs from Amersham) and used for in situ hybridization with preparations of larval brain ganglia of D. nasuta following Pardue (1986).

3. Results

3.1 Restriction digestion of metaphase chromosomes

Examples of stained metaphase plates digested with the different restriction endonucleases are shown in figure 1. It was seen that except for SalI and TaqI, all other enzymes produced a typical C-band staining of metaphase chromosomes; digestion with AluI, EcoRI, HaeIII, Sau3a and SinI caused very reduced Giemsa staining of all euchromatic regions while the heterochromatin blocks on all chromosomes appeared very dark stained as seen after typical C-banding (Lakhotia and Kumar 1978). With these restriction enzymes, the Giemsa staining of Y chromosome (see inset in figure 1b) also closely resembled the pattern seen after C-banding (Lakhotia and Kumar 1978). No notable difference was found between the Giemsa staining pattern of metaphases digested with the above 5 restriction enzymes (figure 1). However, digestion with SalI or TaqI resulted in a significant reduction of Giemsa stainability of both eu- as well as heterochromatin regions
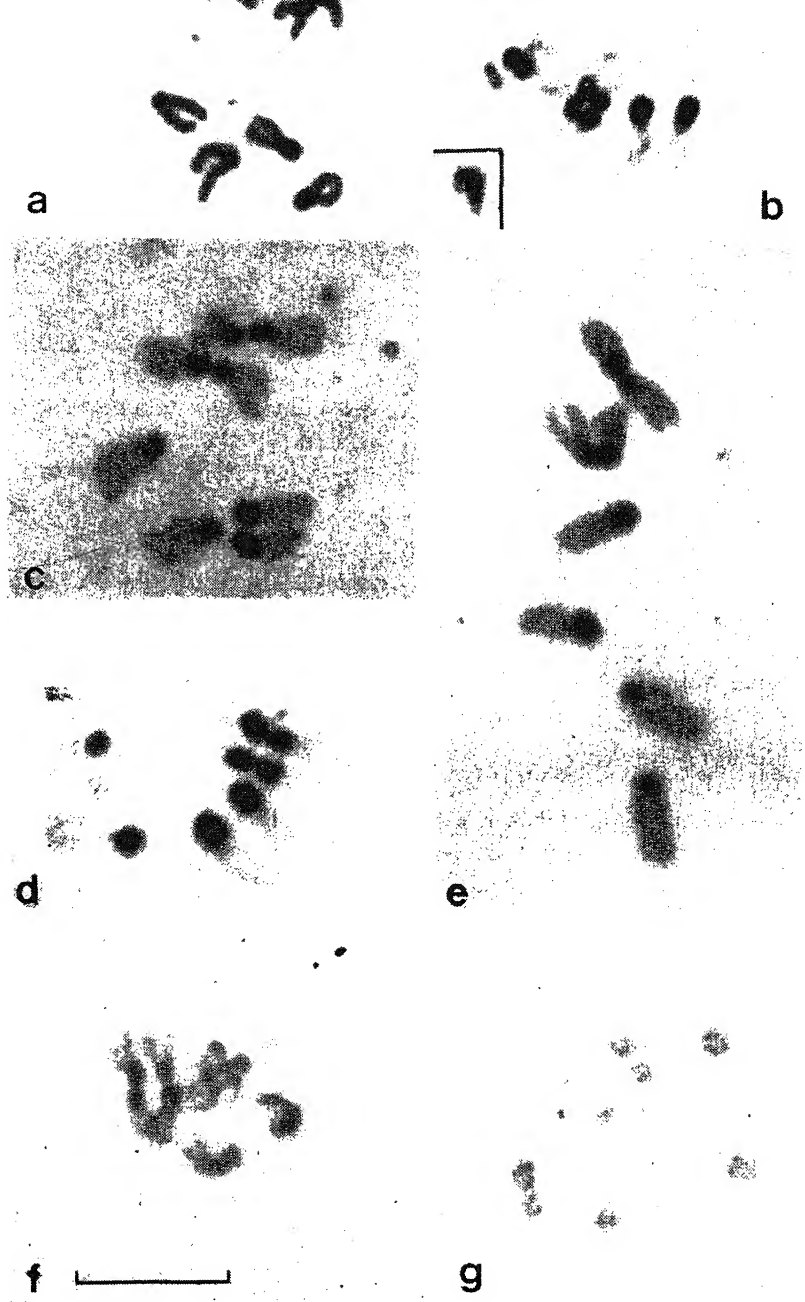
Figure 1. Giemsa stained metaphase plates from brain ganglia of *D. nasuta* larvae.
(a) Control (no enzyme) or after different enzyme treatments. (b) AluI, (c) EcoRI, (d) Sau3a, (e) HaeIII, (f) TaqI, (g) SalI. The inset in (b) shows Y-chromosome from a male metaphase after AluI digestion. The scale bar in this and figures 2, 3 and 5 indicates 10 μm.

(figure 1f, g). None of the enzymes produced any banding in the euchromatin regions (figure 1).

3.2 *Giemsa staining of other cell types after AluI digestion*

AluI-digested polytene chromosomes in squash preparations of salivary glands of *D. nasuta* stained poorly with Giemsa except for the whole of α-heterochromatin in the chromocentre (Kumar and Lakhotia 1977), a band at the base and one band in middle of chromosome 4 (figure 2a). The intranucleolar DNA mass (Lakhotia and Roy 1979) also appeared to be less affected by AluI digestion. AluI digested interphase nuclei from embryos of brain ganglia or larvae, pupae or adult showed intense staining of only the single chromocentre with rest of the nuclear chromatin appearing very light stained.

The follicle and nurse cells in ovaries of adult females endoreplicate, with the latter being highly polyploid (up to 1500C). However, the homologous chromatids in these cell types are not as organized as in larval salivary gland cells and thus no polytene chromosomes are seen in nurse cells. In both cell types, AluI digestion reduced Giemsa staining of all regions except the single chromocentre (figure 2b) which remained as darkly stained as in control nuclei. It is significant that in spite of their very different degrees of endoreplication, the size of the chromocentre was same in these two cell types and was comparable to that in diploid embryonic cells.

Thus in every cell type examined, the heterochromatic chromocentre was found to be completely resistant to AluI digestion.

3.3 *Hoechst 33258 fluorescence pattern of ovarian nurse, follicles and embryonic blastoderm cells*

The Hoechst 33258 stained nuclei both from the large nurse and smaller follicle cells show a single, similar sized brightly fluorescing chromocentre (figure 3b) as seen in larval salivary gland polytene nuclei (Lakhotia 1984). This Hoechst-bright region corresponds with the region that stains dark with Giemsa after AluI digestion (see figure 2b). The early embryonic nuclei do not have compact chromocentres as may be seen in figure 3a. However, the size of the Hoechst-bright regions in these diploid embryonic cells compares with the size in endo-replicated nurse and follicle cells.

3.4 *Restriction endonuclease digestion of genomic DNA and in situ hybridization of AluI resistant DNA*

Ethidium bromide staining of genomic DNA from adult males of *D. nasuta*, digested with the different enzymes mentioned in §2 and separated on 0·8% agarose gels, revealed that after digestion with all enzymes, except TaqI, a high molecular weight DNA band (23 kb) was left undigested (figure 4). As a result, the 23 kb AluI-resistant band appeared very distinct. After TaqI digestion, the 23 kb band was not seen (figure 4).

When the nick translated 23 kb AluI-resistant DNA was hybridized *in situ* with
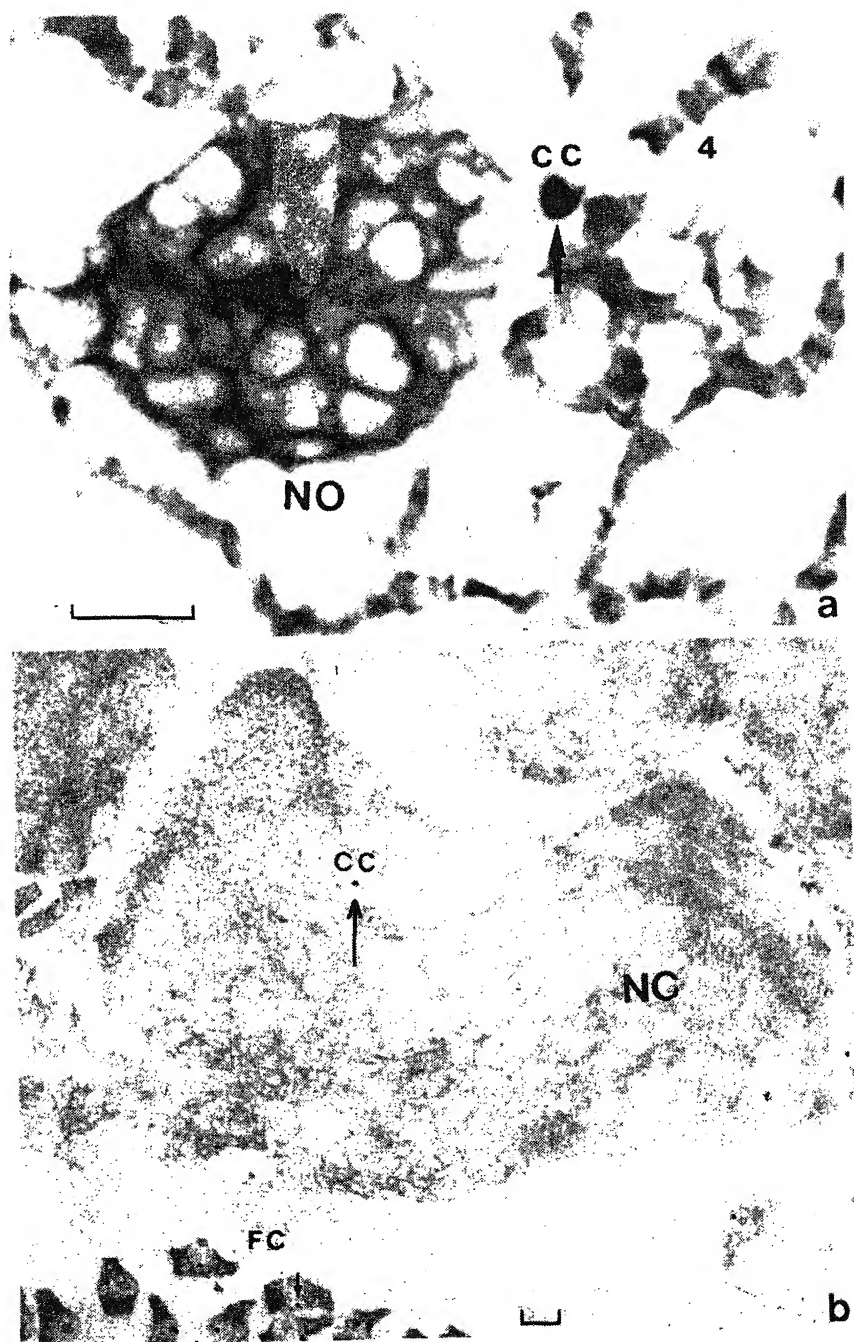
Figure 2. (a) Part of an AluI digested polytene nucleus showing intense staining of the α-heterochromatin (arrow) and of two bands on chromosome 4 (NO = nucleolus). (b) AluI treated large nurse cell (NC) and a group of follicle cells (FC) from adult ovary. Arrow marks the small chromocentre in the highly endoreplicated nurse cell.
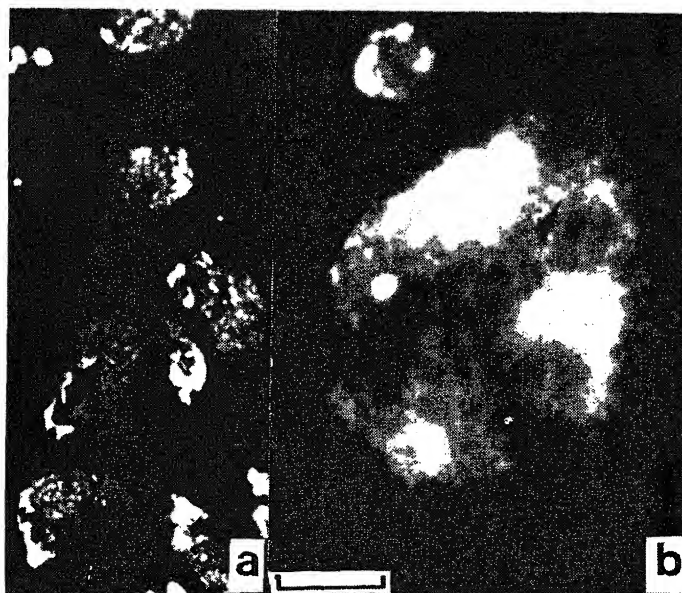
Figure 3. Hoechst 33258 fluorescence stained nuclei from (**a**) early embryos and (**b**) adult ovarian nurse and follicle cells.

brain cell nuclei of *D. nasuta*, the hybridization was more or less restricted to the heterochromatic chromocentre region only (figure 5).

4. Discussion

The effect of restriction enzymes on the fixed chromosome preparations have been variously ascribed to be primarily due to chromatin conformation or to the distribution of the recognition sites for those enzymes in the genome or to both (reviewed by Miller and Miller 1990). However, the view that the availability of recognition sequences play a more important role in the production of restriction bandings, has received significant support from various studies. In the present study, except SalI and TaqI, none of the other restriction enzymes tested affected Giemsa stainability of any of the heterochromatin blocks in cytological preparations of *D. nasuta*, although all euchromatin regions were severely affected. This refractoriness of heterochromatin to the action of these enzymes could be due either to particular properties of chromatin structure and organization of heterochromatin which did not allow action of these enzymes or to the absence of recognition sites for these enzymes in the DNA sequences comprising heterochromatin in *D. nasuta*. Although the first alternative cannot be ruled out, the latter possibility appears more likely in view of the earlier reports in literature (Miller *et al* 1983; Bianchi *et al* 1985; Babu 1988; Lopez-Fernandez *et al* 1989) and our following observations: (i) While AluI did not affect heterochromatin in any of the cell types (interphase cells in embryo or brain ganglia; mitotic cells in larval brain; polytene nuclei in larval salivary glands and polyploid nuclei in ovarian follicle and
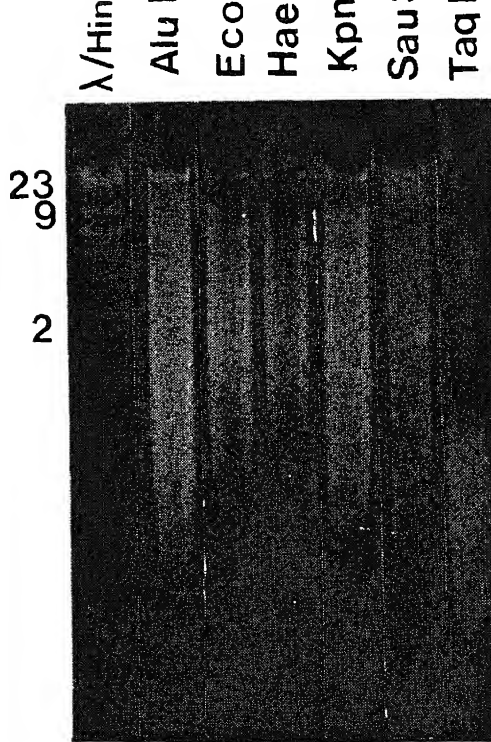
Figure 4. Ethidium bromide staining of genomic DNA of *D. nasuta* digested with different enzymes indicated.

Molecular weights (in kb) of some of the marker bands in HindIII digested λ-DNA lane are indicated. Note the bright band at the top in all genomic DNA lanes except TaqI.

nurse cells), SalI and TaqI appeared to readily affect heterochromatin regions of mitotic cells; thus the condensed heterochromatin regions were not totally refractory to loss of chromicity following restriction endonuclease digestion *in situ.* (ii) A high molecular weight DNA band was left undigested in purified genomic DNA of *D. nasuta* by all those enzymes that also did not affect heterochromatin staining *in situ* while enzymes like TaqI which digested heterochromatin, also did not leave a high molecular weight DNA band in gels. (iii) The specific *in situ* hybridization of the gel purified high molecular weight AluI resistant DNA with chromocentre heterochromatin showed that the heterochromatin of *D. nasuta* contains DNA sequences that do not have or have only infrequent sites for AluI. In a recent detailed study on the mechanism of action of restriction enzymes on fixed and unfixed mammalian metaphase chromosomes, Burkholder (1989) found that while digestion with certain restriction enzymes was influenced to some extent by local chromatin organization, the effects produced by enzymes like AluI, HaeIII, etc., reflected the distribution of restriction sites along the chromosomal DNA. Therefore, in all likelihood the C-band effect of AluI and the other restriction
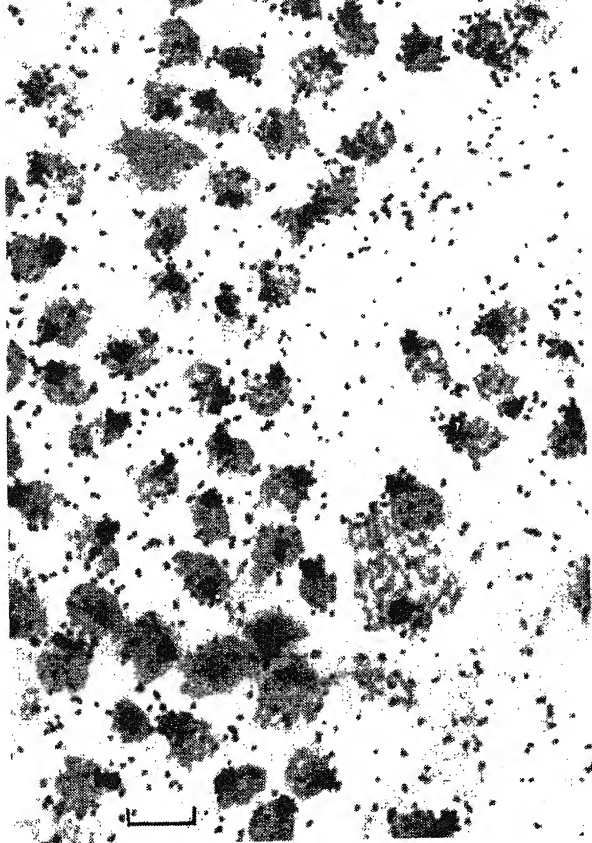
Figure 5. *In situ* hybridization of the 23 kb AluI-resistant DNA with larval brain nuclei.

enzymes seen in this study is due to the DNA sequences in heterochromatin of *D. nasuta* being poor in recognition sites for the enzymes.

Cytologically, the heterochromatin content in *D. nasuta* chromosomes is about 40% of chromosome length (Lakhotia and Kumar 1978) while the single satellite sequence was reported (Ranganath *et al* 1982) to be only about 7–8% of *D. nasuta* genome. If this is indeed so, much of the heterochromatin in *D. nasuta* should be comprised of other non-satellite DNA sequences. In the light of present results it would therefore appear that sites for enzymes like AluI are infrequent in these non-satellite DNA sequences too and that these sequences are more or less uniformly distributed in different blocks of heterochromatin in the population of *D. nasuta* studied by us. The content and distribution of heterochromatin is known to vary intra- as well as inter-specifically in different members of the *D. nasuta* subgroup of species (Ranganath *et al* 1982; Hatsumi *et al* 1988). Application of *in situ* restriction digestion in these instances is expected to help in understanding the basis of polymorphism in heterochromatin content in this group of species.

Satellite and highly repetitive sequences comprising heterochromatin are known to be underreplicated in endoreplicating cells of *Drosophila* (see Spradling and Orr-

the AluI-resistant heterochromatic chromocentre in highly polytenized salivary gland nuclei as well as in the endoreplicating follicle and nurse cells was found to be small. Hammond and Laird (1985) compared the extent of underreplication and the spatial organization of satellite and certain other repetitive sequences in these three cell types of *D. melanogaster* and concluded that in the follicle cells which undergo only 2–3 endoreplication cycles, the satellite DNA sequences remain at 2C level while in the highly endoreplicated nurse cells, the satellite sequences replicate in later endoreplication cycles. These authors also concluded that in the nurse cells, the satellite sequences associated with different heterochromatin blocks are not as tightly held together as in salivary gland polytene nuclei and in rare cases may even be widely separated so that a compact chromocentre perhaps does not exist in nurse cells of *D. melanogaster*. Our present results revealed a different organization of heterochromatin in follicle and nurse cells of *D. nasuta*. The AluI-resistant dark-stained chromocentre in the very highly endoreplicated large nurse cells was as small as in the follicle or early embryonic cells. Moreover, like in embryonic, brain or follicle cells, the AluI-resistant chromocentre was always a single compact block in the ovarian nurse cells of *D. nasuta*, suggesting that the pericentromeric heterochromatin blocks of different chromosomes of *D. nasuta* were as tightly associated with each other as in typical polytene or mitotic cell types. The differences in the spatial organization of heterochromatin in ovarian nurse cells of *D. melanogaster* (Hammond and Laird 1985) and in *D. nasuta* (present results) may be related to the fact that while the heterochromatin in *D. melanogaster* is comprised of more than one type of satellite sequences (Lohe and Roberts 1988), the DNA sequences in heterochromatin of *D. nasuta* are, as noted above, much more similar and thus may condense together. Hammond and Laird's (1985) use of *in situ* hybridization to monitor the quantity (extent of endoreplication) and spatial distribution of heterochromatin would detect the satellite sequences present in the euchromatin domains also. Thus the information obtained cannot be directly correlated to chromocentre. In our case, the cytological identity of chromocentre is very distinct leaving no scope for such ambiguity. Indeed, using Hoechst 33258 fluorescence to locate heterochromatin, we found the chromocentre in ovarian nurse cells of *D. nasuta* to be organized more or less as compactly as in the other cell types.

None of the restriction enzymes used in our study produced any banding pattern in the euchromatin regions of mitotic chromosomes although a majority of these enzymes are known to produce G- or R-bands in mammalian metaphase chromosomes (Babu 1988). Mitotic chromosomes of *Drosophila* do not show G-bands or replication bands also (Holmquist 1989; Raman and Lakhotia 1990). The absence of restriction enzyme-induced banding of mitotic chromosomes of *Drosophila* further supports the view that the functional and higher order organization of mitotic chromosomes is different in *Drosophila* and mammals (Raman and Lakhotia 1990).

Babu A 1988 Heterogeneity of heterochromatin of human chromosomes as demonstrated by restriction endonuclease treatment; in *Heterochromatin-molecular and structural aspects* (ed.) R S Verma (Cambridge: Cambridge University Press) pp 250–275

Bianchi M S, Bianchi N O, Pantelias G E and Wolff S 1985 The mechanism and patterns of banding induced by restriction endonucleases in human chromosomes; *Chromosoma* 91 131–136

Burkholder G D 1989 Morphological and biochemical effects of endonucleases on isolated mammalian chromosomes *in vitro*; *Chromosoma* 98 347–355

Hammond M P and Laird C D 1985 Chromosome structure and DNA replication in nurse and follicle cells of *Drosophila melanogaster*; *Chromosoma* 91 279–296

Hatsumi M, Morishige V and Wakahama K I 1988 Metaphase chromosomes of four species of the *Drosophila nasuta* subgroup; *Jpn. J. Genet.* 63 435–444

Holmquist G P 1989 Evolution of chromosome bands: molecular ecology of noncoding DNA; *J. Mol. Evol.* 28 469–486

Kumar M and Lakhotia S C 1977 Localization of non-replicating heterochromatin in polytene cells of *Drosophila nasuta* by fluorescence microscopy; *Chromosoma* 59 301–305

Lakhotia S C 1984 Replication in *Drosophila* chromosomes. XII. Reconfirmation of under replication of heterochromatin in polytene nuclei by cytofluorometry; *Chromosoma* 89 63–67

Lakhotia S C and Kumar M 1978 Heterochromatin in mitotic chromosomes of *Drosophila nasuta*; *Cytobios* 21 79–89

Lakhotia S C and Roy J K 1981 Effect of Hoechst 33258 on condensation patterns of hetero- and euchromatin in mitotic and interphase nuclei of *Drosophila nasuta*; *Exp. Cell. Res.* 132 423–431

Lakhotia S C and Roy J K 1983 Effects of distamycin A and netropsin on condensation of mitotic chromosomes in early embryos and larval brain cells of *Drosophila*; *Indian J. Exp. Biol.* 21 357–362

Lakhotia S C and Roy S 1979 Replication in *Drosophila* chromosomes. I. Replication of intranucleolar DNA in polytene cells of *D. nasuta*; *J. Cell Sci.* 36 185–197

Lakhotia S C, Roy J K and Kumar M 1979 A study of heterochromatin in *Drosophila nasuta* by the 5-bromodeoxyuridine-Giemsa staining technique; *Chromosoma* 72 249–255

Lima-de-Faria A, Isaksson M and Olsson E 1980 Action of restriction endonuclease on the DNA and chromosomes of *Muntiacus muntjak*; *Hereditas* 92 267–273

Lohe A and Roberts P 1988 Evolution of satellite DNA sequences in *Drosophila*; in *Heterochromatin—molecular and structural aspects* (ed.) R S Verma (Cambridge: Cambridge University Press) pp 148–156

Lopez-Fernandez C, Gosalvez J, Suja J A and Mezzanotte R 1989 Restriction endonuclease digestion of meiotic and mitotic chromosomes in *Pyrgomorpha conica* (Orthoptera, Pyrogomorphidae); *Genome* 30 621–626

Maniatis T, Fritsch E F and Sambrook J 1983 *Molecular cloning. A laboratory manual* (Cold Spring Harbor: Cold Spring Harbor Laboratory)

Mezzanotte R 1986 The selective digestion of polytene and mitotic chromosomes of *Drosophila melanogaster* by the AluI and HaeIII restriction endonucleases; *Chromosoma* 93 249–255

Mezzanotte R, Manconi P E and Ferruci L 1986 On the possibility of localizing *in situ Mus musculus* and *Drosophila virilis* satellite DNAs by AluI and EcoRI restrict endonucleases; *Genetica* 70 107–111

Miller D A, Choi J C and Miller O J 1983 Chromosome localization of highly repetitive human DNAs and amplified ribosomal DNA with restriction enzymes; *Science* 219 395–397

Miller D A and Miller O J 1990 Restriction enzyme banding of metaphase chromosomes; in *Trends in chromosome research* (ed.) T Sharma (Berlin: Springer-Verlag and New Delhi: Narosa) pp 238–250

Pardue M L 1986 In situ hybridization to DNA of chromosomes and nuclei; in *Drosophila — a practical approach* (ed.) D B Robberts (Oxford, Washington: IRL Press) pp 111–137

Raman R and Lakhotia S C 1990 Comparative aspects of chromosome replication in *Drosophila* and mammals; in *Trends in chromosome research* (ed.) T Sharma (Berlin: Springer-Verlag and New Delhi: Narosa) pp 69–89

Ranganath H A, Schmidt E R and Hagele K 1982 Satellite DNA of *Drosophila nasuta* and *D. n. albomicana*: localization in polytene and metaphase chromosomes: *Chromosoma* 85 361–368

Spradling A and Orr-Weaver T 1988 Regulation of replication during *Drosophila* development; *Annu. Rev. Genet.* 21 373–403

Differential reactivity of filarial antigens with human sera from bancroftian filariasis endemic zone

K CHEIRMARAJ, M V R REDDY and B C HARINATH*

Department of Biochemistry, Mahatma Gandhi Institute of Medical Sciences, Sevagram 442 102, India

Abstract. The reacting pattern of circulating filarial antigen fraction-2 from *Wuchereria bancrofti* and soluble antigen from adult *Brugia malayi* with bancroftian filarial sera were analysed by immunoblotting technique and enzyme linked immunosorbent assay. Microfilaraemic sera reacted specifically with proteins of molecular weight 200, 120, 97, 56, 54, 43, 26 and 17 kDa of circulating filarial antigen fraction-2 and 44, 40, 38, 31, 22 and 18 kDa of *Brugia malayi* adult soluble antigen. Clinical filarial sera identified protein molecules of 56, 54 and 42 kDa of circulating filarial antigen fraction-2 and 19, 16 and 14 kDa of *Brugia malayi* adult soluble antigen. Some components of both the antigen preparation were also identified by endemic normal sera *i.e.*, proteins 120, 97, 62, 43 and 33 kDa of circulating filarial antigen fraction-2 and 170, 120, 43, 31 and 12 kDa of *Brugia malayi* adult soluble antigen. One of the sodium dodecyl sulphate-polyacrylamide gel electropherosis fractions of circulating filarial antigen fraction-2 (CFA_2-8) and *Brugia malayi* adult soluble antigen fraction-6 when used in enzyme linked immunosorbent assay could differentiate microfilaraemic sera from endemic normal and clinical filarial sera. The other antigen fractions (CFA_2-2, 6 and 7 and *BmA*-2) showed a high geometric mean titre of filarial immunoglobulin G antibodies in endemic normal sera when compared to microfilaraemia and clinical filarial sera. These proteins need to be further studied to assess their involvement in protecting from filarial infection in an endemic area.

Keywords. *Wuchereria bancrofti*; *Brugia malayi*; filarial antigens; diagnosis; SDS-PAGE; ELISA.

1. Introduction

Bancroftian filariasis is characterized by a wide spectrum of responses to the causative organism *Wuchereria bancrofti*. In an endemic area, a majority of the population does not have microfilariae or clinical symptoms of the disease. This group which has more or less the same degree of exposure to infection as the other infected groups is apparently immune. A small proportion are microfilaraemic; the majority of this group are asymptomatic. Some individuals develop clinical manifestations *viz.*, elephantiasis of limbs, hydrocele etc. Since this clinical spectrum may reflect the diversity in the host's immune response to the infection, analysis of sera of endemic population for filarial antibodies will be useful for stage specific diagnosis and for recognizing immune protective antigens.

Circulating filarial antigen fraction-2 (CFA_2) isolated from microfilaraemic plasma has been demonstrated to be a candidate antigen for use in the diagnosis of

---

(Kazura *et al* 1986; Maizels *et al* 1985; Freedman *et al* 1989; Parab *et al* 1990). Among *B. malayi* antigens, adult worm antigen appeared to be more discriminatory and more specific than antigens from other stages for the detection of filarial antibody (Kaushal *et al* 1984). Lammie *et al* (1990) reported that the humoral immune response was significantly greater to detergent extracted antigens of *B. pahangi* adult worms than to soluble antigenic preparation. Moreover, the surface components may be recovered by sodium dodecyl sulphate (SDS) solublization. The use of surface antigens in serology is logical, since they are the first antigens encountered by the host during infection and the host immune mechanisms probably operate primarily at the parasite surface. Earlier studies showed that antibody raised against *B. malayi* adult SDS extracted antigen proved to be more sensitive in the detection of circulating filarial antigen in bancroftian filarial sera than the antibody to saline-extracted antigen of *B. malayi* (Cheirmaraj *et al* 1990).

The present communication reports a comparative study on the reactive patterns of different groups of filarial endemic sera with CFA_2 and *B. malayi* adult SDS-soluble antigen using the techniques of western blotting analysis and enzyme linked immunosorbent assay (ELISA).

2. Materials and methods

2.1 *Sera samples*

Human sera belonging to different groups *viz.*, normal (endemic and non-endemic) and filarial (microfilaraemia and clinical filariasis) were screened. Filarial blood samples were collected from Sevagram and surrounding villages, which are endemic for nocturnally periodic *W. bancrofti*. The presence of microfilariae was tested by night blood (wet smear) examination. Clinical filarial samples were from individuals with manifestations such as hydrocele, swelling of limbs and elephantiasis. Endemic normal samples were from the healthy individuals living in endemic region for over 5 years having no history of filariasis. Non-endemic normal samples were collected from students coming to this Institute from places like Chandigarh and Kashmir where there is no filariasis. Sera were separated from blood samples and stored at $-20°C$ with sodium azide as preservative.

2.2 CFA_2

CFA was prepared from pooled plasma of microfilaraemic patients (after separation of microfilariae) by 36–75% saturation with ammonium sulphate and further fractionated on ultrogel ACA 34 gel column as described by Reddy *et al* (1986). The fractions of the second protein peak showing filarial antigen were pooled, concentrated by membrane filtration and labelled as CFA_2.

from the peritoneal cavity of jirds, *Meriones unguiculatus*, were homogenized and extracted with phosphate buffer saline (PBS, 0·05 M, pH 7·2) overnight at 4°C. Proteins soluble in PBS were recovered by centrifugation and the pellets were suspended in 5% SDS, 5% 2-mercaptoethanol and 8 M urea in 0·01 M sodium phosphate buffer (SPB, pH 7·2) and extracted overnight at 4°C. The SDS soluble fraction was recovered by centrifugation (15,000 g) at 4°C for 30 min and the supernatant was separated, dialysed and labelled as SDS soluble antigen (*BmA* SDS-S Ag). The protein was estimated by the method of Lowry et al (1951).

2.4 Western blot analysis

The reactivity of filarial antigens with different groups of sera was analysed by immunoblotting technique. In brief, the filarial antigens CFA$_2$ and *BmA* SDS-S Ag (200 μg each) were resolved by SDS-polyacrylamide gel electrophoresis (PAGE) on 10% non-gradient slab gel (12 × 12 cm) as described earlier (Kharat et al 1989). The antigen components were electrophoretically transferred onto nitrocellulose paper (BA 85 of Scleicher and Schuell AG, Switzerland) with 0·6 amps current for 90 min at 4°C as described by Towbin et al (1979). The nitrocellulose sheet was then blocked with 5% skimmed milk powder in 0·05 M PBS, pH 7·2 for 1 h at 37°C followed by washing with 2% SMP in PBS for 5 times. The blot was then cut into strips of 5 mm width. The strips were incubated separately with optimally diluted (1:100) sera of different groups and the bound antibodies were probed with anti human IgG-peroxidase conjugate. The substrate consisted of 3, 3'-diamino benzidine (0·05%) in 0·25 M PBS, pH 7·2 and hydrogen peroxide (0·003%). The standard molecular weight proteins (Sigma Chemical Co., USA) were used in SDS-PAGE to determine the molecular weights of reactive proteins in the antigens.

2.5 Gel elution

In another experiment, the SDS-PAGE gels were sliced horizontally (into 12 slices) at 1 cm intervals and each slice was subjected to mechanical grinding to elute protein into 5 ml of 0·05 M SPB, pH 7·2 (Guellaen et al 1984). The eluates of 12 fractions were dialyzed against excess buffer, concentrated and protein concentration was estimated (Lowry et al 1951). These fractions were used in indirect ELISA to analyse their reactivity with different groups of filarial sera.

2.6 Indirect stick ELISA

The assay was done as described earlier (Parkhe et al 1990) using cellulose acetate membrane fixed plastic sticks coated with optimal concentrations (5 ng) of antigen fractions as sorbent material. Optimal (1:300) and serial two-fold dilutions of sera of different groups were analysed for filarial antibodies. Anti human IgG (Lupin Laboratories, India) was conjugated to enzyme penicillinase (Sigma Chemical Co.,

with 10·64 mg penicillin V and 100 μl of 0·08 M iodine in 3·2 M potassium iodide.

3. Results

In SDS-PAGE, under reduction conditions, CFA_2 showed 21 protein bands (Parkhe *et al* 1990) and *Bm*A SDS-S Ag showed 22 protein bands with molecular weights ranging from 12 kDa to $\geqslant$ 160 kDa (figure 1). Immunoblot analysis of CFA_2 and *Bm*A SDS-S Ag with sera of different groups of endemic residents showed polydispersed nature of both antigenic preparations. In this technique, none of the proteins were recognized by pooled non-endemic normal serum. The sera of endemic residents identified proteins of M_r 160, 140, 78, 66, 37 and 35 kDa of CFA_2 and 200, 140, 100, 80, 63 and 55 kDa of *Bm*A SDS-S Ag. In addition to these, microfilaraemic sera recognized proteins of M_r 200, 120, 97, 56, 54, 43, 26 and 17 kDa of CFA_2 and 44, 40, 38, 31, 22 and 18 kDa of *Bm*A SDS-S Ag (figure 2).
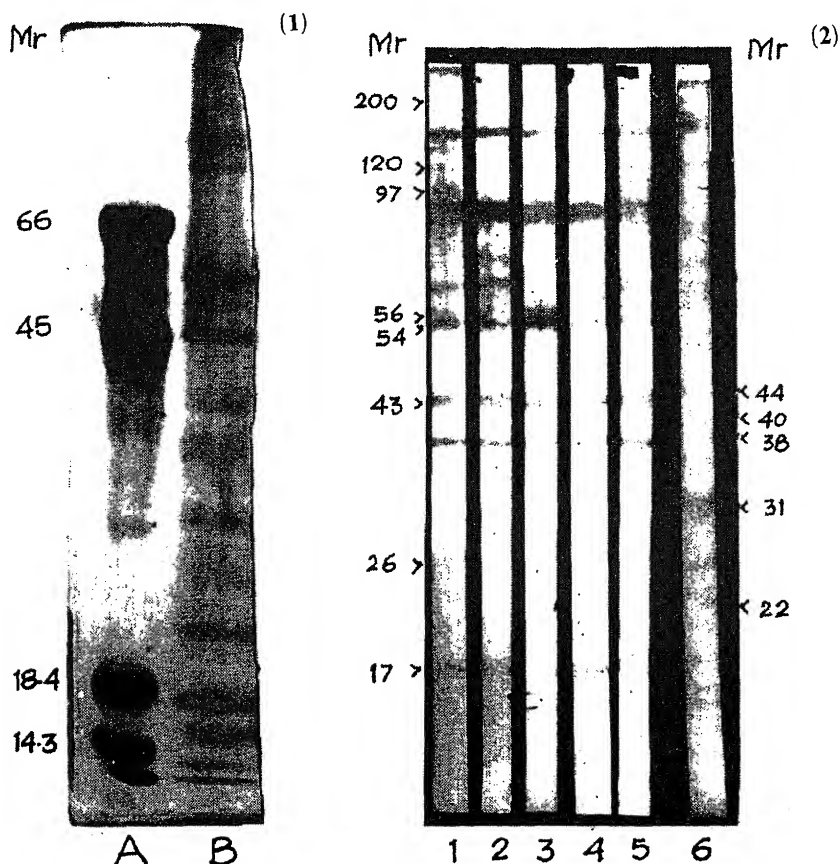
Figure 1 and 2. 1. SDS-PAGE pattern of *B. malayi* adult soluble antigen (*Bm*A SDS-S Ag) (B) and molecular weight markers (A). 2. Recognition of CFA_2 and *Bm*A SDS-S Ag by microfilaraemic sera. Lanes 1–5 individual microfilaraemic sera with CFA_2 and lane 6 pooled microfilaraemic serum with *Bm*A SDS-S Ag.

the antigenic molecules recognized selectively by the endemic normal, micro-filaraemic or clinical filarial sera in blotting studies and the results are shown in figures 5 and 6 respectively. The three SDS-PAGE fractions of CFA_2 viz., CFA_2-2. 6 and 7 (bearing the antigenic molecules of 120, 97, 43 and 33 kDa) showed a higher geometric mean titres of filarial IgG antibodies in endemic normal sera (476, 648 and 688 respectively) compared to microfilaraemic (300, 344 and 300 respectively) and clinical filarial sera (280, 424 and 321 respectively, table 1). CFA_2-8 fraction (with antigenic molecule of 26 kDa) showed higher titres of filarial IgG antibodies (791) in microfilaraemic sera compared to endemic normal
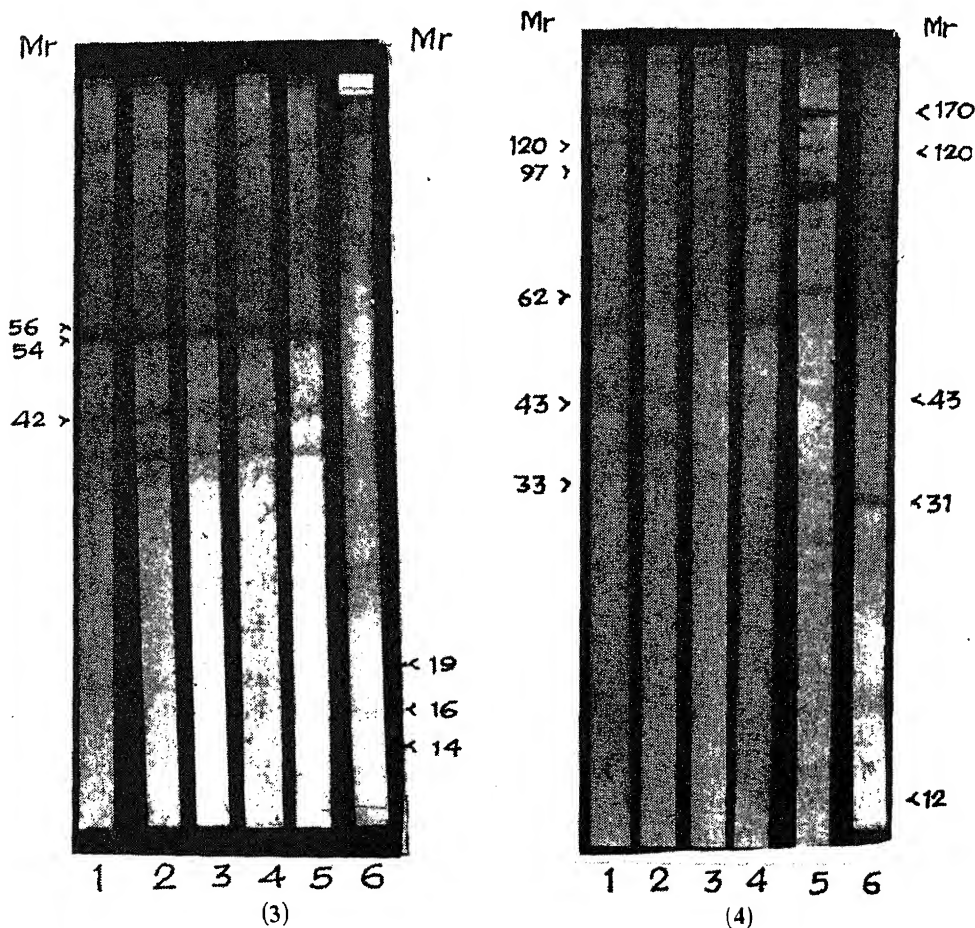
Figures 3 and 4. Recognition of CFA_2 and BmA SDS-S Ag by clinical filarial sera (3) and sera of endemic normals (4). Lanes 1-5 individual clinical filarial sera (3) and endemic normal sera (4) with CFA_2 and lane 6 pooled clinical filarial (3) and endemic normal (4) serum with BmA SDS-S Ag.
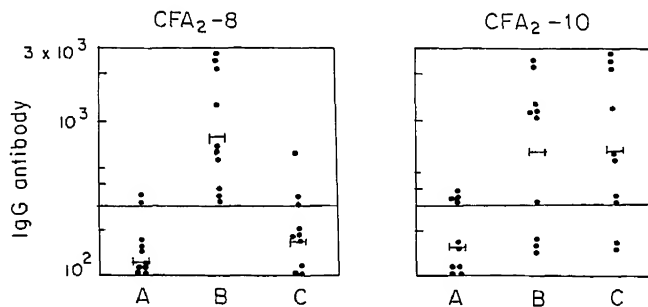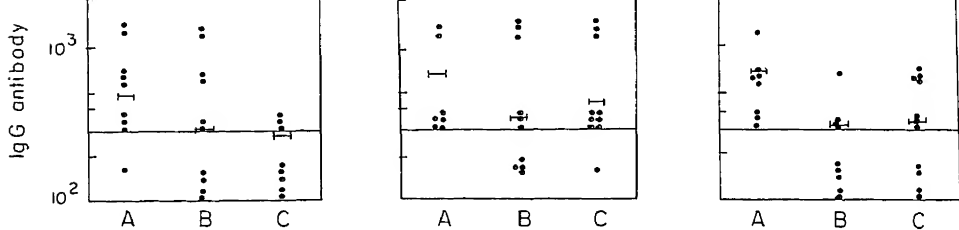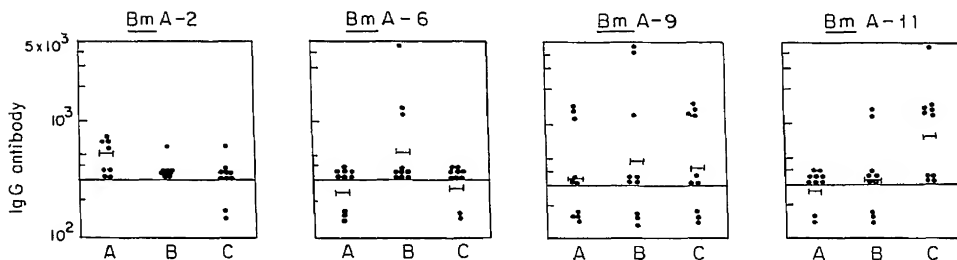
Figures 5 and 6. Filarial antibody levels in sera samples of endemic normals (A), microfilaraemics (B) and clinical filarial (C) patients against CFA$_2$ (5) and *Bm*A SDS-S Ag (6) fractions. Sera dilution at 1:300 was the threshold level for positivity. Horizontal bars represent geometrical mean titre of antibody.

(121) and clinical filarial sera (161) and the difference was statistically significant ($P < 0.01$) by student's t test. CFA$_2$-10 fraction (with antigenic molecule of 17 kDa) showed higher titres of filarial IgG antibodies in microfilaraemic and clinical filarial sera (642 in each group) compared to endemic normal sera (150) and the difference was significant ($P < 0.01$ for Mf *vs* EN and $P < 0.05$ for Ch *vs* EN) by student's t test.

With *Bm*A SDS-S Ag fraction, *Bm*A-2 fraction (bearing the antigenic molecule of 120 kDa) showed higher titres of filarial IgG antibodies in endemic normal sera (522) compared to microfilaraemic (344) and clinical filarial sera (300, table 2). *Bm*A 6 and 9 fractions (having the antigenic molecules of 44, 40, 38 and 22 kDa) showed higher titres of filarial IgG antibodies in microfilaraemic sera

Group	GMT of filarial IgG antibody				
	CFA$_2$-2 (95–160)[a]	CFA$_2$-6 (37–45)[a]	CFA$_2$-7 (31–37)[a]	CFA$_2$-8 (25–31)[a]	CFA$_2$-10 (17–20)[a]
Non-endemic normal	—	—	—	—	—
Endemic normal	476 (89%)	648 (100%)	688 (100%)	121 (20%)	150 (40%)
Micro-filaraemia	300 (60%)	344 (60%)	300 (50%)	791 (100%)	642 (70%)
Clinical filariasis	280 (50%)	424 (90%)	321 (60%)	161 (30%)	642 (80%)

[a]Molecular weight range in kDa.
The percentage of positivity in each group is given in parenthesis (the sera dilution at 1:300 was taken as the threshold level for positivity).

Table 2. Geometric mean of filarial IgG antibody titres in different groups of endemic sera using *Bm*A SDS-S Ag — SDS-PAGE fractions.

Group	GMT of filarial IgG antibody			
	*Bm*A-2 (95–160)[a]	*Bm*A-6 (37–45)[a]	*Bm*A-9 (20–25)[a]	*Bm*A-11 (14–17)[a]
Non-endemic normal	—	—	—	—
Endemic normal	522 (100%)	243 (70%)	344 (60%)	261 (80%)
Micro-filaraemia	344 (100%)	522 (100%)	487 (70%)	321 (70%)
Clinical filariasis	300 (80%)	261 (80%)	424 (70%)	791 (100%)

[a]Molecular weight range in kDa.
The percentage of positivity in each group is given in parenthesis (the sera dilution at 1:300 was taken as the threshold level for positivity).

(522 and 487 respectively) compared to endemic normal (243 and 344 respectively) and clinical filarial sera (261 and 424 respectively). *Bm*A-11 fraction (with the antigenic molecules of 16 and 14 kDa) showed higher titres of filarial IgG antibodies in clinical filarial sera (791) compared to endemic normal (261) and microfilaraemic sera (321). Unfractionated whole *Bm*A SDS-S Ag detected high titres of filarial IgG antibodies in microfilaraemic sera (3393) compared to clinical filarial (700) and endemic normal sera (300).

4. Discussion

In an endemic area for bancroftian filariasis a majority of inhabitants are apparently immune to infection; while a few carry microfilariae in circulation, still

having protective and diagnostic importance. This communication reports analysis of different groups of sera for filarial antibodies using an *in vivo* released filarial antigen (CFA_2) and a heterologous antigen (*BmA* SDS-S Ag) having extensive antigen sharing with *W. bancrofti*.

In western blot analysis of CFA_2, while the non-endemic normal sera did not show any reactivity, the sera of endemic region identified in common several antigenic molecules with the molecular weight in the range of 12 to $\geqslant 160$ kDa. This is expected as all the endemic population is repeatedly exposed to parasitic antigens (Ottesen *et al* 1982). In addition, each of the 3 groups of endemic sera *i.e.*, microfilaraemic, clinical filarial and normal sera identified specifically some proteins. The microfilaraemic sera reacted with bands of M_r 200, 120, 97, 56, 54, 43, 26 and 17 kDa whereas clinical filarial sera reacted with 56, 54 and 42 kDa. Forsyth *et al* (1985) demonstrated filarial antigens of M_r 140, 62, 56 and 52 kDa in sera of filarial patients reacting with Gib 13 monoclonal antibody. Lal *et al* (1987) demonstrated 3 bands with apparent M_r 200, 160 and 78 kDa as the target antigens of CA 101 monoclonal antibody in the circulation of infected filarial patients. Using rabbit anti *BmA* antibodies a high molecular weight antigen ($\simeq 200$ kDa) was recognized in bancroftian filarial sera (Paranjape *et al* 1986; Lunde *et al* 1988). Two protein bands of M_r 67 and 52 kDa was recognized by Gib 13 monoclonal antibody in *W. bancrofti* infected patients (Dissanayake *et al* 1984). Antibodies from human cases of *W. bancrofti* recognized antigens of apparent M_r 59, 51, 34 and 17 kDa in *W. bancrofti* L_3 somatic antigens and 51, 21 and 17 kDa antigen in *Wb* L_3 ES antigens (Maizels *et al* 1986).

With *BmA* SDS-S Ag, microfilaraemic sera reacted with proteins of M_r 44, 40, 38, 31, 22 and 18 kDa and clinical filarial sera reacted with proteins of 19, 16 and 14 kDa. Parab *et al* (1990) showed that microfilaraemic sera reacted with 22, 43, 50, 54, 56, 66, 73, 79 and 88 kDa proteins and chronic sera reacted with 25, 38, 43, 56, 58, 62, 68, 79, 86 and 92 kDa proteins of *B. malayi* mf soluble antigens.

The antigens recognized by microfilaraemic sera particularly 26 and 17 kDa of CFA_2 and 44, 40 and 38 kDa of *BmA* SDS-S Ag may be used as a candidate antigen to differentiate active infection. To confirm this indirect ELISA was carried out to detect the antibodies in all the 3 categories of endemic sera using non-endemic normal sera as a control. The CFA_2-8 fraction (M_r range 25–31 kDa) and *BmA*-6 fraction (M_r range 37–45 kDa) detected antibodies in all the 10 microfilaraemic samples (100%) with high antibody titre when compared to chronic and endemic normal samples. Earlier studies from our laboratory reported that whole CFA_2 detects IgG antibodies in 50% of microfilaraemic samples and 70% of clinical filarial cases (Reddy *et al* 1986) and CFA_2-9 fraction detects IgG antibodies in 60% of microfilaraemics and 73% of clinical filarial cases (Parkhe *et al* 1990).

In immunoblots, endemic normal sera identified antigens of 120, 97, 62, 43 and 33 kDa of CFA_2 and 170, 120, 43, 31 and 12 kDa proteins of *BmA* soluble antigens. The antigens recognized by these putatively immune, infection free individuals (Freedman *et al* 1989) may be involved in the induction of immunity to filarial infection. There is no significant study to demonstrate the existence of protective immunity in 80–90% of endemic normal population except the reports on the presence of cytotoxic antibodies against microfilariae and infective larvae demonstrated by *in vitro* serum dependent cell-mediated cytotoxicity (Subrahmanyam

normals are able to differentiate the endemic normal population from those of microfilaraemic and clinical filarial cases, we carried out indirect ELISA with the fractionated antigens such as CFA_2-2, 6 and 7 and BmA-2. All these fractions detected high antibody levels with 80–100% positivity in endemic normal sera compared to microfilaraemic and chronic sera. Freedman *et al* (1989) showed that a 43 kDa antigen derived from *B. malayi* infective larvae was recognized by endemic normal sera. Amicrofilaraemic human sera had a significantly higher mean antibody titre to 25 kDa antigen of *B. malayi* microfilariae extract (Kazura *et al* 1986). Parab *et al* (1990) suggested that the proteins of M_r 25, 58 and 68 kDa of *B. malayi* mf which reacts with EN and chronic sera may be the candidate antigens to be analysed as protective immunogens. A major antigen of 97 kDa shared by both microfilariae and adult worms of *B. malayi* induced partial resistance to *B. malayi* microfilariae in mice and it was found to be paramyosin the invertebrate muscle protein (Nanduri and Kazura 1989). SDS-extraction of *B. malayi* adult worms yielded antigens at the molecular mass of > 200, 170 to 200, 40 to 44, 33 to 36, 23 to 28, 20 to 22 and 17 to 19 kDa which induced protection in Balb/c mice against challenge with *B. malayi* infective larvae (Hammerberg *et al* 1989). Aggarwal *et al* (1985) identified a microfilarial surface antigen of M_r 110 kDa, reacting with a monoclonal antibody which induce the clearance of microfilariae from circulation in mice on passive immunization. This study reports the usefulness of the antigens (26 kDa of CFA_2 and 44, 40 and 38 kDa of BmA S-Ag) in differentiating microfilaraemics from clinical filarial and endemic normal individuals. Further, antigen recognized by endemic normal sera (120, 97, 43 and 33 kDa of CFA_2 and 120 kDa of BmA-S Ag) may be the candidate antigens requiring further purification and testing as protective immunogens in animal models and by the appropriate cellular immunological studies.

Acknowledgements

References

Aggarwal A, Cuna W, Haque A, Dissous C and Capron A 1985 Resistance against *Brugia malayi* microfilariae induced by a monoclonal antibody which promotes killing by macrophages and recognizes surface antigen(s); *Immunology* **54** 655–663

Avrameas S 1969 Coupling of enzymes to proteins with glutaraldehyde — use of conjugates for the detection of antigens and antibodies; *Immunochemistry* **6** 43–52

Cheirmaraj K, Reddy M V R and Harinath B C 1990 Diagnostic use of polyclonal antibodies raised in mouse ascitic fluid in bancroftian filariasis; *J. Immunoassay* **11** 429–444

Dissanayake S, Forsyth K P, Ismail M M, Mitchell G F 1984 Detection of circulating antigen in bancroftian filariasis by using a monoclonal antibody; *Am. J. Trop. Hyg.* **33** 1130–1140

Forsyth K P, Spark R, Kazura J, Brown C V, Peters P, Heywood P, Dissanayake S and Mitchell G F 1985 A monoclonal antibody based immuno-radiometric assay for detection of circulating antigen in bancroftian filariasis; *J. Immunol.* **134** 1172–1177

Freedman D O, Nutman T B and Ottesen E A 1989 Protective immunity in bancroftian filariasis. Selective recognition of a 43 kD larval stage antigen by infection-free individuals in an endemic area; *J. Clin. Invest.* **83** 14–22

purification procedures (eds) J Craigventer and L Harrison (New York: Alan R Liss) Vol. 2, pp 109–124

Hammerberg B, Nogami S, Nakagaki K, Hayashi Y and Tanaka H 1989 Protective immunity against *Brugia malayi* infective larvae in mice. II. Induction by a T cell-dependent antigen isolated by monoclonal antibody affinity chromatography and SDS-PAGE; *J. Immunol.* **143** 4201–4207

Kaushal N A, Hussain R and Ottesen E A 1984 Excretory-secretory and somatic antigens in the diagnosis of human filariasis; *Clin. Exp. Immunol.* **56** 567–576

Kazura J W, Cicirello H and Forsyth K 1986 Differential recognition of a protective filarial antigen by antibodies from humans with bancroftian filariasis; *J. Clin. Invest.* **77** 1985–1992

Kharat I, Cheirmaraj K, Prasad G B K S and Harinath B C 1989 Antigenic analysis of excretory-secretory products of *Wuchereria bancrofti* and *Brugia malayi* infective larval forms by SDS-PAGE; *Indian J. Exp. Biol.* **27** 681–684

Lal R D, Paranjape R S, Briles D E, Nutman T B and Ottesen E A 1987 Circulating parasite antigen(s) in lymphatic filariasis: Use of monoclonal antibodies to phosphocholine for immunodiagnosis; *J. Immunol.* **138** 3454–3460

Lammie P J, Eberhard M L and Lowrie R C Jr 1990 Differential humoral and cellular immuno-reactivity to saline and detergent extracted filarial antigens; *Trans. R. Soc. Trop. Med. Hyg.* **84** 407–410

Lowry O H, Rosebrough N J, Farr A L and Randall R J 1951 Protein measurement with the Folin-phenol reagent; *J. Biol. Chem.* **193** 265–275

Lunde M N, Paranjape R, Lawley T J and Ottesen E A 1988 Filarial antigen in circulating immune complexes from patients with *Wuchereria bancrofti* filariasis; *Am. J. Trop. Med. Hyg.* **38** 366–371

Maizels R M, Sutanto I, Gomez-Priego A, Lillywhite J and Denham D A 1985 Specificity of surface molecules of adult *Brugia* parasites: cross-reactivity with antibody from *Wuchereria, Onchocerca* and other human filarial infections; *Trop. Med. Parasitol.* **36** 233–237

Maizels R M, Burke J, Sutanto I, Purnomo and Partono F 1986 Secreted and surface antigens from larval stages of *Wuchereria bancrofti*, the major human lymphatic filarial parasite; *Mol. Biochem. Parasitol.* **19** 27–34

Nanduri J and Kazura J W 1989 Paramyosin-enhanced clearance of *Brugia malayi* microfilaraemia in mice; *J. Immunol.* **143** 3359–3363

Ottesen E A, Weller P F, Lunde M N and Hussain R 1982 Endemic filariasis on a Pacific Island. II. Immunologic aspects: immunoglobulin, complement and specific antifilarial IgG, IgM and IgE antibodies; *Am. J. Trop. Med. Hyg.* **31** 953–961

Parab P B, Rajasekariah G R, Carvalho P A and Subrahmanyam D 1990 Differential recognition of *Brugia malayi* antigens by bancroftian filariasis sera; *Indian J. Med. Res.* **91** 138–143

Paranjape R S, Hussain R, Nutman T B, Hamilton R and Ottesen E A 1986 Identification of circulating parasite antigen in patients with bancroftian filariasis; *Clin. Exp. Immunol.* **63** 508–516

Parkhe K A, Reddy M V R, Cheirmaraj K, Ramaprasad P and Harinath B C 1990 Analysis, characterization and diagnostic use of circulating filarial antigen in bancroftian filariasis; *J. Biosci.* **15** 37–46

Reddy M V R, Prasad G B K S and Harinath B C 1986 Isolation and evaluation of antigens from microfilaraemia plasma and immune-complexes for diagnosis of bancroftian filariasis; *Indian J. Pathol. Microbiol.* **29** 179–183

Sim K L, Kwa B H and Mak J W 1982 Immune responses in human *Brugia malayi* infections: Serum dependent cell-mediated destruction of infective larvae *in vitro*; *Trans. R. Soc. Trop. Med. Hyg.* **76** 362–370

Subrahmanyam D, Mehta K, Nelson D S, Rao Y V B G and Rao C K 1978 Immune reactions in human filariasis; *J. Clin. Microbiol.* **8** 228–232

Towbin M, Stachlin T and Gordon J 1979 Electrophoretic transfer of proteins from polyacrylamide gels to nitro-cellulose sheets — Procedure and some applications; *Proc. Natl. Acad. Sci. USA* **76** 4350–4354

Immunoprophylaxis against filarial parasite, *Brugia malayi*: potential of excretory-secretory antigens in inducing immunity

K CHEIRMARAJ, V CHENTHAMARAKSHAN, M V R REDDY and
B C HARINATH*

Department of Biochemistry, Mahatma Gandhi Institute of Medical Sciences,
Sevagram 442 102, India

Abstract. The role of excretory-secretory antigens in inducing immunity in the host against *Brugia malayi* microfilariae and infective larvae was studied by *in vitro* antibody dependent cell-mediated reaction as well as *in vivo* inoculation of filarial parasites within a microchamber in the host. The immune sera of jirds raised against *Brugia malayi* microfilarial and infective larval excretory-secretory antigens (*Bm* Mf ESA and *Bm* L$_3$ ESA) promoted the adherence of peritoneal exudate cells to *Brugia malayi* microfilariae and infective larvae *in vitro* and induced cytotoxicity to the parasites within 48 h. The anti *Bm* Mf ESA serum was more effective than anti *Bm* L$_3$ ESA serum in inducing cytotoxicity to microfilariae and both antisera had a similar cytotoxic effect on infective larvae. In the microchambers implanted in the immune jirds, host cells could migrate and adhere to the microfilariae and infective larvae and kill them within 48–72 h. Further, *Mastomys natalensis* immunized against *Bm* Mf ESA and L$_3$ ESA generated a high degree of protective response against circulating microfilariae. These results suggest that excretory-secretory antigens are effective in inducing resistance against filarial parasites and thus have potential in immunoprophylaxis.

Keywords. *Brugia malayi*; microfilariae; infective larvae; immunoprophylaxis; excretory-secretory antigens.

1. Introduction

Lymphatic filariasis continues to pose a major public health problem in India. The general approach to control filariasis in most endemic areas are reduction of morbidity and interruption of transmission. Despite recent advances both in chemotherapy and in vector control, the filarial disease remains a major cause of morbidity in the developing world. Immunoprophylaxis may serve as an effective adjunct to the existing control measures.

Studies on immunoprophylaxis against filarial infection have been made in several experimental models employing different stages of *Brugia malayi* parasites. The jirds (*Meriones unguiculatus*) and *Mastomys natalensis* are the fully permissive rodent hosts for sub-periodic *B. malayi* and have been found to be very useful in immunological and other studies related to brugian filariasis. Protective immunity against *B. malayi* infection has been demonstrated in jirds using irradiated third stage larvae (Yates and Higashi 1985) or microfilarial antigens (Kazura *et al* 1986). Successful vaccination with attenuated larvae suggested that it would be the excretory-secretory (ES) products or moulting fluid that contains the effective

the substances released by worms (Clegg and Smith 1978; Rajasekariah *et al* 1988). Vaccination with ES products of third stage larvae of *B. pahangi* showed partial immunity (determined by decreased worm numbers and/or absence of circulating microfilariae) in jirds (WHO 1987). Antibody dependent cell-mediated cytotoxicity (ADCC) is believed to be one of the principal immunological mechanisms functional in man and animals and the disappearance of circulating parasites is mainly attributed to this phenomenon (Mehta *et al* 1981b; Chandrashekar *et al* 1985a,b). This communication reports the potential of ES products of *B. malayi* microfilariae and infective larvae in inducing ADCC reaction both *in vitro* and *in vivo* and killing the microfilariae and infective larvae of *B. malayi*.

2. Materials and methods

2.1 *Filarial infection*

Multimammate rats, *Mastomys natalensis* or *M. coucha* (Kruppa *et al* 1990) (GRA Giessen strain) were infected with *B. malayi* (sub-periodic) by sub-cutaneous (sc) inoculation of 100 third stage infective larvae and the infection was monitored as described by Sanger *et al* (1981).

Jirds (*M. unguiculatus*) were infected with 100 *B. malayi* infective larvae by the intraperitoneal (ip) route (McCall *et al* 1973).

2.2 *Filarial parasites*

Infective larvae (L_3) of *B. malayi* were collected following the Baermann's technique (Suzuki and Seregeg 1979). *Aedes aegypti* mosquitoes were fed on the blood from *B. malayi* infected *Mastomys* and two weeks later, they were dissected to recover infective larvae.

Microfilariae (Mf) were obtained by lavage of the peritoneal cavities of jirds which had been infected with *B. malayi* L_3 larvae, 15–20 weeks earlier.

2.3 *Antigen preparation*

2.3a *B. malayi Mf ESA*: Microfilariae were washed with normal saline and RPMI 1640 medium and then plated on a sterile disposable petriplate. The plate was incubated at 37°C for 1 h to remove the hosts' peritoneal cells. An hour later, the microfilariae were recovered, washed and maintained in the same medium at 28°C. After 48 h, culture fluid was centrifuged and the supernatant was dialyzed, freeze-dried and stored at −20°C until use. The protein content was estimated by the method of Lowry *et al* (1951).

2.4 *L_3 ESA*

The infective larvae of *B. malayi* were maintained in Hank's balanced salt solution (HBSS) at 28°C for 48 h as described by Kharat *et al* (1989). The *Bm* L_3 ESA was obtained by processing the culture fluid as described above.

Two groups of jirds were immunized ip, each group with *Bm* Mf ESA or L$_3$ ESA. The first dose consisted of 25 μg of antigenic protein emulsified in Freund's complete adjuvant. The second and third doses of similar amount, emulsified in Freund's incomplete adjuvant were given at intervals of 10 days. Control animals received only saline emulsified in Freund's adjuvant as above. A week after the last dose of antigen, the animals were bled from retro-orbital plexus and immune sera were isolated.

2.6 *Peritoneal exudate cells*

Peritoneal exudate cells (PEC) from normal jirds were collected by peritoneal cavity washings with sterile medium RPMI 1640. The cells were washed with the same medium supplemented with 10% fetal calf serum (FCS) and the viability of the cells was assessed by trypan blue dye exclusion.

2.7 *In vitro cytotoxicity assay*

The cytotoxicity assay was carried out as described by Chandrashekar *et al* (1985a, 1990). Briefly, 100 mf or 6 L$_3$ in 50 μl of RPMI 1640 were incubated with 50 μl of PEC (2×10^3 cells/mf (or) 5×10^4 cells/L$_3$ larva) and 50 μl of normal or immune jird serum in the 96 well culture plate (Costar Inc, MA, USA). The plate was incubated in an atmosphere of 5% CO$_2$ at 37°C. At different periods of incubation (24 and 48 h) the samples were examined microscopically for cellular adherence and cytotoxicity to microfilariae and infective larvae. Percentage of cytotoxicity was expressed by considering the number of immobile or dead parasites within the experimental period.

2.8 *Micropore chambers technique*

Micropore chambers were assembled using 14×2 mm plexi glass rings (Millipore Filter Corp., Bedford, MA, USA) and 3 μm nucleopore polycarbonate membrane (Thomas Scientific, USA) as described by Weiss and Tanner (1979). The micropore chambers were loaded with 100 mf or 10 L$_3$ larvae in RPMI 1640 medium via an aperture (diameter - 1 mm) at the side of the plexi glass ring and then sealed with paraffin wax and subsequently with MF cement (Millipore Filter Corp., USA). The chambers were implanted intraperitoneally into the immunized and control jirds through an incision of 2–3 cm and the skin was sutured. After 24, 48 and 72 h, the chambers were taken out and the contents were removed with pasteur pipette and examined microscopically.

2.9 *In vivo cytotoxicity assay*

Two different groups of *Mastomys*, with five in each group were immunized ip, with *Bm* Mf ESA or L$_3$ ESA as described above. A week after giving the last dose of immunization, the two groups of *Mastomys* along with the control group were inoculated (ip) with 1×10^5 *B. malayi* microfilariae in RPMI 1640 medium. The

3. Results

In the *in vitro* cytotoxic assays, the immune sera of jirds raised against *Bm* Mf ESA and L_3 ESA promoted the adherence of PEC to *B. malayi* microfilariae and infective larvae and induced cytotoxicity to the parasites within 24–48 h (table 1). The anti *Bm* Mf ESA serum was more effective than anti *Bm* L_3 ESA serum in killing microfilariae and the difference was statistically significant ($P < 0.05$) by Student's *t*-test. However, against infective larvae, both the antisera had a similar cytotoxic effect and there was no (statistically) significant difference.

The microscopic observation of the nucleopore chambers implanted in jirds immunized with *Bm* Mf ESA or L_3 ESA showed the migration of host lymphocytes, polymorphonuclear cells and few macrophages into the chambers leading to their adherence and killing of microfilariae or infective larvae within 48–72 h (figures 1 and 2 and table 2). The cytotoxicity in the immunized jirds varied between 38 to 75% in 48 h and 95–100% in 72 h. On the other hand, in the chambers implanted in control jirds, the cytotoxicity to the parasites was only 8–15% in 48 h and 20–35 % in 72 h.

The results of the *in vivo* studies on the effect of immunization on the microfilaraemic state are summarized in table 3. An intraperitoneal injection of 1×10^5 mf in *Mastomys* resulted in the peripheral circulation of microfilariae within 24 h, which was maintained throughout the observation period of 10 days. However in *Mastomys* immunized with *Bm* Mf ESA, very few microfilariae were present in the peripheral circulation, which were also eliminated by day 5 and did not reappear again till day 10. In *Mastomys* immunized with *Bm* L_3 ESA, though the mf count was less in the peripheral circulation compared to control *Mastomys*, they continued to exist till day 10.

4. Discussion

The present study was undertaken to evaluate the role of ES antigens in producing immunity in the host against filarial infection *in vitro* and *in vivo*. Since, in preliminary experiments, no difference in cytotoxicity was observed with intact or

Table 1. Serum dependent cellular cytotoxicity to *B. malayi* parasites *in vitro*.

| Jird serum† | Cytotoxicity (%)* | | | |
| | 24 h | | 48 h | |
	Mf	L_3	Mf	L_3
Control	3 ± 3	–	6 ± 5	33 ± 14
Anti Mf ESA	63 ± 21	8·3 ± 8	100	62·3 ± 24
Anti L_3 ESA	51 ± 22	21·5 ± 13	78 ± 20	82 ± 17

†Sera were collected from 4 animals and tested separately for cytotoxicity.
*Mean ± SD.

(1)

(2)

Figures 1 and 2. Adhesion of PEC to *B. malayi* microfilariae (**1**) and infective larvae (one part) (**2**) in the micropore chamber implanted (ip) in the immunized jird.

decomplement serum, the experiment for ADCC reaction was therefore carried out with sera without heat inactivation. The observations in *in vitro* ADCC reaction showed that the antibodies raised against *Bm* Mf ESA and L_3 ESA induced cytotoxicity to the parasites. This observation, which to our knowledge is the first observation, envisages the definite role of *B.* malayi ES products in inducing immunity in the fully permissive host. The non-living parasites or their extracts have generally failed to confer resistance in fully permissive hosts, although they may do so in animals that are semi-permissive for parasite development (Mehta *et al* 1981a; Carlow and Philipp 1987). The observations in prophylactic studies

| Jirds* | Cytotoxicity (%)[†] | | | | | |
| | 24 h | | 48 h | | 72 h | |
	Mf	L_3	Mf	L_3	Mf	L_3
Control	–	–	8 ± 3	15 ± 5	20 ± 8	35 ± 5
Bm Mf ESA immunized	20 ± 5	5 ± 5	48 ± 2	75 ± 5	100	95 ± 5
Bm L_3 ESA immunized	8 ± 2	15 ± 5	38 ± 6	70	100	100

*Experiments were performed in 6 animals of each group.
[†]Mean ± SD.

Table 3. Effect of immunization on circulating microfilariae in *M. natalensis*.

| Mastomys | Microfilariae* in 10 μl of blood | | | | |
	Day 1	Day 3	Day 5	Day 7	Day 10
Control (n = 3)	10 ± 2	7 ± 3	8 ± 1	9 ± 3	7 ± 2
Bm Mf ESA immunized (n = 5)	0·2 ± 0·1	1 ± 1	0	0	0
Bm L_3 ESA immunized (n = 5)	3 ± 2	2 ± 2	2 ± 1	1 ± 1	1 ± 1

*Mean ± SD

conducted by Rajasekariah *et al* (1988) indicated that the secretory products are a source of protective antigens.

Both antibody and complement mediated effector mechanisms have been shown to operate on microfilariae and infective larvae *in vitro* (Subrahmanyam *et al* 1976, 1978; Mehta *et al* 1980, 1981b; Tanner and Weiss 1978; Haque *et al* 1981; Sim *et al* 1982; Chandrashekar *et al* 1985a, b, 1990). The nematode epicuticle may act as substrate for antibody and complement mediated adherence of host cells that may result in damage to or death of the parasite (Capron *et al* 1982). Neutrophils, macrophages and eosinophils are all known to possess surface receptors for the Fc part of IgG (Rabellino and Metcalf 1975; Wong and Wilson 1975). The predominant isotope responsible for ADCC reaction was found to be IgG (Chandrashekar *et al* 1985a, b; WHO 1987).

Micropore chamber technique was employed to check whether a similar ADCC reaction can occur *in vivo*. These chambers implanted in animals are advantageous since they provide a closer physiological environment than *in vitro* cultures for larval growth and survival and thus for assessing the host effector mechanisms (Weiss and Tanner 1979; Rajasekariah *et al* 1989). In the present study the microfilariae and infective larvae were attacked by host cells which migrated into the chambers implanted in immunized jirds within 48–72 h. In the earlier studies Chandrashekar *et al* (1990) showed that *Bm* L_3 larvae were attacked by the host macrophages and polymorphs in microchambers, 16–24 h after implantation in the immunized rats. Abraham *et al* (1986) observed that it took 10 days for the host

susceptibility to immune attack. These variations in cytotoxicity reactions in *in vivo* conditions suggest that the responsible factors seem to be dependent on parasite species and the host (permissive and non-permissive).

The effect of antibodies raised against *Bm* Mf ESA and L_3 ESA on circulating microfilariae was studied *in vivo* in *Mastomys*. The *Mastomys* immunized against *Bm* Mf ESA generated a high degree of protective response against circulating microfilariae compared to control *Mastomys* and those immunized with *Bm* L_3 ESA. In the earlier studies conducted by Rajasekariah *et al* (1987, 1988) immunization of mice with microfilarial antigens induced an absolute degree of protection against mf and comparatively a highly significant level of immunity against L_3. Kazura and Davis (1982) showed that soluble antigenic preparation derived from *B. malayi* microfilariae has the capacity to induce a high degree of resistance in Swiss–Webster mice against the circulating microfilariae. Rajasekariah *et al* (1988) showed that immunization of Balb/c mice with *B. pahangi* Mf ESM antigens produced partial but significant levels of protection against the establishment of Mf in mice. A vaccine against microfilariae will be useful in blocking transmission and thus in the control of filariasis.

These results suggest that functional antigens are contained in the filarial ES product. Failure to achieve complete protection with the ES products may be due to the presence of substance (s)/antigen (s) which presumably mask the activity of protective antigens. Purification of the ES product may be useful in enhancing protection.

References

Abraham D, Weiner D J and Farrell J P 1986 Protective responses of the jird to larval *Dipetalonema viteae*; *Immunology* **57** 165–169

Capron A, Dessaint J P, Haque A and Capron M 1982 Antibody-dependent cell-mediated cytotoxicity against parasistes; *Prog. Allergy* **31** 234

Carlow C K S and Philipp M 1987 Protective immunity to *Brugia malayi* larvae in Balb/c mice: Potential of this model for the identification of protective antigens; *Am. J. Trop. Med. Hyg.* **37** 597–604

Chandrashekar R, Rao U R, Parab P B and Subrahmanyam D 1985a *Brugia malayi*: Serum-dependent cell-mediated reactions to microfilariae; *Southeast Asian J. Trop. Med. Public Health* **16** 15–21

Chandrashekar R, Rao U R and Subrahmanyam D 1985b Serum-dependent cell-mediated reactions to *Brugia pahangi* infective larvae; *Parasite Immunol.* **7** 633–642

Chandrashekar R, Rao U R and Subrahmanyam D 1990 Antibody-mediated cytotoxic effects *in vitro* and *in vivo* of rat cells on infective larvae of *Brugia malayi*; *Int. J. Parasitol.* **20** 725–730

Clegg J A and Smith M A 1978 Prospects for the development of dead vaccines against helminths; *Adv. Parasitol.* **16** 165–218

Haque A, Ouaissi A, Joseph M, Capron M and Capron A 1981 IgE antibody in eosinophil and macrophage mediated *in vitro* killing of *Dipetalonema viteae* microfilariae; *J. Immunol.* **127** 716–725

zura J W, Cicirello H and McCall J W 1986 Induction of protection against *Brugia malayi* infection in jirds by microfilarial antigens; *J. Immunol.* **136** 1422–1426

arat I, Cheirmaraj K, Prasad G B K S and Harinath B C 1989 Antigenic analysis of excretory-secretory products of *Wuchereria bancrofti* and *Brugia malayi* infective larval forms by SDS-PAGE; *Indian J. Exp. Biol.* **27** 681–684

uppa T F, Iglauer F, Ihnen E, Miller K and Kunstyr I 1990 *Mastomys natalensis* or *Mastomys coucha*. Correct species designation in animal experiments; *Trop. Med. Parasitol.* **41** 219–220

wry O H, Rosebrough N J, Farr A L and Randall R J 1951 Protein measurement with the Folin-phenol reagent; *J. Biol. Chem.* **193** 265–275

:Call J W, Malone J B, Ah H S and Thompson P E 1973 Mongolian Jirds (*Meriones unguiculatus*) infected with *Brugia malayi* by the intraperitoneal route: a rich source of developing larvae, adult filariae and microfilariae; *J. Parasitol.* **59** 436

:hta K, Sindhu R K, Subrahmanyam D and Nelson D S 1980 IgE-dependent adherence and cytotoxicity of rat spleen and peritoneal cells to *Litomosoides carinii* microfilariae; *Clin. Exp. Immunol.* **41** 107–114

:hta K, Subrahmanyam D and Sindhu R K 1981a Immunogenicity of homogenates of the developmental stages of *Litomosoides carinii* in albino rats; *Acta Trop.* **38** 319–324

:hta K, Sindhu R K, Subrahmanyam D, Hopper K E and Nelson D S 1981b Antibody dependent cell-mediated effects in bancroftian filariasis; *Immunology* **43** 117–123

ijasekariah G R and Subrahmanyam D 1987 Isolation of functional antigen and study of their efficacy in induction of protection against filarial infections; *ICMR Research project progress report* pp 11–13

ijasekariah G R, Mukherjee Puri P, Chandrashekar R and Subrahmanyam D 1988 Clearance of *Brugia pahangi* microfilariae in immunized mice; *Immunol. Cell Biol.* **66** 331–336

ijasekariah G R, Monteiro Y M, Nelto A, Deshpande L and Subrahmanyam D 1989 Protective immune responses with trickle infections of the third stage filarial larvae, *Wuchereria bancrofti* in mice; *Clin. Exp. Immunol.* **78** 292–298

bellino E M and Metcalf D 1975 Receptors for C_3 and IgG on macrophage, neutrophil and eosinophil colony cells grown *in vitro*; *J. Immunol.* **115** 688–692

nger I, Lammler G and Kimmig P 1981 Filarial infections of *Mastomys natalensis* and their relevance for experimental chemotherapy; *Acta Trop.* **38** 277–288

n B K, Kwa B H and Mak J W 1982 Immune responses in human *Brugia malayi* infections: Serum dependent cell-mediated destruction of infective larvae *in vitro*; *Trans. R. Soc. Trop. Med. Hyg.* **76** 362–369

orahmanyam D, Rao Y V B G, Mehta K and Nelson D S 1976 The serum-dependent adhesion and cytotoxicity of cells to *Litomosoides carinii* microfilariae; *Nature (London)* **260** 529–530

orahmanyam D, Mehta K, Nelson D S, Rao Y V B G and Rao C K 1978 Immune reactions in human filariasis; *J. Clin. Microbiol.* **8** 228–232

zuki T and Seregeg I G 1979 A mass dissection technique for determining infectivity rate of filariasis vectors; *Jpn. J. Exp. Med.* **49** 117–121

nner M and Weiss N 1978 Studies on *Dipetalonema viteae* (Filarioidea) II. Antibody-dependent adhesion of peritoneal exudate cells to microfilariae *in vitro*; *Acta Trop.* **35** 151–160

eiss N and Tanner M 1979 Studies on *Dipetalonema viteae* (Filarioidea) 3. Antibody-dependent cell mediated destruction of microfilariae *in vivo*; *Tropenmed. Parasitol.* **30** 73–80

orld Health Organization 1987 Protective immunity and vaccination in Onchocerciasis and Lymphatic filariasis: Report of the thirteenth meeting of the scientific working group on filariasis; *WHO Document TDR/FIL/SWG* (13)/87.3 Geneva

ong L and Wilson J D 1975 The identification of Fc and C_3 receptors on human neutrophils; *J. Immunol. Methods* **7** 69–76

tes J A and Higashi G I 1985 *Brugia malayi*: Vaccination of jirds with ^{60}Cobalt-attenuated infective stage larvae protects against homologous challenge: *Am. J. Trop. Med. Hyg.* **34** 1132–1137

Tissue distribution and antileishmanial activity of liposomised Amphotericin-B in Balb/c mice§

IMRAN AHMAD**, ANSHU AGARWAL, AJAY PAL*, P Y GURU*, B K BACHHAWAT** and C M GUPTA†

Division of Membrane Biology and *Division of Parasitology, Central Drug Research Institute, Lucknow 226 001, India

**Liposome Research Centre, University of Delhi, South Campus, Benito Juarez Road, New Delhi 110 021, India

Abstract. Antileishmanial activity and organ distribution of the antifungal drug Amphotericin-B in free and liposomised form have been studied in Balb/c mice infected with *Leishmania donovani*. Results indicate that Amphotericin-B in the liposomised form is significantly more active than the free form. This increase in the activity is perhaps related to the reduced drug toxicity rather than the altered drug distribution at the site of infection.

Keywords. Amphotericin-B; antileishmanial activity; renal toxicity; liposomes; tissue distribution; drug delivery.

1. Introduction

Amphotericin-B (Amp-B) is a very potent antifungal drug which exhibits marked renal toxicity (Graybill and Craven 1983). However, this toxicity is dramatically reduced by incorporating the drug in liposomes (Alving 1986). The liposomised Amp-B is very effective not only against the fungal diseases (Graybill *et al* 1982; Lopez-Berestein *et al* 1983; Trembaly *et al* 1984) but also against the leishmania infections (New *et al* 1981; Berman *et al* 1986).

Earlier studies have shown that availability of Amp-B in various tissues is altered by the fungal infections (Lopez-Berestein *et al* 1984; Ahmad *et al* 1990). Also, altered tissue distribution patterns of this drug have recently been observed in animals suffering from diabetes (Wasan *et al* 1990). To examine whether the *Leishmania donovani* infection would also affect the drug availability in various tissues, we have studied the tissue distribution and antileishmanial activity of liposomised Amp-B in Balb/c mice.

2. Materials and methods

2.1 *Materials*

Fungizone, the lyophilized pharmaceutical preparation of Amp-B in deoxycholate, was obtained from Sarabhai Chemicals, Baroda, and was reconstituted in 5%

217

Dr G Maierhofer. Egg phosphatidylcholine (EPC) was prepared as described earlier (Gupta and Bali 1981). All other reagents used were of analytical grade.

2.2 Animals

Male Balb/c mice weighing 18–22 g were used in all the experiments.

2.3 Parasites

The strain of *L. donovani* (HOM/IN/80/Dd8), originally isolated from a Kala-azar patient from Bihar, was a kind gift from Professor P C C Garnham. The strain is being regularly maintained *in vitro* as promastigotes in NNN medium, and as amastigotes in golden hamsters.

2.4 Infection

Amastigote suspensions (about 10^8 amastigotes/ml) were prepared from the spleen of infected hamsters (> 1 month old) in Lock's solution (8 g NaCl, 0.2 g KCl, 0.2 g $CaCl_2$, 0.3 g KH_2PO_4 and 2.5 g glucose in 1 litre, pH 7.2). A measured aliquot (0.2 ml) of this suspension was administered intravenously to Balb/c mice. The establishment of the infection was confirmed by the presence of a number of amastigotes/500 host cell nuclei in liver and spleen.

2.5 Liposomes

Liposomes were prepared from EPC or SPC and Chol (PC/Chol molar ratio 7:3) as described earlier (Gupta and Bali 1981). Briefly, the lipids (total weight 45 mg) were dissolved in chloroform in a round-bottomed flask and to it 1 mg Amp-B in methanol was then added. The organic solvents were removed under reduced pressure, resulting in formation of a thin lipid film on the wall of the flask. The dried lipid mixture was dispersed in 150 mM saline and sonicated for 30 min under nitrogen using a probe-type sonicator. It was centrifuged at 12,000 g for 30 min (4°C). The supernatant was dialyzed against 150 mM saline to remove free Amp-B, and the amount of Amp-B incorporated in liposomes was determined spectrophotometrically (Mehta *et al* 1984). About 80–85% of Amp-B was found to be associated with the liposomes.

2.6 Drug treatment

About 3 weeks after infecting with *L. donovani*, the animals were divided into 4 groups. While the first group was given free Amp-B, the second group was administered Amp-B incorporated in EPC/Chol or SPC/Chol liposomes. The third group received empty liposomes (free of drug) whereas the fourth group was left untreated. The efficacy of the treatment was ascertained by monitoring the parasite burden in spleen and liver of the treated animals.

Giemsa, and the number of amastigotes/500 host cell nuclei ware counted. Per cent inhibition of the amastigote number was calculated, using untreated animals as controls, as follows:

$$\% \text{ Inhibition} = 100 - \left(\frac{X}{Y} \cdot 100\right),$$

where X and Y denote actual and mean numbers of amastigotes/500 cell nuclei in treated and control animals, respectively.

2.7 Tissue distribution

Tissue distributions of Amp-B in various organs were determined essentially according to the method of Lopez-Berestein et al (1984). The detailed methodology has been described by us earlier (Ahmad et al 1989).

Both normal and infected mice were injected intravenously free or liposomised Amp-B, and 1 h or 24 h after the injection, the animals were sacrificed and various organs (viz., lung, liver, spleen and kidney) taken out, excised and frozen until analysis. The tissue samples from different animals were pooled together, and 0·5 g of each tissue homogenised in methanol. It was centrifuged at 10,000 g for 15 min and the supernatant injected into an HPLC column (μ C_{18} reverse phase) for analysis. The drug concentration in various tissues was obtained after multiplying the observed values with the recovery factor. The recovery factor for various tissues was determined essentially as reported earlier (Ahmad et al 1989). The recovery of Amp-B from different tissues varied from 61 to 75%.

3. Results and discussion

Amp-B was intercalated into the egg PC/Chol or SPC/Chol liposomes bilayers by cosonicating this drug with a mixture of egg PC (or SPC) and Chol. The titanium particles and undispersed lipids were removed by centrifugation, and the free drug from the liposomised Amp-B was separated by extensive dialysis. The drug-loaded liposomes thus obtained were administered intravenously to Balb/c mice infected with L. donovani, and the efficacy of this treatment was assessed by measuring the parasite load in spleens and livers of the treated animals. Results given in table 1 shows that the parasite load in the spleens of infected animals was significantly reduced by incorporating the drug in EPC/Chol or SPC/Chol liposomes. However the drug incorporated in SPC/Chol liposomes appeared to be much less effective in controlling the liver infections as compared to that incorporated in EPC/Chol liposomes. Besides enhancing the drug efficacy, liposomisation of the drug also led to a marked decrease in the drug toxicity; all the animals died at 2 mg/kg dose of free Amp-B. These results are consistent with the earlier studies (New et al 1981; Berman et al 1986).

To determine the tissue distribution, free drug and liposomised drug were injected in both normal and infected animals at 1 mg/kg and 4 mg/kg dose respectively. Free drug dose of 1 mg/kg which was chosen as the LD_{50} of free Amp-

Drug formulation	Drug dose (mg/kg)	Inhibition of infection (%)	
		Spleen	Liver
Liposomised (EPC/Chol)	5·0	70·8 ± 5·7 (10)	79·9 ± 9·6 (10)
	0·8	69·7 ± 7·3 (6)	78·5 ± 16·4 (6)
	0·4	62·5 ± 6·9 (7)	44·7 ± 14·1 (7)
Liposomised (SPC/Chol)	5·0	79·8 ± 3·7 (14)	49·8 ± 8·6 (14)
Free	0·8	32·7 ± 10·9 (10)	55·4 ± 15·0 (10)
EPC/Chol liposomes		21·2 ± 10·2 (7)	ND

Values shown are means ± SE, and have been calculated from the pooled data of 2 separate experiments, using 3–7 animals/group each time.
Numbers in parentheses denote the number of total animals used. At 5·0 mg/kg (or 2·0 mg/kg) dose of free Amp-B, all the animals died spontaneously.
ND, Not determined.

Table 2. Organ concentration of Amp-B after injecting free and liposomised Amp-B in normal and *L. donovani*-infected Balb/c mice.

Tissue	Organ concentration (μg/g tissue)							
	Free Amp-B				Liposomised Amp-B			
	Normal		Infected		Normal		Infected	
	1 h	24 h	1 h	24 h	1 h	24 h	1 h	24 h
Liver	31·4	5·2	31·0	14·2	15·3	29·4	30·8	11·1
Spleen	26·0	7·2	20·4	8·4	7·0	8·1	4·6	11·7
Lung	8·8	6·3	2·5	4·8	9·0	6·5	10·5	6·8
Kidney	7·2	6·0	8·8	20·0	2·5	8·6	5·1	12·2

Liposomes used in these experiments were formed from SPC and Chol. Liposomal Amp-B was given at 4 mg/kg, while the free drug was administered at 1 mg/kg dose. However, for calculating the organ concentration, the free drug dose was adjusted to 4 mg/kg (for details see Lopez–Berestein *et al* 1984). Values shown are means of two independent determinations carried out on drug extracts obtained from pooled organs of 5 mice each time.

B is only about 1·2 mg/kg (Ahmad *et al* 1989). This low dose of the drug if administered in liposomes, can not be accurately detected in various tissues and hence a higher dose (4 mg/kg) of liposomised drug was used. The animals were sacrificed 1 h or 24 h after the drug administration, and various organs taken out and homogenised in methanol. The homogenates were centrifuged, and the organ concentration of Amp-B determined by HPLC as described in §2.

Table 2 shows that the drug concentration in livers of the infected animals was not influenced much by incorporating Amp-B in the liposomes. However, it was appreciably reduced in kidney under identical conditions. Moreover, the drug concentration in the case of the liposomal Amp-B in spleen was smaller, as compared to free Amp-B, at 1 h but not at 24 h after the injection. Besides the liposomisation, the drug distribution in various tissues was influenced also by the infection. This influence was more pronounced in the case of the liposomised drug, compared to the free drug (table 2). It would therefore seem that the Amp-B distribution in biophase is influenced by both the drug incorporation in liposomes and the *L. donovani* infections in animals.

donovani-infected mice, but it does lead to a decrease in the drug concentration in the kidney of these animals. This is quite consistent with earlier studies (Lopez-Berestein *et al* 1984; Ahmad *et al* 1990). It may thus be suggested that the higher efficacy of the liposomised Amp-B observed here is at least partly due to the reduced drug concentration in kidney, as it should lead not only to the decreased drug toxicity (Graybill and Craven 1983) but also to an increased drug tolerance. This is quite consistent with our finding that the drug tolerance is significantly increased by delivering the drug in liposomes. It may thus be concluded that the increased efficacy of the liposomised Amp-B against *L. donovani* infections is perhaps largely due to the enhanced drug tolerance rather than the altered drug distribution at the site of infection.

Acknowledgements

References

Ahmad I, Sarkar A K and Bachhawat B K 1989 Liposomal Amphotericin-B in the control of experimental aspergillosis in mice: Part I—Relative therapeutic efficacy of free and liposomal Amphotericin-B; *Indian J. Biochem. Biophys.* 26 351–356

Ahmad I, Sarkar A K and Bachhawat B K 1990 Effect of cholesterol in various liposomal compositions on the *in vivo* toxicity, therapeutic efficacy, and tissue distribution of Amphotericin-B; *Biotechnol. Appl. Biochem.* 12 550–556

Alving C R 1986 Liposomes as drug carriers in leishmaniasis and malaria; *Parasitol. Today* 2 101–107

Berman J D, Hanson W L, Chapman W L, Alving C R and Lopez-Berestein G 1986 Antileishmania activity of liposome-encapsulated Amphotericin-B in hamsters and monkeys; *Antimicrob. Agents Chemother.* 30 847–851

Graybill J R, Craven C P, Taylor R L, Williams D M and Magee W E 1982 Treatment of murine cryptococcaris with liposome associated Amphotericin-B; *J. Infect. Dis.* 145 748–752

Graybill J R and Craven C P 1983 Antifungal agents used in systemic mycoses: activity and therapeutic use; *Drugs* 25 41–62

Gupta C M and Bali A 1981 Carbamyl analogs of phosphatidylcholines: synthesis, interaction with phospholipases and permeability behaviour of their liposomes; *Biochim. Biophys. Acta* 663 506–515

Lopez-Berestein G, Mehta R, Hopfer R L, Mills K, Kasi L, Mehta K, Fainstein V, Luna M, Hersh E M and Juliano R 1983 Treatment and prophylaxis of disseminated infection due to *Candida albicans* in mice with liposome-encapsulated Amphotericin-B; *J. Infect. Dis.* 147 939–945

Lopez-Berestein G, Rosenblum M G and Mehta R 1984 Altered tissue distribution of Amphotericin-B by liposomal encapsulation: Comparison of normal mice to mice infected with *Candida albicans*; *Cancer Drug Deliv.* 1 199–205

Mehta R, Lopez-Berestein G, Hopfer R, Mills K and Juliano R 1984 Liposomal Amphotericin-B is toxic to fungal cells but not to mammalian cells; *Biochim. Biophys. Acta* 770 230–234

New R R C, Chance M L and Heath S 1981 Antileishmanial activity of amphotericin and other antifungal agents entrapped in liposomes; *J. Antimicrob. Chemother.* 8 371–381

Trembaly C, Barga M, Fiore C and Szoka F 1984 Efficacy of liposome-intercalated Amphotericin-B in the treatment of systemic candidiasis in mice; *Antimicrob. Agents Chemother.* 26 170–173

Wasan K M, Vadiei K, Lopez-Berestein G and Luke D R 1990 Pharmacokinetics, tissue distribution, and toxicity of free and liposomal Amphotericin-B in diabetic rats; *J. Infect. Dis.* 161 562–566

Plasminogen activator: Isolation and purification from lymphosarcoma of ascites bearing mice

M W NULKAR, RUKMINI DARAD, M SUBRAMANIAN and A R PAWSE*

Biochemistry Division, Bhabha Atomic Research Centre, Trombay, Bombay 400 085, India

Abstract. Plasminogen activator secreted by lymphosarcoma (ascites) of mice was purified up to 163-fold by ammonium sulphate fractionation at 35% saturation and chromatography on *p*-aminobenzamidine-Sepharose 4B. The purified activator contained specific activity of 9980 IU/mg. The plasminogen activator displayed homogeneity by polyacrylamide slab gel electrophoresis and high performance liquid chromatography. The activator consisted of a single polypeptide chain with an apparent molecular weight of 66,000 daltons as determined by sodium dodecyl sulphate-polyacrylamide gel electrophoresis under reducing conditions as well as gel filtration on Sephadex G-100. Distinct differences between this activator and urokinase were discernible in respect of specific activities, fibrin affinity and immunochemical properties. The lymphosarcoma activator appears to be of tissue-type origin since it showed gross similarity to standard tissue plasminogen activator in terms of modes of binding to fibrin and immunological attributes.

Keywords. Plasminogen activator; urokinase; fibrinolysis; fibrin; lymphosarcoma.

1. Introduction

Plasminogen activators form a key component of fibrinolytic system with a high specificity for plasminogen yielding the active enzyme plasmin through the hydrolysis of the $Arg_{560}-Val_{561}$ peptide bond (Ranby and Brandstrom 1988; Collen and Gold 1990). Activation also serves as an important source of localized proteolytic activity during tumour invasion, ovulation, cell migration and various physiological processes (Dano *et al* 1985; Loskutoff 1988; Vansetten *et al* 1989). Two functionally and immunologically distinct enzyme species of plasminogen activators (PA) have been identified, the urokinase-type and tissue-type activators present in a wide variety of tissues, body fluids, malignant tumours and transformed cell lines (Hekman and Loskutoff 1987; Gross *et al* 1988). These enzymes have been purified and shown to be serine proteases with high specificity to plasminogen (Prager *et al* 1986; Hajjar and Hamel 1990). Reports of Saksela (1985), Cajot *et al* (1986) and Gross *et al* (1988) suggest that rapidly dividing cells such as tumour cells contain high amounts of plasminogen activator activities. While working with rat Yoshida sarcoma (Nulkar *et al* 1983) and lymphosarcoma system of mice it was observed that fibrinolytic system played an important role during propagation of tumour and metastases. It was therefore of interest to examine lymphosarcoma as a source of plasminogen activator. The present paper relates to the purification and characterization of plasminogen activator secreted by lymphosarcoma of mice.

*Corresponding author.

2. Materials and methods

2.1 Materials

CNBr-activated Sepharose 4B, lysine Sepharose and Sephadex G-100 were obtained from Pharmacia Fine Chemicals AB (Sweden). Human urokinase was purchased from Leo Pharmaceutical Laboratories (Copenhagen) while standard tissue-plasminogen activator ($\simeq 500{,}000$ IU/mg fibrinolytic activity) bovine serum albumin, ε-aminocaproic acid and the electrophoresis calibration kit were the products of Sigma Chemical Co., USA. D-Val-Leu-lysine-p-nitroanilide, bovine fibrinogen (S-2251) were obtained from Kabi, Sweden. Rat plasminogen was prepared by affinity chromatography of plasma on lysine-Sepharose 4B (Deutsch and Mertz 1970). All the other chemicals used were of Analar grade obtained from the standard sources.

2.2 Experimental procedures

2.2a *Isolation of tumour cells*: Inbred male Swiss mice (8–10 weeks old) originally obtained from the Jackson Laboratories, Bar Harbour, Maine, were fed on stock laboratory diet and maintained in the laboratory. From a spontaneously developed lymphosarcoma grown in this laboratory (Podval *et al* 1984) an ascitic variant was established as a subline by repeated transfer of tumour cells from peritoneal fluid into the peritoneum of syngeneic Swiss mice (Thakur *et al* 1990). Ascitic lymphosarcoma cells were harvested from mice on the twentyfirst day after initial ip transplantation ($\simeq 10^3$ cells). The tumour cells were harvested in the presence of 10·0 KIU/ml Aprotinin and washed with buffer containing 0·05 M Tris-HCl, pH 7·5, 0·13 M NaCl, 0·025 M KCl, 0·0025 M MgCl$_2$ by centrifugation at 600 g for 5 min. The washing procedure was repeated twice for removal of traces of blood cells.

2.2b *Purification procedure*: The washed cells were suspended in 4 vol of 0·25 M sucrose, 0·05 M Tris-HCl, pH 7·5, 0·1% Triton X-100, homogenized and centrifuged at 20,000 g for 30 min. The clear supernatant fraction was dialyzed against 0·05 M Tris-HCl buffer pH 7·5 overnight at 4°C and precipitated with ammonium sulphate at 35% saturation. The precipitate was suspended in 0·3 M Tris-HCl containing 0·01% Triton X-100 and was sedimented at 25,000 g for 30 min. The supernatant was dialyzed against 0·05 M Tris-HCl pH 8. The most frequently used affinity matrix for purification (Gilbert and Wachsman 1982) procedure is p-amino-benzamidine-Sepharose chromatography which was utilized for the purification of plasminogen activator of lymphosarcoma. The dialyzed supernatant was passed directly onto a column ($0·8 \times 10$ cm) of amino-caproyl-p-aminobenzamidine-Sepharose 4B that had been equilibrated previously in 0·05 M Tris-HCl buffer, pH 7·5 followed by 50 ml washings of the same buffer. The column was then washed sequentially with 50 ml each with (i) 0·05 M Tris-HCl, 0·8 M NaCl, pH 7·5, (ii) 0·05 M Tris-HCl, 1·0 M NaCl, pH 8 and (iii) 0·05 M Tris-HCl, 0·5 M NaCl, pH 8 with a flow rate of 8 ml/h. The washings of the column were collected in 10 ml fractions and checked for protein [E_{280}] and enzyme activity expressed as plasmin units. The enzyme was eluted (1 ml fraction/tube) from the column in 25 ml using 0·2 M arginine contained in 0·05 M Tris-HCl buffer with 0·5 M NaCl and 0·01% Triton A-100, pH 8.

method as described by Electricwala et al (1985) comparing with standard urokinase preparation. The reaction mixture contained 500 μg of purified fibrinogen, 100 μg of plasminogen, 0·2 ml of activator or urokinase (10 IU), 0·05 ml of thrombin (40 NIH units) and 0·5 ml of 0·02 M sodium phosphate buffer, pH 7·4, 0·15 M NaCl and 0·01% Tween 80. After incubation at 37°C the time of complete lysis of the clot formed was recorded. (iii) Amidolytic activity of the activator was measured according to the method of Cheung et al (1986) in a total volume of 1·0 ml. 0·1 ml of S-2251 (0·3 mM final concentration) was added to 0·1 ml activator or urokinase (10 IU) followed by 0·2 ml plasminogen (3 mM) and 0·6 ml of 20 mM phosphate buffer containing 0·1 M NaCl, pH 7·4. The release of *p*-nitroaniline was monitored at 405 nm at 37°C using Gilford spectrophotometer. The activity has been expressed in urokinase equivalent IU/μg by comparison with the International Reference Preparation for urokinase. The activity of urokinase was checked prior to each use. Simultaneously, the activity was compared with standard commercial preparation of t-PA for identifying the nature of activator.

2.2d *Molecular weight determination*: The molecular weight of plasminogen activator was determined by gel filtration on Sephadex G-100. The Sephadex column (1·5 × 60 cm) equilibrated with Tris-HCl buffer, pH 7·5 was calibrated in the presence of standard proteins including cytochrome C (12,500), trypsin (24,000), ovalbumin (45,000) and serum albumin (66,000).

High performance liquid chromatography (HPLC) of PA or standard protein markers was performed on a 0·75 × 60 cm prepacked TSK G 3000 SW column (Pharmacia, LKB, Germany) using 50 mM Tris-HCl, 100 mM NaCl, pH 7·2 at 280 nm.

2.2e *Other analytical procedures*: Protein content was determined by the method of Lowry et al (1951). Polyacrylamide gel electrophoresis (PAGE) was carried out in 7·5% polyacrylamide slab gels (Lugtenberg et al 1975). Electrophoresis on sodium dodecyl sulphate (SDS)-polyacrylamide gel slabs was conducted by the method of Laemmli (1970) using 4–15% polyacrylamide gradient gel, under reducing conditions in the presence of 0·1% 2-mercaptoethanol along with the calibration kit consisting of the standard protein markers of high molecular weights. The gels were stained with Coomassie blue R-250 and destained with 10% glacial acetic acid. In some experiments they were restained with ammoniacal silver solution as described by Wray et al (1981).

2.2f *Binding of activator to fibrin*: Bovine plasminogen-free fibrinogen (500 μg) isolated by lysine-bound Sepharose 4B column was mixed with 200 μg of activator or urokinase, 0·05 NIH units of thrombin and 0·8 ml of 20 mM sodium phosphate buffer 0·1 M NaCl, pH 7·4. At the end of 5 min the clot formed was incubated at 37°C for 1 h followed by sedimentation at 30,000 *g* for 10 min. The activity was

plasminogen and 0·3 mM S-2251 at 37°C for 30 min. The absorbance was read at 405 nm after termination of the reaction with 0·1 ml glacial acetic acid as described by Cheung *et al* (1986).

2.2g *Immunochemical method*: Antibodies against lymphosarcoma activator were raised in female rabbits by three fortnightly subcutaneous injections of purified activator (200 μg) in Freund's adjuvant. Antiserum was prepared from the blood drawn from the ear vein, one week after the last injection and was stored at $-10°C$. Double immunodiffusion analysis was carried out in 1·5% agar gel as described by Ouchterlony and Nilsson (1973). Wells containing samples were allowed to diffuse overnight by placing the plates at 4°C in a humid atmosphere. The precipitin arcs were stained by 0·25% Coomassie blue and photographed.

3. Results

3.1 *Purification of plasminogen activator of lymphosarcoma of ascites cells*

Preliminary work with lymphosarcoma system indicated that 25% of the homogenate contained substantial amount of PA activity as judged by caseinolytic assay procedure and by the clot lysis time method. For purification of the activator from this source, clear supernatant (20,000 g) fraction was prepared, dialyzed and precipitated by ammonium sulphate at 35% saturation. After extensive dialysis, the supernatant was chromatographed on amino-caproyl-p-aminobenzamidine Sepharose 4B. The flow-through of the column contained about 3–4% of PA activity. Washings with buffers containing varying concentrations of sodium chloride essentially served to eliminate some of the contaminants associated with the activator. Figure 1 shows the activity bound to the column following elution by 0·05 M Tris-HCl buffer containing 0·5 M L-arginine, 0·01% Triton X-100 and 0·5 M NaCl at pH 8. Fractions 15–40 were pooled to study enzymatic activity. About 0·3–0·4% of the protein applied to the column was present in the peak of activity showing 163-fold enhancement in the specific activity (9980 units/mg). As much as 28% of the activity could be recovered from the eluate (table 1). The final yield of the purified enzyme varied between 0·17–0·18 mg/108 ml of tumour cells harvested from 12 mice.

The biological activities of the activator with reference to caseinolytic, fibrinolytic and amidolytic activities are summarized in table 2. In the presence of activator the time required for plasma clot lysis was comparable with that of urokinase while the standard t-PA preparation displayed marginal difference. The activator showed as much as 65 and 85% caseinolytic and amidolytic activities respectively when compared with urokinase. The binding of activator or t-PA to fibrin clot showed that 59 and 66% of activity respectively were accessible to binding with fibrin while with urokinase there was a lack of affinity to fibrin. This would suggest that lymphosarcoma activator had relatively high affinity to fibrin when compared to urokinase.

Polyacrylamide slab gel electrophoretic analysis of protein samples from each step of purification is shown in figure 2. Although the resolution of protein bands
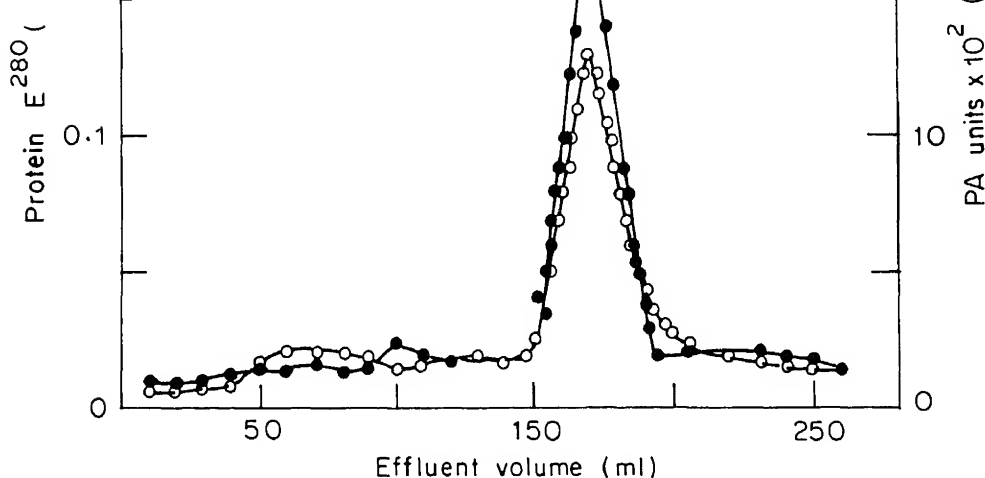
Figure 1. Chromatography in plasminogen activator of lymphosarcoma of ascites on *p*-aminobenzamidine Sepharose.

The clear dialyzed ammonium sulphate precipitated preparation (11·5 ml) was applied to a column of *p*-aminobenzamidine Sepharose equilibrated in 0·05 M Tris-HCl buffer, pH 7·5. After collecting the flow-through of the column ($\simeq 3\%$ of enzyme activity) the column was washed with the equilibrating buffer. The enzyme was eluted subject to three changes of buffer ($\simeq 150$ ml) as described in § 2·2. At the time of elution, 1 ml fractions (corresponding to effluent volume 151–200 ml) were collected and 15 μl aliquots were analysed for enzyme activity. The arrow indicates the start of elution in the effluent.

Table 1. Purification of plasminogen activator of lymphosarcoma of ascites (LS-A).

Fraction	Volume (ml)	Total protein (mg)	Specific activity (units/mg)	Recovery (%)	Purification (fold)
20,000 *g* supernatant	108	81·36	62	100 (4962)	1
Ammonium sulphate precipitate	12	38·04	105	80·4 (3994·2)	1·7
p-Amino-benzamidine-Sepharose eluate	25	0·177	9982	35·6 (1776·8)	163

Enzyme activity (PA) is expressed as plasmin units. A unit of plasmin is defined as the amount of enzyme giving rise to an increase of 1×10^3 extinction per min at 280 nm.

by PAGE showed a few major bands in the crude preparations, only one Coomassie blue stainable band was evident in the *p*-aminobenzamidine peak suggesting the apparent homogeneity of the preparation. This experiment was essentially conducted to show the reduction in the number of protein components

Enzyme	Caseinolytic activity (units/μg)	Amidolytic activity (units/μg)	Fibrinolytic activity (lysis time) (min)	Binding to fibrin (%)
Lymphosarcoma (LS-A)	11·05	0·21	14·0	59·0
Standard t-PA	18·1	0·27	11·5	66·0
Urokinase	17·0	0·25	13·5	0·42

Enzymatic assays were performed as described in § 2·2. Amidolytic activity is expressed as follows. Unit of amidolytic activity = Amount of activity that converts one mol of substrate per second under standard conditions. Per cent binding to fibrin was determined by reading the absorbance (405 nm) following incubation of supernatant with plasminogen and S-2251 for 30 min at 37°C.
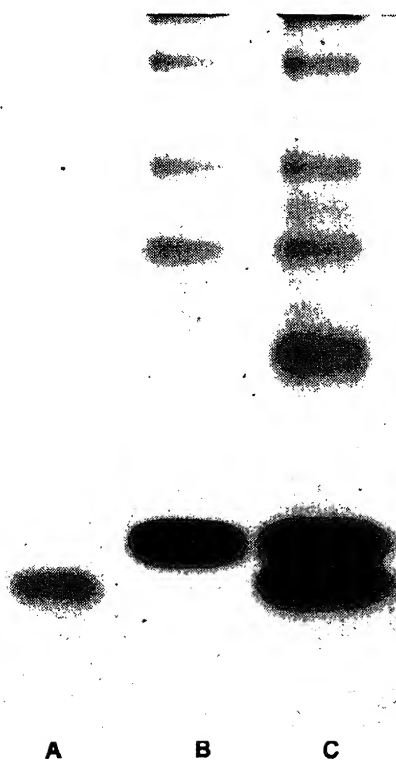
Figure 2. Polyacrylamide slab gel electrophoresis of lymphosarcoma (LS-A) derived plasminogen activator preparations.

Electrophoresis was conducted by the procedure of Lugtenberg *et al* (1975) at 6 mA for 18 h in 7·5% polyacrylamide gels followed by staining with Coomassie blue. (A) Dialyzed 20,000 *g* supernatant fraction (100 μg); (B) ammonium sulphate fractionated extract (100 μg); (C) eluate (15 μg) from *p*-aminobenzamidine-Sepharose 4B peak.

during the purification protocol, particularly following the affinity chromatography. The standard protein markers were therefore not run alongside.

Purity of the samples obtained during the stages of purification was also

purification protocol the number of Coomassie blue-stainable, protein bands were marginally decreased. The stained bands when restained by silver staining procedure (Wray *et al* 1981) did not show any additional sensitivity. The purified preparation of activator in the peak fraction migrated as a single protein band indicating the presence of a single polypeptide chain, the apparent molecular weight of which corresponded to about 66,000 daltons under reducing conditions. Gel filtration of the activator on Sephadex G-100 was also in keeping with this estimated figure derived from standard calibration curve of several proteins of known molecular weights.

The purity of the activator was further checked by running its HPLC profile. The elution pattern is depicted in figure 4 which shows a single protein peak on HPLC confirming its purity. A comparison of its migration with authentic standard proteins also revealed an apparent molecular weight of ~66,000 daltons.

Immunodiffusion analysis was performed to define the nature of lymphosarcoma activator. Antibodies against this activator were produced in rabbit to examine specificity and immunological cross-reactivity between lymphosarcoma activator, Yoshida sarcoma activator (Nulkar and Pawse 1991), standard t-PA and urokinase.
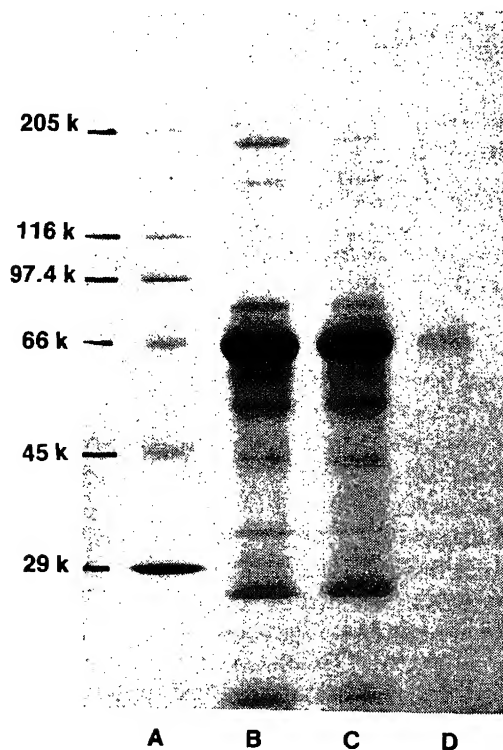
Figure 3. Analysis by SDS-PAGE of activator during stages of purification.

Protein samples were electrophoresed in the presence of 0·1% mercaptoethanol and 0·1% SDS in a 4·5% polyacrylamide gradient gel according to the procedure of Laemmli (1970). (A) Standard marker protein (10 μg); (B) dialyzed 20,000 g supernatant extract (20 μg); (C) ammonium sulphate fractionated extract (15 μg); (D) p-aminobenzamidine Sepharose peak material (10 μg).
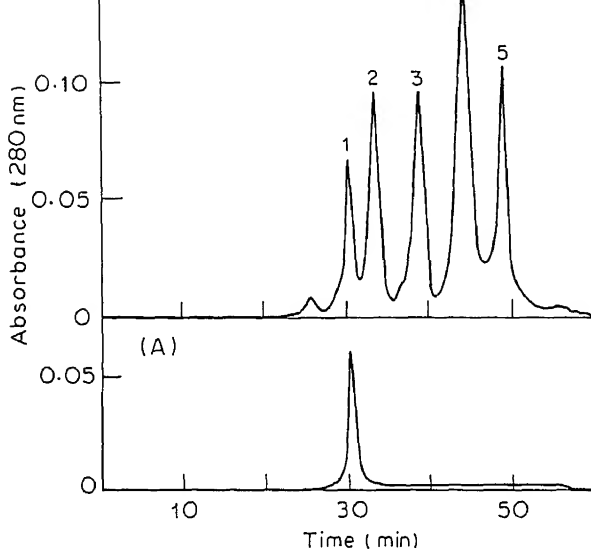
Figure 4. HPLC of t-PA.

Purified LS-A (40 μg) was analysed by HPLC on a TSK G 3000 SW column (0·75 × 60 cm) equilibrated with 50 mM Tris-HCl, 100 mM NaCl, pH 7·2. The same buffer was used to elute the protein at a flow rate of 0·5 ml/min. Absorbance was monitored at 280 nm. (A) Lymphosarcoma activator, (B) Standard mixture of protein (50 μg each) of known molecular weights. (1) Bovine serum albumin (66,000); (2) ovalbumin (45,000); (3) carbonic anhydrase (29,000); (4) chymotrypsinogen (24,000); (5) cytochrome (12,500).

Ouchterlony's double immuno-diffusion analysis revealed that lymphosarcoma activator and Yoshida sarcoma activator cross-reacted with a rabbit antiserum showing a positive precipitin reaction. Similarly, standard t-PA also reacted positively in contrast to urokinase which did not show precipitin arc (figure 5). Serum of the non-immune rabbit did not exhibit precipitin arc with either of the activators or urokinase. These experiments with lymphosarcoma point to its immunological identity with tissue-type plasminogen activator thus differing distinctly from urokinase. The antibodies raised against LS-A did not appear to be highly specific because of the cross-reaction with other tissue-type PAs.

4. Discussion

The results described above reveal that cells of lymphosarcoma contained plasminogen activating potential. The fibrinolytic activity of this activator was assessed by comparing with standard t-PA and urokinase. Reports concerning the purification procedures of plasminogen activators emphasise the use of affinity matrices such as arginine or lysine, Sepharose 4B, Con A-Sepharose 4B, zinc chelate Sepharose 4B and immunoadsorbents (Kluft *et al* 1983; Wallen *et al* 1983; Einarsson *et al* 1985). In the present work purification procedure for
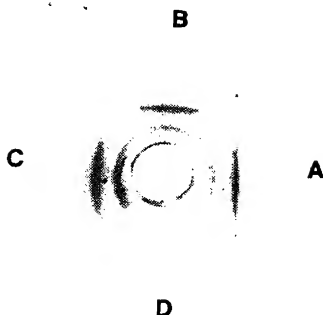
Figure 5. Ouchterlony double immunodiffusion analysis.
Central well, Rabbit antiserum (10 μl from antiserum diluted 4 times with saline). (**A**) Lympho sarcoma activator (20 μg); (**B**) standard tissue plasminogen activator (20 μg); (**C**) Yoshida sarcoma activator (20 μg); (**D**) urokinase (20 μg).

lymphosarcoma activator was devised by affinity chromatography on amino-caproyl-*p*-aminobenzamidine-Sepharose 4B avoiding extremes of pH or denaturing conditions. The loss of activity associated with the tumour cells was minimized by avoiding multistep chromatographic procedures. The peak of enzymatic activity contained about 0·3–0·4% of protein applied to the column. The final preparation showed a specific activity of approximately 9982 IU/mg. The activator has a lower specific activity as compared to the standard t-PA. This may suggest a possible difference in the fibrinolytic potential of this activator and standard t-PA. Variations in specific activities of tissue plasminogen activators in non-malignant cells and a number of cell lines have been reported (6000–90,000 IU/mg) depending on the use of assay procedure. About 0·17 mg of the purified enzyme could be obtained from tumour cells of 12 mice. The lymphosarcoma activator contained a single polypeptide chain of apparent molecular weight of 66,000 daltons as revealed by SDS-PAGE.

Plasminogen activators of variable molecular sizes have been identified by SDS-PAGE technique (Hoal *et al* 1983; Dodd *et al* 1986). The binding studies indicate that the activation of plasminogen gets enhanced in the presence of fibrin by lymphosarcoma activator or standard t-PA but not by urokinase. Immunodiffusion analysis further indicated that antiserum of this activator did not' react with urokinase. The activator behaved in a manner similar to Yoshida sarcoma PA in terms of immunological response and other properties. It would seem that lymphosarcoma derived plasminogen activator activity could be of tissue-type origin as judged by fibrin binding and immunological studies. It is necessary to mention that plasma when incubated with either activator or standard t-PA at 37°C for 24 h displayed negligible breakdown of fibrinogen while urokinase induced significant fibrinogenolysis. Implicit in this discussion are the reports of Katzenberger *et al* (1987, 1988) suggesting the presence of urokinase like plasminogen activator in fast growing cells and showing possible implications in the tumour growth. Recently, correlations of plasminogen activator and plasmin-like activities with fibrinolytic activity have been documented in growth of an

functional roles in invasive processes and thrombolysis respectively (Collen *et al* 1989). Tissue-type of plasminogen activators are hence getting recognition as effective therapeutic agents for treatment of various cardiovascular diseases (Verstraete 1990). Activity of lymphosarcoma activator remains to be evaluated in respect of fibrin-dissolving potential.

References

Cajot J F, Kruithof E K O, Schleuning W D, Sordat B and Bachmann F 1986 Plasminogen activators, plasminogen activator inhibitors and procoagulant analysed in twenty human cell lines; *Int. J. Cancer* **38** 719–727

Cheung A, Lau H K F and Yuen P 1986 A plasminogen activator from benign ovarian cystadenoma: Partial purification and characterization; *Thromb. Res.* **41** 717–729

Collen D C and Gold H K 1990 New developments in thrombolytic therapy; *Thromb. Res. Suppl.* **10** 105–131

Collen D, Lijnen H R, Todd P A and Goa K L 1989 Tissue-type plasminogen activator: A review of its pharmacology and therapeutic use as a thrombolytic agent; *Drug* **38** 346–388

Dano K, Andreasen P A, Grondahl–Hansen J, Kristensen P, Nielsen L S and Skriver L 1985 Plasminogen activators, tissue degradation and cancer; *Adv. Cancer Res.* **44** 139–266

Deutsch D G and Mertz E T 1970 Plasminogen: Purification from human plasma by affinity chromatography; *Science* **170** 1095–1096

Dodd I, Jalalpour S, Southwick W, Newsome P, Browne M J and Robinson J H 1986 Large scale, rapid purification of recombinant tissue-type plasminogen activator; *FEBS Lett.* **209** 13–17

Einarsson M, Brandt J and Kaplan L 1985 Large scale purification of human tissue-type plasminogen activator using monoclonal antibodies; *Biochim. Biophys. Acta* **830** 1–10

Electricwala A, Ling R J, Sutton P M, Griffiths B, Riley P A and Atkinson T 1985 *In vitro* studies on the fibrinolytic, thrombolytic and fibrinogenolytic properties of a tissue plasminogen activator from guinea pig keratocytes; *Thromb. Haemostasis* **53** 200–203

Gilbert L C and Wachsman J T 1982 Characterization and partial purification of the plasminogen activator from human neuroblastoma cell line, sk-n-sh; *Biochim. Biophys. Acta* **704** 450–460

Gross J L, Behrens D L, Mullins D E, Kornblith P L and Dexter D L 1988 Plasminogen activator and inhibitor activity in human glioma cells and modulation by sodium butyrate; *Cancer Res.* **48** 291–296

Hajjar K A and Hamel N M 1990 Identification and characterization of human endothelial cell membrane binding sites for tissue-plasminogen activators and urokinase; *J. Biol. Chem.* **265** 2908–2916

Hekman C M and Loskutoff D J 1987 Fibrinolytic pathways and endothelium; *Semin. Thromb. Hemostasis* **13** 514–527

Hoal E G, Wilson E L and Dowdle E B 1983 The regulation of tissue-plasminogen activator activity by human fibroblasts; *Cell* **34** 273–279

Johnson A J, Kline D J and Alkjaersig N 1969 Determination of caseinolytic activity for plasminogen activation; *Thromb. Diath. Haemorrh.* (*Stuttg.*) **21** 259–272

Katzenberger G J, Lea M A and Suriender Kumar 1987 Presence of urokinase like plasminogen activator in fast growing cells; *Fed. Proc.* **46** 1963

Katzenberger G J, Lea M A and Suriender Kumar 1988 Plasminogen activator activity of rat hepatomas; *Fed. Am. Soc. Exp. Biol.* **2** A388

Kluft C, Van Wezel A L, Van der Velden C A M, Emeis J J, Verheijen J H and Wijngaards G 1983 The molecular form of α_2-antiplasmin with affinity for plasmin is selectively bound to fibrin by factor XIII; in *Advances in biotechnological processes* (eds) A Mizrahi and A L Van Wezel (New York: Alan R Liss) pp 97–110

Laemmli U K 1970 Cleavage of structural proteins during the assembly of the head of bacteriophage T_4; *Nature* (*London*) **227** 680 685

Loskutoff D J 1988 Type 1 plasminogen activator inhibitor and its potential influence on thrombolytic therapy; *Semin. Thromb. Hemostasis* **14** 100–109

Lugtenberg B, Meijers J, Peter R, Vander Hock P and Van Alpem L 1975 Electrophoretic resolution on the major outer membrane protein of *E. coli* K12 into four bands; *FEBS Lett.* **58** 254–258

Nulkar M W, Chanderkar L P, Pawse A R and Nadkarni G B 1983 Possible methylation of plasma proteins involved in coagulation and fibrinolysis; *Indian J. Biochem. Biophys.* **20** 338–343

Nulkar M W and Pawse A R 1991 Isolation and purification of plasminogen activator from Yoshida ascites sarcoma of rats; *Indian J. Biochem. Biophys.* **28** 46–51

Ouchterlony O and Nilsson L A 1973 *Handbook of experimental immunology* 2nd edition (ed.) D W Weir (Oxford: Blackwell) Chapter 19, pp 1–39

Poduval T B, Seshadri M and Sundaram K 1984 Enhanced host resistance to transplantable murine lymphosarcoma in Swiss mice by combined immunostimulation with BCG and polyinolinic-polycytidylic acid; *J. Natl. Cancer. Inst.* **72** 139–144

Preger M D, Nelson N F, Cieplak W and Dacus S C 1986 Characterization of plasminogen activator from 2 human renal-carcinoma cell lines and effect of differentiation inducing agents; *Proc. Am. Assoc. Cancer Res.* **27** 3

Ranby M and Brandstrom A 1988 Biological control of tissue plasminogen activator-mediated fibronolysis; *Enzyme* **40** 130–143

Rijken D C and Collen D 1981 Purification and characterization of the plasminogen activator secreted by human melanoma cells in culture; *J. Biol. Chem.* **256** 7035–7041

Saksela O 1985 Plasminogen activation and regulation of pericellular proteolysis; *Biochem. Biophys. Acta* **823** 35–65

Thakur V S, Seshadri M, Poduval T B, Shah D H and Sundaram K 1990 Allosensitisation induced suppression of various murine tumors: Role of non-H-2 antigens in antitumour immunity; *Indian J. Exp. Biol.* **28** 706–710

Tozser J, Hamvas A, Rady P, Kertai P and Elodi P 1989 Plasminogen activator and plasminlike activities in experimental rat tumours; *Acta Biochim. Biophys. Hung.* **24** 119–129

Vansetten G B, Salonen E M, Vaheri A, Beuerman R W, Hietanen J, Tarkkanen A and Tervo T 1989 Plasmin and plasminogen activator activity in tear fluid during corneal wound healing after anterior keratectomy; *Curr. Eye Res.* **8** 1293–1298

Verstraete M 1990 Newer thrombolytic agents; in *Cardiology Update Reviews for Physicians* (ed.) E. Rapaport (New York, Amsterdam, London: Elsevier) pp 99–111

Wray W, Boulikas T, Wray V P and Hancock R 1981 Silver staining of proteins in polyacrylamide gels; *Anal. Biochem.* **118** 197–203

Wallen P, Pohl G, Bergsdorf N, Ranby M, Ny T and Jornvall H 1983 Purification and characterization of a melanoma cell plasminogen activator; *Eur. J. Biochem.* **132** 681–686

Relationship between fatty acid binding proteins, acetyl-CoA formation and fatty acid synthesis in developing human placenta

TANYA DAS, GAURISANKAR SA, ANUP K BANDYOPADHYAY
and MANJU MUKHERJEA*

Department of Biochemistry, University College of Science, University of Calcutta, 35, Ballygunge Circular Road, Calcutta 700 019, India

Abstract. The relationship between fatty acid binding proteins, ATP citrate lyase activity and fatty acid synthesis in developing human placenta has been studied. Fatty acid binding proteins reverse the inhibitory effect of palmitoyl-CoA and oleate on ATP citrate lyase and fatty acid synthesis. In the absence of these inhibitors fatty acid binding proteins activate ATP citrate lyase and stimulate $[1-^{14}C]$ acetate incorporation into placental fatty acids indicating binding of endogenous inhibitors by these proteins. Thus these proteins regulate the supply of acetyl-CoA as well as the synthesis of fatty acids from that substrates. As gestation proceeds and more lipids are required by the developing placenta fatty acid binding protein content, activity of ATP citrate lyase and rate of fatty acid synthesis increase indicating a cause and effect relationship between the demand of lipids and supply of precursor fatty acids during human placental development.

Keywords. ATP citrate lyase; fatty acid binding proteins; fatty acid synthesis; placenta; correlation.

1. Introduction

During embryogenesis when demand of lipid is very high to supply energy and to synthesize cellular membranes for the developing placenta, more lipids and precursor fatty acids are to be synthesized. The rate of fatty acid synthesis and total activities of the synthesizing enzymes are positively correlated in several animal systems. In chicken liver, fatty acid synthesis and the activities of acetyl-CoA carboxylase (Goodridge 1973), malic enzyme and ATP citrate lyase (Goodridge 1968; Silpananta and Goodridge 1971) are correlated when neonatal chicks are fed. Activities of these enzymes are determined largely by the relative concentrations of enzyme activators and inhibitors as well as by the composition of long chain fatty acids and acyl-CoA pool. The long chain fatty acids and their CoA esters may be compartmentalized in the cell and changes in their distribution might affect lipogenesis. It has been suggested that intracellular trafficking of these inhibitors might be affected partly by their binding to fatty acid binding proteins (FABPs) (Spener and Mukherjea 1990). These proteins belong to a class of low molecular mass (14–15 kDa) non-enzymic proteins which bind hydrophobic ligands and are abundantly present in the cytosol of many mammalian cells (Bass 1985; Sweetser *et al* 1987; Das *et al* 1989). FABPs are distinct from the recently discovered 10 kDa

acids (Mogensen *et al* 1988). Besides having an important role in the cellular transport and metabolism of fatty acids, these proteins have been reported to regulate many fatty acid synthesizing enzymes (Paulussen and Veerkamp 1990; Spener *et al* 1989) either by directly enhancing delivery of substrates in a usable form, targeting substrates to particular metabolic fates or eliminating inhibitory effects of long chain fatty acids.

It is known that synthesis of palmitic acid from malonyl-CoA and acetyl-CoA is catalyzed by fatty acid synthase, a multienzyme complex. The extra mitochondrial acetyl-CoA is supplied by ATP citrate lyase and the reducing power required for fatty acid synthesis is furnished mainly by glucose-6-phosphate dehydrogenase (G6PD). All these enzymes get inhibited by fatty acids and their CoA esters (Glatz and Veerkamp 1985; Kawaguchi and Bloch 1974). Earlier reports from this laboratory show that FABPs protect G6PD from the detrimental effect of fatty acids and fatty acyl-CoA esters in human placenta and fetal tissues (Das *et al* 1988, 1989; Sa *et al* 1989). The present work aims at studying the relationship between FABPs, ATP citrate lyase activity and fatty acid synthesis in developing human placenta.

2. Materials and methods

ATP, bovine serum albumin (BSA), DEAE-cellulose, malate dehydrogenase, malonyl-CoA, NADH, oleic acid, palmitoyl-CoA (PAL-CoA) and Sephacryl S-200 were purchased from Sigma Chemical Co., St. Louis, Mo, USA. [1-^{14}C] acetate was a gift from Dr K D Mukherjee, Federal Centre of Lipid Research, Munster, Germany. All other chemicals used were of analytical grade and were purchased locally.

Human placentas of gestational ages between 5–30 weeks were collected from patients undergoing legal abortion either by suction or *via* hysterotomy from the Department of Obstetrics and Gynecology, National Medical College and Hospital, Calcutta. Placentas above 30 weeks were obtained from patients delivering still born babies and term placentas were collected at the time of parturition or *via* caesarean section from different hospitals in Calcutta. Tissues were collected within 15 min of operation/delivery and kept in ice. Gestational ages were calculated from the period of amenorrhea and by crown-rump length of the fetus (Chaudhuri *et al* 1982).

2.1 *Preparation of human placental supernatant*

Placentas were excised, fragmented and washed with 0·9% NaCl to remove blood. Fragments were homogenized in 10 mM Tris-HCl buffer (pH 8·5) in a Teflon glass homogenizer and centrifuged at 105,000 g for 1 h. The supernatant was heated at 50°C for 20 min, shaken vigorously with 25% butanol (v/v) for 1 min and centrifuged at 36,000 g for 30 min to remove lipids and denatured proteins. The delipidated supernatant was lyophilized for complete removal of butanol.

2.2 *Preparation of human placental FABPs*

Isoforms of human placental FABPs (DE-I, DE-II and DE-III) were purified by the

procedure as described by Das *et al* (1988). The proteins were routinely characterized by UV spectroscopy and by SDS-PAGE to ensure single band of about 14,000 molecular weight and were stored at 0–4°C as lyophilized powder.

2.3 *Effect of PAL-CoA, oleate and FABPs on ATP citrate lyase*

Human placental cytosol (105,000 *g* supernatant) was prepared in 0·25 M sucrose. ATP citrate lyase activity was measured in a Hitachi spectrophotometer, Model U 3210, following the decrease in extinction at 340 nm according to the method of Takeda *et al* (1969). Inhibition of the enzyme was studied in the reaction mixture in presence of different concentrations of PAL-CoA or oleate. The isoforms of FABPs were added separately in the reaction mixture containing the inhibitors.

2.4 *Fatty acid synthesis*

Tissue slices of human placenta were incubated with 0·25 μCi of [1–^{14}C] acetate at 37°C for 3 h and homogenized with 8 ml of chloroform/methanol (2:1) mixture. The homogenate was kept at room temperature for 4–6 h under N_2 with occasional shaking. After centrifugation the chloroform layer containing lipids was washed with 0·7% NaCl and concentrated in the presence of N_2. Individual lipids were separated by thin layer chromatography (TLC) and identified by using standard lipids. Fatty acid synthesis was studied by observing the amount of radioactivity incorporated throughout the gestation. Role of FABPs, PAL-CoA and oleate on fatty acid synthesis were examined.

2.5 *Estimation of protein*

Protein was estimated according to the method of Lowry *et al* (1951) using bovine serum albumin as standard.

2.6 *Statistical analysis*

Data were treated statistically using student's *t* test. In order to study the extent of correlation between any two of the relevant variables involved, correlation coefficients were computed. The variability of the data was presented as mean $\pm$ SEM. Differences at $P < 0.05$ were considered to be significant.

3. Results

3.1 *Modulation of ATP citrate lyase activity by PAL-CoA, oleate, and FABPs*

Results of figure 1 indicate that human placental ATP citrate lyase is sensitive to PAL-CoA and oleate. Less than 75 μM PAL-CoA or 100 μM oleate completely inhibit the enzyme. Inhibition of this enzyme has been found to be a function of PAL-CoA and oleate concentrations. DE-II and DE-III fractions of FABPs protect the placental ATP citrate lyase against such inhibitions (figure 1). To assess the
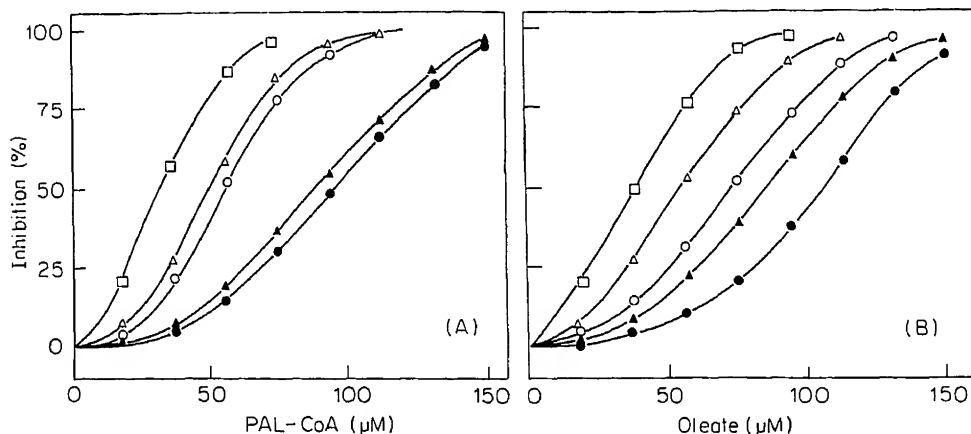
Figure 1. Protection of human placental ATP citrate lyase against PAL-CoA (A) and oleate (B) inhibition by various amounts of FABPs. (□) Control; (○) 15 μg DE-II; (△) 15 μg DE-III; (●) 25 μg DE-II; (▲) 25 μg DE-III. Assay conditions are those described under § 2.

relative protection afforded by FABPs, concentrations of PAL-CoA or oleate required for 50% inhibition of this enzyme in the presence and absence of FABPs have been calculated. In the presence of 25 μg of DE-II, 2·25 and 1·8 times higher amounts of PAL-CoA and oleate, respectively were required for 50% inhibition. To achieve the same protection, about the same amount of DE-III was required in the case of PAL-CoA inhibition but more than one and half times of DE-III was needed in the case of oleate. DE-I fraction of FABP showed no such protective effect.
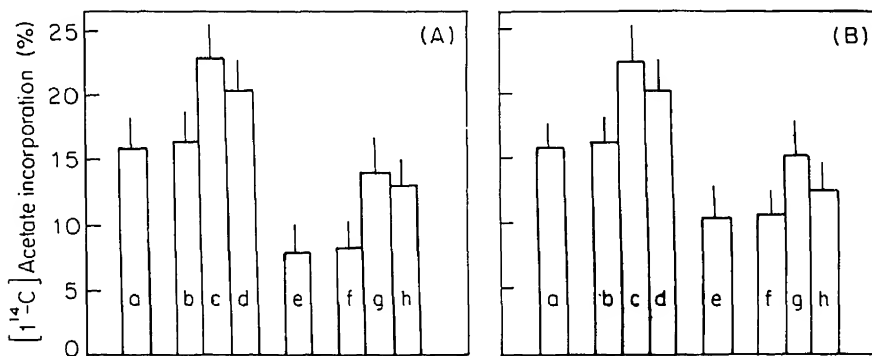
Figure 2. Role of FABPs in regulating the inhibition of human placental fatty acid synthesis by PAL-CoA (A) and oleate (B). Control (a); with 15 μg DE-I (b)/DE-II (c)/DE-III (d) per g tissue; with 25 μM PAL-CoA/oleate (e); with 25 μM PAL-CoA/oleate and 15 μg DE-I (f)/DE-II (g)/DE-III (h) per g tissue. Values are mean ± SEM of 3 sets of experiments.

3.2 *Role of FABPs in regulating fatty acid synthesis*

PAL-CoA and oleate (figure 2) inhibit fatty acid synthesis. In the presence of a fixed

inhibition in the case of oleate. When no inhibitor is present, FABPs increase fatty acid synthesis.

3.3 Ontogeny of human placental FABPs

Table 1 shows the ontogenic profiles of FABPs in human placenta. Concentration of DE-II remains maximum throughout the gestation, while that of DE-III is minimum. From early stage of intrauterine development, levels of all these FABPs increase sharply up to 25–30 weeks of gestation. The rate of increase slows down afterwards.

3.4 Development of ATP citrate lyase activity and fatty acid synthesis in human placenta

Table 2 indicates that ATP citrate lyase activity is discernable in human placenta as early as at 5–10 weeks of gestation. Enzyme activity increases in parallel with gestation up to 25–30 weeks but shows a decreasing trend at term. The amount of $[1-^{14}C]$ acetate incorporation into placental fatty acids increases steadily from 5–10 weeks of gestation up to term, though the rate of fatty acid synthesis slows down slightly after 25–30 weeks.

3.5 Correlation coefficients between the developmental profiles of FABFs, ATP citrate lyase and fatty acid synthesis

The results of table 3 show that the developmental patterns of FABP levels, ATP

Table 1. Ontogenic profile of different fractions of FABP in human placenta.

| Group | Gestational ages (weeks) | Amount of FABP* in different fractions | | | |
		DE-I	DE-II	DE-III	Total
I	5–10	3·1 ± 0·6	9·8 ± 1·6	1·4 ± 0·3	14·3 ± 0·9
II	10–15	4·8 ± 0·9	11·9 ± 1·0	2·2 ± 0·5	18·9 ± 1·2
III	15–20	6·6 ± 1·1	16·6 ± 1·4	3·0 ± 0·7	26·2 ± 1·4
IV	20 25	8·4 ± 1·6	21·1 ± 1·9	3·8 ± 0·8	33·3 ± 1·7
V	25–30	10·0 ± 1·2	24·7 ± 2·1	4·6 ± 1·3	39·3 ± 2·1
VI	30–35	10·6 ± 1·0	25·7 ± 2·6	5·2 ± 1·0	41·5 ± 3·0
VII	35–40	10·8 ± 1·5	26·3 ± 2·0	5·6 ± 1·1	42·7 ± 2·4

Values are mean ± SEM of 3 sets of experiments in each case.

Group II vs I		—	—	—	$P < 0.05$
Group III vs II		—	$P < 0.05$	—	$P < 0.025$
Group IV vs III		—	—	—	$P < 0.05$
Group V vs IV		—	$P < 0.05$	—	—
Group VI vs V		—	—	—	—
Group VII vs VI		—	—	—	—

*mg FABP/mg protein $\times 10^{-3}$.

Group	Gestational ages (weeks)	ATP citrate lyase (nM NADP produced/ min/mg protein)	Fatty acid synthesis (% [1–^{14}C] acetate incorporated)
I	5–10	2·01 ± 0·27	3·95 ± 0·35
II	10–15	2·97 ± 0·43	7·10 ± 0·54
III	15–20	4·39 ± 0·60	9·18 ± 0·74
IV	20–25	7·21 ± 0·82	12·11 ± 0·59
V	25–30	12·80 ± 1·12	15·78 ± 0·86
VI	30–35	11·74 ± 1·03	15·48 ± 1·25
VII	35–40	10·26 ± 0·96	14·56 ± 0·98

Values are mean ± SEM of 3 sets of experiments in each case.

Group	II vs I	—	$P < 0.005$
Group	III vs II	—	$P < 0.05$
Group	IV vs III	$P < 0.05$	$P < 0.025$
Group	V vs IV	$P < 0.01$	$P < 0.02$
Group	VI vs V	—	—
Group	VII vs VI	—	—

Table 3. Correlation co-efficients between the developmental profiles of FABPs, ATP citrate lyase activity and fatty acid synthesis in human placenta.

Correlation between	Correlation co-efficient (r)	Significant values (P)
FABPs vs ATP citrate lyase	0·950	$P < 0.001$
ATP citrate lyase vs fatty acid synthesis	0·973	$P \ll 0.001$
Fatty acid synthesis vs FABPs	0·983	$P \ll 0.001$

citrate lyase activity and fatty acid synthesis are highly correlated ($P < 0.001$) in human placenta.

4. Discussion

Placenta is considered to be the sole purveyor of all fetal needs and regulator of the development and maintenance of the fetus. It also serves as an important organ for lipid metabolism for the fetus until the fetal liver becomes more competent. Thus any regulation of placental lipid metabolism must be important for the fetal health. In view of their remarkable abundance in the placental cytosol (3–4%) FABPs may play a major role in regulating G6PD-fatty acid interaction (Das et al 1988). The present study indicates that FABPs regulate ATP citrate lyase which supplies acetyl-CoA, and also influence [1–^{14}C] acetate incorporation into fatty acids. Human placental FABPs may thus take part in overall metabolic regulation of fatty acid synthesis by affecting substrate and cofactor production as well as fatty acid synthesis itself. Although albumin and other proteins have been reported to cause similar effect (Goodridge 1972; Sa et al 1989), the demonstration that FABPs are

effect may be specific in the intact cell. Such effect of FABPs on the inhibition of fatty acid synthesis is attributable to binding of long chain fatty acids and their CoA thioesters rather than a direct effect of the proteins on the lipogenic enzymes. In the absence of externally added inhibitors FABPs stimulate ATP citrate lyase and fatty acid synthesis may be by binding endogenous inhibitors. This conjecture is supported by the finding that almost similar enhanced activity of controls are obtained when dialyzed preparations were used to remove the ligand inhibitors. The actions of fatty acids and fatty acyl-CoAs on the native enzyme structure of ATP citrate lyase are not clear yet. It may be due to the change of active to inactive oligomeric conformation of the enzyme by binding of the inhibitors. Protective effects of DE-II and DE-III have been found to be almost similar when the inhibitor used was PAL-CoA, however, in the case of oleate DE-II was more effective. Such differences may be due to different affinities of these proteins for palmitic acid and oleic acid (Das *et al* 1988).

Correlation coefficients of developmental profiles of FABPs, ATP citrate lyase activity as well as fatty acid synthesis indicate that these parameters are highly correlated in human placenta. Thus with advancement of pregnancy, demand of lipids increases with a parallel increase in FABP content to supply more fatty acids for lipid synthesis. It is known that fetal fatty acids can be derived from two sources: from maternal plasma, in the form of free fatty acids or from placental breakdown of triglycerides and phospholipids, or from direct placental fatty acid synthesis (Beaconsfield and Ginsburg 1979). Thus placental FABPs not only serve the placental need but also indirectly help the fetus to meet its demand of fatty acids for lipogenesis. Near term, when amount of fetal liver FABPs becomes sufficient and this organ can synthesize ample fatty acids, need of placental FABPs subsides. The rate of increase in FABP content therefore slows down in placenta near term whereas the same remains constant up to birth in fetal liver (Das *et al* 1989).

Acknowledgements

References

Bass N M 1985 Function and regulation of hepatic and intestinal fatty acid binding protein; *Chem. Phys. Lipids* **38** 95–114

Beaconsfield P and Ginsburg J 1979 Carbohydrate, fat and protein metabolism in the placenta: a clinicians view; in *Placenta: a neglected experimental animal* (eds) P Beaconsfield and C Villie (Oxford: Pergamon Press) pp 34–62

Chaudhuri D, Kushari J and Mukherjea M 1982 Occurrence of phosphodiesterase IV in the developing human brain, liver and placenta; *Eur. J. Obstet. Gynecol. Reprod. Biol.* **13** 309-316

Das T, Sa G and Mukherjea M 1989 Human fetal liver fatty acid binding proteins: Role on glucose 6 phosphate dehydrogenase activity; *Biochim. Biophys. Acta* **1002** 164–172

Das T, Sa G, Ghosh P K, Mukhopadhyay D and Mukherjea M 1989 Isolation of fatty acid binding proteins from human fetal intestine and heart: Comparison with corresponding hepatic proteins; *Med. Sci. Res.* **17** 985–986

Glatz J F C and Veerkamp J H 1985 Intracellular fatty acid binding proteins; *Int. J. Biochem.* **17** 13–22

Goodridge A G 1968 Citrate-cleavage enzyme, malic enzyme and certain dehydrogenases in embryonic and growing chicks; *Biochem. J.* **108** 663–666

Goodridge A G 1972 Regulation of the activity of acetyl coenzyme A carboxylase by palmitoyl coenzyme A and citrate; *J. Biol. Chem.* **247** 6946–6952

Goodridge A G 1973 On the relationship between fatty acid synthesis and the total activities of acetyl coenzyme A carboxylase and fatty acid synthetase in the liver of prenatal and early postnatal chick; *J. Biol. Chem.* **248** 1932–1938

Kawaguchi A and Bloch K 1974 Inhibition of glucose 6 phosphate dehydrogenase by palmitoyl coenzyme A; *J. Biol. Chem.* **249** 5793–5800

Lowry O H, Rosebrough N J, Farr A L and Randall R J 1951 Protein measurement with the folin phenol reagent; *J. Biol. Chem.* **193** 265–275

Lunzer M A, Manning J A and Ockner R K 1977 Inhibition of rat liver acetyl coenzyme A carboxylase by long chain acyl coenzyme A and fatty acid; *J. Biol. Chem.* **252** 5483–5487

Mogensen I B, Schulenberg-Schell H, Hansen H O, Spener F and Knudsen J 1988 A novel acyl-CoA binding protein from bovine liver. Effect on fatty acid synthesis; *Biochem. J.* **241** 189–192

Paulussen R J A and Veerkamp J H 1990 Intracellular fatty acid binding proteins, characteristics and function; *Sub-Cell. Biochem.* **16** 175–226

Sa G, Das T and Mukherjea M 1989 Purification and characterization of fatty acid binding proteins from human fetal lung; *Exp. Lung Res.* **15** 619–634

Silpananta P and Goodridge A G 1971 Synthesis and degradation of malic enzyme in chick liver; *J. Biol. Chem.* **246** 5754–5761

Spener F, Borcher T and Mukherjea M 1989 On the role of fatty acid binding proteins in fatty acid transport and metabolism; *FEBS Lett.* **244** 1–5

Spener F and Mukherjea M 1990 Nonenzymatic proteins mediating intracellular lipid transport and metabolism: current status and emerging trends; *Sub-Cell. Biochem.* **16** 1–19

Sweetser D A, Heuckeroth R O and Gordon J I 1987 The metabolic significance of mammalian fatty acid binding proteins; *Annu. Rev. Nutr.* **7** 377–359

Takeda Y, Suzuki F and Iwoue H 1969 ATP citrate lyase (citrate-cleavage enzyme); *Methods Enzymol.* **13** 153–160

Effect of griseofulvin on lipid composition and membrane integrity in *Microsporum gypseum*

INDU BALA CHUGH, M P GUPTA and G K KHULLER*

Department of Biochemistry, Postgraduate Institute of Medical Education and Research, Chandigarh 160 012, India

Abstract. The effect of griseofulvin on lipid constituents and membrane permeability of *Microsporum gypseum* has been investigated. Mycelia grown in medium containing griseofulvin (IC_{50} concentration) possessed a lower content of total lipids, phospholipids and sterols. This inhibitory effect was further supported by decreased incorporation of [^{14}C] acetate in total lipids, total phospholipids and sterols. Decrease in total phospholipids was also reflected to a varying extent in all individual phospholipids. An increase in the unsaturated to saturated fatty acid ratio was observed in mycelia grown in medium containing griseofulvin. Membrane permeability was affected by griseofulvin as shown by increased K^{+}-efflux and greater leakage of intracellular [^{32}P] labelled components from prelabelled cells. Our results suggest that the antifungal activity of griseofulvin is partially due to its secondary effect on lipid constituents of *Microsporum gypseum*.

Keywords. *Microsporum gypseum*; griseofulvin; phospholipids; membrane integrity.

1. Introduction

Griseofulvin is an orally effective antimicrobial agent for superficial fungal infections of the skin (Shah 1980). It is thought to be essentially fungistatic rather than fungicidal (Kerridge 1986) and its fungistatic action has been suggested to be due to interference with the synthesis of cell wall chitin (Blank *et al* 1960). This view was later rejected due to a lack of correlation between alterations in chitin level and the growth inhibitory action of griseofulvin. McNall (1960) observed a partial reversal of griseofulvin action by purines, pyrimidines and other nucleotides, thus suggesting the fungistatic action through direct interference with the synthesis of nucleic acids. However, Weinstein and Blank (1960) reported that griseofulvin is bound to lipids within the cell but not to RNA or DNA. Although the growth inhibitory activity of a number of antimycotics has been shown to be mediated through their interactions with lipid constituents (Kerridge 1986), no study has been initiated to examine the effect of griseofulvin on lipid constituents in dermatophytes. In the present paper, we have studied alterations caused by griseofulvin in lipid composition of *Microsporum gypseum*. As lipids are important membrane components, further experiments were conducted to examine the effect of the drug on membrane permeability and activity of membrane-bound enzymes.

2. Materials and methods

2.1 *Materials*

Griseofulvin and adenosine 3′, 5′-cyclic monophosphate were procured from Sigma

*Corresponding author.

Chemical Co., St. Louis, Mo, USA. *Naja naja* snake venom was obtained from V P
Chest Institute, New Delhi. Aminonaphtholsulphonic acid and trichloroacetic acid,
2, 5-diphenyloxazole (PPO) and 1, 4-bis (5-phenyloxazolylbenzene) (PPOP) were
purchased from Sisco Research Laboratories Pvt. Ltd., Bombay and peptone was
purchased from Centron Research Laboratories, Bombay. $[^{14}C]$ acetate (sp.
activity, 60.3 mCi/mmol) was obtained from the Bhabha Atomic Research Centre,
Bombay.

2.2 *Organism and growth conditions*

M. gypseum (NCPF 412) obtained from the Mycological Reference Laboratory,
School of Medicine, London, was maintained on Sabouraud's dextrose-agar slants
(pH 5.4–5.6) at 27°C. The culture was regrown in liquid Sabouraud's medium (pH
5.4–5.6) containing 4% glucose and 1% peptone on a shaker (60 RPM) at 27°C. To
determine IC_{50} and minimum inhibitory concentration (MIC) doses of griseofulvin,
cultures were grown in the presence of the drug at concentrations ranging from 0·1
to 0·8 μg/ml. The drug was dissolved in ethanol (0·2 mg/ml) and the concentration
of the solvent in growth medium did not exceed 0·1%, at which fungal growth or
lipid constituents remain unaffected (Bansal and Khuller 1981). IC_{50} and MIC
doses were derived from the graph prepared by plotting dry weight of mycelia at
mid log phase (96 h old culture) versus concentration of griseofulvin in the medium.

2.3 *Lipid composition*

Effect of griseofulvin in growing mycelia was studied by growing *M. gypseum* in
Sabouraud's broth containing IC_{50} dose of the drug (0·21 μg/ml). Control cultures
were grown in the same medium without drug. Cells were harvested at mid-log
phase (after 96 h) to analyse various lipid constituents. Lipids were extracted from
mycelia by the method of Folch *et al* (1957) and were quantitated gravimetrically.
Total phospholipids (TPL) were estimated by measuring inorganic phosphorus
content in lipid extracts according to the method of Marinetti (1962). Sterols were
extracted by the method of Singh *et al* (1979) and measured by the method of
Zlatkis *et al* (1953).

2.4 *Identification of lipid components*

Individual phospholipids were separated on silica gel H plates by using
chloroform: methanol:ammonia (65:25:4, v/v) solvent system as described by
Kates (1972). Individual phospholipid components were localized by staining with
iodine vapours and quantitated by measuring lipid phosphorus. To assay
phospholipid fatty acids, these were converted to methyl esters by transesterification
with methanol and thionyl chloride according to the modified method of
Prabhudesai (1978) and analysed on 5700 AIMIL Nucon gas chromatograph by
using a column containing 20% diethylene glycol succinate (DEGS) on 60–80 mesh
Chromosorb W. Fatty acids were identified by comparing their retention time with

2.5 *Incorporation of [^{14}C] acetate in lipids of M. gypseum*

The effect of griseofulvin on lipid biosynthesis in mid-log phase mycelia of *M. gypseum* was studied by the method of Khuller *et al* (1984). Mid-log phase mycelia were harvested and suspended in sterile 10 mM citrate phosphate buffer (pH 6·5) containing MIC dose (0·5 μg/ml) of griseofulvin and preincubated on a shaker at 27°C for 3 h. To study the biosynthesis of total lipids (TL), TPL and sterols, mycelia were further incubated with [^{14}C] acetate (1·5 μCi/g/15 ml) at 27°C for 0 and 120 min. After incubation with [^{14}C] acetate, mycelia were separated, washed to remove adsorbed radioactivity and subjected to lipid extraction (Folch *et al* 1957) or sterol extraction (Singh *et al* 1979). Phospholipids were separated from neutral lipids by thin-layer chromatography of TL using acetone as the solvent. Radioactivity in TL, TPL and sterols fractions was determined using toluene based scintillation fluid.

2.6 *Measurement of K^+-efflux*

Membrane permeability of drug-treated mycelia was monitored by studying K^+-efflux. Mid log phase untreated mycelia were transferred into 10 mM citrate phosphate buffer (pH 6·5). Total intracellular K^+ content and the level of K^+ in filtrate was measured on a Na^+/K^+ Analyser 4020 (Orion Research, USA). Griseofulvin was then added to the cell suspension at 15 X MIC (7·5 μg/ml) and 30 X MIC (15 μg/ml) doses and percentage stimulation in K^+-efflux was measured after 15, 30, 45 and 60 min of incubation with the drug. The amount of K^+ release was expressed as a percentage of total intracellular K^+ as described by Chen *et al* (1977).

2.7 *Leakage of [^{32}P] labelled material from prelabelled cells*

Mid-log phase mycelia were harvested, transferred to fresh medium containing [^{32}P] labelled orthophosphoric acid (0·5 mCi/g cells in 100 ml growth medium) and incubated on a shaker at 27°C for 3 h. Mycelia were then isolated, washed thoroughly with chilled isotonic saline and transferred again into fresh medium containing griseofulvin at a dose of 10 X MIC (5 μg/ml) or only carrier solvent (ethanol 0·5%, v/v). Aliquots of the mycelial suspension were removed after 0, 1, 2, 3 and 4 h of incubation with the drug and filtrate was collected and used for monitoring the leakage of intracellular [^{32}P] by measuring radioactivity. Percentage release of intracellular [^{32}P] was calculated as described earlier (Gupta *et al* 1991).

2.8 *Assay of membrane bound enzymes*

Mid-log phase mycelia were harvested, and incubated in fresh sterile Sabouraud's medium containing $10 \times$ MIC of griseofulvin (5 μg/ml) for 3 h at 27°C. Mycelia were separated again, washed with isotonic saline and resuspended (approximately 1 g cell/5 ml) in 40 mM Tris HCl buffer (pH 7·5) and disrupted by sonication in a

Parameter	Control cultures	Griseofulvin grown
	(mg/g dry weight)	
Total lipids	86·14 ± 10·23	58·88 ± 2·57**
Total phospholipids	16·24 ± 0·13	9·39 ± 1·5**
Total sterols	14·60 ± 0·05	9·10 ± 1·6**
Lysophosphatidylcholine	1·91 ± 0·05	1·26 ± 0·33**
Phosphatidylserine + Phosphatidylinositol	3·53 ± 0·80	1·94 ± 0·19*
Phosphatidylcholine (PC)	6·17 ± 0·70	4·12 ± 0·32**
Phosphatidylethanolamine (PE)	2·88 ± 0·27	0·97 ± 0·21***
Unknown phospholipids	1·70 ± 0·11	1·00 ± 0·34*
PC/PE ratio	2·14	4·24

Values are mean ± SD of three independent batches analysed in duplicate. $*P < 0.05$; $**P < 0.01$; $***P < 0.001$; IC_{50}–0·21 μg/ml.

cold centrifugation at 4°C at 10,000 g for 30 min. Post 10,000 g supernatant was taken in a dialysis bag (exclusion limit 6,000 daltons) and dialysed against 20 mM Tris HCl (pH 7·5) buffer for 7–8 h at 4°C. The dialysate was used to assay the activity of phosphodiesterase (PDE) by the method of Aboud and Burger (1971) and activity of 5′-nucleotidase was measured by the method of Heppel and Hilmoe (1951).

3. Results

3.1 *Lipid composition of control and griseofulvin-grown mycelia*

Table 1 shows the lipid composition of control and griseofulvin grown (IC_{50}) mycelia. Content of TL, TPL and sterols were found to decrease significantly ($P < 0.01$) by 32, 42 and 38%, respectively in griseofulvin grown mycelia. Analysis of individual phospholipid fractions of control and griseofulvin grown mycelia is also shown (table 1). A significant decrease in the level of lysophosphatidylcholine ($P < 0.01$), phosphatidylserine and phosphatidylinositol ($P < 0.05$), phosphatidylcholine ($P < 0.01$), phosphatidylethanolamine ($P < 0.001$) and unidentified phospholipids ($P < 0.05$) was seen in griseofulvin grown mycelia. The ratio of PC/PE increased from 2·14 to 4·24 in griseofulvin grown cells as compared to control.

The relative percentage of fatty acids in phospholipids from control and griseofulvin grown cultures have been shown in table 2. Griseofulvin grown mycelia showed a considerable decrease in myristic acid (32%) and palmitic acid (16%) with an increase in stearic acid content. However the levels of palmitoleic acid and oleic acids did not change significantly. The ratio of unsaturated to saturated fatty acids was 1·5 in control while it was 1·8 in the griseofulvin grown mycelia.

3.2 *Effect of griseofulvin on lipid biosynthesis*

Figure 1 shows lipid biosynthesis from [^{14}C]acetate in control and drug treated (0·5 μg/ml) mycelia. Uptake at 0 min was 10–20 times less than the 120 min value

Fatty acids	Relative percentage of phospholipid fatty acids	
	Control	Griseofulvin grown
Myristic acid (14:0)	6·82	4·61
Palmitic acid (16:0)	24·60	20·20
Palmitoleic acid (16:1)	3·66	3·97
Stearic acid (18:0)	8·57	10·66
Oleic acid (18:1)	18·82	18·87
Linoleic acid (18:2)	37·56	41·66
Unsaturated/saturated fatty acid ratio	1·5	1·8

Values are mean of two independent observations. IC$_{50}$ − 0·21 µg/ml.
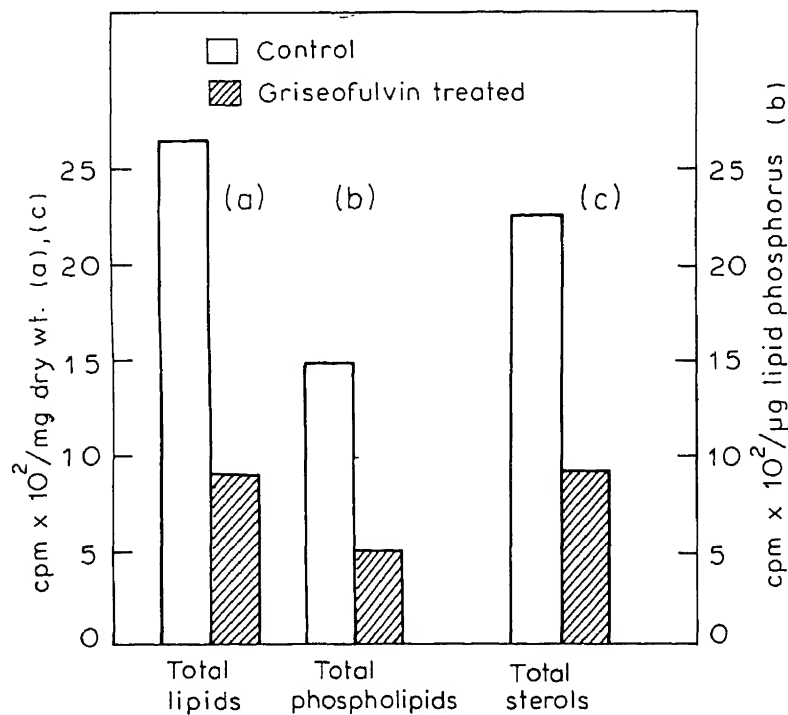
Figure 1. Effect of minimum inhibitory concentration of griseofulvin (0·5 µg/ml) on incorporation of [^{14}C] acetate into TL, TPL and total sterols of *M. gypseum* mycelia.

by 33·9, 33 and 39·9% respectively due to the presence of griseofulvin.

3.3 *Effect of griseofulvin on leakage of cellular constituents*

Griseofulvin treatment (10 X MIC) of mid log phase cells resulted in a significant stimulation in leakage of intracellular $[^{32}P]$ from prelabelled cells (174% in griseofulvin treated cells in comparison to 82% in control cells) after 4 h of treatment with drug (table 3).

3,4 *Effect of griseofulvin on K^+-efflux*

Griseofulvin at 15 X MIC and 30 X MIC doses caused a stimulation in K^+-efflux by 18 and 28% respectively (figure 2) after 60 min of incubation with the drug. There was no efflux of K^+ for 60 min in the absence of the drug.

Table 3. Effect of griseofulvin on leakage of radioactivity from control and griseofulvin treated (10 X MIC) mycelia previously labelled with $[^{32}P]$ (H_3PO_4).

| Incubation time (h) | Percentage increase in $[^{32}P]$ leakage | |
	Control	Griseofulvin treated
1	37·5 (3)	71·9 (3)
2	84·8 (3)	137·3 (3)
3	87·6 (3)	160·9 (3)
4	81·7 (3)	174·3 (3)

Values in parenthesis represent number of independent batches analysed in duplicate. Experiment was started with same number of counts in control and griseofulvin treated cultures.
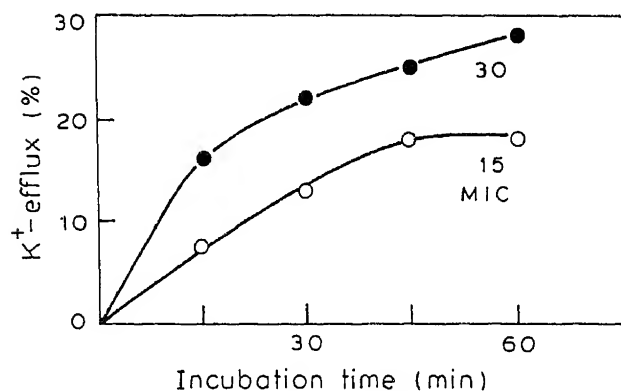
Figure 2. Effect of griseofulvin at 15 X MIC and 30 X MIC on K^+-efflux in *M. gypseum* cells. Values are average of three batches analysed in duplicate (O), 15 X MIC; ( ), 30 X MIC.

Activity of phosphodiesterase was not affected by griseofulvin. The enzyme activities were 24.6 ± 3.0 and 28.0 ± 4.0 nmol/min/mg protein in control and griseofulvin treated (10 X MIC) mycelia, respectively. There was no effect of griseofulvin on the activity of 5'-nucleotidase which was 10.0 ± 1.9 nmol/min/mg protein in control.

4. Discussion

Biochemical events leading to the growth inhibitory action of griseofulvin are yet not clear except for its inhibitory effects on chitin (Brian 1960) and nucleic acid synthesis (McNall 1960). In the present study, cells grown in the presence of IC_{50} dose of griseofulvin exhibited significantly lower levels of TL, TPL and sterols (table 1). This is probably due to the effect of the drug or its metabolites on the enzymes of lipid biosynthesis/degradation or through some alternate mechanism. However, experimental evidence is required to negate this hypothesis.

Further, an increase in K^+-efflux was observed from the mycelia treated with high doses of griseofulvin (15 X MIC and 30 X MIC; figure 2). This observation is supported by earlier reports by Iwata et al (1973) according to which high concentrations of clotrimazole caused leakage of various small molecules like K^+, amino acids, sugars and inorganic phosphates. Increased K^+ -efflux caused by clotrimazole (Iwata et al 1973) is known to decrease the cellular pH which has been proposed to activate certain lytic enzymes leading to enhanced degradation of some cellular constituents (Lampen 1966). In the present study, the observed increase in leakage of $[^{32}P]$ components from griseofulvin treated cells (table 3) can be attributed to these facts. Antifungal drugs (e.g., polyenes and imidazoles) are also known to influence certain membrane-bound enzymes including phosphodiesterase and 5'-nucleotidase in *Candida albicans* (Surarit and Shephard 1987). However, griseofulvin did not alter the activity of these enzymes in *M. gypseum*.

On the basis of results presented here, it is clear that griseofulvin exerts its fungistatic effect through alterations in lipid composition and membrane permeability, in addition to the previously reported inhibitory effect on nucleic acid synthesis.

References

Aboud M and Burger M 1971 Cyclic 3', 5'-adenosine monophosphodiesterase and the release of catabolic repression of beta galactosidase by exogenous cyclic 3', 5'-adenosine monophosphate; *Biochem. Biophys. Res. Commun.* **43** 174–182

Bansal V S and Khuller G K 1981 Changes in phospholipids of Microsporum species in the presence of ethanol; *Arch. Microbiol.* **130** 248–249

Blank H, Taplin D and Roth F J 1960 Electron microscopic observations of the effects of griseofulvin on dermatophytes; *Arch. Dermatol.* **81** 667–679

Chen W C, Sud I J, Chou D L and Feingold S 1977 Selective toxicity of the polyene antibiotics and their methyl ester derivatives; *Biochem. Biophys. Res. Commun.* **74** 480–487

Folch J, Lees M and Stanley G H S 1957 A simple method for isolation and purification of total lipids from animal tissues; *J. Biol. Chem.* **226** 497–509

Gupta M P, Kapur N, Bala I and Khuller G K 1991 Studies on the mode of action of tolnaftate in *Microsporum gypseum*; *J. Med. Vet. Mycol.* **29** 45–52

Heppel L A and Hilmoe R J 1951 5'-nucleotidase of seminal plasma. Assay method; *Methods Enzymol.* **2** 546–550

Iwata K, Yamaguchi H and Hiratini T 1973 Mode of action of clotrimazole; *Sabouraudia* **11** 158–166

Kates M 1972 Techniques of lipidology: Isolation, analysis and identification of lipids; in *Laboratory Techniques in Biochemistry and Molecular Biology* (eds) T S Work and E Work (London: North-Holland and New York: Elsevier) pp 269–610

Kerridge D 1986 Mode of action of clinically important antifungal drugs; *Adv. Microbiol. Physiol.* **27** 1–72

Khuller G K, Dogra A, Malik U and Asotra S 1984 Macromolecular biosynthesis in *Mycobacterium smegmatis* ATCC-607 in the presence of antiserum to mannophosphoinositides; *J. Gen. Microbiol.* **130** 1795–1798

Lampen J O 1966 *Interference by polyence antifungal antibiotics (especially nystatsin and fillipin) with specific membrane functions* 16th Symposium of Society of General Microbiologists (London) (London: Cambridge University Press) pp 111–130

Marinetti G V 1962 Chromatographic separation, identification and analysis of phospholipids; *J. Lipid Res.* **3** 1–11

McNall E G 1960 Biochemical studies on the metabolism of Griseofulvin; *Arch. Dermatol.* **81** 657–661

Prabhudesai A V 1978 *Chemical synthesis of lipids* Ph. D. thesis, Poona University, Pune

Shah V P 1980 *Griseofulvin absorption per OS and percutaneous Preusser* (eds) Med. Mycology, Zbl, Bakt. Suppl.-8, (Stuttgart, New York: Gustav Fischer Verlag) pp 223–239

Singh M, Jayakumar A and Prasad R 1979 Lipid composition and polyene antibiotic sensitivity in isolates of *Candida albicans*; *Microbios* **24** 7–17

Surarit R and Shepherd M G 1987 The effect of azole and polyene antifungals on the plasma membrane enzymes of *Candida albicans*; *J. Med. Vet. Mycol.* **25** 403–413

Weinstein G D and Blank H 1960 Quantitative determination of griseofulvin by a spectrophotometric assay; *Arch. Dermatol.* **81** 746–749

Zlatkis A, Zak B and Boyles A J 1953 A new method for the direct determination of serum chlosterol; *J. Lab. Clin. Med.* **41** 486–492

AUTHOR INDEX

Journal of Biosciences

ACKNOWLEDGEMENTS

Dr N Kochupillai, New Delhi
Dr V Kothekar, New Delhi
Dr G Kulandaivelu, Madurai
Dr S C Lakhotia, Varanasi
Dr N Lakshmiah, Hyderabad
Dr Lalji Singh, Hyderabad
Dr Madhav Gadgil, Bangalore
Dr Madhoolika Agrawal, Varanasi
Dr S Mahadevan, Bangalore
Dr Mahdi Hasan, Aligarh
Dr I Manorama Thomas, Bangalore
Dr Margret Biswas, Bangalore
Dr Mary Jacob, Vellore
Dr A F Mascarenhas, Pune
Dr S Mathavan, Madurai
Dr Meena Augustus, Bangalore
Dr V M Meher–Homji, Pondicherry
Dr Mewa Singh, Mysore
Mr Milind G Watve, Bangalore
Dr H Y Mohan Ram, Delhi
Dr C V Mohan, Mangalore
Dr B K Mukherjee, New Delhi
Dr R Muniayappa, Guam, USA
Dr K Muralidhar, Delhi
Dr P S Murthy, Delhi
Dr B Nagarajan, Madras
Dr R C Nageshwar Rao, Patancheru
Dr Namita Surolia, Bangalore
Dr V Nanjundiah, Bangalore
Dr S Narendra Prasad, Dehra Dun
Dr R Nayak, Bangalore
Dr S A Newman, New York, USA
Dr J Newport, California, USA
Dr G Padmanaban, Bangalore
Dr T J Pandian, Madurai
Dr A H Parulekar, Goa
Dr N Pattabiraman, Washington,
  USA
Dr T N Pattabiraman, Manipal
Dr Peter Ashton, Massachusetts,
  USA
Dr Phyllis Lee, Cambridge, UK
Dr M K K Pillai, Delhi
Dr R S Pirta, Simla
Dr R M Pitchyappan, Madurai
Dr M Pradhan, Bangalore
Dr V Prakash, Mysore

Dr Priya Davidar, Pondicherry
Dr A S Raghavendra, Hyderabad
Dr P V Rai, Bangalore
Dr D Rajagopala Rao, Mysore
Dr C Rajamanickam, Madurai
Dr Rakesh Tuli, Bombay
Dr Rama S Singh, Ontario, Canada
Dr A Ramaiah, New Delhi
Dr P S Ramakrishnan, New Delhi
Dr T Ramakrishnan, Bangalore
Dr C Ramakrishnan, Bangalore
Dr Raman K Roy, Bangalore
Dr S Ramani, Bangalore
Dr T Ramasarma, Bangalore
Dr Ramesh Maheshwari, Bangalore
Dr Ramesh S Paranjape, Madras
Dr Ranjit R J Daniels, Bangalore
Dr A J Rao, Bangalore
Dr G R Rao, Bangalore
Dr M R S Rao, Bangalore
Dr S R V Rao, Delhi
Dr N H Ravindranath, Bangalore
Dr Renu–Khanna Chopra, New Delhi
Dr Rita G Adiyodi, Calicut
Dr U P Roos, Zurich, Switzerland
Dr C J Saldanha, Bangalore
Dr Sandip K Basu, Chandigarh
Dr Sarala K Subba Rao, New Delhi
Dr Saraswathi Vishveshwara,
  Bangalore
Dr P S Sastry, Bangalore
Dr H S Savithri, Bangalore
Dr Shail K Sharma, New Delhi
Dr M S Shaila, Bangalore
Dr A K Sharma, Calcutta
Dr N S Shekhawat, Jodhpur
Dr A R Sheth, Bombay
Dr P S Shetty, Bangalore
Dr Shyamal Roy, Calcutta
Dr O Siddiqi, Bombay
Dr R N Singh, Bombay
Dr M Singh, Calcutta
Dr J S Singh, Varanasi
Dr V Sitaramam, Pune
Dr S Subramanya, Bangalore
Dr Sudha Bhattacharya, New Delhi
Dr Sudha G Gangal, Bombay